



Three dimensional depth visualization using image sensing to detect artefact in space

by

Raymond. D. Nell

Thesis submitted in fulfilment of the requirements for the degree

Doctor of Technology: Electrical Engineering

in the Faculty of Engineering

at the Cape Peninsula University of Technology

Supervisor: Prof. MTE. Kahn

Bellville

2014

CPUT copyright information

The thesis may not be published either in part (in scholarly, scientific or technical journals), or as a whole (as a monograph), unless permission has been obtained from the University.

DECLARATION

I, **Raymond. D. Nell**, declare that the contents of this dissertation/thesis represent my own unaided work, and that the dissertation/thesis has not previously been submitted for academic examination towards any qualification. Furthermore, it represents my own opinions and not necessarily those of the Cape Peninsula University of Technology.



Signed

12 June 2014

Date

ABSTRACT

Three-dimensional (3D) artefact detection can provide the conception of vision and real time interaction of electronic products with devices. The orientation and interaction of electrical systems with objects can be obtained. The introduction of electronic vision detection can be used in multiple applications, from industry, in robotics and also to give orientation to humans to their immediate surroundings. An article covering holograms states that these images can provide information about an object that can be examined from different angles. The limitations of a hologram are that there must be absolute immobilization of the object and the image system. Humans are capable of stereoscopic vision where two images are fused together to provide a 3D view of an object. In this research, two digital images are used to determine the artefact position in space. The application of a camera is utilized and the 3D coordinates of the artefact are determined. To obtain the 3D position, the principles of the pinhole camera, a single lens as well as two image visualizations are applied. This study explains the method used to determine the artefact position in space. To obtain the 3D position of an artefact with a single image was derived. The mathematical formulae are derived to determine the 3D position of an artefact in space and these formulae are applied in the pinhole camera setup to determine the 3D position. The application is also applied in the X-ray spectrum, where the length of structures can be obtained using the mathematical principles derived. The XYZ coordinates are determined, a computer simulation as well as the experimental results are explained. With this 3D detection method, devices can be connected to a computer to have real time image updates and interaction of objects in an XYZ coordinate system.

Keywords: 3D point, xyz-coordinates, lens, hologram

Acknowledgements

I want to thank my supervisor Prof. MTE Kahn who guided me through the process

I also want to thank all others that had discussions and support me with this project

Dedication

I, Raymond Nell dedicate this thesis to all my children who kept my spirit high during this research. The enthusiasms that a child gives were from Zaakirah, Aamirah, Raymonde, Ashmaa, Naa'ilah and Rozeena. I also dedicate this thesis to Zoeleigha and Lilian who travelled with me to overseas congresses and even waited long hours at the airport if I had to travel alone to a congress. Sometimes they waited till late at night at home for a call from me from a country more than 10000km away. I give great thanks to my Creator who kept me safe during the overseas journeys.

TABLE OF CONTENTS

Declaration.....	iii
Abstract.....	iv
Acknowledgements.....	v
Glossary.....	xix
Dedication.....	vi

CHAPTER 1: BACKGROUND AND SCOPE OF STUDY

1.1	Introduction.....	1
1.2	Background to the research problem.....	1
1.3	Literature review.....	2
1.4	Research topic.....	3
1.5	Hypothesis.....	4
1.6	Purpose of the research.....	4
1.7	Research Objectives.....	4
1.8	Research methodology.....	4
1.9	Layout of the thesis.....	5
1.9.1	Chapter 1: Background and Scope.....	5
1.9.2	Chapter 2: Principles of stereoscopic vision.....	5
1.9.3	Chapter 3: Stereoscopic vision with a pinhole camera.....	5
1.9.4	Chapter 4: Method to determine the 3D xyz-coordinates of an artefact.....	5
1.9.5	Chapter 5: Mathematical model to determine the xyz-coordinates of an object using a linear two camera system.....	6
1.9.6	Chapter 6: Method to determine linear 3D measurements.....	6
1.9.7	Chapter 7: The use of 3D electronic vision for effective utilization of solar power in a hybrid electrical supply setup.....	6
1.9.8	Chapter 8: Measuring the light intensity of a hybrid powered CFL and LED lighting using 3D electronic vision in rotation of the solar panel.....	6
1.9.9	Chapter 9: Determine the 3D-coordinates of the X-ray focus.....	6
1.9.10	Chapter 10: A method to determine and calculate the distance between the X-ray focus and the patient skin surface without any interaction with the patient.....	7
1.9.11	Chapter 11: A method to perform 3D measurements on routine AP and LAT X-ray examinations.....	7
1.9.12	Chapter 12: Summary.....	7

CHAPTER 2: Imaging systems used to determine the 3D position of an artefact

2.1	Introduction to Principles of stereoscopic vision.....	8
2.2	The 3D object.....	8
2.3	Principles of stereoscopic vision.....	9
2.4	Principles of a lens camera.....	10
2.5	Principles of a pinhole camera.....	12
2.6	Characteristics of a pinhole camera.....	12
2.7	Summary, pinhole camera.....	13

CHAPTER 3: Stereoscopic vision with a pinhole camera

3.1	Introduction.....	14
3.2	Method to determine the xyz-coordinates from 2D images.....	15
3.3	Mathematical method to determine the intersecting point of two lines in 3D.....	17
3.4	Determine the distance of the shortest line.....	22
3.5	Simulation.....	24
3.6	Simulation of the 3D pinhole camera method.....	26
3.6.1	Method for computer simulation.....	27
3.6.2	Method for computer simulation.....	27
3.7	Experiment to determine the artefact position in space.....	29
3.7.1	The origin of the setup.....	31
3.7.2	The artefact images.....	31
3.7.3	Application of the formulae to calculate artefact position.....	34
3.7.4	Application of the formulae to calculate artefact position.....	35
3.7.5	Summary of experimental results.....	38
3.8	Conclusion of Chapter 3.....	38

CHAPTER 4: A method to determine the 3D xyz-coordinates of an artefact with a single lens image

4.1	Introduction.....	40
4.2	Characteristics of a lens image.....	40
4.3	Determine the object position from centre of lens.....	42
4.4	Determine the height of the object.....	42
4.5	Example: Extract from example in Sears page 95.....	44
4.6	Determine the 3D xyz-coordinates.....	45
4.7	Determine the x-coordinate.....	47
4.8	Determine the y-coordinate.....	47
4.9	Determine the z-coordinate.....	48

4.10	Thick lens.....	48
4.11	Principle points and focal points of different thick lenses.....	50
4.12	Determine the xyz-coordinates of an object with a thick lens.....	51
4.13	Formulae to determine the xyz-coordinates with a single image from a thick lens.....	51
4.14	Determine the xyz-coordinates of an object with a compound lens.....	53
4.15	Determine the xyz-coordinates of compound lens and a telescopic lens.....	53
4.16	Limitations to consider.....	53
4.17	Summary.....	54
4.18	Conclusion of chapter 4.....	55

CHAPTER 5: A mathematical model to determine the xyz-coordinates of an object using a linear two camera system

5.1	Introduction.....	56
5.2	Aim.....	56
5.3	The 3D-camera setup.....	56
5.4	Method to determine the xyz-coordinates of the COP.....	58
5.5	Mathematical method to determine the intersecting point of two lines in 3D....	59
5.6	Determine the COP for a camera setup.....	62
5.7	Determining the position of the object point.....	64
5.8	The xyz-coordinates of the object point.....	65
5.9	MATLAB simulation.....	68
5.10	Discussion.....	69
5.11	Limitations to consider.....	70
5.12	Conclusion of chapter 5.....	70

CHAPTER 6: Method to determine linear 3D measurements

6.1	Introduction.....	71
6.2	Aim.....	71
6.3	The value of 3D measurements.....	71
6.4	The 3D camera setup.....	71
6.5	Method to determine 3D measurement.....	73
6.6	MATLAB Simulation.....	75
6.7	Conclusion of chapter 6.....	78

CHAPTER 7: The use of 3D electronic vision for effective utilization of solar power in a hybrid electrical supply setup

7.1	Introduction.....	79
7.2	Solar energy and sun-tracking.....	79
7.3	Aim.....	81
7.4	Hybrid system.....	82
7.5	The 3D visualization system.....	82
7.6	Accuracy of the 3D visualization system.....	84
7.7	Repositioning of the solar panel.....	86
7.8	Experimental results with solar panel in sunlight.....	87
7.9	Solar panel voltage output with no load connected.....	87
7.10	Solar panel voltage output with a load of 29.9Ω connected.....	89
7.11	Solar panel voltage output with a load of 55.5Ω connected.....	90
7.12	Solar panel voltage output with a load of 131.3Ω connected.....	92
7.13	Output power characteristics of the solar panel in direct sunlight.....	94
7.14	Output power characteristics of the solar panel in half shadow.....	94
7.15	Output power characteristics of the solar panel in full shadow.....	95
7.16	Comparison of the output power of the solar panel in direct sunlight, half shadow and full shadow.....	96
7.17	The use of the renewable energy or the national grid electrical supply.....	96
7.18	Limitations to consider.....	97
7.19	Conclusion of chapter 7.....	97

CHAPTER 8: Measuring the light intensity of a hybrid powered CFL and LED lighting using 3D electronic vision in rotation of the solar panel

8.1	Introduction.....	98
8.2	Solar energy and angle of sunlight.....	98
8.3	Aim.....	99
8.4	The hybrid system.....	99
8.5	Direction of sun's rays.....	100
8.6	Solar panel output angulated against the sunrays.....	102
8.7	Solar panel output angulated against the sunrays.....	103
8.8	Solar panel output angulated against the sunrays.....	104
8.8.1	Light intensity output measured of the incandescent, CFL, LED and lights connected to the solar panel.....	104
8.9	Results obtained.....	106
8.10	Limitations to consider.....	107
8.11	Results.....	107

CHAPTER 9: A model to determine the 3D-coordinates of the X-ray focus

9.1	Introduction.....	108
9.2	Aim.....	108
9.3	The X-ray focus.....	108
9.4	Method.....	109
9.5	Points used to generate the two image lines.....	111
9.6	Mathematical method to determine the intersecting point of two lines in 3D.....	111
9.7	Mathematical method to determine the shortest distance between two lines in 3D.....	113
9.8	Coordinates of the focus point.....	116
9.9	Discussion.....	118
9.10	Limitations to consider.....	119
9.11	Conclusion of chapter 9.....	120

CHAPTER 10: Method to determine and calculate the distance between the X-ray focus and the patient skin surface without any interaction with the patient

10.1	Introduction.....	121
10.2	Aim.....	121
10.3	The X-ray focus.....	121
10.4	Point of interest on patient skin surface.....	122
10.5	Method to determine the distance.....	122
10.6	Coordinates of the focus point.....	123
10.7	Method to determine the xyz-coordinates of the point on the patient skin surface.....	125
10.8	Converting the radius and Euler angles to xyz-coordinates.....	126
10.9	The distance between the X-ray focus and a point of interest on the patient skin surface.....	127
10.10	Setup to measure the distance from the X-ray focus to patient skin surface..	128
10.11	Limitations to consider.....	129
10.12	Conclusion of chapter 10.....	130

CHAPTER 11: A method to perform 3D measurements on routine AP and LAT X-ray examinations

11.1	Introduction.....	131
-------------	--------------------------	------------

11.2	Aim.....	132
11.3	Method to perform 3D measurements with a routine AP and LAT X-ray examination.....	132
11.4	The X-ray focus.....	134
11.5	Points used to generate the two image lines.....	135
11.6	Coordinates of the focus point.....	137
11.7	Determining the 3D-coordinates on the AP and LAT views.....	139
11.8	Experimental results in 3D measurements with set diameter of a radiopaque structure.....	141
11.9	Conclusion.....	142

CHAPTER 12: Conclusion

12.1	Introduction to conclusion.....	143
12.2	Mathematical method to determine the intersecting point of two lines in 3D.....	143
12.3	Formulae to determine the shortest distance between two line segments in 3D.....	144
12.4	Determining the 3D xyz-position using two pinhole cameras.....	150
12.5	Determining the 3D xyz-position using a single lens image.....	151
12.6	Determine the Centre of Projection of a camera setup.....	151
12.7	Determining the 3D xyz-position of an X-ray focus.....	152
12.8	Determining the 3D measurements on an AP and LAT X-ray Image	153
12.9	Experimental comparison of methods derived and application.....	154
12.10	Conclusion.....	155
12.11	Recommendations for further study	156
	Reference.....	157

List of Tables

Table 3.1: Results of two lines intersect in 3D.....	25
Table 3.2: Results of two line segments in 3D that do not intersect.....	26
Table 3.3: Table with the coordinate values calculated with the formulae.....	28
Table 3.4: Comparing the calculated values with the computer simulation model.....	28
Table 3.5: The pinhole positions, artefact image positions as well as the artefact position calculated.....	35
Table 3.6: Comparing the calculated values with the experimental results to determine the position of the artefact.....	37
Table 4.1: Display the focal length, focal point and principle points of different thick lenses.....	50
Table 7.1a: Comparison between calculated x-values and measured x-values.....	84
Table 7.1b: Comparison between calculated x-values and measured x-values.....	84
Table 7.1c: Comparison between calculated x-values and measured x-values.....	84
Table 7.2: Display the difference in length for each xyz-coordinate.....	85
Table 7.3: Display the % accuracy for all three coordinates and the overall accuracy.....	86
Table 7.4a: Display the difference in output power of the solar panel with no load connected in direct sunlight.....	88
Table 7.4b: Display the difference in output power of the solar panel with no load connected in half shadow.....	88
Table 7.4c: Display the difference in output power of the solar panel with no load connected in full shadow.....	88
Table 7.5a: Display the difference in output power of the solar panel in direct sunlight with a load of 29.9 Ω connected.....	89
Table 7.5b: Display the difference in output power of the solar panel in half shadow with a load of 29.9 Ω connected.....	90
Table 7.5c: Display the difference in output power of the solar panel in full shadow with a load of 29.9 Ω connected.....	90
Table 7.6a: Display the difference in output power of the solar panel in direct sunlight with a load of 55.5 Ω connected.....	91
Table 7.6b: Display the difference in output power of the solar panel in half shadow with a load of 55.5 Ω connected.....	91
Table 7.6c: Display the difference in output power of the solar panel in full shadow with a load of 55.5 Ω connected.....	92

Table 7.7a: Display the difference in output power of the solar panel in direct sunlight with a load of 131.3Ω connected.....	93
Table 7.7b: Display the difference in output power of the solar panel in half shadow with a load of 131.3Ω connected.....	93
Table 7.7c: Display the difference in output power of the solar panel in full shadow with a load of 131.3Ω connected.....	93
Table 7.8: Display the difference in output power of the solar panel in direct sunlight.....	94
Table 7.9: Display the difference in output power of the solar panel in half shadow.....	94
Table 7.10: Display the difference in output power of the solar panel in full shadow.....	95
Table 8.1: Difference in output power at different angles.....	102
Table 8.2a: Light intensity with room light on. Room luminance measured is 45.2lux..	105
Table 8.2b: Light intensity with room light off, window not covered. Room luminance measured is 0.16lux.....	105
Table 8.2c: Light intensity with room light off, window covered. Room luminance is 0.0lux.....	106
Table 11.1: Results measurement of the coin with 1 st point selected	139
Table 11.2: Results measurement of the coin with 2 nd point selected.....	139
Table 11. 3: Results measurement of the 1 st point selected on the AP and LAT view	141
Table 11.4: Results measurement of the 2 nd point selected on the AP and LAT view.....	141

LIST OF FIGURES

Figure 2.1: Stereoscopic vision. Two images viewed are merged together to form a 3D image.....	9
Figure 2.2: Image projected on a screen through a convex lens.....	10
Figure 2.3: An electronic flat panel sensor.....	11
Figure 2.4: Display the internal structure of a camera.....	11
Figure 2.5: Principle of a pinhole camera.....	12
Figure 3.1: Two pinhole cameras are positioned next to each other and two images are obtained from the same object.....	14
Figure 3.2: A setup to determine the position in space using two image planes with a pinhole opening in front.....	15
Figure 3.3: The boxtype pinhole cameras setup to produce two pinhole images.....	15
Figure 3.4: The setup of two image planes with two pinhole positions to detect the artefact position.....	16
Figure 3.5: The setup to measure the shortest distance between the two lines in 3D.....	17
Figure 3.6: Setup to determined the shortest distance between two lines in 3D.....	18
Figure 3.7: MATLAB simulation of two lines intersect in 3D.....	25
Figure 3.8: MATLAB simulation of two line segments in 3D that do not intersect.....	26
Figure 3.9: Computer model displaying the coordinates of the artefact, pinhole positions as well as the position of the artefact image points on image plane 1 and 2.....	27
Figure 3.10: The position of the artefact as simulated by the computer model was within the same range as those calculated by the formulae derived.....	29
Figure 3.11: Schematic setup position for the experiment with P1 as the origin.....	30
Figure 3.12: The setup position for the experiment with the pinhole camera.....	30
Figure 3.13: The pinhole artefact image with the camera at the position one.....	32
Figure 3.14: Schematic of pinhole artefact image with the camera at the position one.....	33
Figure 3.15: The pinhole artefact image with the camera at the position two.....	33
Figure 3.16: Schematic of pinhole artefact image with the camera at the position two.....	34
Figure 3.17: The values inserted on the schematic images.....	35
Figure 3.18: The setup to measure the artefact point.....	36
Figure 3.19: The value measured of the artifact.....	37
Figure 3.20: Summery of the experiment.....	38

Figure 4.1: Image formation by a thin lens.....	41
Figure 4.2: The formulae to determine the object height and object distance.....	44
Figure 4.3: Example to determine the object height and object distance.....	45
Figure 4.4: Display the object distance (s) and object height (y) in 3D format.....	46
Figure 4.5: Display the 3D xyz-coordinates in a 3D lens setup.....	47
Figure 4.6. Display different types of thick lenses with radii.....	49
Figure 4.7: Display principle points, H and H', of a thick lens.....	53
Figure 4.8: A compound lens system with lenses sharing the same horizontal axis.....	53
Figure 5.1a: COP of a camera setup.....	57
Figure 5.1b: 3D camera setup.....	57
Figure 5.1c: 3D camera setup with the COP and object point.....	59
Figure 5.2: Setup to determine the xyz-coordinates of the COP.....	59
Figure 5.3: Setup to determined the shortest distance between two lines in 3D.....	60
Figure 5.4: Setup to determine the COP.....	62
Figure 5.7: Setup for the origin.....	65
Figure 5.7a: Setup for P1, P2, P3 and P4.....	66
Figure 5.8: MATLAB Simulation to determine the object point.....	68
Figure 5.9: Schematic of the setup to determine the 3D-distance with two images on the 3D-vision camera.....	69
Figure 6.1: 3D camera setup.....	72
Figure 6.2: 3D camera setup with the COP and object point.....	73
Figure 6.3 Setup to determine the 3D distance between two points in 3D.....	74
Figure 6.4 Setup to perform 3D measurements.....	75
Figure 6.5 Setup to determined the shortest distance between two lines in 3D.....	76
Figure 7.1: Display of a solar panel that is partly covered by a shadow which can reduce its output efficiently.....	80
Figure 7.2: When a solar panel is partly covered by a shadow, it will be moved into direct sunlight.....	81
Figure 7.3: A hybrid system that provides electrical supply from the national grid as well as the renewable energy system.....	82
Figure 7.4: Camera setup to determine the xyz-coordinates of the object at point A.....	83
Figure 7.4.1: XY-positioning of the solar panel.....	86
Figure 7.5: Setup to measure output power of the solar panel with no load connected.....	87
Figure 7.6: Setup to measure output power of the solar panel with the 55.5Ω and 60Ω resisters connected in parallel. The measured resistance was 29.9Ω	89

Figure 7.7: Setup to measure output power of the solar panel with a single 55.5Ω resistor connected.....	91
Figure 7.8: Setup to measure output power of the solar panel with the 55.5Ω and 60 Ω resistors connected in series. The measured resistance was 131.3 Ω.....	92
Figure 7.9: The voltage (V) and current (I) curve of the solar panel in direct sunlight.....	94
Figure 7.10: The voltage (V) and current (I) curve of the solar panel in half shadow.....	95
Figure 7.11: The voltage (V) and current (I) curve of the solar panel in full shadow.....	95
Figure. 7.12: Comparison of the output power of the solar panel in direct sunlight, half shadow and full shadow.....	96
Figure 7.13: Display the two different plugs.....	97
Figure 8.1: The sun's rays' falls at an angle onto the solar panel.....	99
Figure 8.2: A hybrid system that provides electrical supply to the light sources.....	100
Figure 8.3: Display the angles created by the sun's rays.....	100
Figure 8.4: Solar panel angulated towards the incoming sunrays.....	102
Figure 8.5: Graph of the different output power with the solar panel angled at different angles. Open circuit voltage.....	103
Figure 8.6: Rotation of the solar panel.....	104
Figure 8.7: Connection and setup of the solar panel with the incandescent, CFL, and LED light.....	104
Figure 8.8: Displays both the power as well as the lux measured for every light at room luminance of 0.0lux.....	107
Figure 9.1: X-ray tube with X-rays being generated.....	109
Figure 9.2: 3D Setup to determine the position of the pinhole and pinhole images.....	110
Figure 9.2a: Method to determine the xyz-position of the pinhole and pinhole images.....	110
Figure 9.3: Setup to determined the shortest distance between two lines in 3D.....	111
Figure 9.4: Focus point of the X-ray tube setup.....	116
Figure 9.5: Schematic of the setup to determine the 3D distance with an AP and LAT view.....	119
Figure 10.1: X-ray tube with X-rays being generated.....	121
Figure 10.2: Measuring the distance between the patient skin surface and the X-ray focus.....	122

Figure 10.3: Points of interest to measure the distance between the patient skin surface and the X-ray focus.....	123
Figure 10.4: Focus point of the X-ray tube setup.....	123
Figure 10.5: Display of the radius and the rotations.....	126
Figure 10.6: Setup to measure the distance from the X-ray focus to patient skin surface.....	128
Figure 11.1: Schematic presentation of a 3D AP and LAT with the X-ray foci and the 3D measurement.....	129
Figure 11.1.1: Schematic of obtaining the 3D distance from proximal and distal points of an anatomical structure.....	133
Figure 11.2: X-ray tube with X-rays being generated.....	135
Figure 11.3: AP and LAT X-ray image.....	136
Figure 11.4: Displays an AP and LAT view of a coin.....	137
Figure 11.5: The LAT image in view and the measurement position on the LAT view.....	138
Figure 11.6: AP image in view and the measurement position on the AP view.....	138
Figure 11.7 Measuring the radial transverse distance.....	140
Figure 11.8: Measuring the radial transverse distance.....	140
Figure 12.1: Determine the 3D co-ordinates of two lines in 3D.....	145
Figure 12.2: Setup to determine the COP	152
Figure 12.3: Focus point of the X-ray tube setup	153
Figure 12.4: Measuring the radial transverse distance	154

GLOSSARY

Nomenclature

AP (Anterior posterior)	An X-ray picture in which the X-ray beams pass from the front-to-back.
LAT (Lateral)	An X-ray picture in which the X-ray beams pass from the side.
Centre of Projection (COP)	The vanishing point of any given line in space is located at the point in the image where a parallel line through the centre of projection intersects the image plane.
azimuth angle	The angle between the projected vector and a reference vector on the reference plane is called the azimuth. Azimuth angle is the arc of the horizon between the observer's meridian and the vertical circle of an object, measured either from the north or south, to the right or clockwise, or to the left or counter clockwise, through 90° or 180°. It must be labelled north or south (as a prefix) and east or west (as a prefix) to indicate the direction of measurement.
altitude angle	The azimuth of an object is the angular distance along the horizon to the location of the object. By convention, azimuth is measured from north towards the east along the horizon.
Stereoscopic Vision	Two images are presented at slightly different angles so that they can be merged into a single image in three dimensions .
Binocular vision	Binocular vision is the process of viewing a scene with both eyes and fusing the images in one.
Parallax	Objects in the distance have a larger shift as objects that are close by to the viewer.
Optical system	The visible spectrum is the portion of the electromagnetic spectrum that is visible to (can be detected by) the human eye. An optical system is a system that uses the visible spectrum for imaging.
Incandescent light bulb	A light bulb that uses a filament.
Luminance	Brightness of light. Measured in LUX.
Hybrid electrical supply	A power supply system with renewable electrical energy, solar power and wind power.
National grid	Electricity supplied by the national department of a country.
X-ray	A high-energy stream of electromagnetic radiation having a frequency higher than that of ultraviolet light

but less than that of a gamma ray (in the range of approximately 10^{16} to 10^{19} hertz). X-rays are absorbed by many forms of matter, including body tissues, and are used in medicine and industry to produce images of internal structures.

Pinhole camera	In a pinhole camera, light passes from an object through a pinhole to the image plane
X-ray focus	The area on the anode of an x-ray tube or the target of an accelerator that is struck by electrons and from which the resulting x-rays are emitted.
Bucky	A bucky is typically used for table or wall mounted x-ray systems and holds the x-ray cassette and grid. A bucky, is a device found underneath the exam table, a drawer like device that the cassette and grid is slid into before shooting x-ray.
X-ray cassette	A device used in radiography for holding a sheet of x-ray film or a digital X-ray screen.
Radiopaque	Radiodensity (or radiopacity) refers to the relative inability of electromagnetic radiation, particularly X-rays, to pass through a particular material.
C-arm	A c-arm unit used for surgical procedures with an X-ray tube on one side a fluoroscopy unit of the other side.
Fine focus	An X-ray tube with a focal spot smaller than 0.5 millimetres.
Broad focus	An X-ray tube with a focal spot larger than 0.5 millimetres.
Actual focal spot	The section of a focal spot on which there is intersection of an electron beam with an anode of an x-ray tube.
Artefact	A structure that is present under observation.
Reverse square rule	A specified physical quantity or intensity is inversely proportional to the square of the distance from the source of that physical quantity.
Hologram	A product that uses a technique which enables three-dimensional images to be made. It involves the use of a laser, interference, diffraction, light intensity recording and suitable illumination of the recording. The image changes as the position and orientation of the viewing system changes in exactly the same way as if the object were still present, thus making the image appear three-dimensional.

Brachytherapy	Brachytherapy is a type of radiotherapy that can be used to treat many types of cancer.
Electromagnetic spectrum	The electromagnetic spectrum is the range of all possible frequencies of electromagnetic radiation.
Visual spectrum	The visible spectrum (or sometimes called the optical spectrum) is the part of the electromagnetic spectrum that is visible to the human eye.
3D	A system that has three dimensional form or appearance.
2D	A system that has two dimensional form or appearance.
Dot product	Scalar product: a real number (a scalar) that is the product of two vectors.
Gaussian form of a lens equation	The formula, $1/p + 1/i = 1/f$, $\left(\frac{1}{p} + \frac{1}{i} = \frac{1}{f} \right)$, is called the Gaussian form of the thin-lens formula.
Newtonian form of a lens equation	The Newtonian form, is obtained by considering the distance x from the object to the first focal point and the distance x' from the second focal point to the image.
Thick Lens	In a thick lens, there is a significant difference in diameter between the surfaces of the lens.
Compound lenses	Compound lenses are regarded as multiple lenses positioned in such a way that share the same horizontal axis.
Telescopic lenses	A telescopic lens is a compound lens with multiple lenses in a lens system sharing the same horizontal plane. The properties of a telescopic lens is that it has a short image distance measured from the lens closest to the image in comparison to the long object distance measured from the lens closest to the object.
Principle point of a lens	The principle points (H, H') of a lens is described as the first vertical line where the image line interacts with the vertical line.
Index of a lens	The ratio of the velocity of light in a vacuum to the velocity of light of a particular wave length in any substance is called the index of refraction of the substance for light of that particular wave length.
Focal point of a lens	The first focal point of a lens may be defined as that object point on the lens axis which is imaged by the lens at infinity. The second focal point of a lens may be defined as the image point of an infinity distant point object on the lens axis.

Abbreviations

AP	Anatomical Position
LAT	Lateral
DICOM	Digital Imaging and Communication in Medicine
3D	Three-dimensional
2D	Two-dimensional
f	focal length
H	Principle point of a lens
s	Object distance
s'	Image distance
m	magnification
COP	Centre of Projection
rpp	radians per pixel
DC	Direct Current
AC	Alternating Current
LED	Light Emitting Diode
CFL	Compact Fluorescent Lamp
SANS	South African National Standard
W	WATT

SID	Source-to-image-distance
SRD	Source-to-rotation-distance
SOD	Source-to-object-distance
IRD	Image-to-rotation-distance

CHAPTER 1

BACKGROUND AND SCOPE OF STUDY

1.1 Introduction

To determine the position of an artefact or object in a visual domain, two different images of the object are required to determine the three-dimensional (3D) position of the artefact. Stereoscopic vision is the application of two different images fused together to form a 3D image. Humans are capable of stereoscopic vision and produce two different images of the same object in each eye. When these two images are fused together, a 3D image of the object is produced.

Having an electronic product that detect 3D imaging can be of great value as applications can be implemented in industry, artefact detection and even in robotics where electronics and motors can be used to interact with the artefact (Engineering Talk. 2008).

In general two images are used to determine the 3D position of an object in space, but in this research a method a novel concept was derived to determine the 3D position on an object using only a single image.

In applying the stereoscopic principles, the mathematical model was derived to determine the 3D position of an artefact using two images. This mathematical model was applied in the pinhole camera setup and with a camera setup utilizing the centre of projection method.

1.2 Background to the research problem

An article covering holograms states that these images can provide information about an object that can be examined from different angles. The limitations of a hologram are that there must be absolute immobilization of the object and the image system (Ball et. al. 1989:340).

With this method proposed, images of an object in the visual spectrum are used to determine the 3D position and if needed, real time interaction can be obtained. Also

the techniques developed in the visual spectrum are applied in the X-ray spectrum to perform measurements of the internal structures of objects. Nell (2006:21) developed a method to detect a 3D point in space with a single X-ray view. The method explained by Nell (2006:21) was the use of linear intersection of two image lines to determine the position of an artefact. Bester et al. (1998:336) explained that both the sine and cosine formulae can be used to determine unknown sides of triangles and can also be used in 3D detection. With this research propose, it will provide a method to determine the 3D coordinates of an object, using two-dimensional (2D) imaging techniques with the intersection of two image lines. The sine and cosine formulae will be used to determine the 3D position. A stereoscopic method will be introduced using 2D image projection and the 3D coordinates will be mathematically calculated using the relationships of sin, cosine and tan formulae. The origin of the 3D coordinate system will be part of the projected system.

The objective is to determine different method to derive the 3D position of an artefact.

The method introduced will determine the 3D position of an artefact in the visual and X-ray spectrum.

1.3 Literature review

Having an electronic product that detect 3D imaging can be of great value as applications can be implemented in industry, artefact detection and even in robotics where XYZ motors can be used to interact with the artefact (Engineering Talk.2008).

Stereoscopic vision is fundamental to depth perception. Humans are capable of stereoscopic vision as they are able to focus both eyes on a single object (<http://education.vetmed.vt.edu/Curriculum/VM8054/EYE/BINOCS.HTM>). Figure 2.1 demonstrates how two images are visualized and merged together. These two images are fused together which produce a 3D orientation of the object.

Stereoscopic cameras have been utilized to determine the lander track in the autonomous operations of the microrover the Mars surface. The application and utilization of stereoscopic vision stretch far beyond the borders of industry and the earth. (Fontaine et. al. 2000)

Ball et. al (1989:341) explained with the parallax method, objects in the distance have a larger shift as objects that are close by to the viewer. This shift is when the viewer move horizontal, then the object shift is also horizontal. This phenomena is observed when traveling in a motor vehicle and the hills far away on the horizon move at a much slower rate than the trees close to the roadside.

The principles of stereoscopic vision, binocular vision and the parallax effect are all principles in the vision process to determine 3D orientation.

Thakare et. al. (2012) explained in a research paper on artificial intelligence with stereo-vision that stereo-vision is the field of computer vision and is related to artificial intelligence. Stereo vision can be used in many applications in field of artificial intelligence and robotics. Stereoscopic imaging can be applied in motion and position detection and to calculate distance of any object

1.4 Research topic

The title of this study is:

“Three dimensional depth visualization using image sensing to detect artefact in space”

An object consists of multiple points. These points are in a xyz-coordinate system. For object detection, edge detection needs to be performed to obtain the outside rim of the object. Hollingworth et al. (2000:1078) explained that edge detection is a form of high-pass filtering because edges in an image are associated with high spatial frequencies, that is, areas with fast changing content. Edge detection is an important pre-processing technique applied in a computer vision system, because it defines the boundary of an object. For edge detection, high-pass filtering can be used which results in the edges be available for processing in an image. Matrices are spread sheets of numbers (Joubert et al. 1997:148). When obtaining these two images, edge detection of the images can be performed using matrix manipulation and with these edge image information, the 3D surface points of the object can be calculated (Liu et al. 2007:22). To obtain the external surface of the object, the external points of the surface can be connected in a triangle format (www.emeraldinsight.com).

1.5 Hypothesis

Depth visualization of artefacts can be obtained using image sensing to detect the xyz-position in space.

1.6 Purpose of the research

The purpose of the research is to determine the 3D xyz-coordinates of an artefact in space using a 2D image system.

1.7 Research Objectives

The objective of the research is to determine the 3D xyz-coordinates of an artefact in space using different imaging methods including a 2D image system.

Also in determining the 3D xyz-coordinates of an artefact, the mathematical formulae in utilization of the properties of stereoscopic vision can be applied to determine the 3D position of an artefact.

1.8 Research methodology

The methods used by the researcher are:

- Conceptualize the method to determine the artefact position in space.
- Draw a schematic image projection to detect the artefact using two different images.
- Derive the mathematical formulae to determine the position of the artefact in space.
- Draw up a simulation application of the schematic projection.
- Apply the mathematical formulae and determine if the simulation results confirm with the conception, image projection as well as the calculated results.
- Determine the artefact position in a special domain.
- Apply the electronic 3D detection pinhole camera in experimental results to detect an artefact and test if the results correlate with the measurements of the xyz position of the artefact.

- Using the mathematical formulae in application of the centre of projection (COP) method with a two camera setup to calculate the 3D position of an artefact in space.
- Utilizing the methods and formulae derive to determine the 3D position of an artefact in space, the distance of the X-ray focus to the patient skin surface will be derived.
- By applying the methods to determine the 3D position in the X-ray spectrum, the internal measurements of the body structures can be measured.

1.9 Layout of the thesis

This thesis discusses different methods to determine the 3D xyz-coordinates of an artefact. In order to achieve the objectives of the study, the following chapters and contents of the dissertation are structured as follow:

1.9.1 Chapter 1: Background and Scope.

This chapter explains the title of the research as well as the layout, objectives and methodology.

1.9.2 Chapter 2: Imaging systems used to determine the 3D position of an artefact.

This chapter explains the different imaging systems used to determine the 3D position of an artefact

1.9.3 Chapter 3: Stereoscopic vision with a pinhole camera.

This chapter explains the method how the 3D position of an artefact can be obtained using the pinhole imaging method.

1.9.4 Chapter 4: Method to determine the 3D-coordinates of an artefact with a single lens image.

This chapter explains the method how the 3D position of an artefact can be obtained using a single image obtained from a lens imaging system. This method can also be

used in a multi lens camera, but still only a single image is used to determine the 3D-position in space.

1.9.5 Chapter 5: Mathematical model to determine the xyz-coordinates of an object using a linear two camera system.

This chapter explains the method how the 3D position of an artefact can be obtained using a 3D camera setup where two images are obtained in an electronic format and the 3D-coordinates of the artefact are calculated.

1.9.6 Chapter 6: Method to determine linear 3D measurements.

This chapter explains the method how to perform measurements in 3D using the linear camera system.

1.9.7 Chapter 7: The use of 3D electronic vision for effective utilization of solar power in a hybrid electrical supply setup.

This chapter explains the benefit using the 3D vision system in the effective utilization of solar power in a hybrid electrical supply setup.

1.9.8 Chapter 8: Measuring the light intensity of a hybrid powered CFL and LED lighting using 3D electronic vision in rotation of the solar panel.

This chapter explains the benefit using the 3D vision system using in a lighting system by measuring the light intensity of a hybrid powered CFL and LED lighting system using 3D electronic vision information for the rotation of the solar panel.

1.9.9 Chapter 9: Determine the 3D-coordinates of the X-ray focus.

This chapter explains a method to determine the 3D-coordinates of the X-ray focus.

1.9.10 Chapter 10: A method to determine and calculate the distance between the X-ray focus and the patient skin surface without any interaction with the patient.

This chapter explains a method to determine the distance from the patient skin surface to the X-ray focus.

1.9.11 Chapter 11: A method to perform 3D measurements on routine AP and LAT X-ray examinations.

This chapter explains the method to perform 3D measurements on routine AP and LAT X-ray examinations.

1.9.12 Conclusion

This chapter provides a conclusion of the methods and results obtained.

With the objectives and the layout, different 3D position detection methods will be investigated. All these methods provide the 3D-coordinates and these coordinates can be inserted into robotic arm for interaction with the objects.

CHAPTER 2

Imaging systems used to determine the 3D position of an artefact

2.1 Introduction to stereoscopic vision

Stereoscopic vision uses two different images of the same object fused together. By using the concepts and principles of stereoscopic vision, it can be applied in a mathematical formula to calculate the 3D position of an object.

These different imaging methods will be used to determine the 3D coordinates of the object.

With this research propose, it will provide a method to determine the 3D coordinates of an object, using two-dimensional (2D) imaging techniques and the intersection of two image lines.

Lazaros (2008) explained that Stereo vision is a flourishing field and new approaches are presented every year. Latest trends in the field mainly pursue real-time execution speeds, as well as decent accuracy and detecting conjugate pairs in stereo images is a challenging research problem known as the correspondence problem, i.e., to find for each point in the left image, the corresponding point in the right one is a continuous challenge. In this research an algorithm was developed in the form of a computer program to detect the conjugate pairs in stereo images.

2.2 The 3D object

An object consists of multiple points. These points are in a xyz-coordinate system.

The method introduced will determine the 3D position of an artefact in the visual spectrum.

To detect the position of an artefact in space, the two different images of an object are used to determine the three-dimensional (3D) image of the artefact.

2.3 Principles of stereoscopic vision

Stereoscopic vision is the application of two different images fused together to form a 3D image.

The principles of stereoscopic vision, binocular vision and the parallax effect are all principles in the vision process to determine 3D orientation.

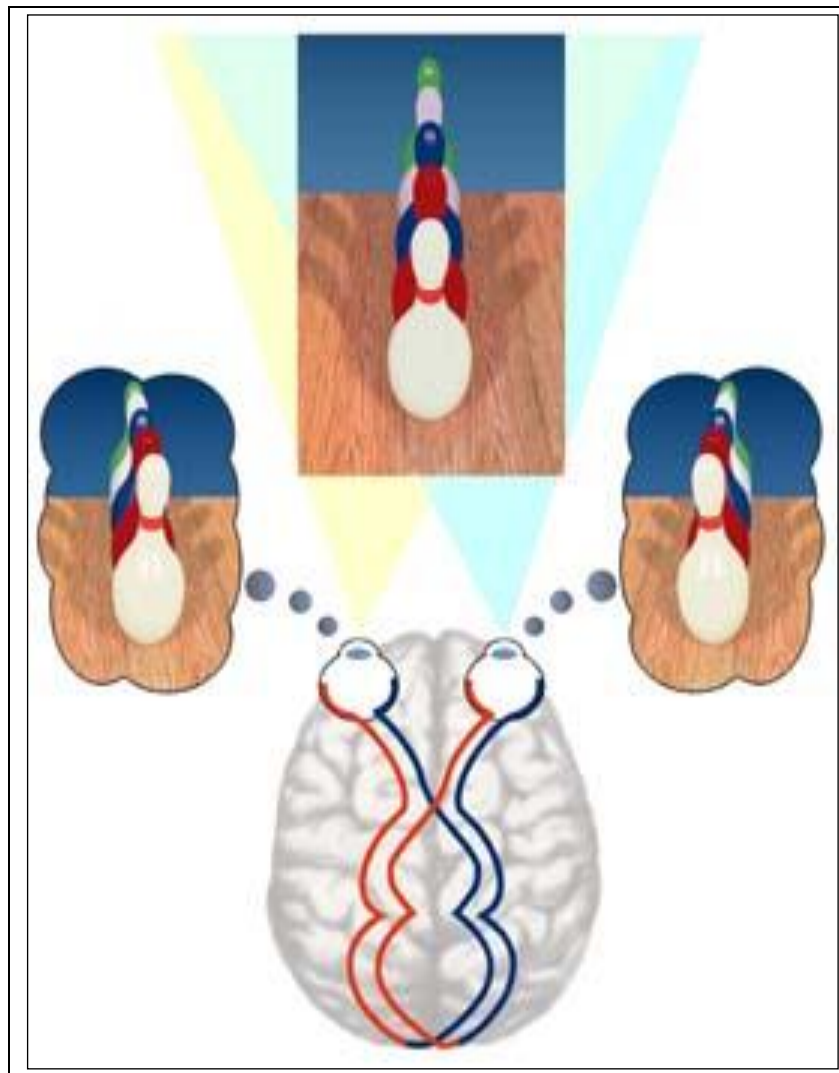


Figure 2.1: Stereoscopic vision. Two images viewed are merged together to form a 3D image (<http://www.vision3d.com/stereo.html>)

2.4 Principles of a lens camera

With a lens camera, a lens optical system is used to project the image on an image plane. In a lens camera, depth of view is important as all objects are not in focus with a lens.

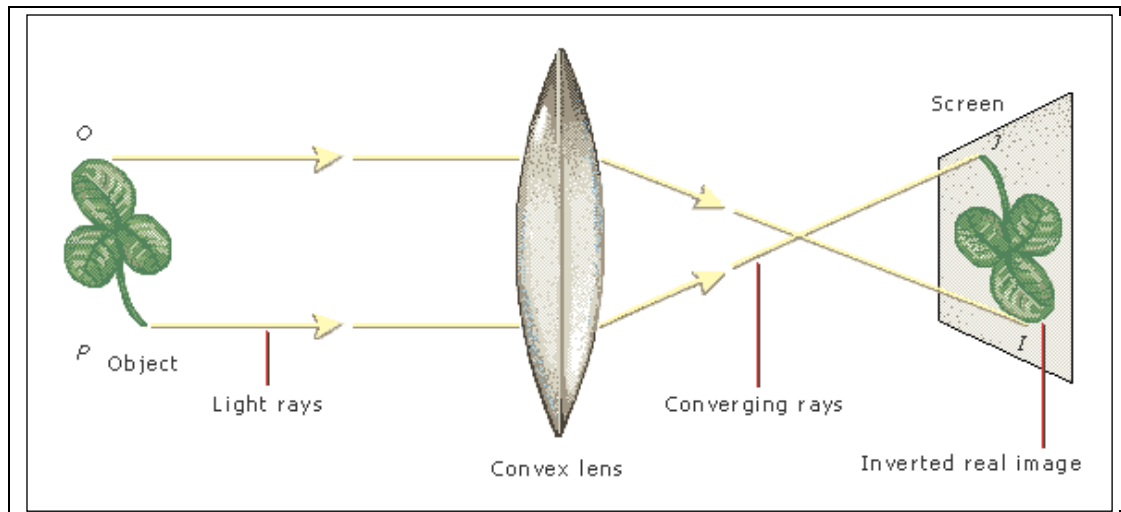


Figure 2.2: Image projected on a screen through a convex lens
(Microsoft Encarta Encyclopedia, 2003)

The focal points of the lens must also be taken in consideration as the light of the object is projected onto the image plane. To obtain a focused image, the lens is adjusted. Some cameras can have multiple lenses and can also have mirrors to ensure the best colour and image is captured.

The capturing screen of a camera can be an electronic flat panel device. The position of the electronic flat panel is normally fixed in the camera and the lens is adjusted to ensure the image is in focus. With a lens camera, the shutter opening, the refractive index of the lens and the light path from the object to the image as well as the position of the image plane all contribute to ensure the image is in focus.

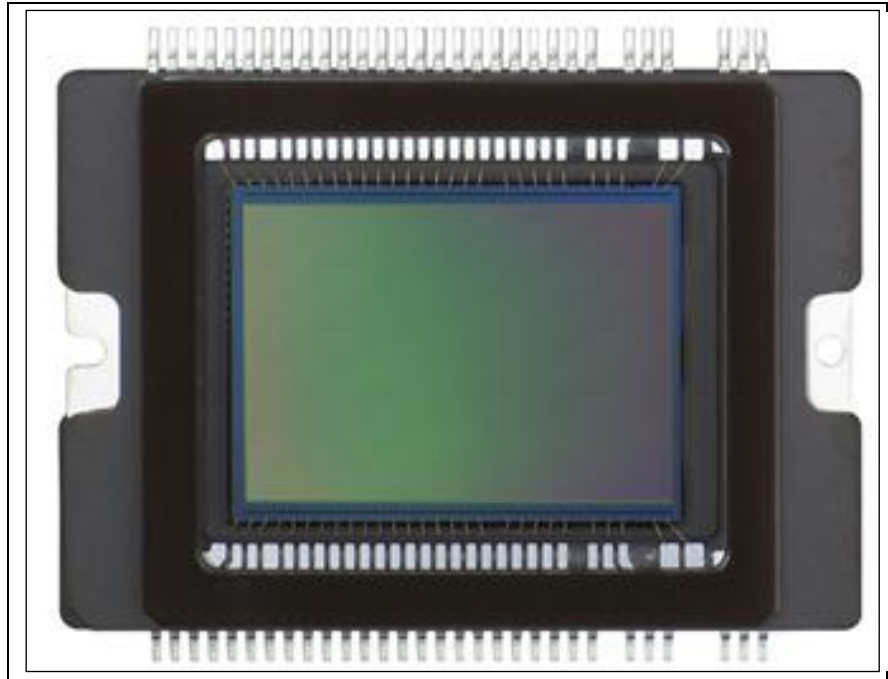


Figure 2.3: An electronic flat panel sensor

[\[http://inphotos.org/tag/canon/\]](http://inphotos.org/tag/canon/)



Figure 2.4: Display the internal structure of a camera

[\[http://inphotos.org/tag/canon/\]](http://inphotos.org/tag/canon/)

2.5 Principles of a pinhole camera

The principle of a pinhole camera is that light passes from an object through a pinhole to the image plane (Anderson. 2008). The resulted image is inverted as depicted in figure 2.5.

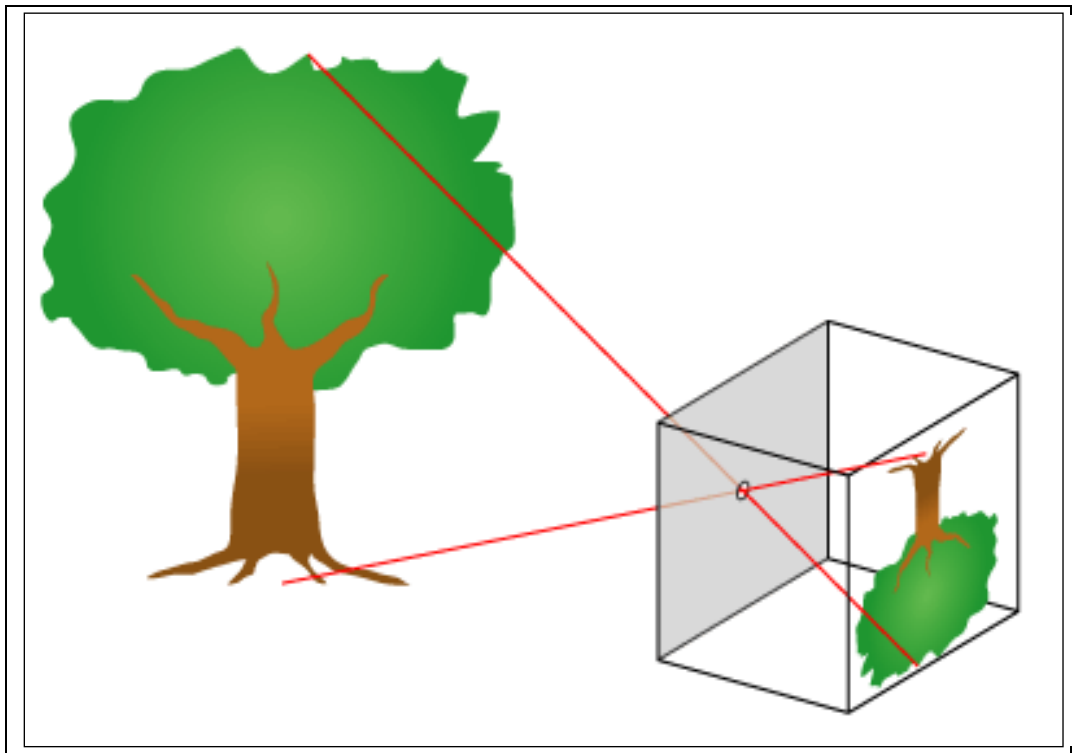


Figure 2.5: Principle of a pinhole camera
[www.techdigest.tv/Pinhole-camera.png]

The image of a pinhole camera can be recorded on a charge couple device (CCD) for electronic applications. The recorded image is upside down and focused because the light rays, which travel in straight lines, do not cross each other inside the box and indicated in the Technology Teacher (2009).

2.6 Characteristics of a pinhole camera

The advantage of using the pinhole is that light only passes through the single point, the pinhole (<http://andrewrreed.com/Writings/curricula/articles-of-potential-interest/pinhole-camera>). The disadvantage is that very little light reaches the image plane and a long exposure time is needed (<http://pinhole-camera.deviantart.com/>). With a pinhole camera, there is nearly infinite depth of view due to that the light only passes through the pinhole

(<http://photo.net/pinhole/pinhole.htm>). Light rays travel in straight lines and if these lines came from an artefact point, it will produce a point on the image plane.

To determine the size of the pinhole the pinhole-to-image plane has to be known. The formula to determine the pinhole size is:

$$d = 1.9\sqrt{f\lambda} \quad (2.1)$$

(<http://andrewreed.com/Writings/curricula/articles-of-potential-interest/pinhole-camera>)

where d is the diameter, f is the focal length (distance from pinhole to sensor plate) and λ is the wavelength of light. The visible spectrum of light is from violet to red as depicted by Adonis & Kahn, 2006. Often the value of the yellow-green spectrum is used which is about 0.00055mm. Cameras with a small aperture act as pinhole cameras (<http://pinhole-camera.deviantart.com/>).

2.7 Summary, pinhole camera

The above methods explain the different methods of projection of an image of an object onto an image plane. Having these images from two different cameras at the same time of the same object, the 3D coordinates can be calculated due to the parallax effect. The parallax effect causes a slight change in position of the object image on the two different projections and using this shifting the 3D coordinates are calculated.

In the following chapter, the use of the parallax effect and the pinhole camera is used to determine the 3D xyz-coordinates of an artefact point.

CHAPTER 3

Stereoscopic imaging with a pinhole camera

3.1 Introduction

The method described to determine the 3D depth is based on stereoscopic vision, using two 2D-images to determine the xyz-coordinates (www.techdigest.tv/Pinhole-camera.png). A method to determine the 3D position of an object is the use of two pinhole cameras that are positioned next to each other as described in figure 3.1. This will result in two different images.

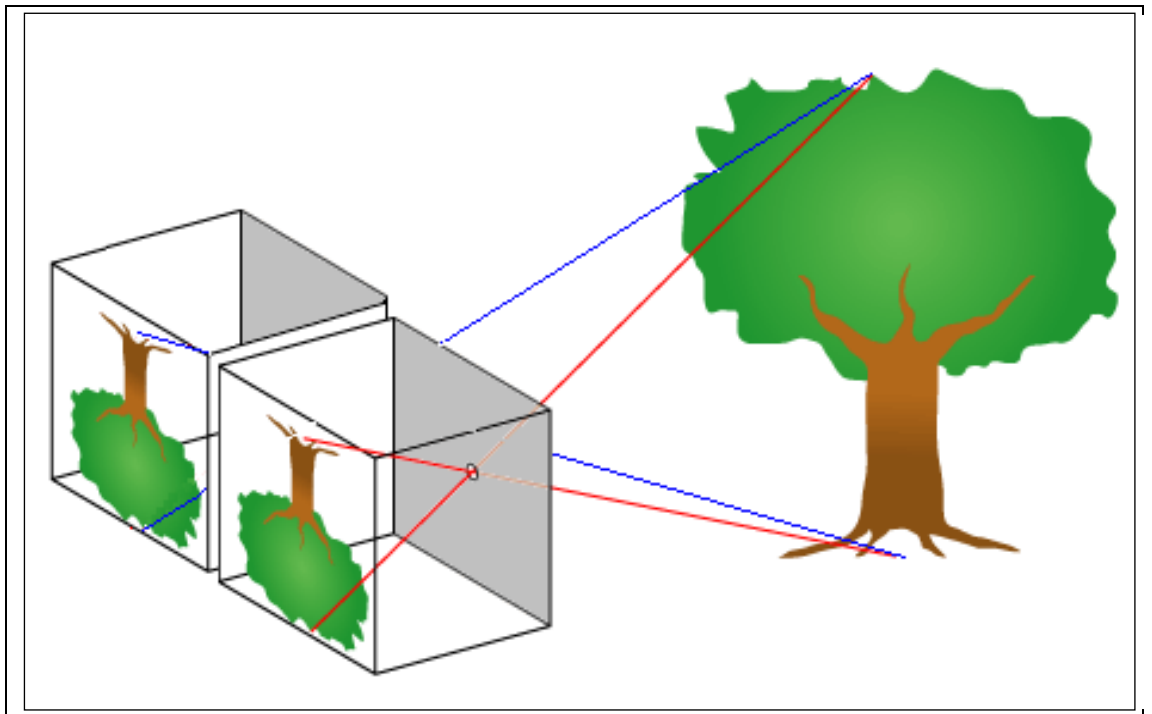


Figure 3.1: Two pinhole cameras are positioned next to each other and two images are obtained from the same object

The characteristics of these two images produced are that due to the different pinhole positions and different image planes, two slightly different images are produced from the same object at the same time. The method is graphically explained in figure 3.2 where an artefact point is projected through two pinhole cameras and different image points are projected on the two image planes. Due to the parallax effect, objects in the distance have a larger shift as objects that are close by to the viewer (Ball et al. 1989:341).

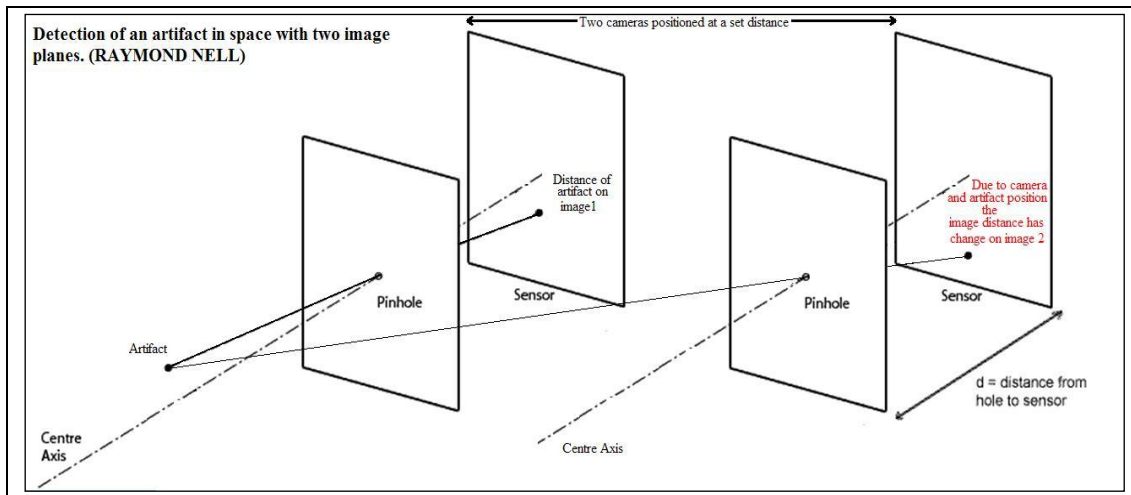


Figure 3.2: A setup to determine the position in space using two image planes with a pinhole opening in front

3.2 Method to determine the 3D-coordinates from 2D images

The method used to determine the 3D xyz-coordinates is the use of a pinhole camera box (two pinhole cameras in a single box setup) with the pinhole positions known. The origin for the calculation and measurement of the artefact position is the right pinhole position. The position is determined with respect to the origin which is as at the right pinhole position.

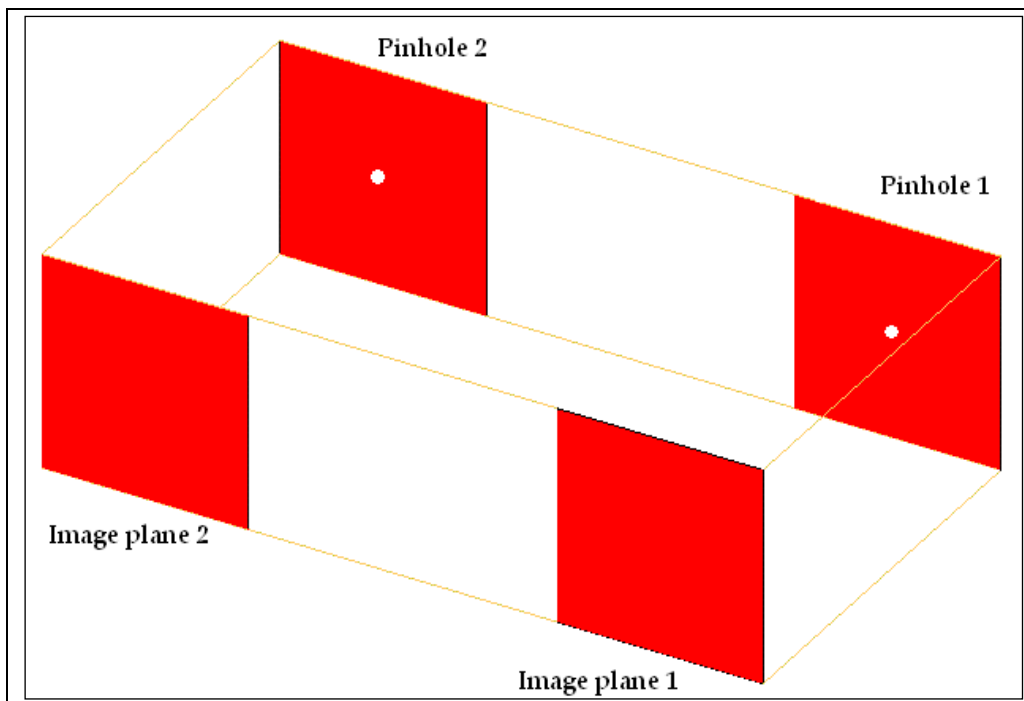


Figure 3.3: The boxtype pinhole cameras setup to produce two pinhole images

To determine the xyz-coordinates of the artefact position, the pinhole, the artefact image as well as the artefact position is given labels from P1 to P5 as displayed in figure 3.4.

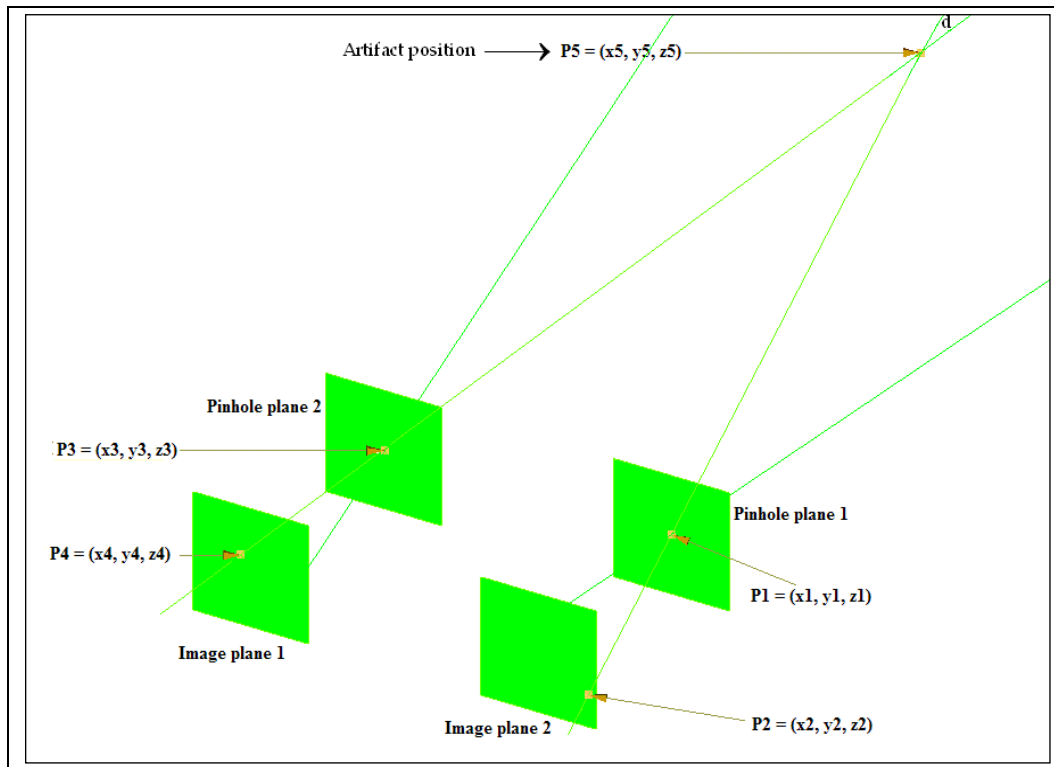


Figure 3.4: The setup of two image planes with two pinhole positions to detect the artefact position

In figure 3.4, the pinhole coordinates of P1 and P3 will be known, and the image position of the artefact that is at points P3, P4 will be determined from the image planes.

The method to determine the xyz-coordinates of the intersecting point is to determine the coordinates of the midpoint of the line segment with the shortest distance between line P1P2 and line P3P4.

If the distance of the shortest line is zero, then the coordinates of the midpoint is the coordinates of the intersecting point.

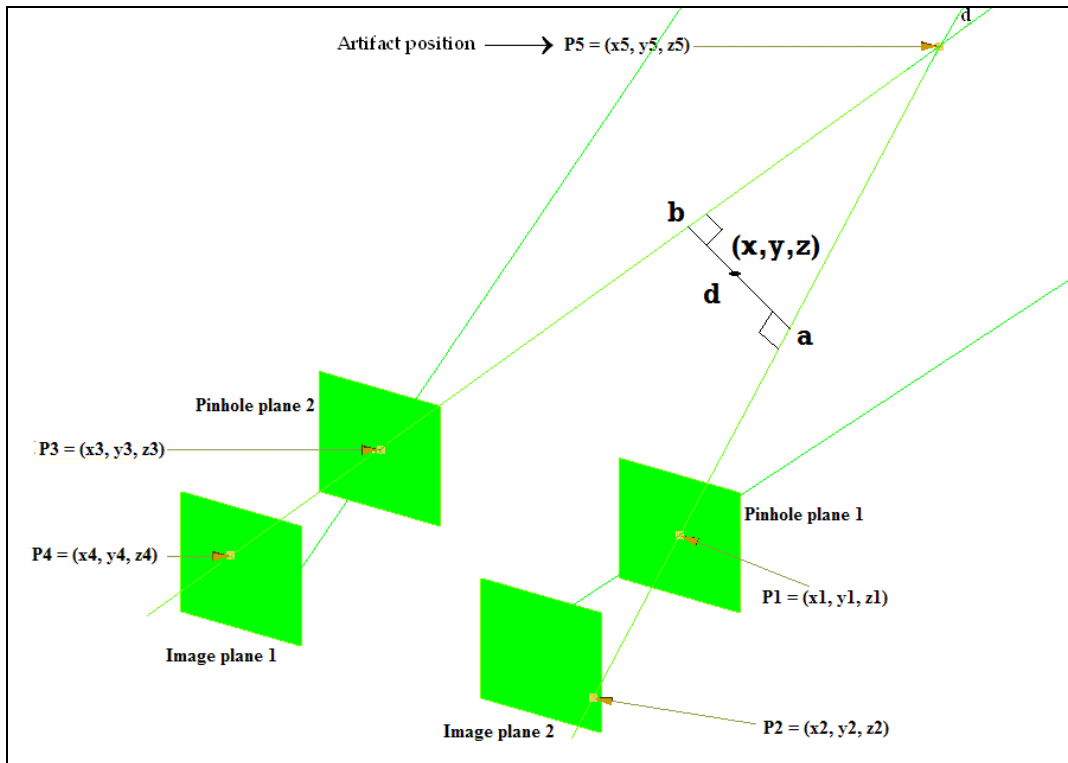


Figure 3.5: The setup to measure the shortest distance between the two lines in 3D

3.3 Mathematical model to determine the intersecting point of two lines in 3D

The following describe the mathematical model of a line in 3D and obtaining the intersection point of the two lines.

Figure 3.6 describes two lines in 3D. As all lines do not intersect in 3D, the xyz-coordinates of the midpoint of the shortest distance between the two lines will be determined.

The length of the shortest line between the two 3D lines will also be calculated. By using this length and if this length is zero, then an intersection point is obtained. Definitions can be inserted; example if the length is less than a hundred of a millimetre, then it can be interpreted as a intersecting point.

The following describe in general the method to determine the xyz-coordinates of the midpoint of the shortest distance between two lines in 3D.

In figure 3.6, the setup to determine the shortest distance between two lines in 3D is depicted.

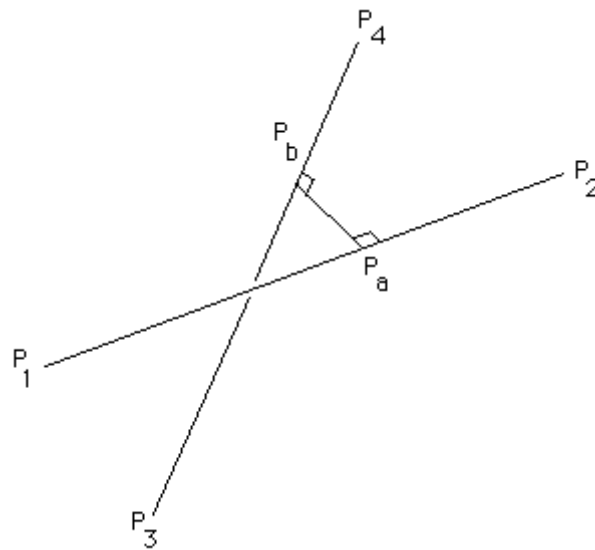


Figure 3.6: Setup to determined the shortest distance between two lines in 3D

An article by Paul Bourke (1998) indicated that if a line segment is described by P_1, P_2 as displayed in figure 3.6, then:

Point “a” (P_a) on line segment P_1P_2 is defined as:

$$P_a = P_1 + \mu_a (P_2 - P_1) \quad (3.1)$$

and point “b” (P_b) is defined as

$$P_b = P_3 + \mu_b (P_4 - P_3) \quad (3.2)$$

The values of μ_a and μ_b are constants, depending on the positions of the points $(P_1, P_2), (P_3, P_4)$ and range from negative to positive infinity and the line segments between P_1, P_2 and P_3, P_4 have their corresponding μ between 0 and 1.

The shortest line segment between the two lines, P_1P_2 and P_3P_4 , will be perpendicular to the two lines as confirmed by Raju (2004). If one line is perpendicular to another line in 3D,

then their dot product is zero. As the line segment is perpendicular to both segments, the dot product of P_aP_b and P_1P_2 is zero as well as P_aP_b and P_3P_4 .

The dot product for the line segments can be written as:

$$(P_a - P_b) \text{ dot } (P_2 - P_1) = 0 \quad (3.3)$$

$$(P_a - P_b) \text{ dot } (P_4 - P_3) = 0 \quad (3.4)$$

Expanding these give the equation

$$(P_1 - P_3 + \mu_a (P_2 - P_1) - \mu_b (P_4 - P_3)) \text{ dot } (P_2 - P_1) = 0 \quad (3.5)$$

$$(P_1 - P_3 + \mu_a (P_2 - P_1) - \mu_b (P_4 - P_3)) \text{ dot } (P_4 - P_3) = 0 \quad (3.6)$$

Expanding these in terms of the coordinates the result is as follows

$$d_{1321} + \mu_a d_{2121} - \mu_b d_{4321} = 0 \quad (3.7)$$

$$d_{1343} + \mu_a d_{4321} - \mu_b d_{4343} = 0 \quad (3.8)$$

with

$$d_{1343} = ((x_1 - x_3)(x_4 - x_3)) + ((y_1 - y_3)(y_4 - y_1)) + ((z_1 - z_3) - (z_4 - z_3)) \quad (3.9)$$

$$d_{4321} = ((x_4 - x_3)(x_2 - x_1)) + ((y_4 - y_3)(y_2 - y_1)) + ((z_4 - z_3) - (z_2 - z_1)) \quad (3.10)$$

$$d_{1321} = ((x_1 - x_3)(x_2 - x_1)) + ((y_1 - y_3)(y_2 - y_1)) + ((z_1 - z_3) - (z_2 - z_1)) \quad (3.11)$$

$$d_{4343} = ((x_4 - x_3)(x_4 - x_3)) + ((y_4 - y_3)(y_4 - y_3)) + ((z_4 - z_3) - (z_4 - z_3)) \quad (3.12)$$

$$d_{2121} = ((x_2 - x_1)(x_2 - x_1)) + ((y_2 - y_1)(y_2 - y_1)) + ((z_2 - z_1) - (z_2 - z_1)) \quad (3.13)$$

where

$$d_{mnop} = (x_m - x_n)(x_o - x_p) + (y_m - y_n)(y_o - y_p) + (z_m - z_n)(z_o - z_p) \quad (3.14)$$

but

$$d_{mnop} = d_{opmn} \quad (3.15)$$

then mu_a is:

$$mu_a = \frac{d_{1343}d_{4321} - d_{1321}d_{4343}}{d_{2121}d_{4343} - d_{4321}d_{4321}} \quad (3.15)$$

By substituting mu_a in:

$$d_{1343} + mu_a d_{4321} - mu_b d_{4343} = 0 \quad (3.16)$$

gives

$$mu_b = \frac{d_{1343} + mu_a d_{4321}}{d_{4343}} \quad (3.17)$$

Then by inserting (mu_a) and (mu_b) into equations:

$$P_a = P_1 + mu_a (P_2 - P_1) \quad (3.18)$$

and

$$P_b = P_3 + \mu_{b_3} (P_4 - P_3) \quad (3.19)$$

with

$$x_a = P_a(x) \quad y_a = P_a(y) \quad z_a = P_a(z)$$

and

$$x_b = P_b(x) \quad y_b = P_b(y) \quad z_b = P_b(z)$$

gives the xyz-coordinates of point(a) and point(b) as:

Point(a):

$$(x_a, y_a, z_a) = (P_a(x), P_a(y), P_a(z)) \quad (3.20)$$

Point(b):

$$(x_b, y_b, z_b) = (P_b(x), P_b(y), P_b(z)) \quad (3.21)$$

then

$$(x_a, y_a, z_a) = (x_1, y_1, z_1) + \mu_{a_1} ((x_2, y_2, z_2) - (x_1, y_1, z_1)) \quad (3.22)$$

$$(x_b, y_b, z_b) = (x_3, y_3, z_3) + \mu_{b_3} ((x_4, y_4, z_4) - (x_3, y_3, z_3)) \quad (3.23)$$

P_a describes the xyz-coordinates of point (a) and

P_b describes the xyz-coordinates of point (b) in figure 3.

3.4 Determine the distance of the shortest line

Bester, et. al. (1998, page 374), explained if the coordinates of two points are available, then the distance formulae can be used to determine the distance between these two points.

$$d_{ab} = \sqrt{(x_a - x_b)^2 + (y_a - y_b)^2 + (z_a - z_b)^2} \quad (3.24)$$

and the xyz-coordinates of the midpoint (x_{ab} , y_{ab} , z_{ab}) are:

$$x_{ab} = \frac{(x_a + x_b)}{2} \quad (3.25)$$

$$y_{ab} = \frac{(y_a + y_b)}{2} \quad (3.26)$$

$$z_{ab} = \frac{(z_a + z_b)}{2} \quad (3.27)$$

From equation 3.22 and equation 3.23 with mu_a and mu_b describe in equation 3.15 and equation 3.17 gives:

$$x_a = \left(x_1 + \left(\frac{(((d1343)(d4321)) - ((d1321)(d4343)))}{(((d2121)(d4343)) - ((d4321)(d4321)))} \right) (x_2 - x_1) \right) \quad (3.28)$$

$$x_b = \left(x_3 + \left(\frac{\left(\left(\frac{d1343 + d4321 \left(\frac{(((d1343)(d4321)) - ((d1321)(d4343)))}{(((d2121)(d4343)) - ((d4321)(d4321)))} \right)} \right)}{d4343} \right) (x_4 - x_3) \right) \right) \quad (3.29)$$

$$y_a = y_1 + \left(\left(\frac{(((d1343)(d4321)) - ((d1321)(d4343)))}{(((d2121)(d4343)) - ((d4321)(d4321)))} \right) (y_2 - y_1) \right) \quad (3.30)$$

$$y_b = y_2 + \left(\left(d1343 + \frac{\left((d4321) \left(\frac{\left(\left((d1343) (d4321) \right) - \left((d1321) (d4343) \right)}{\left(\left((d2121) (d4343) \right) - \left((d4321) (d4321) \right)} \right) \right)}{d4343} \right) \right) \right) (y_4 - y_3) \right) \quad (3.31)$$

$$z_a = z_1 + \left(\frac{\left(\frac{\left(\left((d1343) (d4321) \right) - \left((d1321) (d4343) \right)}{\left(\left((d2121) (d4343) \right) - \left((d4321) (d4321) \right)} \right) \right)}{d4343} \right) (z_2 - z_1) \quad (3.27)$$

$$z_b = z_3 + \left(\frac{\left((d1343) + \left((d4321) \left(\frac{\left(\left((d1343) (d4321) \right) - \left((d1321) (d4343) \right)}{\left(\left((d2121) (d4343) \right) - \left((d4321) (d4321) \right)} \right) \right) \right)}{d4343} \right) (z_4 - z_3) \right) \quad (3.32)$$

With

$$d1343 = ((x_1 - x_3)(x_4 - x_3)) + ((y_1 - y_3)(y_4 - y_1)) + ((z_1 - z_3) - (z_4 - z_3)) \quad (3.33)$$

$$d4321 = ((x_4 - x_3)(x_2 - x_1)) + ((y_4 - y_3)(y_2 - y_1)) + ((z_4 - z_3) - (z_2 - z_1)) \quad (3.34)$$

$$d1321 = ((x_1 - x_3)(x_2 - x_1)) + ((y_1 - y_3)(y_2 - y_1)) + ((z_1 - z_3) - (z_2 - z_1)) \quad (3.35)$$

$$d4343 = ((x_4 - x_3)(x_4 - x_3)) + ((y_4 - y_3)(y_4 - y_3)) + ((z_4 - z_3) - (z_4 - z_3)) \quad (3.36)$$

$$d2121 = ((x_2 - x_1)(x_2 - x_1)) + ((y_2 - y_1)(y_2 - y_1)) + ((z_2 - z_1) - (z_2 - z_1)) \quad (3.37)$$

then inserting (P_{ab}) with $P1$, $P2$, $P3$ and $P4$ gives:

$$x_{ab} = \frac{x_a + x_b}{2} \quad (3.38)$$

$$y_{ab} = \frac{y_a + y_b}{2} \quad (3.39)$$

$$z_{ab} = \frac{z_a + z_b}{2} \quad (3.40)$$

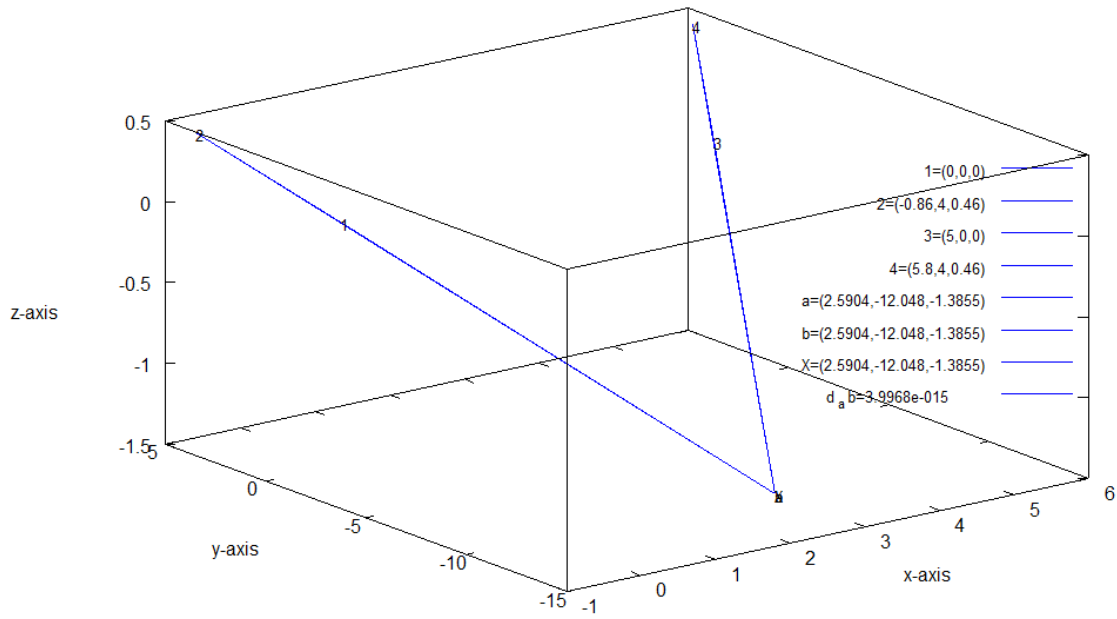
With:

The distance between point (a) and point (b) as:

$$d_{ab} = \sqrt{(x_a - x_b)^2 + (y_a - y_b)^2 + (z_a - z_b)^2} \quad (3.41)$$

3.5 Simulation

To determine the distance between point (a) and point (b), the distance formulae (d_{ab}) is used. MATLAB is an engineering program that can be used for 3D simulation. Figure 3.7 displays a simulation of two lines intersecting in 3D using MATLAB.



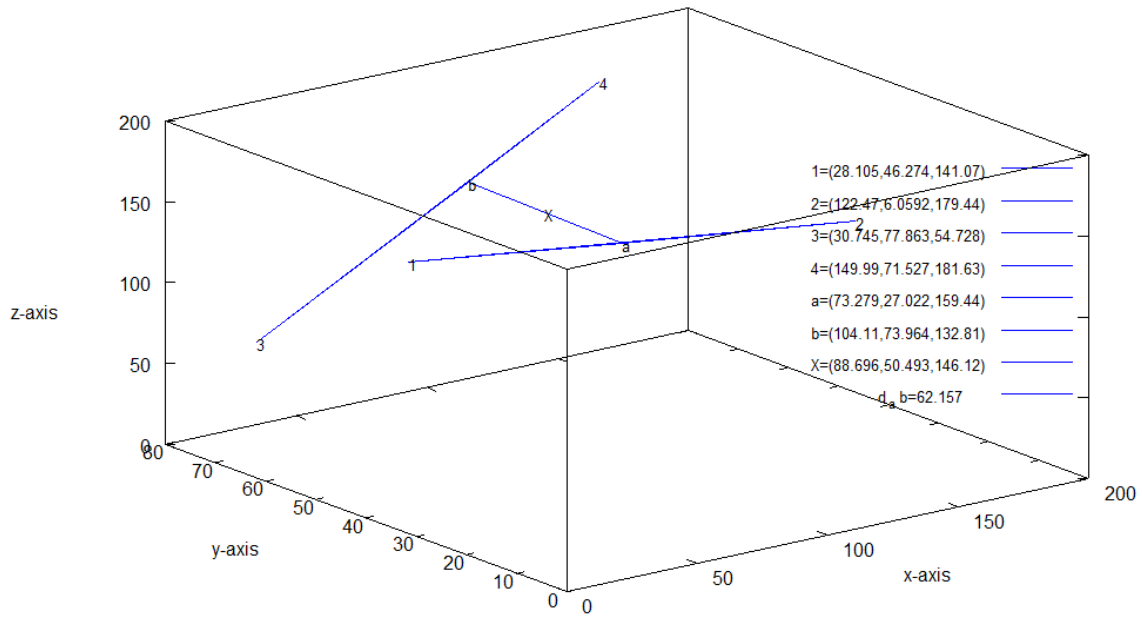
view: 60.0000, 322.500 scale: 1.00000, 1.00000

Figure 3.7: MATLAB simulation of two lines intersect in 3D

Table 3.1: Results of two lines intersect in 3D

	P1	P2	P3	P4	(x,y,z)	d_{ab}	Pa	Pb
x	0	-0.86	5	5.8	2.59	0	2.59	2.59
y	0	4	0	4	-12.05		-12.05	-12.05
z	0	0.46	0	0.46	-1.39		-1.39	-1.39

Also figure 3.8 displays the simulation from MATLAB to indicate the xy-z-coordinates of the shortest distance between two lines in 3D.



view: 60.0000, 322.500 scale: 1.00000, 1.00000

Figure 3.8: MATLAB simulation of two line segments in 3D that do not intersect

Table 3.2: Results of two line segments in 3D that do not intersect

	P1	P2	P3	P4	(x,y,z)	d_{ab}	Pa	Pb
x	28.10	122.47	3.075	149.99	88.70	62.16	73.28	104.11
y	46.27	6.06	77.86	71.53	50.49		27.02	73.96
z	141.07	179.44	54.73	181.63	146.12		149.44	159.44

3.6 Simulation of the 3D pinhole camera method

The following depict a computer simulation to determine the 3D position of an artefact using the two pinhole camera setup.

3.6.1 Method for computer simulation

The method used was to insert the formulae for the xyz-coordinate system into a 3D computer imaging program. The coordinate points on the images planes and the pinhole points were inserted into a mathematical program.

The calculated values for the position of the artefact point are compared with the values determined with the 3D imaging values of the artefact point.

3.6.2 Method for computer simulation

Figure 3.9 displays the computer model with simulation values.

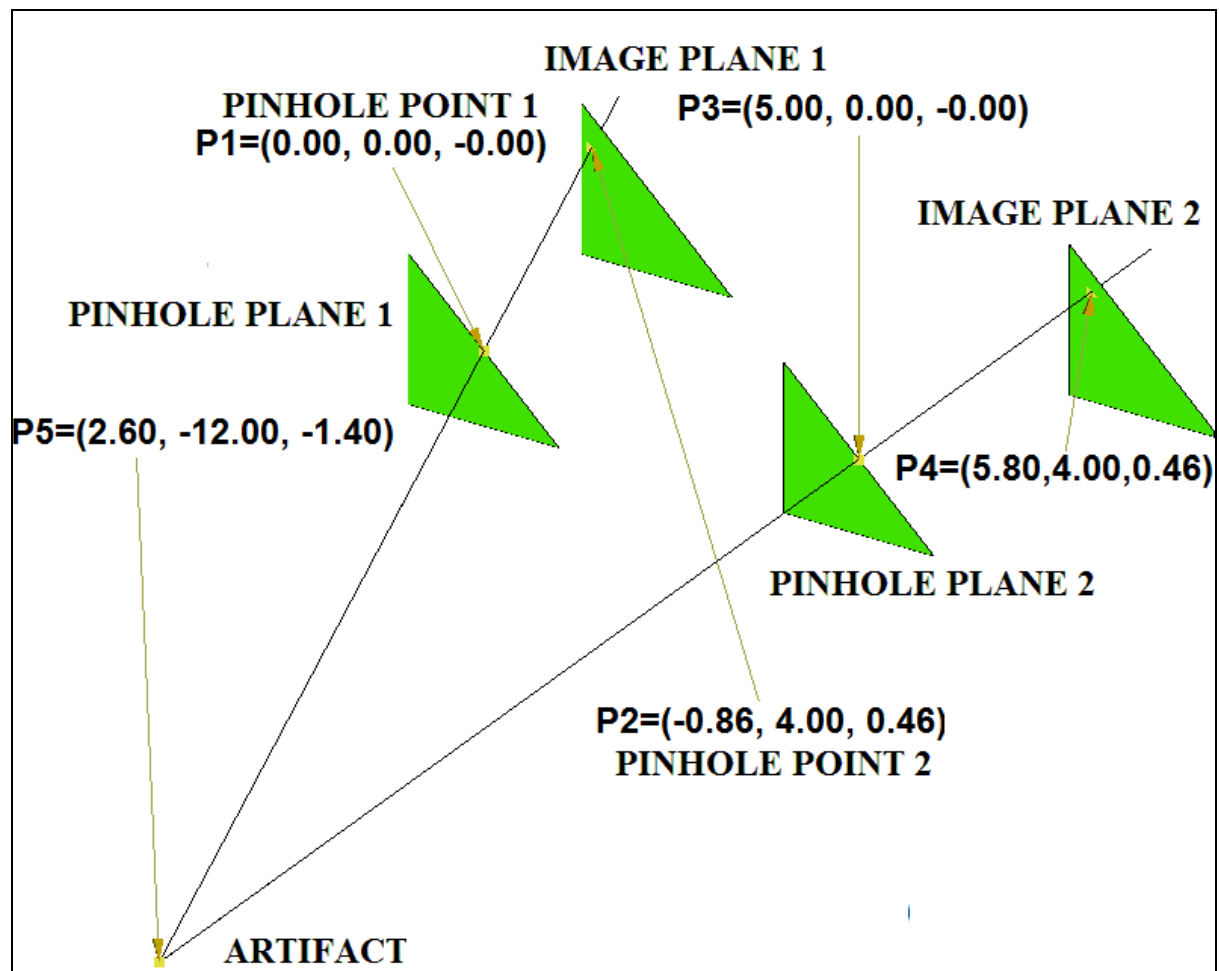


Figure 3.9: Computer model displaying the coordinates of the artefact, pinhole positions as well as the position of the artefact image points on image plane1 and 2

The coordinates of the pinhole positions, the position of the artefact image points on image planes were inserted into the program and the xyz-coordinates were calculated.

Table 3.3: Table with the coordinate values calculated with the formulae

x1	y1	z1	x2	y2	z2	x3	y3	z3	x4	y4	z4	x	y	z
0	0	0	-0.86	4	0.46	5	0	0	5.8	4	0.46	2.59	-12.05	-1.38

The values of the xyz-coordinates were calculated as displayed in table 3.4. These calculated values were compared to the values from the computer model. The calculated results correspond with the values of the graphic simulation program.

Table 3.4: Comparing the calculated values with the computer simulation model

Coordinate	Simulation value	Calculated value
x	2.60	2.59
y	-12.00	-12.05
z	-1.40	-1.38

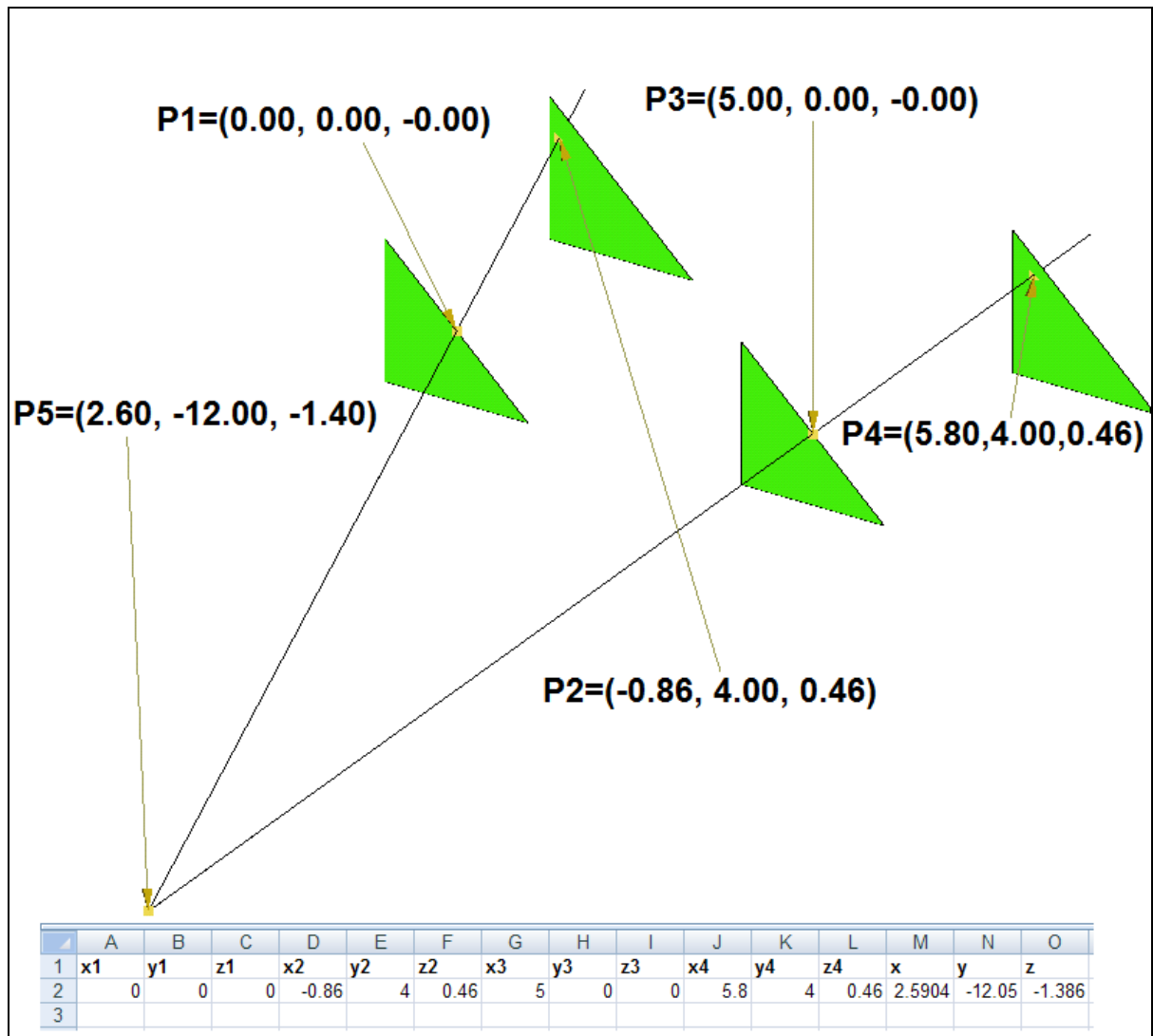


Figure 3.10: The position of the artefact as simulated by the computer model was within the same range as those calculated by the formulae derived

3.7 Experiment to determine the artefact position in space

A practical experiment was done and the formulae to determine the xyz-coordinates were applied in the experiment.

The setup was to position the pinhole camera at position one, the first camera position, a picture of the artefact was taken and then another picture was taken with the pinhole camera at position two. The distance between the two pinhole positions was measured as well as the distance of the pinhole to the image plane.

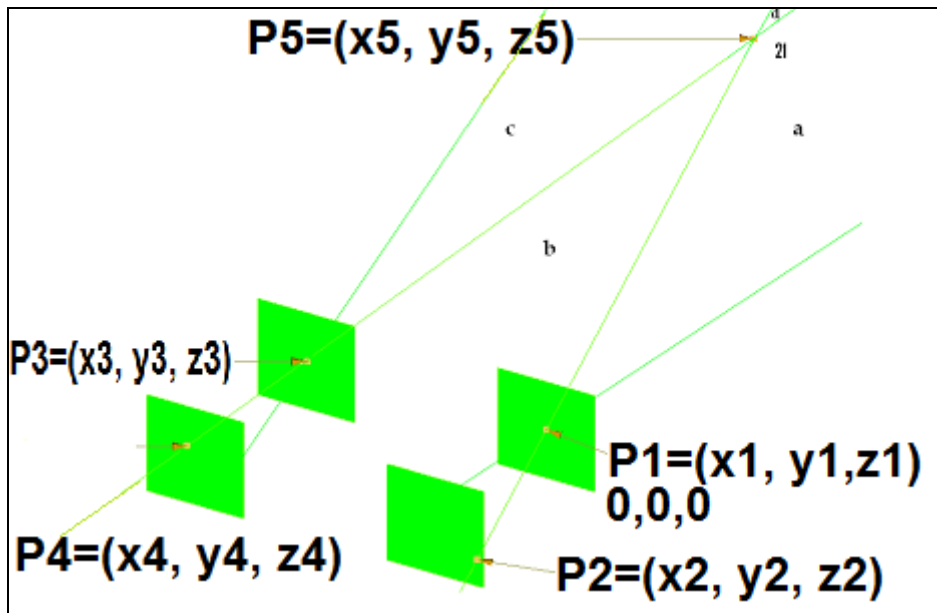


Figure 3.11: Schematic setup position for the experiment with P1 as the origin

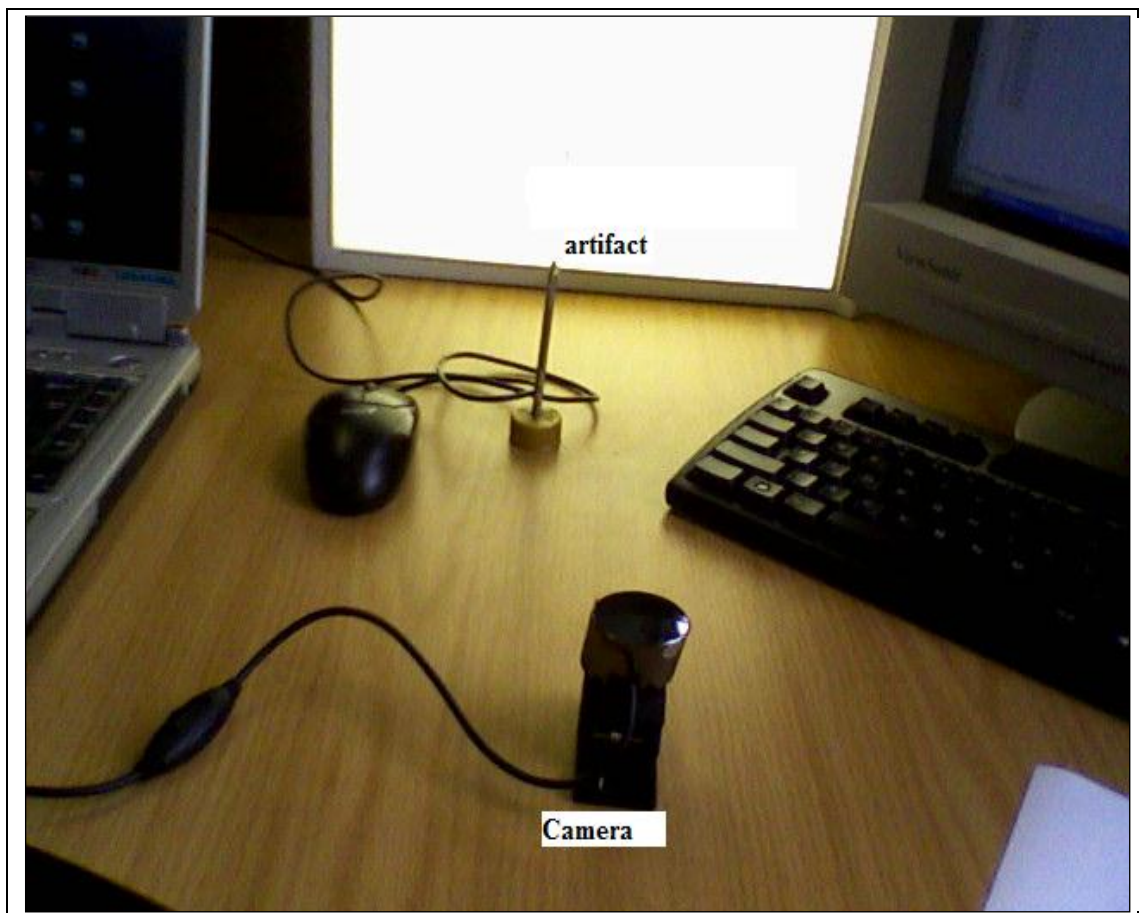


Figure 3.12: The setup position for the experiment with the pinhole camera

3.7.1 The origin of the setup

The origin of the setup was at the position of the right pinhole. The value of the pinhole to image plane was 10mm.

The setup was as projected on figure 3.12. The pinhole positions as per the setup were inserted in the formulae to calculate the artefact position.

From this setup as explained above and depicted in figure 3.12, the two pinhole images were obtained and the artefact image projection were determined from these two 2D images.

3.7.2 The artefact images

In figure 3.13, the artefact image is displayed with the camera at position 1. The image is viewed at a light background and the artefact was a small metal object. The image is inverted as the image is projected through the pinhole.

The sensor size is 4.88mm X 3.64mm. This is a very small sensor size with a pixel value of 640 X 480 pixels. This produces a pixel length size of 0.007625mm for the width and 0.007583mm for the height. The width and height movements are very sensitive due to the small sensor size and this can influence the accurate measurement of the artefact image on the screen.

In figure 3.15, the artefact image is displayed with the camera at position 2. Due to the camera shift, the image has also shifted. The shift in image was obtained and this value is inserted into the formulae to calculate the artefact position.



Figure 3.13: The pinhole artefact image with the camera at the position one

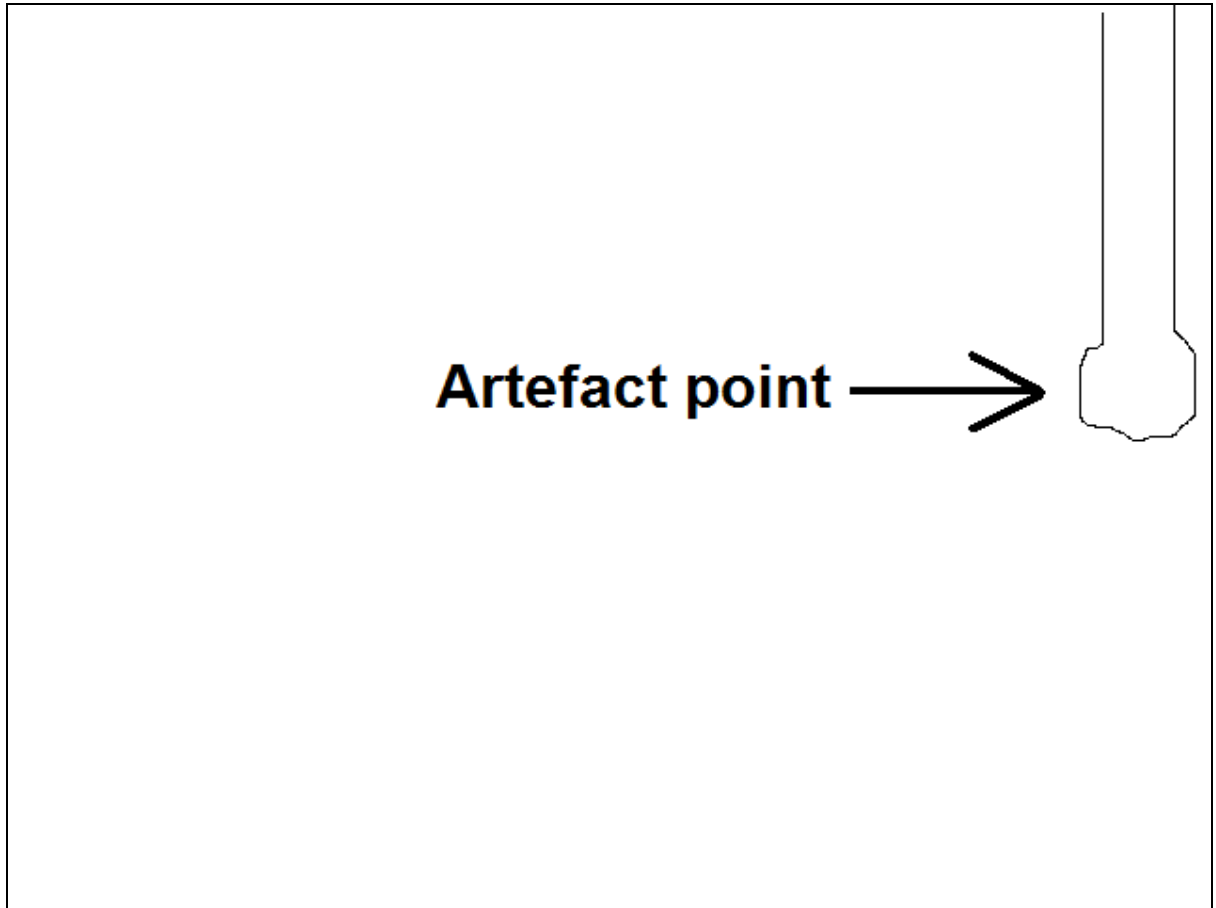


Figure 3.14: Schematic of pinhole artefact image with the camera at the position one



Figure 3.15: The pinhole artefact image with the camera at the position two

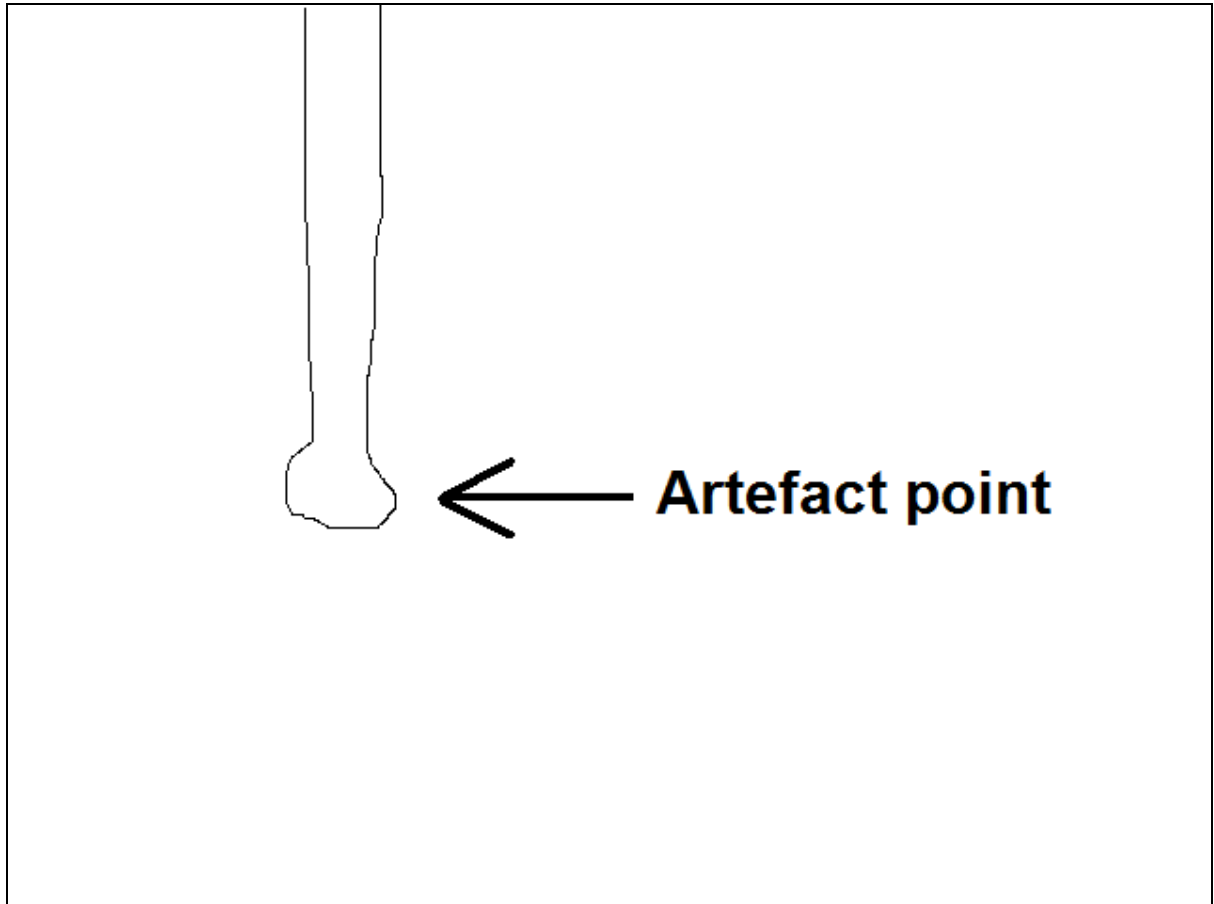


Figure 3.16: Schematic of pinhole artefact image with the camera at the position two

The values of the pinhole positions as well as the positions of the artefact image points were inserted into the formula and the artefact position was calculated.

3.7.3 Application of the formulae to calculate artefact position

As described above, the values of the artefact image points were obtained from each image with the cameras at the two different positions. With the pixel height and length known, the position of the artefact on the image was determined.

Figure 3.17 depict the values inserted of the camera and image model setup.

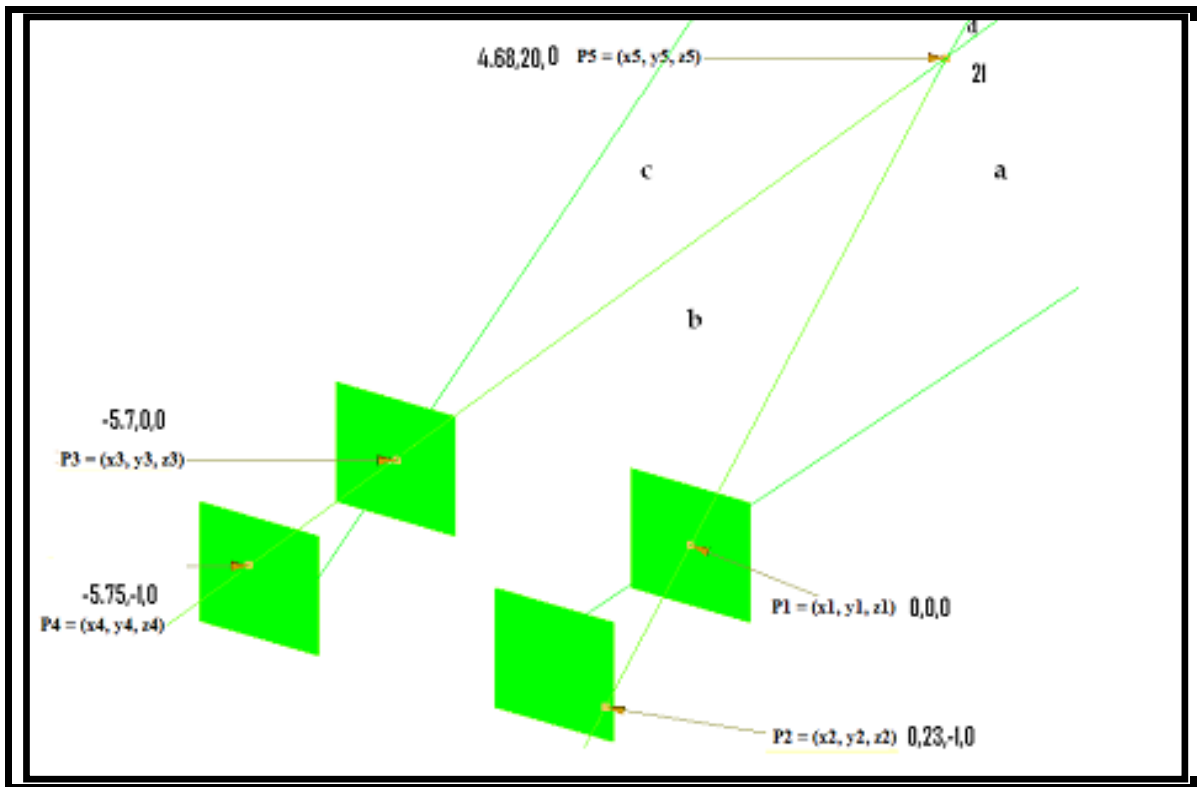


Figure 3.17: The values inserted on the schematic images

Table 3.5 displays the different values inserted as well as the calculated values (x,y,z).

Table 3.5: The pinhole positions, artefact image positions as well as the artefact position calculated

x1	y1	z1	x2	y2	z2	x3	y3	z3	x4	y4	z4	x	y	z
0	0	0	0.23	-1	0	0	0	-5.75	-1	0	0	4.68	20.35	0

3.7.4 Application of the formulae to calculate artefact position

With the setup of the image system, the origin of the visualization system is at the right pinhole camera position. To measure the artefact position, the distance from the right pinhole point to the artefact was measure.



Figure 3.18: The setup to measure the artefact point

The artefact point was measured at 25.3cm as demonstrated in figure 3.19. During the measurement of the artefact position, the artefact must not be disturbed and the measurement must be as accurate as possible.

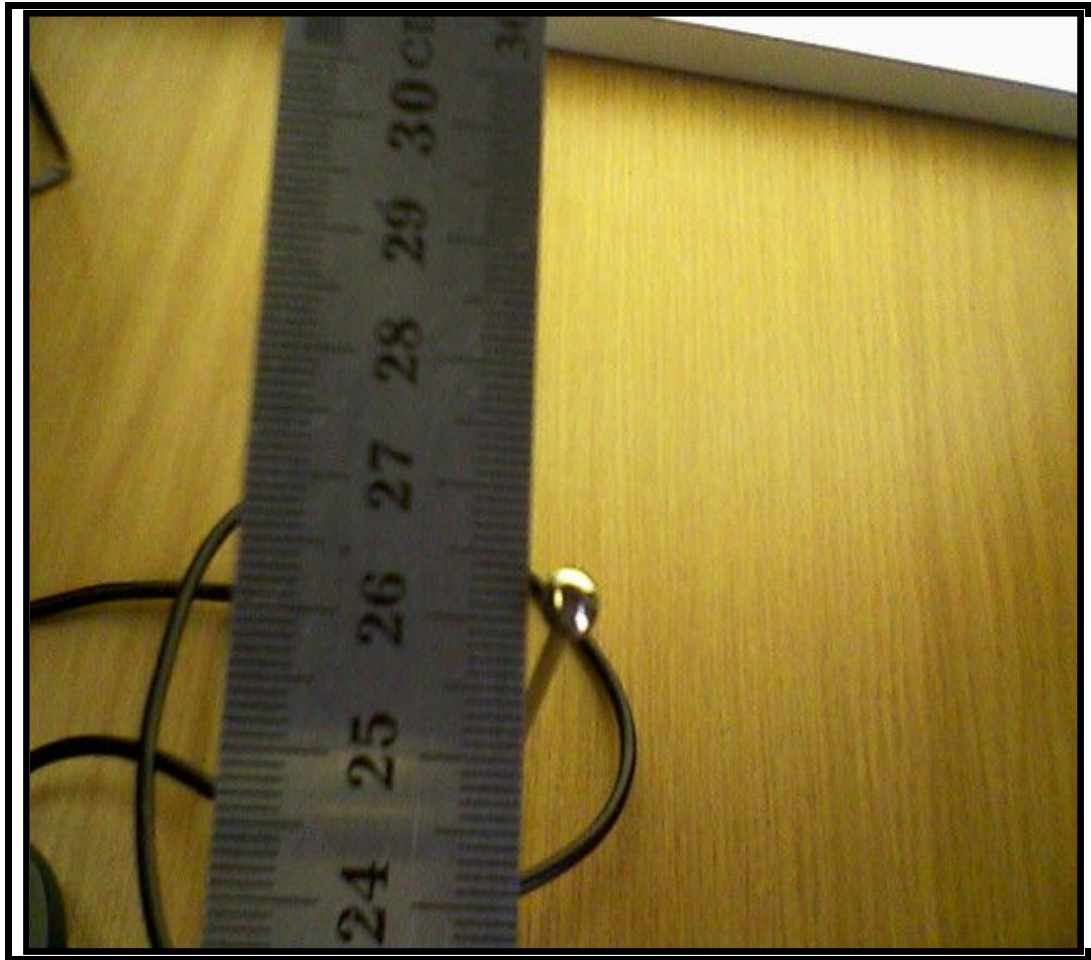


Figure 3.19: The value measured of the artefact

Table 3.6 displays the calculated values with the measured values.

Table 3.6: Comparing the calculated values with the experimental results to determine the position of the artefact

Coordinate	Value as calculated when applying the formulae	Value as measured in experiment
x	4.68	6
y	20.35	25.3
z	0	0

3.7.5 Summary of experimental results

The measurement result was 25.3cm and the calculated result was 20.35cm. The measurement was in the range of 5cm. The difference in the value could be due to the small sensor size, and this in turn has an influence on the calculation of the artefact point.

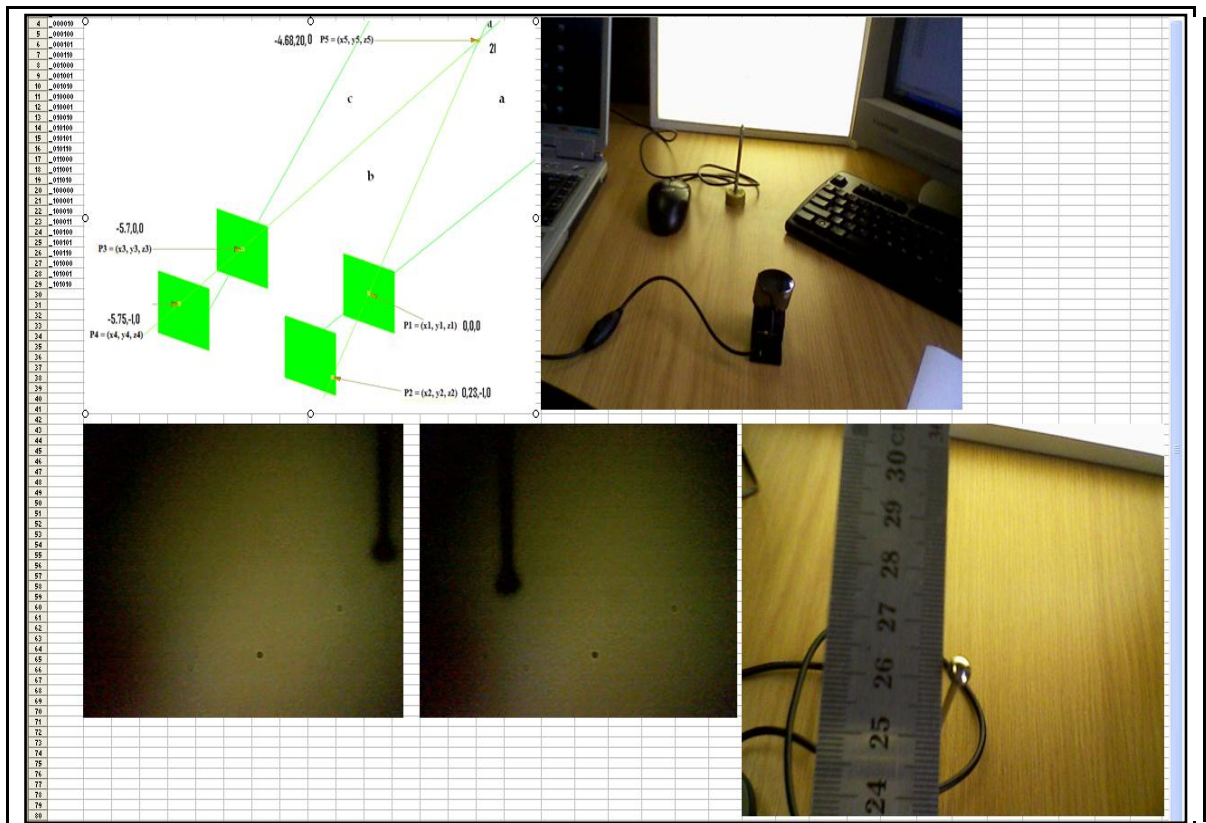


Figure 3.20: Summary of the experiment

3.8 Conclusion of Chapter 3

The position of an artefact point in space was determined using two image planes. Two pinhole camera images were captured. The formulae to determine the xyz-coordinates of the artefact were used and the calculated values were within the range of the measured value in the experiment.

The setup of the pinhole camera system is such that the origin was at the right pinhole position. All other points are determined with reference to the right pinhole position. The coordinates of the right pinhole was determined with the camera setup and the image

position of the artefact point on the two image planes were measured with reference to the right pinhole origin position. The coordinates of the artefact point were given with reference to the right pinhole point.

The benefits in the use of a pinhole camera are that there is nearly infinite depth of view. The pinhole camera method was used to derive the formulae of the image lines which were projected from the artefact point, through the pinhole of the camera and onto the image plane.

As two image planes were used, two image lines were generated from the same artefact point. These two image lines intersect at the artefact point.

The formulae for the xyz-coordinates were derived and these formulae can be inserted into a computer program for real time update of the artefact position in an xyz-coordinate system.

The above explanation and method provide the formulae and application to determine the 3D position of an artefact with two pinhole images. The origin is at the right pinhole position. A practical application is that the artefact can be translated to any origin, rotated around the any axis, translated and rotated or even move in 3D space.

The significance of translation and rotation is that the xyz-coordinates can be transferred to a robotic arm at any origin away from the visualization system and be able to interact with the artefact, example sorting or picking up objects.

CHAPTER 4

A method to determine the 3D xyz-coordinates of an artefact with a single lens image

4.1 Introduction

Three dimensional (3D) depth visualization can provide the ability of electronic devices to interact with objects (Klank. et.al., 2012). Moravec, 2012, from the Robotics institute in Pennsylvania explained that stereoscopic vision is the use of two images to determine the depth of an object. For 3D stereoscopic imaging, two images are viewed of the same object at the same time (DiBiase, 2012). Information from these two images is used to determine the 3D position of an artefact.

This method explained will use a single image to determine the 3D xyz-coordinates of an artefact.

The additional benefit of having 3D-position detection with a single lens image is that image processing can be reduced and still provide the 3D-cordinants of the artefact. Real time localization with 3D reconstruction is of value. In electronics and robotics, this can free up space for additional electronic equipment and instrumentation to be loaded.

With this chapter, a method to determine the 3D xyz-coordinates of an artefact position with a single lens image will be discussed. The mathematical formulae to determine the xyz-coordinates will be provided.

4.2 Characteristics of a lens image

In figure 4.1, a thin lens is described and with a thin lens, the entire deviation of any light ray passing through the thin lens is considered to take place through the centre of the lens (Sears, 1958).

The focal point (f) of the lens is also depicted in figure 4.1. Let (s) be the distance of the object to the centre of the lens and (s') be the distance of image to the centre of the lens.

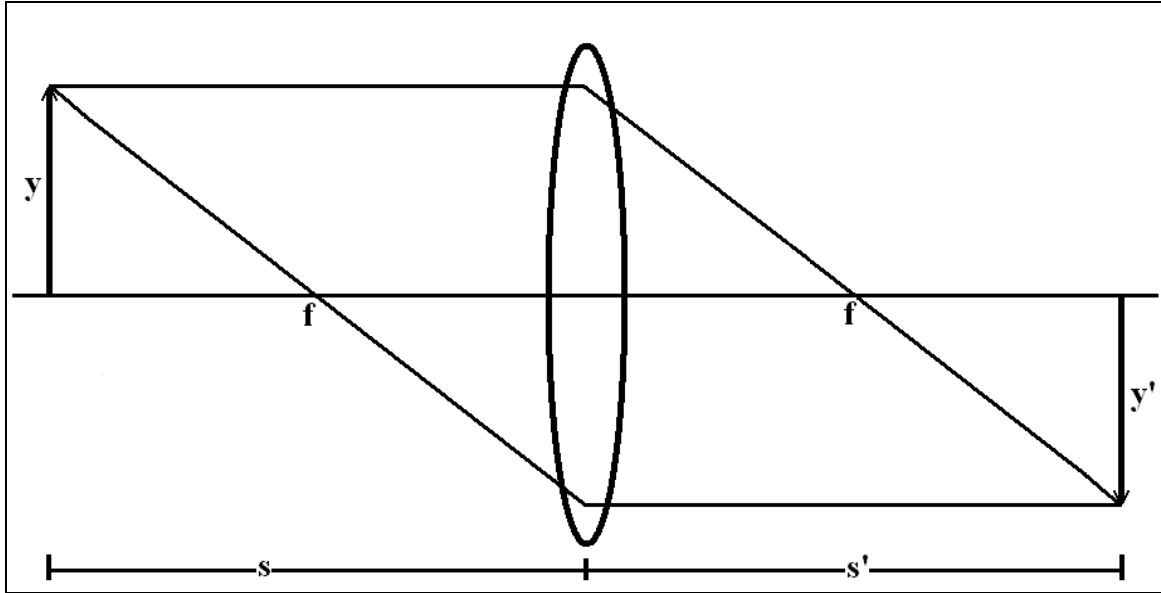


Figure 4.1: Image formation by a thin lens

Equation 4.1 describes the Gaussian form of a lens equation (Dektar, 2012).

$$\frac{1}{s} + \frac{1}{s'} = \frac{1}{f} \quad (4.1)$$

The lateral magnification (m) is described as:

$$m = -\frac{s}{s'} \quad (4.2)$$

Sears also indicated that the lateral magnification is the ratio of y' to y , the length of the object (y) in comparison of the length of the image (y').

Then the lateral magnification (m) can also be described as:

$$m = \frac{y}{y'} \quad (4.3)$$

As depicted in figure 4.1, the height, y' , of the image can be determined from the image on the image plane, and also the distance of the image screen to the centre of the lens (s').

The value of s' is the distance of the image plane to the centre of the lens. The value of y' is the vertical image height from the horizontal centre plane of the lens.

4.3 Determine the object position from centre of lens

By using the Gaussian form of a lens equation described in *equation 4.1*, the object position (s) can be determined from the image position (s') and if the focal point (f) is known.

From equation 4.1 which is:

$$\frac{1}{s} + \frac{1}{s'} = \frac{1}{f}$$

By obtaining (s), rearrange the formula, the object position is determined which is:

$$s = \frac{fs'}{s' - f} \tag{4.4}$$

The value (s) is the distance of the object from the centre of the lens. By only using information of the lens and the image, with *equation 4.4*, the object distance can be determined.

4.4 Determine the height of the object

The method to determine the distance, (s), of the object from the centre of the lens was previously described. Another distance to determine is the height of the object.

This section explains a method to determine the height of the object.

From the two magnifying equations, *equation 4.2* and *equation 4.3*, *equation 4.5* is derived and is also explained by Sears.

$$\frac{y^{(m)}}{y'} = -\frac{s^{(m)}}{s'} \quad (4.5)$$

The aim is to obtain the object height and by rearranging *equation 4.5* to obtain (y) the subject of the formula then:

$$y = -s \left(\frac{y'}{s'} \right) \quad (4.6)$$

But (s) as per *equation 4.4* which is:

$$s = \frac{fs'}{s' - f}$$

Inserting *equation 4.4* into *equation 4.6* gives the height of the object.

Then the height of the object is:

$$y = \frac{fy'}{f - s'} \quad (4.7)$$

Figure 4.7 displays the formulae for the height (y) of the object.

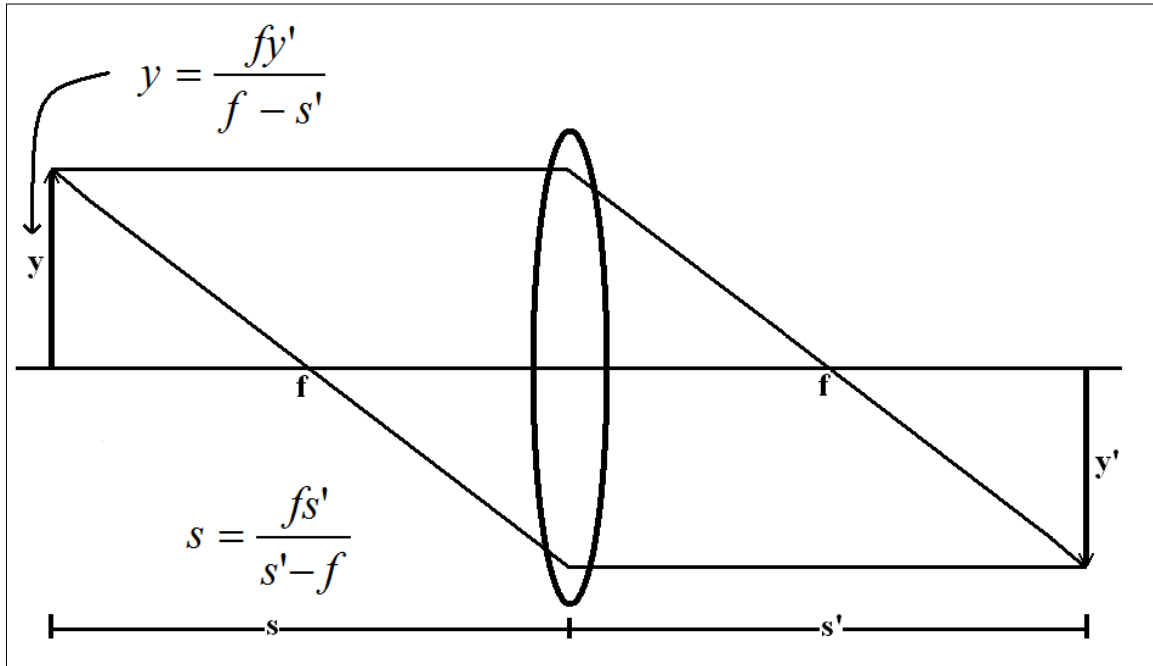


Figure 4.2: The formulae to determine the object height and object distance

4.5 Example: Extract from example in Sears page 95

A thin lens of focal length 20cm project an inverted image 6cm tall on an image screen that is 60cm to the right of a thin lens. Determine the object height and distance of the object to the left of the lens.

The object height is determined using *equation 4.7* which is:

$$y = \frac{fy'}{f - s'}$$

Inserting the focal length (20cm) and image size (6cm) gives an object height of 3cm.

The object distance is determined using *equation 4.4* which is:

$$s = \frac{fs'}{s' - f}$$

Inserting the focal length (20cm) and image distance (60cm) gives an object distance of 30cm.

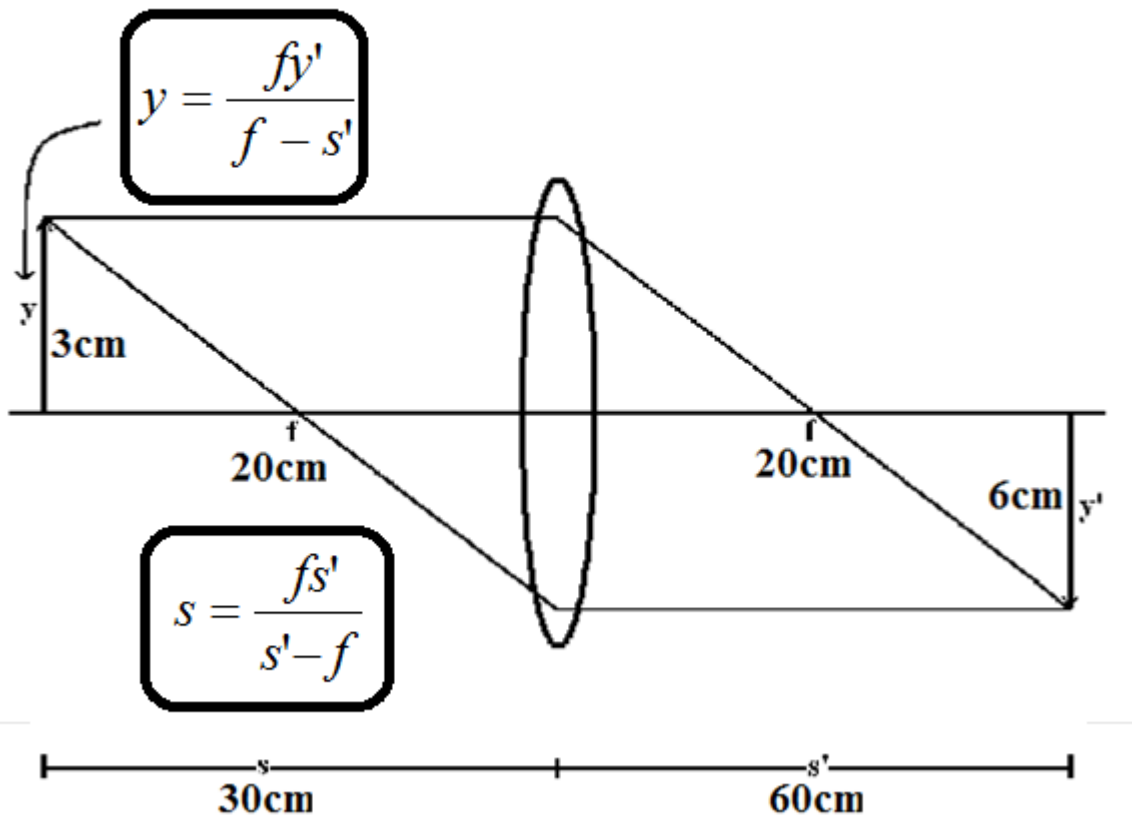


Figure 4.3: Example to determine the object height and object distance

4.6 Determine the 3D xyz-coordinates

A lens displays a 2D image of a 3D object. The object is viewed on an image plane and the object has to be in focus to produce a clear image. Only a thin layer of the object will be in focus with the lens, producing a clear focused image. With modern cameras, a wider range of depth is displayed in an acceptable focus image.

To determine the 3D xyz-coordinates, the imaging method described by Sears where the vertical point of an object is displayed in focus on the image plane is used. If only a point is considered, then with the point in focus, the 3D xyz-coordinates of the point can be calculated

Figure 4.4 displays the 3D-coordinates of an image displayed through a lens onto an image plane.

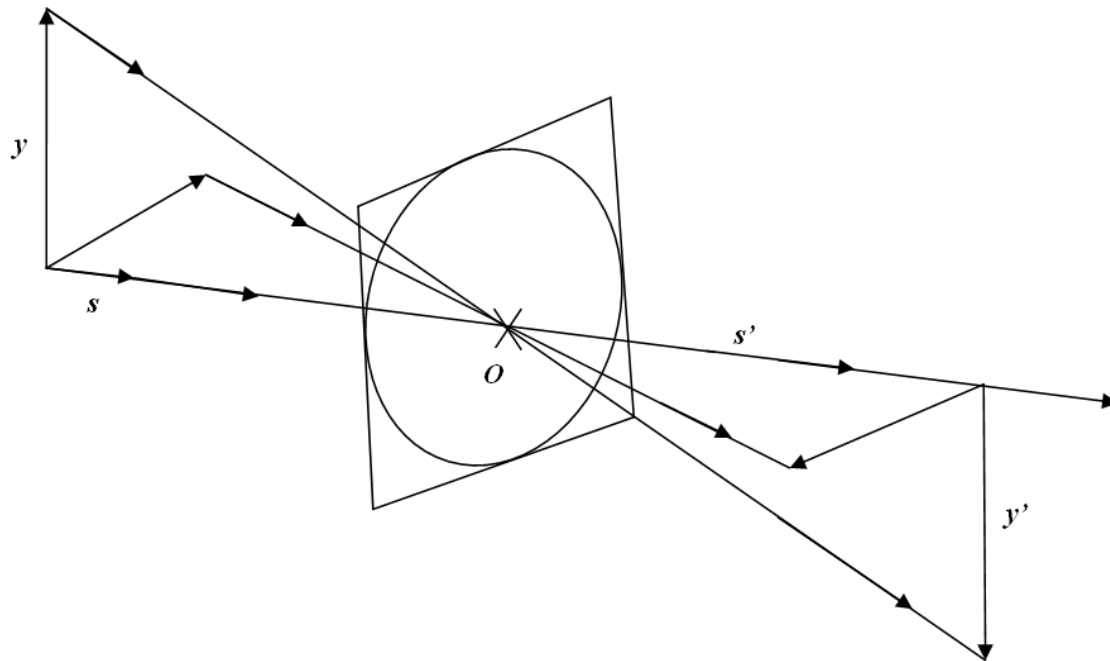


Figure 4.4: Display the object distance (s) and object height (y) in 3D format

By applying the formulae to determine the object distance and the object height in 2D format in the 3D setup, the 3D coordinates can be determined.

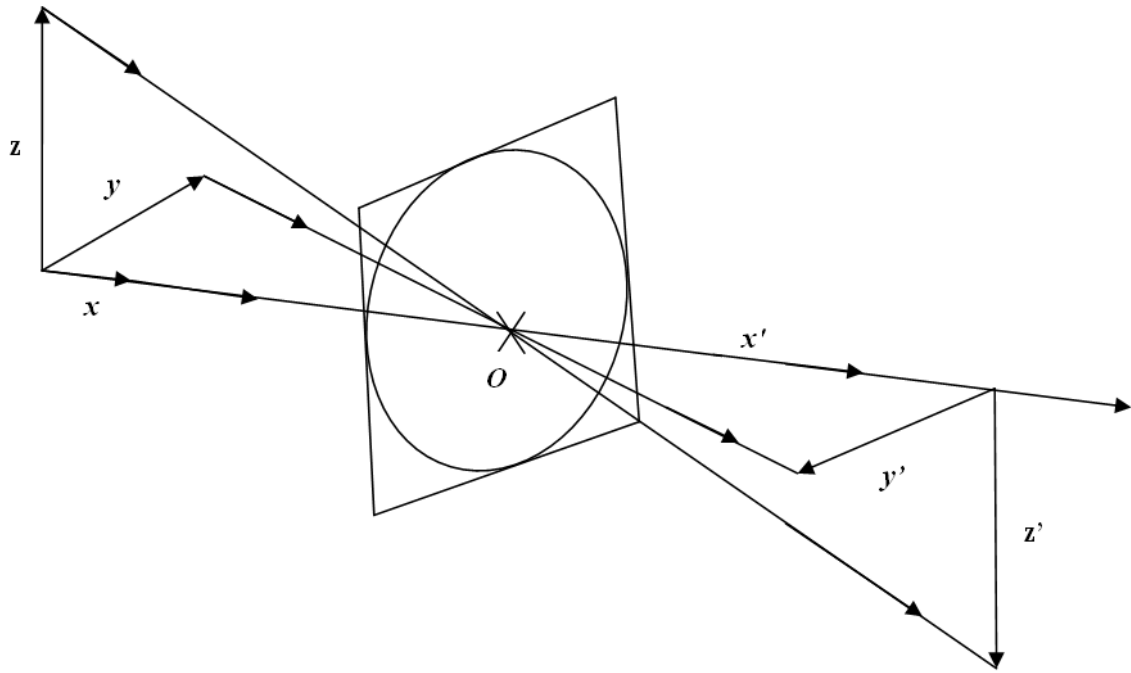


Figure 4.5: Display the 3D xyz-coordinates in a 3D lens setup

4.7 Determine the x-coordinate

To determine the 3D xyz-coordinates of an object, the origin of the system is at the centre point of the lens as depicted in figure 4.5.

The distance of the object to the lens is the *x-value* of the artefact point. By substituting (*s*) with *x* in equation 4.4, the *x-coordinate* of the artefact point is calculated.

The formula for the *x-value* is:

$$x = \frac{fx'}{x' - f} \quad (4.8)$$

The origin of the system is at the centre point of the lens as depicted in figure 4.5.

4.8 Determine the y-coordinate

The *y-coordinate* is determined by calculating the y-height of the object. By substituting (*y*) with (*y*) and (*y'*) with (*y'*) in equation 4.7, the *y-coordinate* of the artefact point is calculated.

Then the formula for the y-coordinate is:

$$y = -\frac{fy'}{s'-f} \quad (4.9)$$

4.9 Determine the z-coordinate

The z-coordinate is determined by calculating the z-height of the object. By substituting (y) with (z) and (y') with (z') in equation 4.7, the z-coordinate of the artefact point is calculated.

Then the formula for the z-coordinate is:

$$z = -\frac{fz'}{s'-f} \quad (4.10)$$

The above formulae are applicable in determine the xyz-coordinates of an artefact point imaged by a thin lens. Thick lenses, multiple lenses, compound lenses and telescopic lenses are also used to visualize the object and their xyz-coordinates can also be determined.

The following describe a method how to determine the xyz-coordinates of an object imaged with a thick lens, multiple lens system, compound lens system and telescopic lens system.

4.10 Thick lens

In a thick lens, there is a significant difference in diameter between the surfaces of the lens. The Gaussian formulae and the Newtonian formulae also applied to a thick lens, but the principle points of the thick lens have to be determined.

The principle points (H, H') of a lens is described as the first vertical line where the image line interacts with that vertical line. The second principle point is described as the second vertical line where the image line interacts with that vertical line. With the distance between these principle points obtained, the image distance and object distance can be calculated. The image and object distances are calculated from the position of the principle points.

Figure 4.6 displays an image of different thick lenses and figure 4.7 displays the schematic of the thick lens with the focus and principle points.

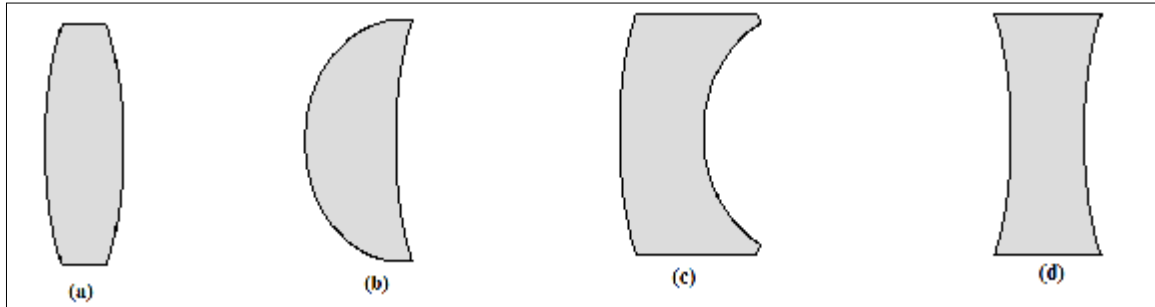


Figure 4.6: Display different types of thick lenses with radii
(a) Double-convex, (b) Meniscus, (c) Meniscus, (d) Double-concave

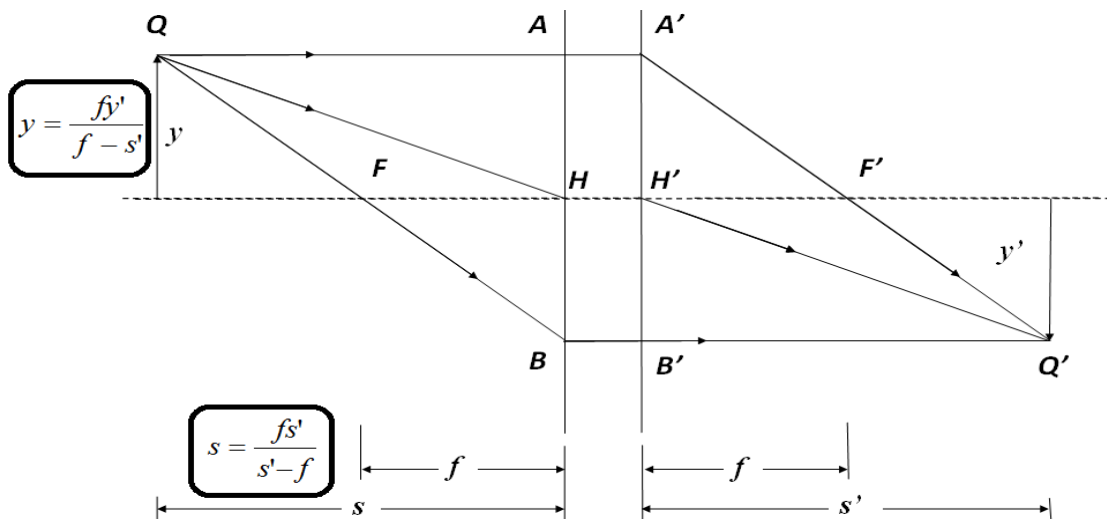





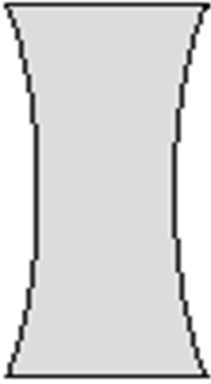
Figure 4.7: Display principle points, H and H', of a thick lens

4.11 Principle points and focal points of different thick lenses

Different types of thick lenses are displayed in Table 4.1. Also displayed in Table 4.1 are the focal lengths, the focal points and the position of the principle points. In this example the axial thickness of each lens is 10mm, the index is 1.50 and the radii of each lens are displayed.

Table 4.1: Display the focal length, focal point and principle points of different thick lenses

Example described in Sears (page: 372)

	Lens 1	Lens 2	Lens 3	Lens 4
				
Radii	$R_1 = +100\text{mm}$ $R_2 = -100\text{mm}$	$R_1 = +100\text{mm}$ $R_2 = +200\text{mm}$	$R_1 = +200\text{mm}$ $R_2 = +100\text{mm}$	$R_1 = -100\text{mm}$ $R_2 = +100\text{mm}$
Focal length	+101.7	+387.1	-413.8	-98.4
Focal point. Distance from first vertex(mm)	$F = -98.3$ $F' = +108.3$	$F = -393.5$ $F' = +384.2$	$F = +427.6$ $F' = -396.9$	$F = +101.6$ $F' = -91.6$
Position of the principle points. Distance from first vertex(mm)	$H = +3.4$ $H' = +6.6$	$H = -6.4$ $H' = -2.9$	$H = +13.8$ $H' = +16.9$	$H = +3.2$ $H' = +6.8$

4.12 Determine the xyz-coordinates of an object with a thick lens

As displayed in figure 4.7, the object distance (s) and the image distance (s') are measured respectively from the first and the second principle points (H, H'). If a thick lens, multiple lens, compound lens or a telescopic lens is used, then the focal point need to be available or calculated to determine the object distance and the object height.

4.13 Formulae to determine the xyz-coordinates with a single image from a thick lens

As depicted in figure 4.7, the object distance (s) is determined from the first principle point in a thick lens. In figure 4.1, the object distance is calculated from the centre of a thin lens. By obtaining a point in the middle of the principle points as reference, then the object distance measured from the centre point between the principle points is:

$$s = \frac{fs'}{s'-f} + \frac{H' - H}{2} \quad (4.11)$$

As from equation 4.11 it is clear that if H and H' coincide as in the case of a thin lens, the formulae to determine the object distance is described by a thin lens.

The magnification formulae of a lens are used to determine the y-coordinate and the z-coordinate. The magnification by a thick lens is described as:

$$m = \frac{y}{y'} \quad (4.11.1)$$

Where (y) is the object height and (y') is the image height.

The formula to determine the y-coordinate and the z-coordinate is as per equation 4.9 and 4.10 namely:

$$y = -\frac{fy'}{s'-f} \tag{4.12}$$

$$z = -\frac{fz'}{s'-f} \tag{4.13}$$

Then the formulae to determine the xyz-coordinates of an artefact point with a single image obtained from a thick lens are:

The x-coordinate is:

$$x = \frac{fs'}{s'-f} + \frac{H' - H}{2} \tag{4.14}$$

The y-coordinate is:

$$y = -\frac{fy'}{s'-f} \tag{4.15}$$

The z-coordinate is:

$$z = -\frac{fz'}{s'-f} \tag{4.16}$$

4.14 Determine the xyz-coordinates of an object with a compound lens

Compound lenses are regarded as multiple lenses positioned in such a way that share the same horizontal axis. Figure 4.8 displays a setup of a compound lens system.

By obtaining the focus point of every lens, the position of the lens in the compound system and the index of the lens, the overall focus point and the principle points of the compound system can be determined.

With the principle points and the focus points available, the formulae to determine the xyz-coordinates as applied in a thick lens can be used to determine the xyz-coordinates in a compound lens.

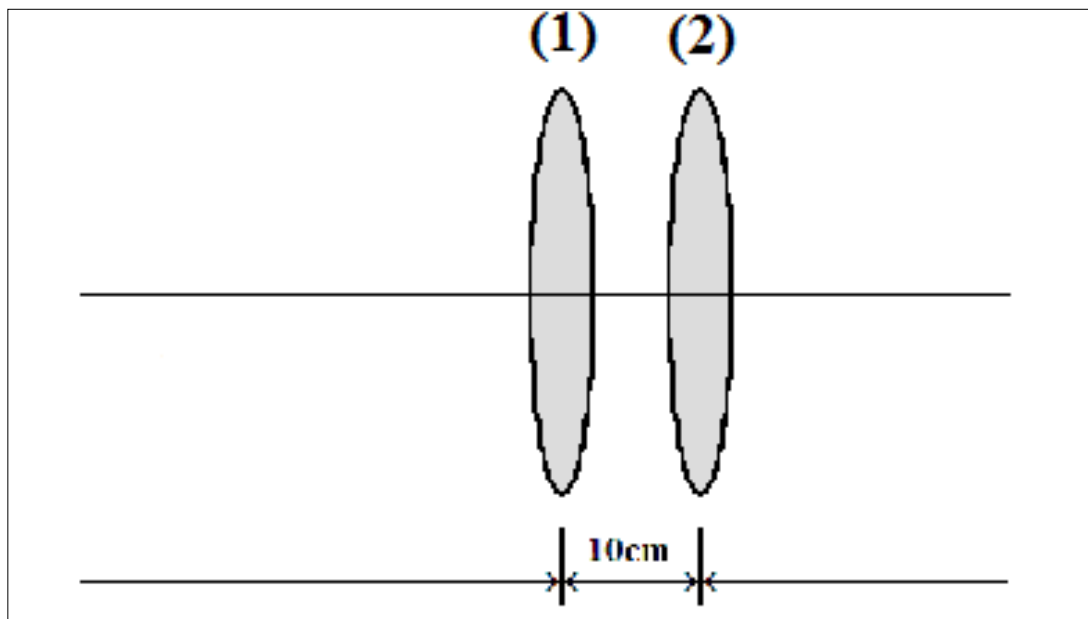


Figure 4.8: A compound lens system with lenses sharing the same horizontal axis

4.15 Determine the xyz-coordinates of compound lens and a telescopic lens

A telescopic lens is a compound lens with multiple lenses in a lens system sharing the same horizontal plane.

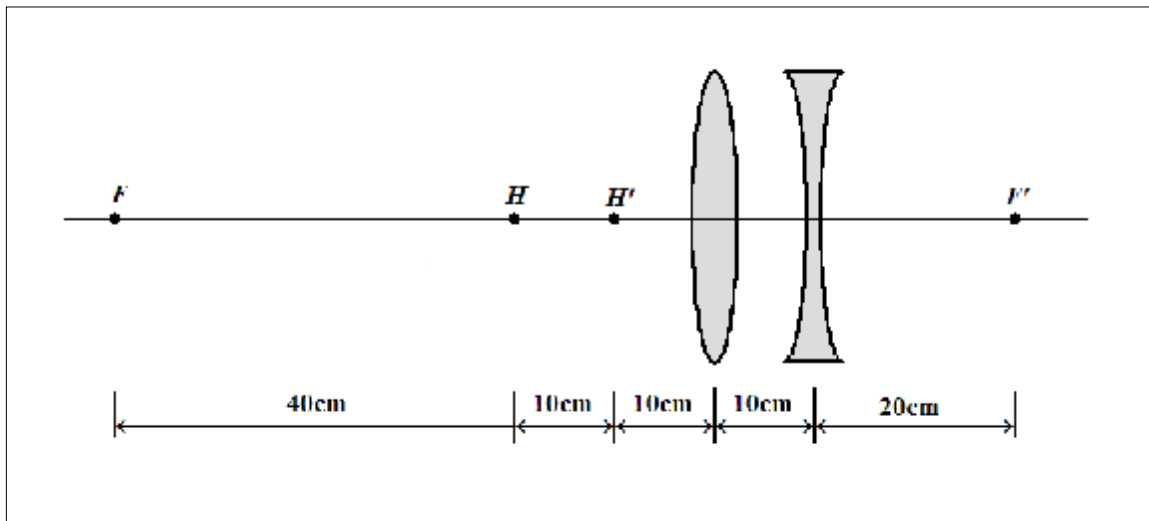


Figure 4.9: A telescopic lens system

The properties of a telescopic lens is that it has a short image distance measured from the lens closest to the image in comparison to the long object distance measured from the lens closest to the object. The setup produces a focused imaged on the focus plane and this property ensures that the camera can be small as a short image distance is required to obtain a focused imaged (Sears, 1958, page: 108).

To obtain the xyz-coordinates from a single image obtain from a telescopic lens system, the formulae used to determine the xyz-coordinates in a thick lens or a compound lens are used. To use the formulae, the principle points and the focus points of the telescopic lens system needs to be determined.

4.16 Limitations to consider

A telescopic lens is a compound lens with multiple lenses in a lens system sharing the same horizontal axis. The formulae derived applicable to a thin lens can be utilized by obtaining the focus points of the lens. When the formulae is applied in a thick, compound or telescopic lens, the principle points as well as the focus points on the lens-system needs to be determined.

To determine the focus points of the lens system, the overall focus point can be calculated if the individual focus points of the lenses are available.

To obtain the principle points of the lens system, the position of every lens in the setup needs to be known or additional equipment need to be used.

The artefact point must not be on the centre axis of the lens.

Additional research needs to be conducted to have practical values in application of the above formulae to determine the xyz-position of an artefact.

4.17 Summary

To determine the xyz-coordinates with a single thin lens image the following formulae have been derived.

The x-coordinate is:

$$x = \frac{fx'}{x' - f}$$

The y-coordinate is:

$$y = -\frac{fy'}{s' - f}$$

The z-coordinate is:

$$z = -\frac{fz'}{s' - f}$$

To determine the xyz-coordinates with a single lens image from a thick lens, compound lens and telescopic lens, the following formulae were derived.

The x-coordinate is:

$$x = \frac{fs'}{s'-f} + \frac{H' - H}{2}$$

The y-coordinate is:

$$y = -\frac{fy'}{s'-f}$$

The z-coordinate is:

$$z = -\frac{fz'}{s'-f}$$

The origin is at the centre of the two principle points.

4.18 Conclusion of chapter 4

The mathematical model to determine the formulae for the 3D xyz-coordinates using only a single image have been derived.

The properties of a lens, the focus point and the magnification formulae were used to determine the coordinates.

In a thick lens, compound and telescopic lens both the focus point and the principle points are used to determine the xyz-coordinates of the artefact point and the magnification formula is also applied.

The method derived provides the opportunity to determine the xyz-coordinates with a single image and if this method is used in robotics, minimal space for products is required.

Having only a single image with an electronic product to determine the 3D xyz-coordinates, processing can be minimized. This in turn free up additional space that can be used for other application in a robotic vision system.

CHAPTER 5

A mathematical model to determine the xyz-coordinates of an object using a linear two camera system

5.1 Introduction

The 3D-position of the object is required when there is a need to interact with objects (Mine, 1996). This could be for sorting, re-arranging of objects or selecting specific objects that are part of a group of other objects (Deneubourg, 1990). If the xyz-coordinates of an object are determined, this can be used as input coordinates to a robotic system and have accurate selection of the identified object. With this system proposed, the xyz-coordinates of multiple objects can also be determined, even if they are at different levels. This chapter describes a mathematical model to determine the xyz-coordinates of an object using a 3D-vision system. Raju, 2004, explained that the centre of projection (COP) is where all image lines merge from an image plane as displayed in figure 5.1a. This 3D-vision system is a setup of two cameras. Using the centre of projection (COP), the 3D-position of the object is determined.

In this chapter, a mathematical model to determine the 3D-coordinates of the object point will be described.

5.2 Aim

The aim is to derive a mathematical formula to determine the 3D xyz-coordinates of an object using a 3D-vision system.

5.3 The 3D-camera setup

The setup is to have two cameras positioned linearly next to each other. The COP is where all image lines merge from an image plane.

Figure 5.1a displays the COP of a camera setup. From figure 5.1a, it indicates that the image lines merge at the COP. Figure 5.1a also depicts that when a pixel is selected on the image plane, a line segment is formed from the pixel position to the COP.

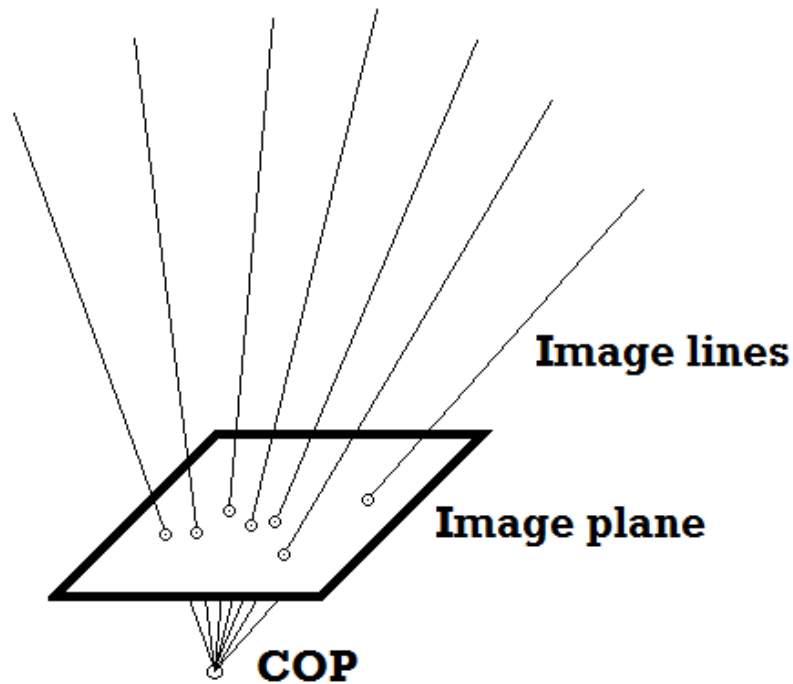


Figure 5.1a: COP of a camera setup

Figure 5.1b displays a 3D-camera setup. The cameras are positioned linearly to each other, in this case vertical. When an image on each camera is captured of the same object at the same time, the one image will be slightly displayed in comparison with the other due to the parallax effect (Ball. et. al., 1989).

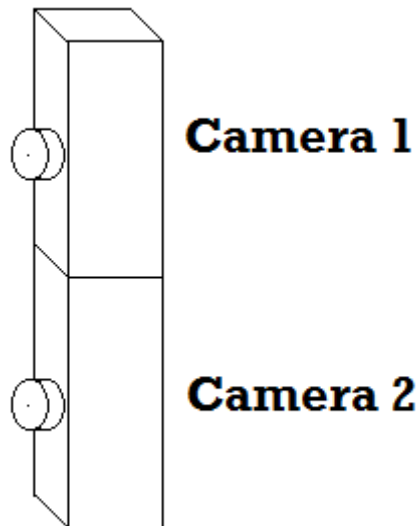


Figure 5.1b: 3D camera setup

Figure 5.1c displays a 3D-camera setup with the COP and object point. In figure 5.1c, only the image planes, the image pixel and the COP are displayed. A line segment is formed from each image pixel to the COP of each camera. Two line segments are formed when two cameras are used. As these two lines, originate from the same object point, they will

intersect at the object point. By determining the intersecting point, the object point can be calculated.

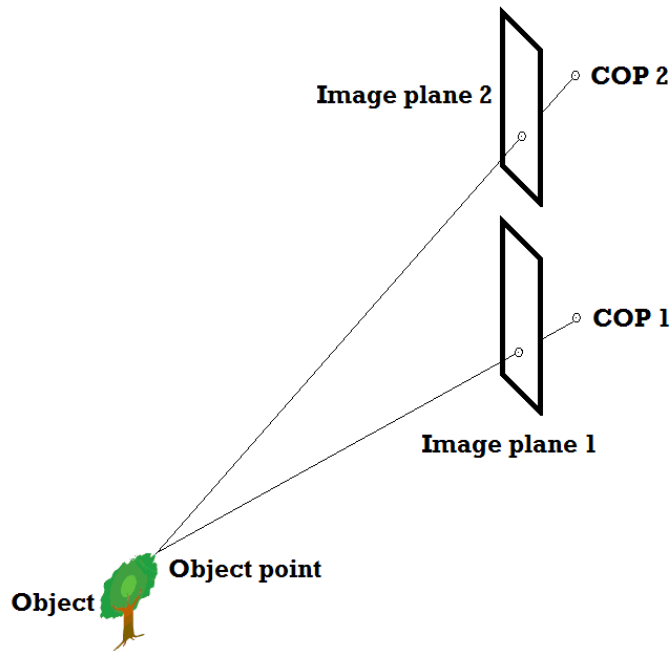


Figure 5.1c: 3D camera setup with the COP and object point

As the object consists of multiple object points, by identifying a central point on the object, the object position can be determined.

5.4 Method to determine the xyz-coordinates of the COP

The following describes a method to obtain the 3D xyz-coordinates of the COP of a camera. As depicted in figure 5.1a, the image lines from the object, projects through the image plane to the COP.

The image plane has a set height and width. By setting the origin at the centre pixel on the image plane, all pixels on the image plane can be described in an xyz-coordinate system.

If the size-per-pixel is known, with the centre pixel as (0,0,0), then the xyz-position of each pixel on the image can be determined by utilizing the xyz-coordinates with the size-per-pixel.

Secondly if the xyz-coordinates of an artefact that is being visualized are determined, then an image line will be formed from the artefact point to the pixel position. Figure 5.2 displays the setup to determine the xyz-coordinates of the COP.

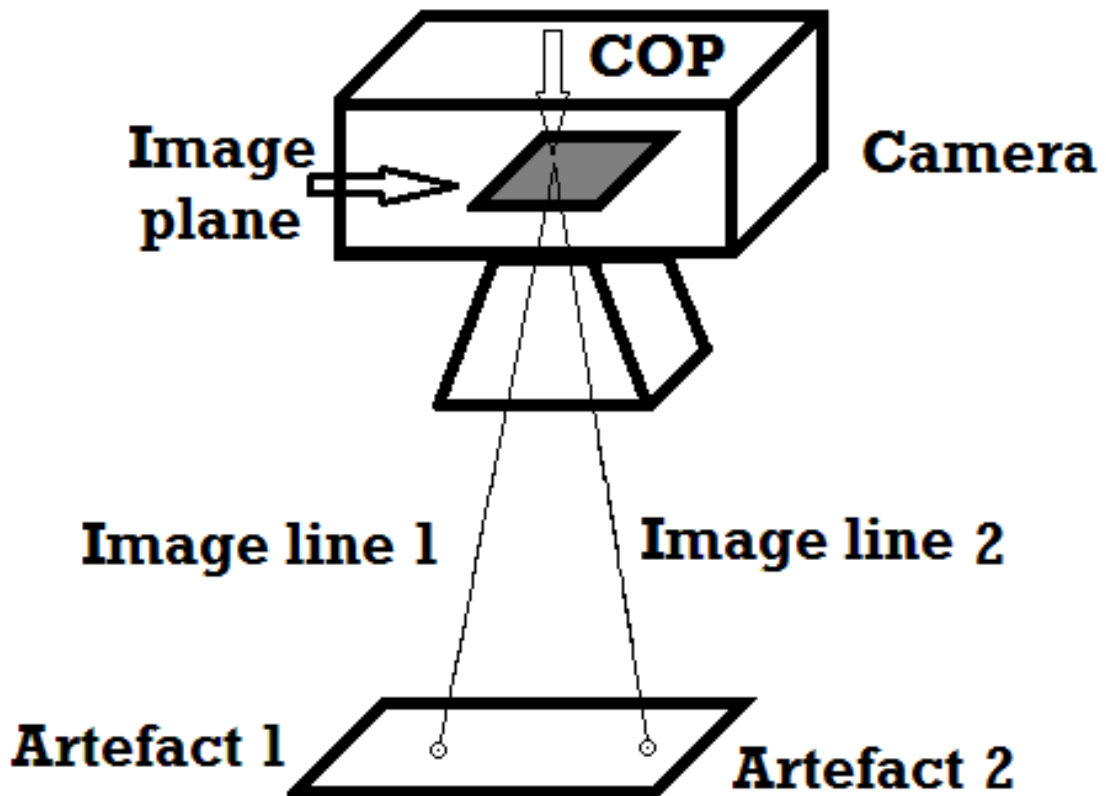


Figure 5.2: Setup to determine the xyz-coordinates of the COP

As from figure 5.2, it indicates that the intersecting point from the two image lines will produce the xyz-coordinates of the COP. To obtain the xyz-coordinates of the COP, the mathematical method to determine the intersecting point of two lines in 3D will be described.

The following describe the method to determine the intersecting point of two lines in 3D.

5.5 Mathematical formulae to determine the intersecting point of two lines in 3D

Figure 5.3 depicts two lines in 3D. As all lines do not intersect in 3D, the xyz-coordinates of the midpoint of the shortest distance between the two lines will be determined.

In figure 5.3 the setup to determine the shortest distance between two lines in 3D will be used.

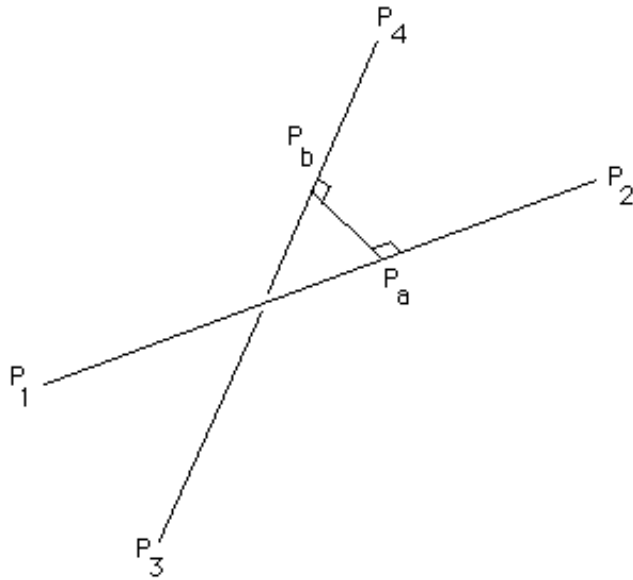


Figure 5.3: Setup to determined the shortest distance between two lines in 3D

If

$$P_1 = (x_1, y_1, z_1)$$

$$P_2 = (x_2, y_2, z_2)$$

$$P_3 = (x_3, y_3, z_3)$$

$$P_4 = (x_4, y_4, z_4)$$

As displayed in figure 5.3,

Then as per equation (3.25), equation (3.26) and equation (3.27), the coordinates of the COP are:

$$x_{ab} = \frac{x_a + x_b}{2} \tag{5.1}$$

$$y_{ab} = \frac{y_a + y_b}{2} \tag{5.2}$$

$$z_{ab} = \frac{z_a + z_b}{2} \tag{5.3}$$

with $x_a, y_a, x_b, y_b, z_a, z_b$ as:

$$x_a = \left(x_1 + \left(\frac{(((d1343)(d4321)) - ((d1321)(d4343)))}{(((d2121)(d4343)) - ((d4321)(d4321)))} \right) (x_2 - x_1) \right) \tag{5.5}$$

$$x_b = \left(x_3 + \left(\frac{d1343 + d4321 \left(\frac{(((d1343)(d4321)) - ((d1321)(d4343)))}{(((d2121)(d4343)) - ((d4321)(d4321)))} \right)}{d4343} \right) \right) (x_4 - x_3) \quad (5.6)$$

$$y_a = y_1 + \left(\frac{(((d1343)(d4321)) - ((d1321)(d4343)))}{(((d2121)(d4343)) - ((d4321)(d4321)))} \right) (y_2 - y_1) \quad (5.7)$$

$$y_b = y_2 + \left(\left(d1343 + \left(\frac{(d4321) \left(\frac{(((d1343) (d4321)) - ((d1321) (d4343)))}{(((d2121) (d4343)) - ((d4321) (d4321)))} \right)}{d4343} \right) \right) \right) (y_4 - y_3) \quad (5.8)$$

$$z_a = z_1 + \left(\frac{(((d1343) (d4321)) - ((d1321)(d4343)))}{(((d2121) (d4343)) - ((d4321) (d4321)))} \right) (z_2 - z_1) \quad (5.9)$$

$$z_b = z_3 + \left(\frac{\left((d1343) + \left((d4321) \left(\frac{(((d1343) (d4321)) - ((d1321) (d4343)))}{(((d2121) (d4343)) - ((d4321) (d4321)))} \right) \right) \right)}{d4343} \right) (z_4 - z_3) \quad (5.10)$$

and

$$d1343 = ((x_1 - x_3)(x_4 - x_3)) + ((y_1 - y_3)(y_4 - y_1)) + ((z_1 - z_3) - (z_4 - z_3)) \quad (5.11)$$

$$d4321 = ((x_4 - x_3)(x_2 - x_1)) + ((y_4 - y_3)(y_2 - y_1)) + ((z_4 - z_3) - (z_2 - z_1)) \quad (5.12)$$

$$d1321 = ((x_1 - x_3)(x_2 - x_1)) + ((y_1 - y_3)(y_2 - y_1)) + ((z_1 - z_3) - (z_2 - z_1)) \quad (5.13)$$

$$d4343 = ((x_4 - x_3)(x_4 - x_3)) + ((y_4 - y_3)(y_4 - y_3)) + ((z_4 - z_3) - (z_4 - z_3)) \quad (5.14)$$

$$d2121 = ((x_2 - x_1)(x_2 - x_1)) + ((y_2 - y_1)(y_2 - y_1)) + ((z_2 - z_1) - (z_2 - z_1)) \quad (5.15)$$

5.6 Determine the COP for a camera setup

Figure 5.4 displays the single camera setup with the image plane and COP. Define (P_1, P_3) as the two artefact points and (P_2, P_4) as the two image points on the image plane.

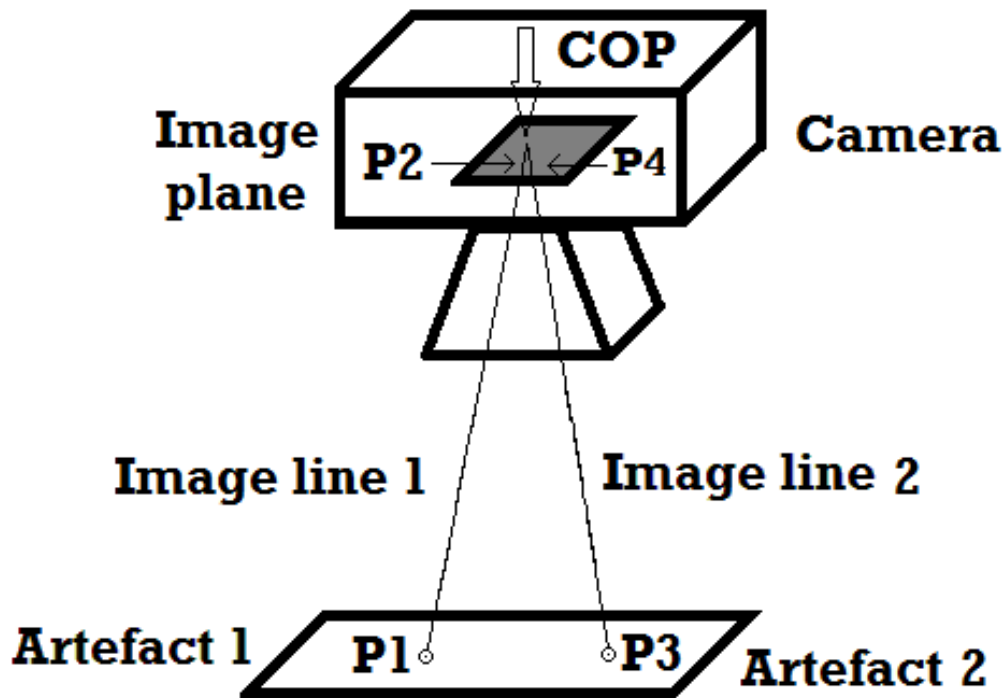


Figure 5.4: Setup to determine the COP

Let

$$P_1 = (x_1, y_1, z_1)$$

$$P_2 = (x_2, y_2, z_2)$$

$$P_3 = (x_3, y_3, z_3)$$

$$P_4 = (x_4, y_4, z_4)$$

Then as per equation (3.25), equation (3.26) and equation (3.27), the coordinates of the COP are:

$$x_{ab} = \frac{x_a + x_b}{2} \quad (5.16)$$

$$y_{ab} = \frac{y_a + y_b}{2} \quad (5.17)$$

$$z_{ab} = \frac{z_a + z_b}{2} \quad (5.18)$$

with $x_a, y_a, x_b, y_b, z_a, z_b$ as:

$$x_a = \left(x_1 + \left(\frac{(((d1343)(d4321)) - ((d1321)(d4343)))}{(((d2121)(d4343)) - ((d4321)(d4321)))} \right) (x_2 - x_1) \right) \quad (5.19)$$

$$x_b = \left(x_3 + \left(\frac{\left(d1343 + d4321 \left(\frac{(((d1343)(d4321)) - ((d1321)(d4343)))}{(((d2121)(d4343)) - ((d4321)(d4321)))} \right) \right)}{d4343} \right) (x_4 - x_3) \right) \quad (5.20)$$

$$y_a = y_1 + \left(\frac{(((d1343)(d4321)) - ((d1321)(d4343)))}{(((d2121)(d4343)) - ((d4321)(d4321)))} (y_2 - y_1) \right) \quad (5.21)$$

$$y_b = y_2 + \left(\left(d1343 + \left(\frac{(d4321) \left(\frac{(((d1343)(d4321)) - ((d1321)(d4343)))}{(((d2121)(d4343)) - ((d4321)(d4321)))} \right)}{d4343} \right) \right) (y_4 - y_3) \right) \quad (5.22)$$

$$z_a = z_1 + \left(\frac{(((d1343)(d4321)) - ((d1321)(d4343)))}{(((d2121)(d4343)) - ((d4321)(d4321)))} (z_2 - z_1) \right) \quad (5.23)$$

$$z_b = z_3 + \left(\frac{\left((d1343) + \left((d4321) \left(\frac{(((d1343)(d4321)) - ((d1321)(d4343)))}{(((d2121)(d4343)) - ((d4321)(d4321)))} \right) \right) \right)}{d4343} (z_4 - z_3) \right) \quad (5.24)$$

and

$$d1343 = ((x_1 - x_3)(x_4 - x_3)) + ((y_1 - y_3)(y_4 - y_1)) + ((z_1 - z_3) - (z_4 - z_3)) \quad (5.25)$$

$$d4321 = ((x_4 - x_3)(x_2 - x_1)) + ((y_4 - y_3)(y_2 - y_1)) + ((z_4 - z_3) - (z_2 - z_1)) \quad (5.26)$$

$$d1321 = ((x_1 - x_3)(x_2 - x_1)) + ((y_1 - y_3)(y_2 - y_1)) + ((z_1 - z_3) - (z_2 - z_1)) \quad (5.27)$$

$$d4343 = ((x_4 - x_3)(x_4 - x_3)) + ((y_4 - y_3)(y_4 - y_3)) + ((z_4 - z_3) - (z_4 - z_3)) \quad (5.28)$$

$$d2121 = ((x_2 - x_1)(x_2 - x_1)) + ((y_2 - y_1)(y_2 - y_1)) + ((z_2 - z_1) - (z_2 - z_1)) \quad (5.29)$$

5.7 Determining the position of the object point

With the COP determine, it can be used to determine the position of the artefact point.

As per figure 5.1a when two cameras are used, then two COPs' will be available.

Also as in figure 5.7, two image lines will be generated from the object point, through the image planes and to the COPs'.

Set the origin at the centre pixel of the first cameras as displayed in figure 5.7.

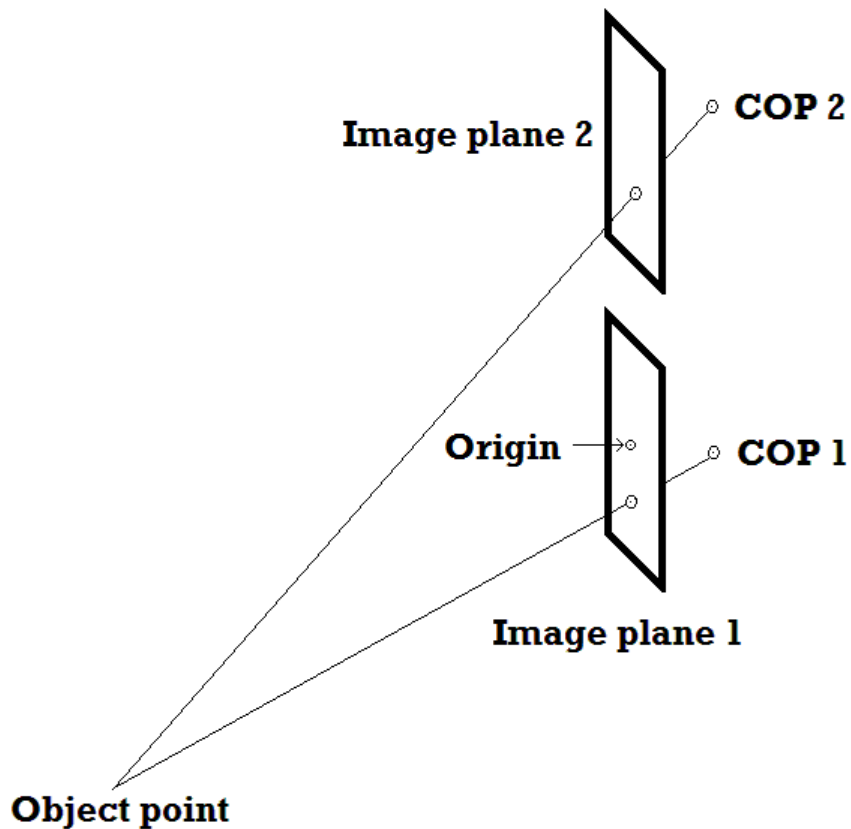


Figure 5.7: Setup for the origin

5.8 The xyz-coordinates of the object point

The xyz-coordinates of the object point is the intersecting point of the line generated from the pixel on image plane1 to COP1 and the line generated from the pixel on image plane 2 to COP2.

Set

P1 as the xyz-coordinates of the pixel on image plane1,
 P2 as the xyz-coordinates of the COP of camera1,
 P3 as the xyz-coordinates of the pixel on image plane2 and
 P2 as the xyz-coordinates of the COP of camera2
 as displayed in figure 5.7a

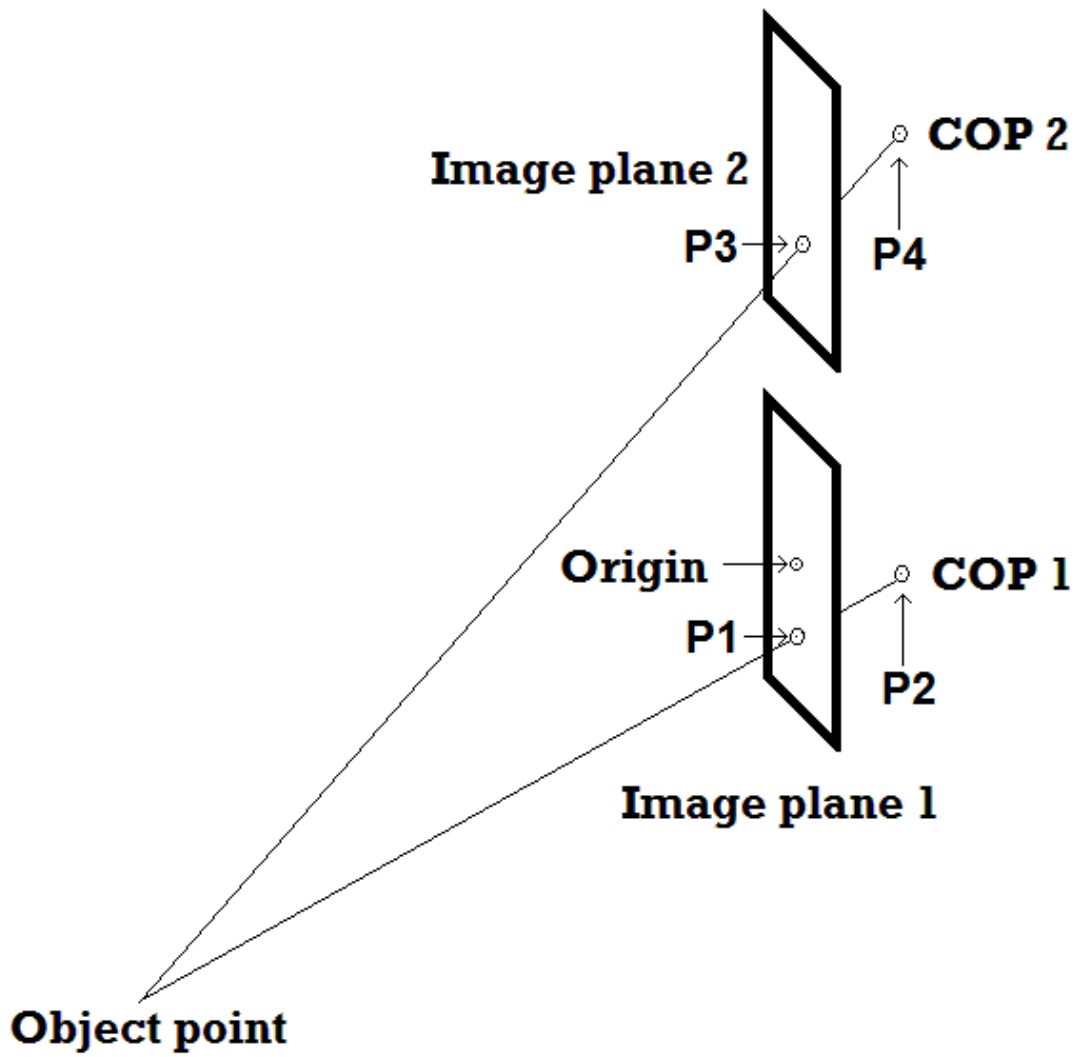


Figure 5.7a: Setup for P1, P2, P3 and P4

Then the formulae for the xyz-coordinates of the object point are:

$$x_{ab} = \frac{x_a + x_b}{2} \quad (5.30)$$

$$y_{ab} = \frac{y_a + y_b}{2} \quad (5.31)$$

$$z_{ab} = \frac{z_a + z_b}{2} \quad (5.32)$$

$$d_{ab} = \sqrt{(x_a - x_b)^2 + (y_a - y_b)^2 + (z_a - z_b)^2} \quad (5.33)$$

with $x_a, y_a, x_b, y_b, z_a, z_b$ as:

$$x_a = \left(x_1 + \left(\frac{(((d1343)(d4321)) - ((d1321)(d4343)))}{(((d2121)(d4343)) - ((d4321)(d4321)))} \right) (x_2 - x_1) \right) \quad (5.34)$$

$$x_b = \left(x_3 + \left(\frac{\left(d1343 + d4321 \left(\frac{(((d1343)(d4321)) - ((d1321)(d4343)))}{(((d2121)(d4343)) - ((d4321)(d4321)))} \right) \right)}{d4343} \right) (x_4 - x_3) \right) \quad (5.35)$$

$$y_a = y_1 + \left(\frac{(((d1343)(d4321)) - ((d1321)(d4343)))}{(((d2121)(d4343)) - ((d4321)(d4321)))} (y_2 - y_1) \right) \quad (5.36)$$

$$y_b = y_2 + \left(\left(d1343 + \frac{\left((d4321) \left(\frac{(((d1343) (d4321)) - ((d1321) (d4343)))}{(((d2121) (d4343)) - ((d4321) (d4321)))} \right) \right)}{d4343} \right) (y_4 - y_3) \right) \quad (5.37)$$

$$z_a = z_1 + \left(\frac{(((d1343) (d4321)) - ((d1321)(d4343)))}{(((d2121) (d4343)) - ((d4321) (d4321)))} (z_2 - z_1) \right) \quad (5.38)$$

$$z_b = z_3 + \left(\frac{\left((d1343) + \left((d4321) \left(\frac{(((d1343) (d4321)) - ((d1321) (d4343)))}{(((d2121) (d4343)) - ((d4321) (d4321)))} \right) \right) \right)}{d4343} (z_4 - z_3) \right) \quad (5.39)$$

and

$$d1343 = ((x_1 - x_3)(x_4 - x_3)) + ((y_1 - y_3)(y_4 - y_1)) + ((z_1 - z_3) - (z_4 - z_3)) \quad (5.40)$$

$$d4321 = ((x_4 - x_3)(x_2 - x_1)) + ((y_4 - y_3)(y_2 - y_1)) + ((z_4 - z_3) - (z_2 - z_1)) \quad (5.41)$$

$$d1321 = ((x_1 - x_3)(x_2 - x_1)) + ((y_1 - y_3)(y_2 - y_1)) + ((z_1 - z_3) - (z_2 - z_1)) \quad (5.42)$$

$$d4343 = ((x_4 - x_3)(x_4 - x_3)) + ((y_4 - y_3)(y_4 - y_3)) + ((z_4 - z_3) - (z_4 - z_3)) \quad (5.43)$$

$$d2121 = ((x_2 - x_1)(x_2 - x_1)) + ((y_2 - y_1)(y_2 - y_1)) + ((z_2 - z_1) - (z_2 - z_1)) \quad (5.44)$$

5.9 MATLAB simulation

Figure 5.8 displays the MATLAB Simulation to determine the object point. The two image line segments are projected from the pixel position on camera1 to the COP of camera1 and from the pixel position on camera2 to the COP of camera2.

The object point will be the intersecting point of these two image lines.

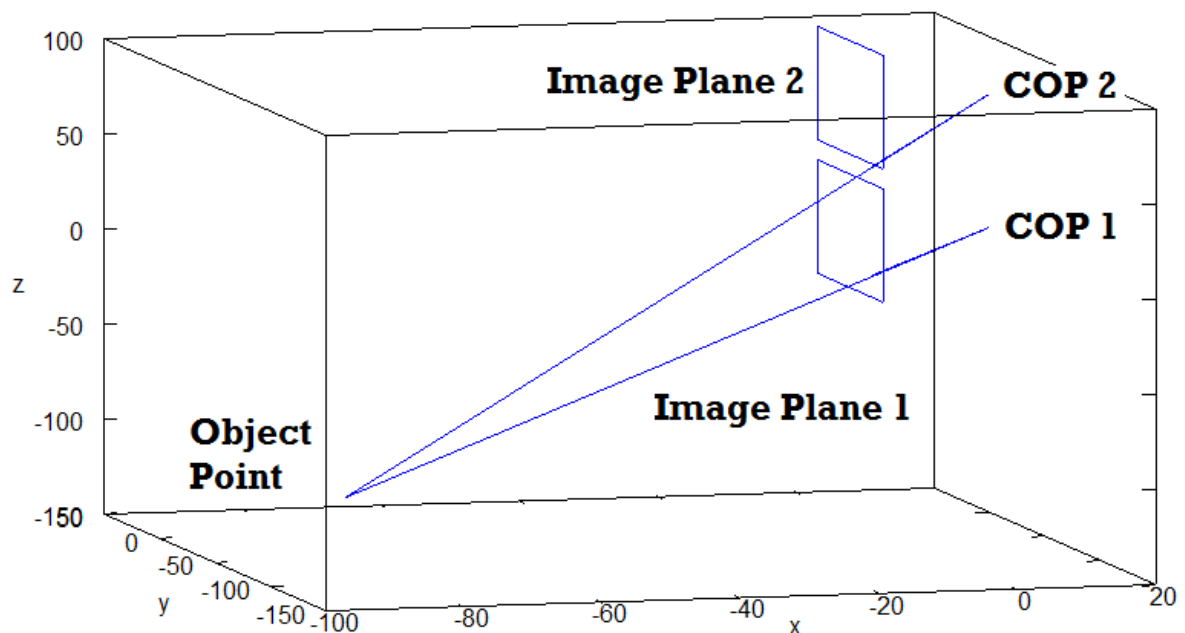


Figure 5.8: MATLAB Simulation to determine the object point

5.10 Discussion

By obtaining the xyz-coordinates of COP, linear 3D-measurements can be performed if two images and the image points are obtained.

To obtain the linear distance between two points in 3D, the following distance formula is used:

$$d = \sqrt{(x_2 - x_1)^2 + (y_2 - y_1)^2 + (z_2 - z_1)^2} \quad (5.45)$$

This indicates that if the xyz-coordinates of two 3D points are determined, then the relative distance in 3D space can be obtained.

Then by identifying two points on the two images on the 3D-vision camera, the distance can be calculated. Figure 5.9 displays a schematic of the setup to determine the 3D measurement with two images on the 3D-vision camera.

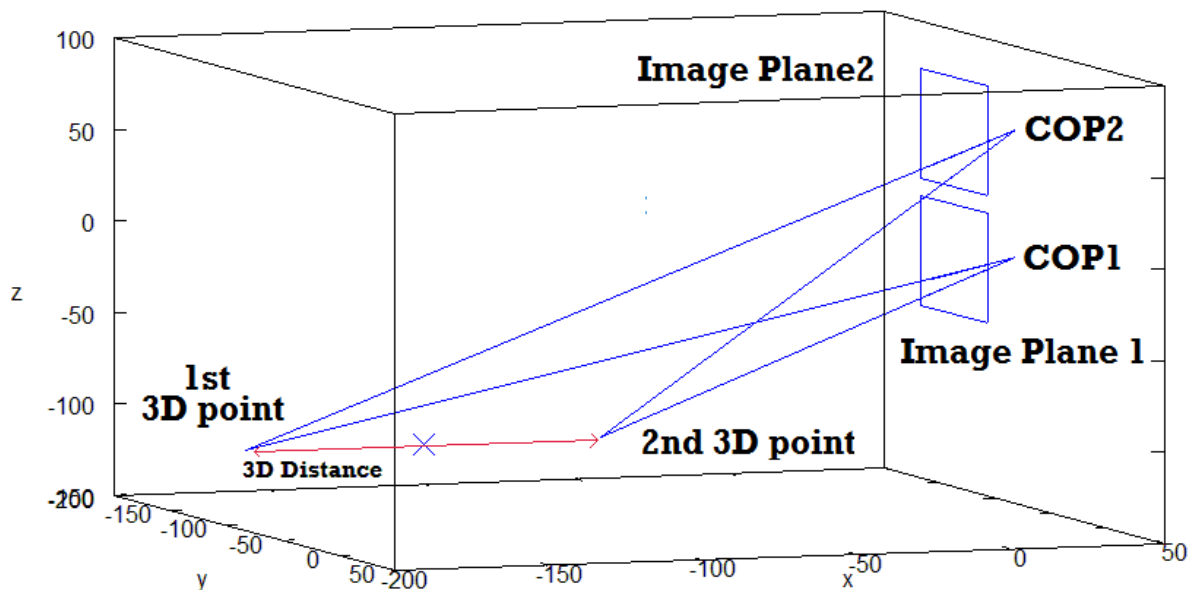


Figure 5.9: Schematic of the setup to determine the 3D-distance with two images on the 3D-vision camera

If two laser pointers are used to identify the two points to obtain the distance, then another application is when the xyz-coordinates of the two laser points are determined, then the 3D distance between these two laser points can be calculated. This can be determined when the xyz-coordinates of the COPs' of a two camera system are available. With the position of the

COPs' and the position of the laser pointers, the relative 3D distance between these two laser points can be determined.

This chapter describes the mathematical model to determine the 3D xyz-coordinates of an object using a 3D-vision system.

5.11 Limitations to consider

When using a 3D-vision camera setup, the origin is described as being at the centre of the lower image plate. For this, the position of the image sensor-plate needs to be determined to obtain the centre position.

Also if two separate image sensor-plates are used, the image plates needs to be aligned with each other. If the image plates are not aligned, the angle needs to be determined and the method for rotation around another point other than the origin needs to be applied.

5.12 Conclusion of chapter 5

The mathematical model to determine the 3D-coordinates of the object was determined.

By determine the positioning of the COP; it can be used to determine the 3D position of the artefact point. With this 3D position available, the co-ordinates can be used for interaction of equipment and machinery with objects.

As the 3D length of an object can also be determined, this method can be used to perform 3D measurements with no interaction with an object.

CHAPTER 6

Method to determine linear 3D measurements

6.1 Introduction

In this chapter, the 3D measurement is determined using a linear two camera setup. The 3D position of an object is needed if interaction of equipment with the object is required.

Cameras are commonly used in the visualization of objects, and by using a camera setup to determine the 3D position of an object, can be added to the features of a camera or a cell phone application.

6.2 Aim

The aim is to describe the method to perform 3D linear measurements using a camera setup.

6.3 The value of 3D measurements

Cameras project a 2D image of a 3D environment. This indicates that if any measurements are done on the image, then a 2D linear distance is measured on the image plane. These 2D measurements are done on the image plane, and only produce measurements in that image plane.

A linear measurement in 3D can be in any direction and orientation. The object that is being captured is from a 3D environment and by having a 3D measurements technique; 3D measurements can be done using the 2D images.

The value of 3D measurements is that measurements of objects can be done in 3D, without interaction with the objects.

6.4 The 3D camera setup

The 3D-camera setup is as explained in section 5.3 with the two cameras positioned linear next to each other.

Figure 6.1 displays the 3D camera setup. The cameras are positioned linearly to each other. When an image on each camera is obtained of the same object at the same time, one image will be slightly displayed differently in comparison with the other.

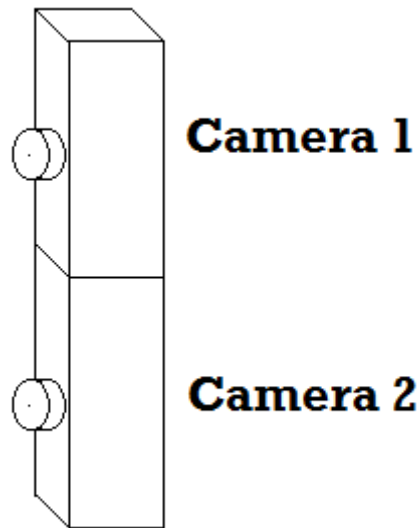


Figure 6.1: 3D camera setup

Figure 6.2 displays 3D camera setup with the COP and object point. In figure 6.2 the image planes are displayed with the image pixel and COP. A line segment is formed from each image pixel to the COP of each camera. Two line segments are formed. As these two lines, originate from the same object point, they will intersect at the image point. By determining the intersecting point, the object point can be calculated.

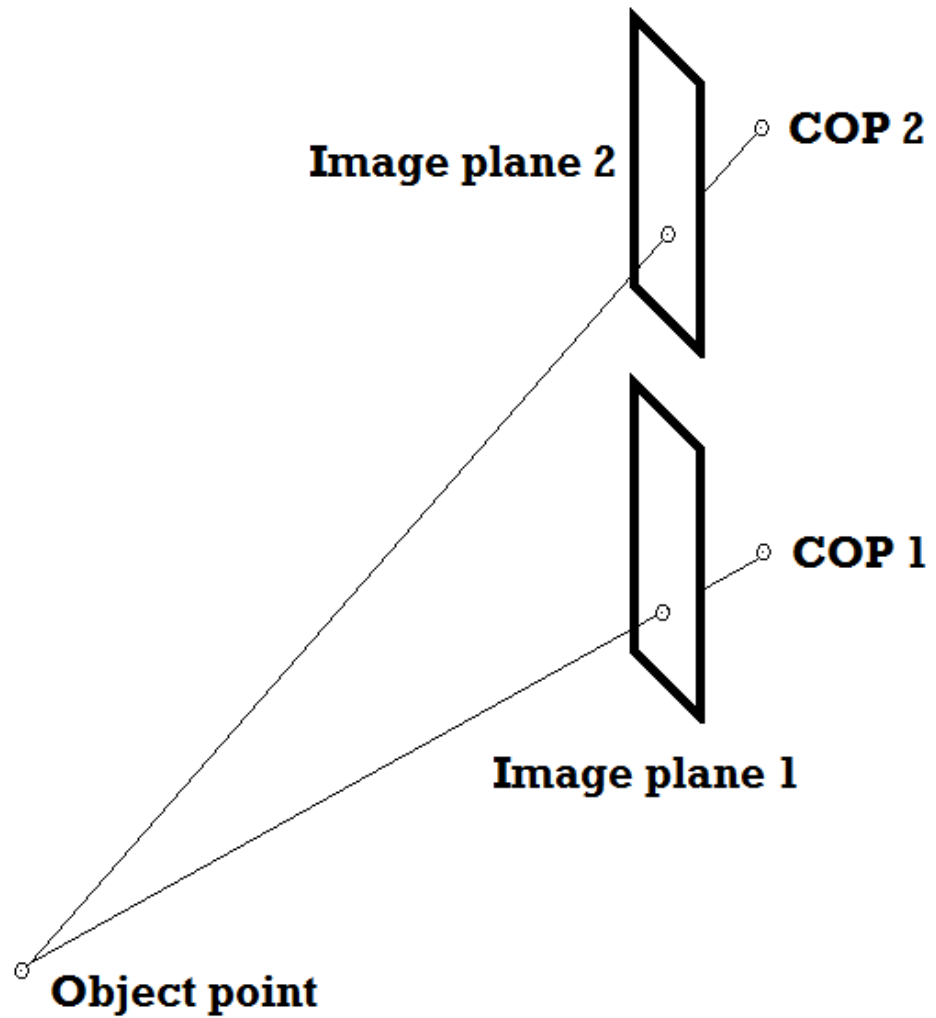


Fig 6.2: 3D-camera setup with the COP and object point

6.5 Method to determine 3D measurement

The method to determine the 3D measurement is by obtaining the 3D positions of two object points, then using the linear formula to calculate the 3D distance between two points.

Figure 6.3 depicts the setup to determine the 3D distance between two points in 3D.

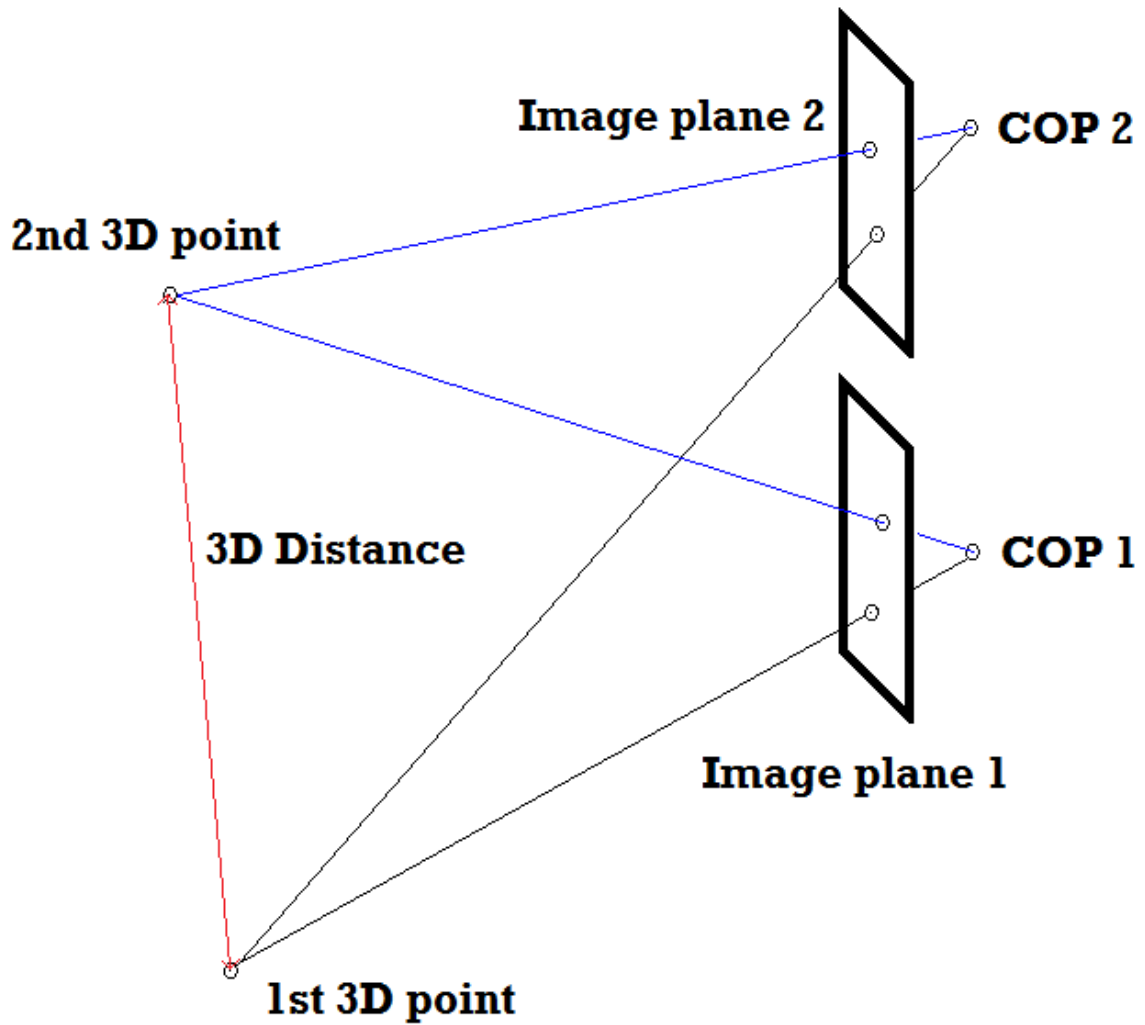


Figure 6.3 Setup to determine the 3D distance between two points in 3D.

The formulae to determine the 3D distance is:

$$d_{ab} = \sqrt{(x_a - x_b)^2 + (y_a - y_b)^2 + (z_a - z_b)^2}$$

where

(x_a, y_a, z_a) is the 3D-coordinates of the 1st point and

(x_b, y_b, z_b) is the 3D-coordinates of the 2nd point

From Chapter 4, the 3D position of a point can be determined as the object produces the same point on two different images. This indicates the user selects one point of the the same object point on the two images which are slightly shifted.

Each camera has a COP and by using the COPs' and the pixel positions, the 3D position is determined. Two points has to be selected from where the 3D measurement needs to be determined.

This will generate two 3D points and these 3D points are used to determine the 3D linear distance.

6.6 MATLAB Simulation

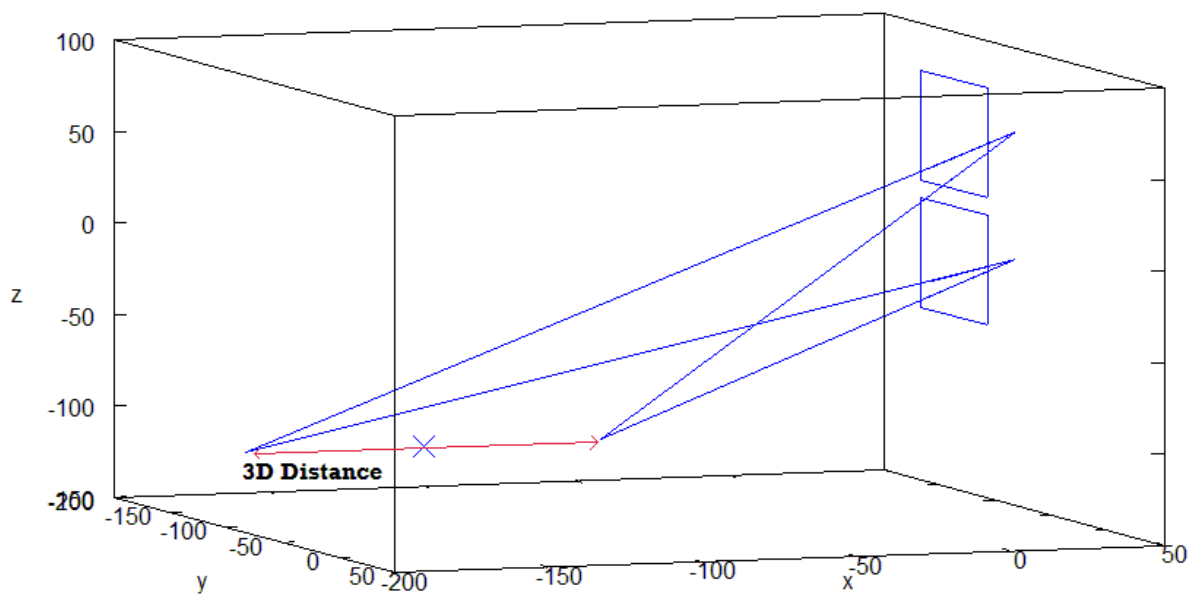


Figure 6.4 Setup to perform 3D measurements

The formulae to determine an intersecting point in 3D is:

Let

$$P_1 = (x_1, y_1, z_1)$$

$$P_2 = (x_2, y_2, z_2)$$

$$P_3 = (x_3, y_3, z_3)$$

$$P_4 = (x_4, y_4, z_4)$$

As displayed in figure 6.5

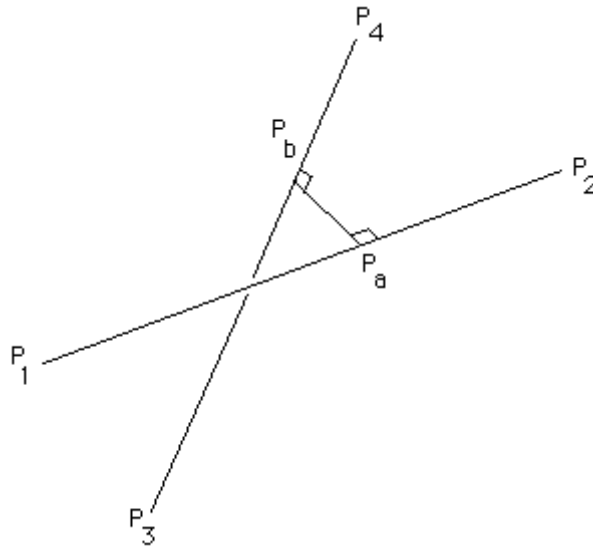


Figure 6.5: Setup to determined the shortest distance between two lines in 3D

Then as per equation (3.25), equation (3.26) and equation (3.27), the coordinates of the COP are:

$$x_{ab} = \frac{x_a + x_b}{2} \quad (6.1)$$

$$y_{ab} = \frac{y_a + y_b}{2} \quad (6.2)$$

$$z_{ab} = \frac{z_a + z_b}{2} \quad (6.3)$$

with $x_a, y_a, x_b, y_b, z_a, z_b$ as:

$$x_a = \left(x_1 + \left(\frac{(((d1343)(d4321)) - ((d1321)(d4343)))}{(((d2121)(d4343)) - ((d4321)(d4321)))} \right) (x_2 - x_1) \right) \quad (6.4)$$

$$x_b = \left(x_3 + \left(\frac{\left(\left(\left(\left(d1343 + d4321 \right) \left(\frac{(((d1343)(d4321)) - ((d1321)(d4343)))}{(((d2121)(d4343)) - ((d4321)(d4321)))} \right) \right) \right) \right)}{d4343} \right) (x_4 - x_3) \right) \quad (6.5)$$

$$y_a = y_1 + \left(\left(\frac{(((d1343)(d4321)) - ((d1321)(d4343)))}{(((d2121)(d4343)) - ((d4321)(d4321)))} \right) (y_2 - y_1) \right) \quad (6.6)$$

$$y_b = y_2 + \left(\left(d1343 + \frac{\left((d4321) \left(\frac{(((d1343) (d4321)) - ((d1321) (d4343)))}{(((d2121) (d4343)) - ((d4321) (d4321)))} \right) \right)}{d4343} \right) (y_4 - y_3) \right) \quad (6.7)$$

$$z_a = z_1 + \left(\frac{(((d1343) (d4321)) - ((d1321) (d4343)))}{(((d2121) (d4343)) - ((d4321) (d4321)))} (z_2 - z_1) \right) \quad (6.8)$$

$$z_b = z_3 + \left(\left(\frac{\left((d1343) + \left((d4321) \left(\frac{(((d1343) (d4321)) - ((d1321) (d4343)))}{(((d2121) (d4343)) - ((d4321) (d4321)))} \right) \right) \right)}{d4343} \right) (z_4 - z_3) \right) \quad (6.9)$$

and

$$d1343 = ((x_1 - x_3)(x_4 - x_3)) + ((y_1 - y_3)(y_4 - y_1)) + ((z_1 - z_3) - (z_4 - z_3)) \quad (6.10)$$

$$d4321 = ((x_4 - x_3)(x_2 - x_1)) + ((y_4 - y_3)(y_2 - y_1)) + ((z_4 - z_3) - (z_2 - z_1)) \quad (6.11)$$

$$d1321 = ((x_1 - x_3)(x_2 - x_1)) + ((y_1 - y_3)(y_2 - y_1)) + ((z_1 - z_3) - (z_2 - z_1)) \quad (6.12)$$

$$d4343 = ((x_4 - x_3)(x_4 - x_3)) + ((y_4 - y_3)(y_4 - y_3)) + ((z_4 - z_3) - (z_4 - z_3)) \quad (6.13)$$

$$d2121 = ((x_2 - x_1)(x_2 - x_1)) + ((y_2 - y_1)(y_2 - y_1)) + ((z_2 - z_1) - (z_2 - z_1)) \quad (6.14)$$

If two points are selected on the one image and two points on the second image, then two 3D points will be determined. Then by using the distance formula, the distance in 3D can be calculated.

The distance formula is:

$$d_{ab} = \sqrt{(x_a - x_b)^2 + (y_a - y_b)^2 + (z_a - z_b)^2}$$

6.7 Conclusion of chapter 6

The determining of the 3D linear distance is dependable on the points selected. This indicates two points' needs to be selected on the first image and the corresponding two points on the second image.

Also as a camera setup is used, no interaction with the object is needed. This provides a 3D measurement method with no interaction with the object.

CHAPTER 7

The use of 3D electronic vision for effective utilization of solar power in a hybrid electrical supply setup

7.1 Introduction

Three-dimensional (3D) electronic vision can provide recognition of objects and orientation of an object to its surrounding. With recognition of objects, possible interaction can be obtained and readjustment of their position (www.nasa.gov/news, 2011). When a solar panel is used in a hybrid electrical supply setup, recognition of objects and their casting shadow can be used to reposition a solar panel to obtain effective utilization of sunlight. Appleyard, 2009, wrote that a number of sun-tracking systems have been designed example the single-axis tracking system that rotates around one axis and azimuthally moving from east to west. A fully shaded solar cell can lose between 80%-90% of its output power (www.greentoronto.me. 2011). Having a hybrid setup (electrical supply, wind energy and solar energy) in a confined space, repositioning the solar panel to obtain direct sunlight when a shadow is cast onto it, can improve efficiency. This paper will explain how 3D electronic vision can be used to maximise the use of a solar panel in a hybrid electrical supply setup.

7.2 Solar energy and sun-tracking

Sun-tracking systems are designed to track the solar azimuth angle on a single axis or to track the solar azimuth and solar altitude angles on two axes (Sungur, 2011). Maximum output of a solar panel can be obtained if the solar panel is in direct sunlight. Solar panel conversion efficiency depends on many factors including incident solar radiation levels, temperature, and load condition (Tse. et.al. 2002). Many sun-tracking systems have been developed and can be computer controlled or microprocessor controlled. These sun-tracking systems can include single and double axis trackers which can boost daily energy production. Kansal (2008) indicated that with a sun-tracking system, data needs to be obtained regarding the best option to position the solar panel.

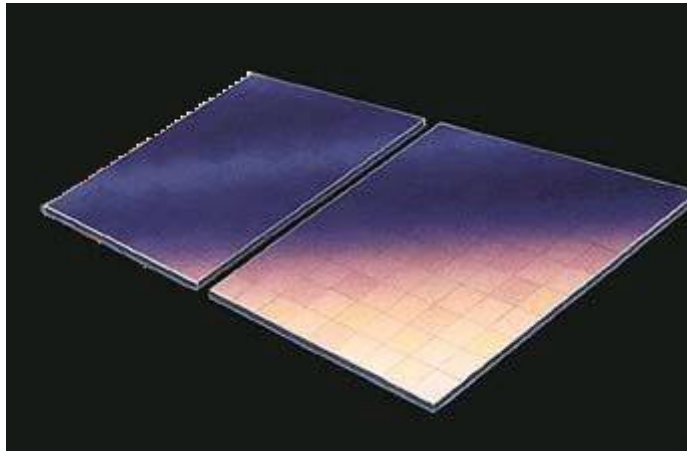


Figure 7.1: Display of a solar panel that is partly covered by a shadow which can reduce its output efficiently

Ibrahim (2010) explained that there is a difference in behaviour of a solar cell when a shadow is cast onto it. With this method of 3D electronic vision designed, the data can be obtained with a visual system. The data of the position of the solar panel, surrounding structures and the position of their casting shadow can be determined in 3D.

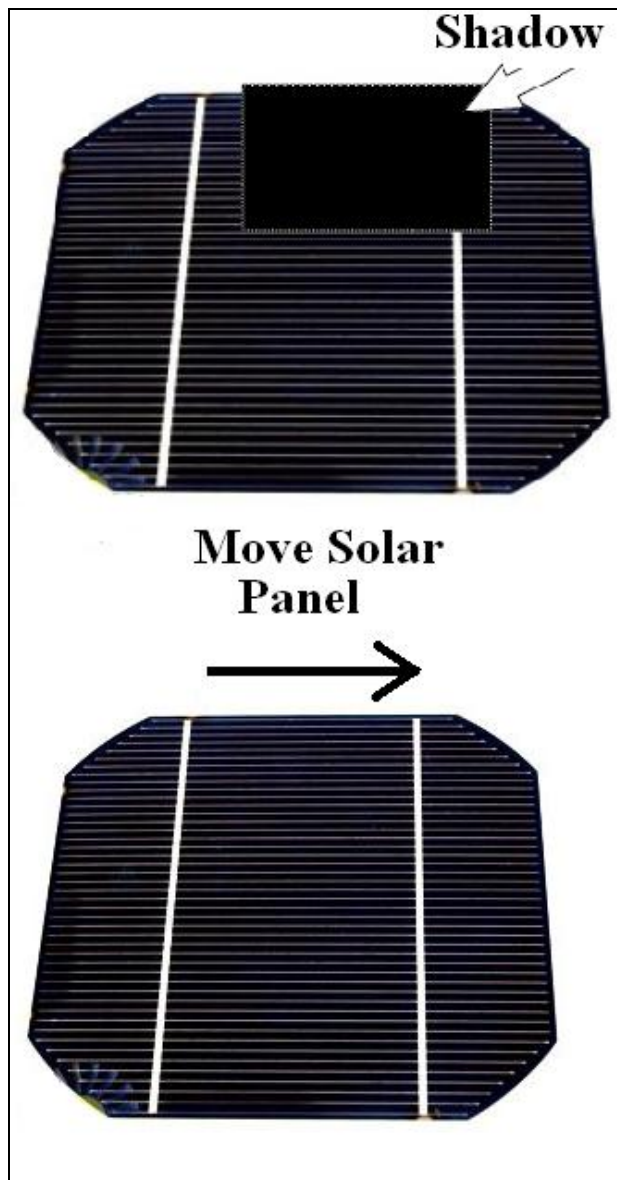


Figure 7.2: When a solar panel is partly covered by a shadow, it can be moved into direct sunlight

7.3 Aim

The aim is to explain how 3D electronic vision can be used for effective utilization of solar power in a hybrid electrical supply system and to measure the output power of the solar panel in direct sunlight, half shadow and full shadow.

7.4 Hybrid system

A hybrid system with electrical supply power as well as renewable electrical energy (solar power and wind power) can all be used in a hybrid electrical supply system to supply power.

The high power systems will use the electrical grid supply and the low power systems will use the renewable energy supply. The renewable energy will be in the form of solar power as well as wind energy.

Figure 7.3 displays a hybrid system that provides electrical supply from the national grid as well as the renewable energy system. Machinery as well as high power equipment can be connected to the national grid where low power equipment example lights can be connected to the renewable energy system.

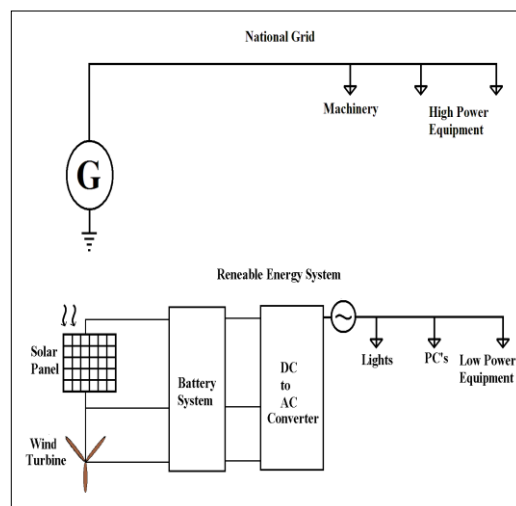


Figure 7.3: A hybrid system that provides electrical supply from the national grid as well as the renewable energy system.

As from figure 7.3, the batteries in the renewable energy system are charged by the wind turbine as well as the solar panel. To obtain maximum output power from the solar panel, the solar panel has to be positioned in direct sunlight with no shadow cast onto it.

7.5 The 3D visualization system

The setup for the renewable energy system can be in a confined space, example the rooftop of a building. With the solar panel in a confined space, the wind turbine, other equipment and surrounding buildings can cast a shadow onto the solar panel that can reduce its output power.

The 3D visualization system work on the basis of two cameras positioned at a set distance from each other and has the solar panel and the surrounding structures in view. The xyz-coordinates of an object in view can be calculated. Figure 7.4 displays the camera setup. With the set distance between the cameras, angle B and angle C determined, then the xyz-coordinates of the object at point A can be determined.

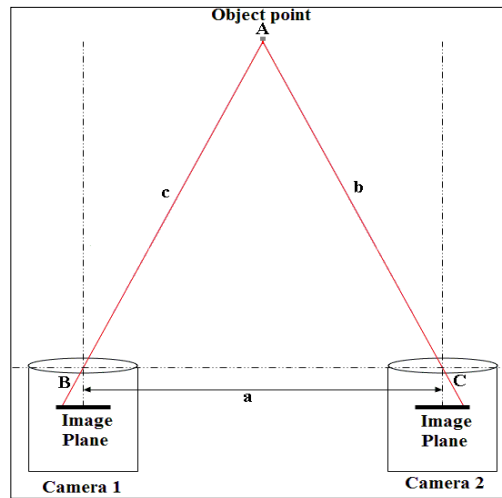


Figure 7.4: Camera setup to determine the xyz-coordinates of the object at point A

By using the sine rule to calculate the length b and c displayed in figure 7.4 and the sum of the inside angles of a triangle is 180° , the formulae for the xyz-coordinates of A is determined which is:

$$x = \left[\left[\frac{a \sin B}{\sin(180^\circ - B - C)} \right] \cos C \right] \quad (7.1)$$

$$y = \left[\frac{a \sin B \sin C}{\sin(180^\circ - B - C)} \right] \quad (7.2)$$

$$z = \left[\left[\frac{a \sin B \sin C}{\sin(180^\circ - B - C)} \right] \tan D \right] \quad (7.3)$$

The angle D is the vertical displacement of the object.

7.6 Accuracy of the 3D visualization system

The setup for the renewable energy system can be in a confined space, example on a rooftop.

In the application of the formulae, 10 random positions of an object were determined. Using the 3D vision system and the xyz formulae, the 10 xyz-coordinates were calculated.

To determine the angles B and C, two images were obtained and the angles were determined with the pixel position multiplied by the number of pixels from the centre position. The radians per pixel were calculated with a known distance for calibration and it was determined as:

$$\text{radians per pixel} = 0.0010445012 \text{ radians/pixel } (0.0598455129 \text{ degrees/pixel})$$

The 3D vision system has an overall accuracy of 96.24% from the calculated distances and a variation of 0.22cm between the calculated distances and the measured distance. With the overall accuracy determined, the detection of the position of the solar panel, surrounding objects and casting shadow, is within 3% of their positions. Table 7.1a, table 7.1b and table 7.1c display the calculated xyz-values and the measured xyz-values.

Table 7.1a:

Comparison
between
calculated
x-values and
measured
x-values

Table 7.1b:

Comparison
between
calculated
y-values and
measured
y-values

Table 7.1c:

Comparison
between
calculated
z-values and
measured
z-values

Calcu- lated x	Mea- sured x	Calcu- lated y	Mea- sured y	Calcu- lated z	Mea- sured z
x	xm	y	ym	z	zm
-1.59	-2.00	25.85	26.20	2.82	2.00
-6.83	-7.00	20.86	21.00	2.42	2.20
-2.66	-2.80	24.12	24.50	2.82	1.60
-2.90	-3.00	17.53	17.50	2.62	1.70
5.74	5.80	39.61	38.00	3.05	2.50
-6.02	-6.00	23.75	23.00	-4.08	-4.00
-3.64	-3.60	15.80	15.00	-1.67	-1.50
-8.24	-8.00	25.55	25.00	-4.31	-4.40
-4.18	-4.50	27.15	27.00	6.00	6.00
-0.39	-0.50	22.38	23.00	-0.96	-0.70

Table 7.2 displays the difference between the calculated and measured xyz-values. Table 7.3 displays the % error of the calculated and measured values. The last rows displays the average of the ten measurements

Table 7.2: Display the difference in length for each xyz-coordinate

Difference Cacl(x)-Meas(x)	Difference Cacl(y)&Meas(y)	Difference Cacl(z)&Meas(z)
ddx	ddy	ddz
0.41	-0.35	0.82
0.17	-0.14	0.22
0.14	-0.38	1.22
0.10	0.03	0.92
-0.06	1.61	0.55
-0.02	0.75	-0.08
-0.04	0.80	-0.17
-0.24	0.55	0.09
0.32	0.15	0.00
0.11	-0.62	-0.26
0.09	0.24	0.33

Table 7.3: Display the % accuracy for all three coordinates and the overall accuracy. The last row displays the average of the ten measurements

%Accuracy x-value	%Accuracy y-value	%Accuracy z-value
% error(x)	% error(y)	% error(z)
-25.557	-1.351	29.169
-2.479	-0.687	8.992
-5.218	-1.585	43.307
-3.566	0.193	35.128
-1.003	4.071	18.120
0.374	3.151	2.076
1.083	5.068	10.350
2.958	2.155	-2.132
-7.642	0.569	0.061
-27.040	-2.764	27.071
-6.808	0.882	17.214
Overall accuracy		3.763

7.7 Repositioning of the solar panel

The solar panel, surrounding objects and the casting shadows are all in view by the visual system. With the visual data from the visual system, the position of the solar panel to be moved away from the casting shadow into direct sunlight can be obtained.

The solar panel can be positioned in the xy-direction with inputs to the two xy-motors as depicted in figure 7.4.1. The visual system provides the feedback of the system.

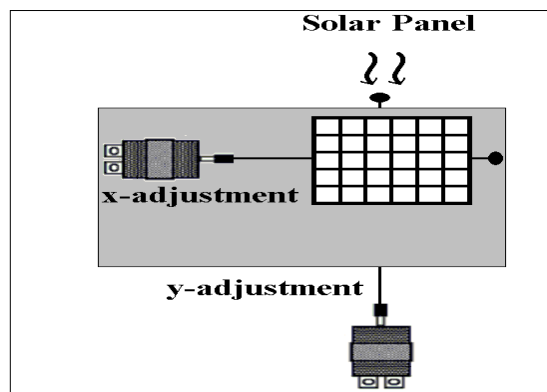


Figure 7.4.1: XY-positioning of the solar panel

7.8 Experimental results with output of the solar panel in sunlight

To obtain the results to determine the output power of a solar panel in full sunlight, half shadow and full shadow, a 200Wp rated solar panel was used and a load of 55.5Ω and 60Ω was connected in parallel, series to the solar panel. The voltage readings were collected every 5 minutes over a period of 30 minutes.

The output power has decreased by 12% when a half shadow was cast onto the solar panel and the output power was decreased by 89%, when a full shadow is cast onto the solar panel as compared to direct sunlight on the solar panel.

7.9 Solar panel voltage output with no load connected

Figure 7.5 displays the setup to measure the output voltage with no load connected to the solar panel. Tables 7.4a, 7.4b and 7.4c display the measurement every 5 minutes over a period of 30 minutes. The average voltage in direct sunlight and no load connected was 30.31V, with the solar panel covered in half shadow was 28.09V and when the solar panel was covered in full shadow, the average voltage reading was 26.11V over a period of 30 minutes

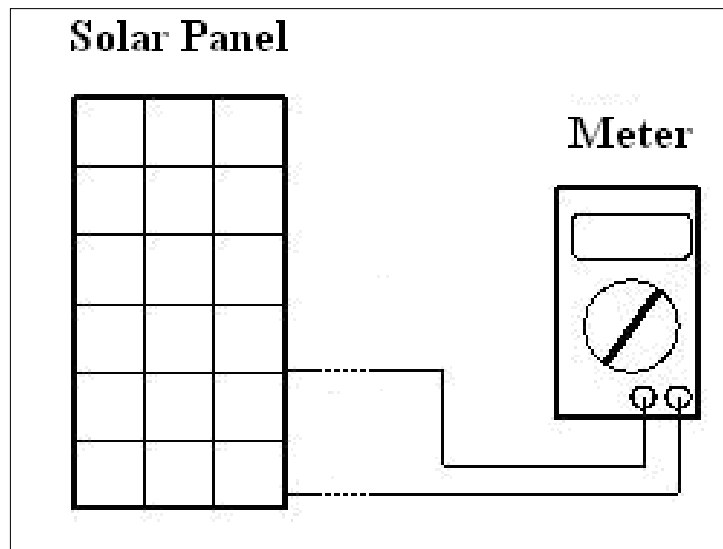


Figure 7.5: Setup to measure output power of the solar panel with no load connected

Table 7.4a: Display the difference in output power of the solar panel with no load connected in direct sunlight

Time (min)	Voltage	Output power in direct sunlight
0	30.45V	0W
5	30.93V	0W
10	30.56V	0W
15	29.91V	0W
20	29.86V	0W
25	30.71V	0W
30	29.78V	0W
Average	30.31V	0W

Table 7.4b: Display the difference in output power of the solar panel with no load connected in half shadow

Time (min)	Voltage	Output power in half shadow
0	28.26V	0W
5	29.04V	0W
10	28.48V	0W
15	28.57V	0W
20	24.45V	0W
25	28.31V	0W
30	29.51V	0W
Average	28.09V	0W

Table 7.4c: Display the difference in output power of the solar panel with no load connected in full shadow

Time (min)	Voltage	Output power in full shadow
0	25.32V	0W
5	25.48V	0W
10	25.48V	0W
15	25.10V	0W
20	28.55V	0W
25	27.07V	0W
30	25.78V	0W
Average	26.11V	0W

7.10 Solar panel voltage output with a load of 29.9Ω connected

Figure 7.6 displays the setup to measure the output voltage with a load of 29.9Ω connected to the solar panel. Tables 7.5a, 7.5b and 7.5c display the measurement every 5 minutes over a period of 30 minutes. The average voltage with direct sunlight and with a load of 29.9Ω connected was 28.57V, the solar panel covered in half shadow was 17.39V and when the solar panel was covered in full shadow, the average voltage reading was 4.92V over a period of 30 minutes. The output power as calculated over the load is displayed in Tables 7.5a, 7.5b and 7.5c.

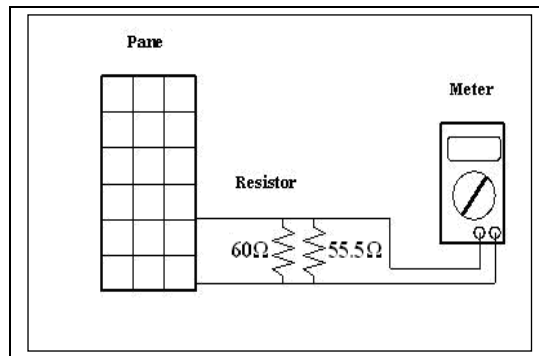


Figure 7.6: Setup to measure output power of the solar panel with the 55.5Ω and 60Ω resistors connected in parallel. The measured resistance was 29.9Ω

Table 7.5a: Display the difference in output power of the solar panel in direct sunlight with a load of 29.9Ω connected

Time (min)	Load resistance (Ω)	Voltage	Output power in direct sunlight
0	29.9Ω	28.68V	27.51W
5	29.9Ω	28.97V	28.07W
10	29.9Ω	29.44V	28.99W
15	29.9Ω	29.39V	28.89W
20	29.9Ω	29.23V	28.58W
25	29.9Ω	26.09V	22.77W
30	29.9Ω	28.21V	26.62W
Average		28.57V	27.34W

Table 7.5b: Display the difference in output power of the solar panel in half shadow with a load of 29.9Ω connected

Time (min)	Load resistance (Ω)	Voltage	Output power in half shadow
0	29.9Ω	15.22V	7.75W
5	29.9Ω	17.39V	10.11W
10	29.9Ω	18.14V	11.01W
15	29.9Ω	18.40V	11.32W
20	29.9Ω	18.08V	10.93W
25	29.9Ω	16.41V	9.01W
30	29.9Ω	18.06V	10.91W
Average	29.9Ω	17.39V	10.15W

Table 7.5c: Display the difference in output power of the solar panel in full shadow with a load of 29.9Ω connected

Time (min)	Load resistance (Ω)	Voltage	Output power in full shadow
0	29.9Ω	3.28V	0.36W
5	29.9Ω	6.83V	1.56W
10	29.9Ω	4.10V	0.56W
15	29.9Ω	5.31V	0.94W
20	29.9Ω	5.62V	1.06W
25	29.9Ω	3.88V	0.50W
30	29.9Ω	5.41V	0.98W
Average	29.9Ω	4.92V	0.85W

7.11 Solar panel voltage output with a load of 55.5Ω connected

Figure 7.7 displays the setup to measure the output voltage with a load of 55.5Ω connected to the solar panel. Tables 7.6a, 7.6b and 7.6c display the measurements every 5 minutes over a period of 30 minutes. The average voltage with direct sunlight and with a load of 55.5Ω connected was 29.07V, the solar panel covered in half shadow was 18.03V and when the solar panel was covered in full shadow, the average voltage reading was 7.09V. The output power as calculated over the load is also displayed in Tables 7.6a, 7.6b and 7.6c.

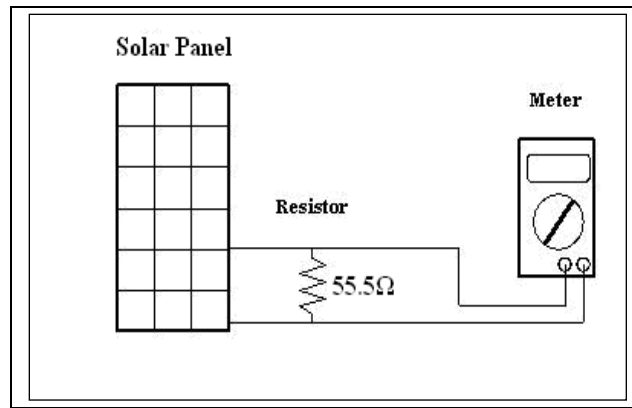


Figure 7.7: Setup to measure output power of the solar panel with a single 55.5Ω resistor connected

Table 7.6a: Display the difference in output power of the solar panel in direct sunlight with a load of 55.5Ω connected

Time (min)	Load resistance (Ω)	Voltage	Output power in direct sunlight
0	55.5Ω	28.60V	14.87W
5	55.5Ω	29.13V	15.43W
10	55.5Ω	29.14V	15.44W
15	55.5Ω	29.14V	15.44W
20	55.5Ω	29.03V	15.32W
25	55.5Ω	29.12V	15.42W
30	55.5Ω	29.34V	15.65W
Average		29.07V	15.37W

Table 7.6b: Display the difference in output power of the solar panel in half shadow with a load of 55.5Ω connected

Time (min)	Load resistance (Ω)	Voltage	Output power in half shadow
0	55.5Ω	18.12V	5.97W
5	55.5Ω	18.11V	5.96W
10	55.5Ω	18.12V	5.97W
15	55.5Ω	17.80V	5.76W
20	55.5Ω	18.12V	5.97W
25	55.5Ω	17.77V	5.74W
30	55.5Ω	18.14V	5.98W
Average		18.03V	5.91W

Table 7.6c: Display the difference in output power of the solar panel in full shadow with a load of 55.5Ω connected

Time (min)	Load resistance (Ω)	Voltage	Output power in full shadow
0	55.5Ω	7.26V	0.96W
5	55.5Ω	7.23V	0.95W
10	55.5Ω	6.95V	0.88W
15	55.5Ω	6.84V	0.85W
20	55.5Ω	6.95V	0.88W
25	55.5Ω	7.20V	0.94W
30	55.5Ω	7.17V	0.93W
Average		7.09V	0.91W

7.12 Solar panel voltage output with a load of 131.3Ω connected

Figure 7.8 displays the setup to measure the output voltage with a load of 131.3Ω connected to the solar panel. Tables 7.7a, 7.7b and 7.7c display the measurements taken every 5 minutes over a period of 30 minutes. The average voltage with direct sunlight and with a load of 131.3Ω connected was 30.46V, 28.57V in half shadow and 9.61V in full shadow over a period of 30 minutes. The output power as calculated over the load is also displayed in Tables 7.7a, 7.7b and 7.7c.

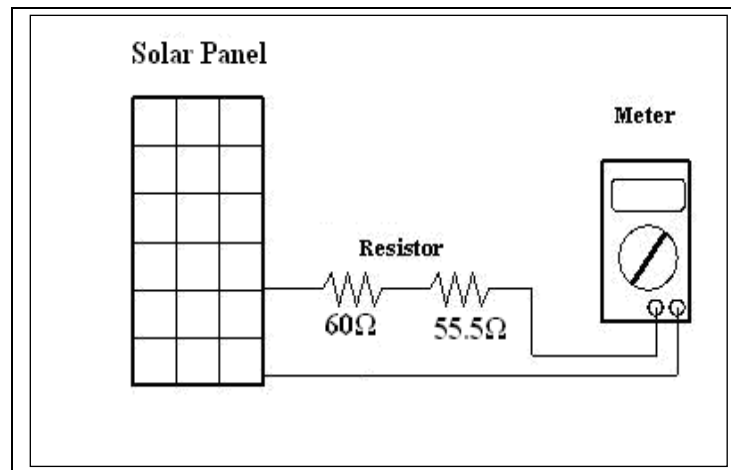


Figure 7.8: Setup to measure output power of the solar panel with the 55.5Ω and 60 Ω resistors connected in series. The measured resistance was 131.3 Ω

Table 7.7a: Display the difference in output power of the solar panel in direct sunlight with a load of 131.3Ω connected

Time (min)	Load resistance (Ω)	Voltage	Output power in direct sunlight
0	131.3Ω	29.82V	6.77W
5	131.3Ω	30.51V	7.09W
10	131.3Ω	30.74V	7.20W
15	131.3Ω	29.85V	6.79W
20	131.3Ω	30.93V	7.29W
25	131.3Ω	30.74V	7.20W
30	131.3Ω	30.63V	7.15W
Average		30.46V	7.07W

Table 7.7b: Display the difference in output power of the solar panel in half shadow with a load of 131.3Ω connected

Time (min)	Load resistance (Ω)	Voltage	Output power in half shadow
0	131.3Ω	28.32V	6.11W
5	131.3Ω	28.49V	6.18W
10	131.3Ω	28.47V	6.17W
15	131.3Ω	28.62V	6.24W
20	131.3Ω	28.65V	6.25W
25	131.3Ω	28.79V	6.31W
30	131.3Ω	28.68V	6.26W
Average		28.57V	6.22W

Table 7.7c: Display the difference in output power of the solar panel in full shadow with a load of 131.3Ω connected

Time (min)	Load resistance (Ω)	Voltage	Output power in full shadow
0	131.3Ω	14.07V	1.51W
5	131.3Ω	8.23V	0.52W
10	131.3Ω	10.45V	0.83W
15	131.3Ω	8.72V	0.58W
20	131.3Ω	11.62V	1.03W
25	131.3Ω	7.11V	0.39W
30	131.3Ω	7.08V	0.38W
Average		9.61V	0.75W

7.13 Output power characteristics of the solar panel in direct sunlight

Table 7.8 displays the output power when the solar panel is in direct sunlight. Figure 7.9 displays the voltage and current curve of the solar panel in direct sunlight.

Table 7.8: Display the difference in output power of the solar panel in direct sunlight

Resistance	Voltage	Current	Power
Open Circuit	30.31V	0.00A	0.00W
131.3Ω	30.46V	0.232A	7.07W
55.5Ω	29.07V	0.535A	15.37W
29.9Ω	28.57V	0.953A	27.35W

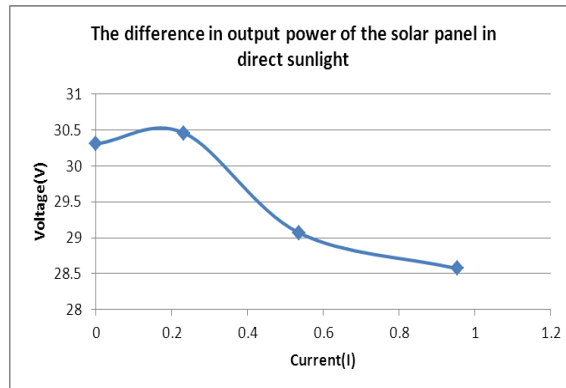


Figure 7.9: The voltage (V) and current (I) curve of the solar panel in direct sunlight

7.14 Output power characteristics of the solar panel in half shadow

Table 7.9 displays the output power when the solar panel is in half shadow. Figure 7.10 displays the voltage and current curve of the solar panel in half shadow.

Table 7.9: Display the difference in output power of the solar panel in half shadow

Resistance	Voltage	Current	Power
Open Circuit	28.09V	0.00A	0.00W
131.3Ω	28.57V	0.218A	6.22W
55.5Ω	18.03V	0.325A	5.91W
29.9Ω	17.39V	0.582A	10.15W

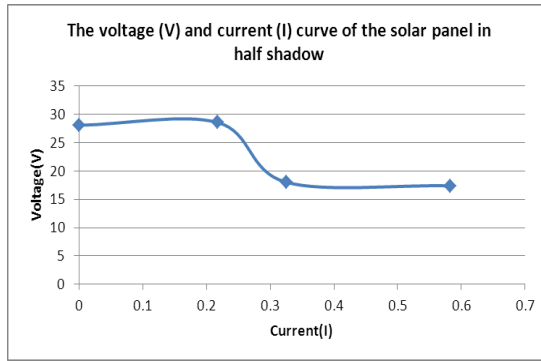


Figure 7.10: The voltage (V) and current (I) curve of the solar panel in half shadow

7.15 Output power characteristics of the solar panel in full shadow

Table 7.9 displays the output power when the solar panel is in half shadow. Figure 7.10 displays the voltage and

Table 7.10 displays the output power when the solar panel is in full shadow. Figure 7.11 displays the voltage and current curve of the solar panel in full shadow.

Table 7.10: Display the difference in output power of the solar panel in full shadow

Resistance	Voltage	Current	Power
Open Circuit	26.11V	0.00A	0.00W
131.3 Ω	9.61V	0.073A	0.75W
55.5 Ω	7.09V	0.128A	0.91W
29.9 Ω	4.92V	0.165A	0.85W

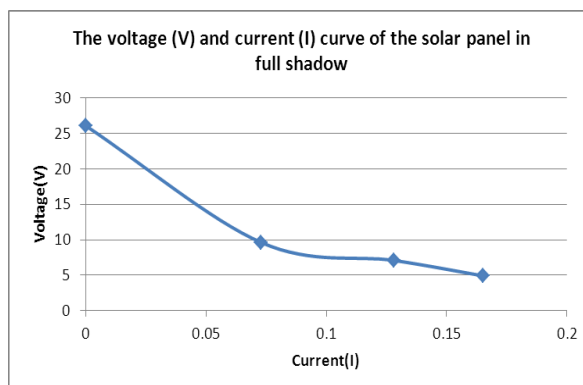


Figure 7.11: The voltage (V) and current (I) curve of the solar panel in full shadow

7.16 Comparison of the output power of the solar panel in direct sunlight, half shadow and full shadow

Figure 7.12 displays the characteristics of the solar panel in direct sunlight, half shadow and full shadow.

Due to the casting of the shadow on the solar panel, there is a significant difference in output power.

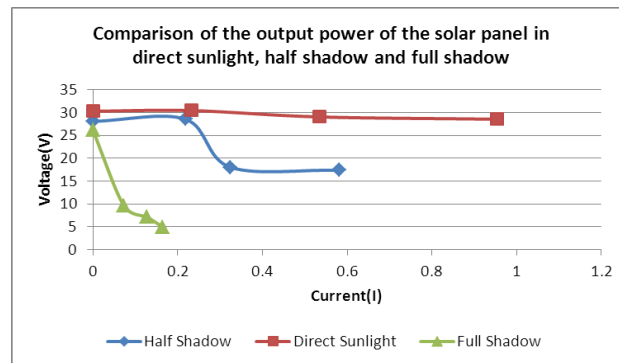


Figure 7.12: Comparison of the output power of the solar panel in direct sunlight, half shadow and full shadow

7.17 The use of the renewable energy or the national grid electrical supply

In section 7.4, the hybrid system is explained and both the national grid as well as the renewable energy system is available to the user. The user can choose to use electricity from the national grid system or from the renewable energy system.

By introducing two types of electrical wall plugs, a green plug for the renewable system and the white plug for the national grid that can be connected to the national supply system, the user can choose between the two energy supply systems. The green plug is designed in such a way that it can be connected to the renewable energy system as well as the national supply where the white plug can only be connected to the national supply. With the DC to AC converter, the supply to the renewable energy system is the same as that of the national grid.

Figure 7.13 displays the design of the green plug and the white plug and the features that allow the green plug to be connected to the renewable energy system as well as the national grid system whereas the white plug can only be connected to the national grid system.

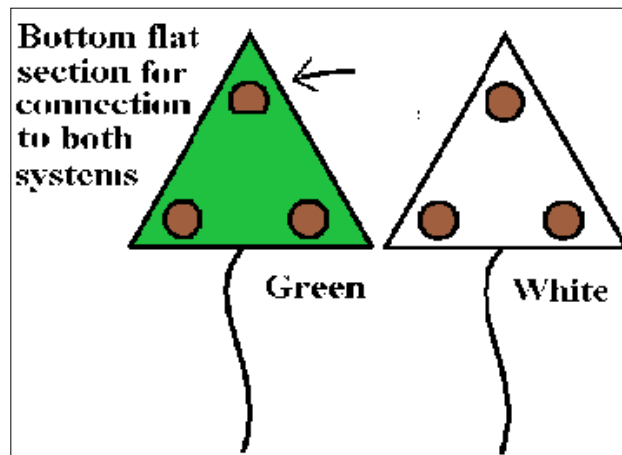


Figure 7.13: Display the two different plugs

7.18 Limitations to consider

The system provides a description on how 3D vision can be used for observation and feedback to optimally use the solar panel. In this experiment, the solar panel was manually moved, but a more in-depth experiment needs to be conducted with a motorised solar panel and the visual system intact. Research also needs to be conducted to investigate why the calculated resistance is different as that of the measured resistance. Walker (2010) indicated that temperature also plays a role in the output performance of a solar panel. An additional temperature reading must be included in future studies.

7.19 Conclusion of chapter 7

The hybrid electrical supply setup with a solar panel can be utilized in a confined space in industry and the solar panel can be reposition to improve efficiency. The description of the implementation of 3D vision for reposition was described. The experimental results indicated that the solar panel produced a 89% increase in efficiency with direct sunlight as when a full shadow is cast on to it.

CHAPTER 8

Measuring the light intensity of a hybrid powered CFL and LED lighting using 3D electronic vision in rotation of the solar panel

8.1 Introduction

In this setup, incandescent, CFL and LED lights are connected to a solar panel and the light intensity is measured. Lighting is required in buildings. Even during daytime, some occupants will have some lights switched on. Buildings can be designed for optimal use of sunlight, but there can be areas that are poorly lighted during daytime. Lighting might be needed in internal rooms and passages. For these areas, lighting powered by a solar panel can be used. An acceptable intensity is required. There are minimum average values of maintained illuminance required and are set out in the Health and Safety Act. These specify 300lux for general offices, 200lux for classrooms and 75lux for passages and lobbies at floor level (<http://www.gbcsa.org.za>). As described by the South African National Standard (SAN 10400 in conjunction with SANS 204-1), the illuminance required for domestic residence with 2 people/bedroom is 100lux.

For electrical supply, a hybrid electrical setup with a solar panel and battery is used. Sungur, 2009, explained to obtain maximum utilization, the solar panel is rotated. The solar panel output is used to power the incandescent, CFL or LED lights. If the output of the solar panel is more than is required, the additional power can be used to charge the battery for night time. If the battery and the solar power are both too low, then the grid power can be used for lighting as well as powering the battery. During daytime, the minimum power must be used for lighting. This paper will explain how 3D electronic vision can be used for rotation of a solar panel in the use of incandescent, CFL or LED lighting and measuring the light intensity.

8.2 Solar energy and angle of sunlight

Maximum output of the solar panel can be obtained when the sun's rays are perpendicular to the solar panel. To ensure the sun's rays fall perpendicular on the solar panel, tracking of the azimuth and solar altitude angles can be used. In this tracking system proposed, 3D vision is used to determine the angle between the sun's rays and the solar panel. The 3D vision system is explained by Nell. et al. 2009. With the angle information available, the solar panel is rotated to ensure the sun's rays fall perpendicular on the solar panel.

Figure 8.1 displays the sun's rays falls at an angle onto the solar panel.

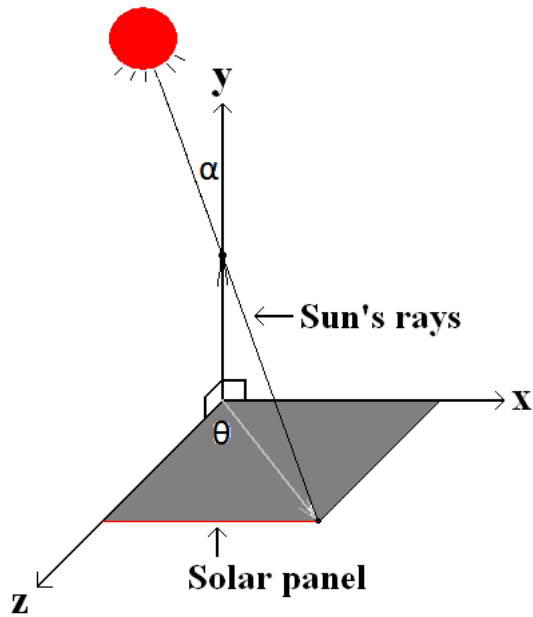


Figure 8.1: The sun's rays falls at an angle onto the solar panel

8.3 Aim

The aim is to describe how 3D electronic vision can be used in rotation of the solar panel for optimal use of sunlight. The light intensity from incandescent light, CFL and LED lighting powered by the solar panel is measured and how the solar panel, battery setup and grid supply can be used in a hybrid electrical setup for both daytime and night time lighting.

8.4 Aim

A hybrid system in this setup is a solar panel connected to a battery system that is in turn connected to a DC to AC converter. To obtain maximum output of the solar panel, the 3D vision system is used to determine the angle between the sun's rays and the solar panel. This angle is used to rotate the solar panel 90° to the sun's rays. Mokoena, 2011 wrote that an efficient lighting system in buildings is of great value.

Figure 8.2 displays a hybrid system that is used to provide power to the light sources to determine the light intensity.

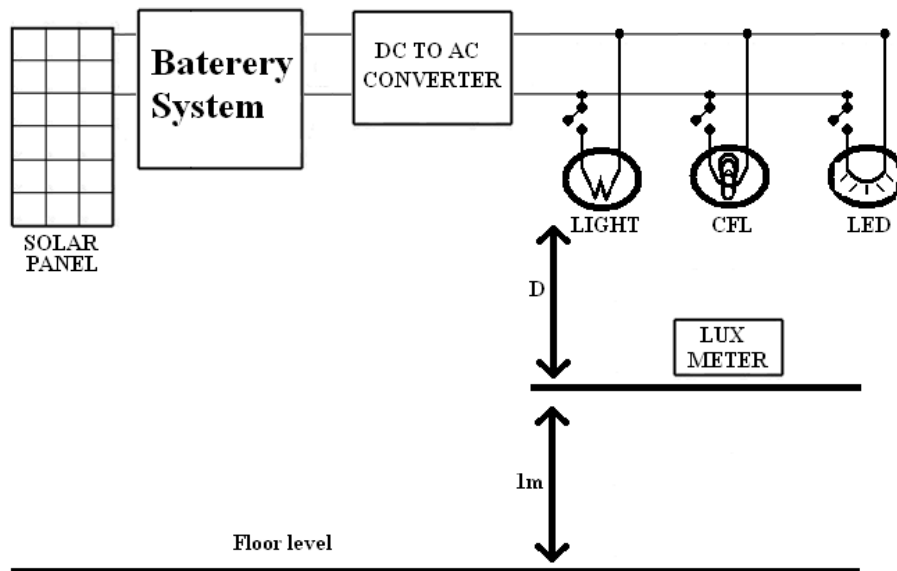


Figure 8.2: A hybrid system that provides electrical supply to the light sources

8.5 Aim

As the solar panel is flat, the horizontal surface of the solar panel is used as the xz -plane as depicted in figure 8.3. When the sun's rays fall at an angle onto the solar panel and a perpendicular reference line is used, then an angle on the xz -plane between the shadow of the erect line and the z -axis and another angle is created between the sun's rays and the y -axis as displayed in figure 8.3. For calculation of these angles, the points X_n , Y_n and Z_n are marked as depicted in figure 8.3.

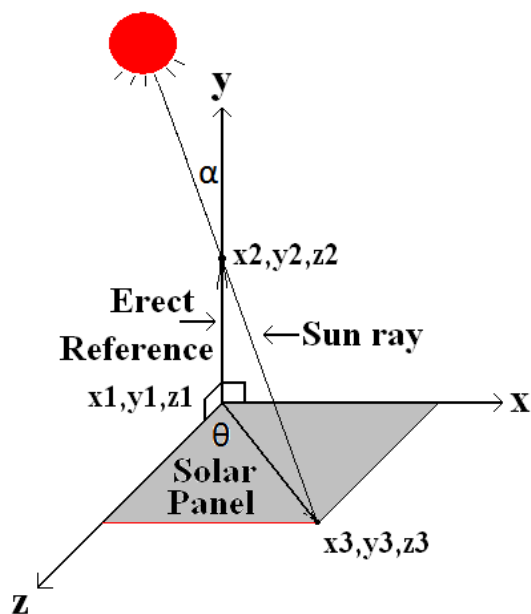


Figure 8.3: Display the angles created by the sun's rays

If the points are reference as (x_1, y_1, z_1) , (x_2, y_2, z_2) and (x_3, y_3, z_3) then the angle α and θ are:

$$\theta = \tan^{-1}\left(\frac{x_3}{z_3}\right) \quad (8.1)$$

$$\alpha = \tan^{-1}\left(\frac{\sqrt{(x_3 - x_1)^2 + (y_3 - y_1)^2}}{y_2}\right) \quad (8.2)$$

or α is,

$$\alpha = \tan^{-1}\left(\frac{\sqrt{y_3^2 + x_3^2}}{y_2}\right) \quad (8.3)$$

By obtaining the angle θ and α , the solar panel can be rotated to ensure the sun's rays are perpendicular to the solar panel.

To obtain the angle as displayed in equations 8.1, 8.2 and 8.3 the coordinates (x_1, y_1, z_1) , (x_2, y_2, z_2) and (x_3, y_3, z_3) need to be determined. To determine these coordinates, the 3D vision camera is used.

Nell. et. al., 2011, described a 3D electronic vision system that can be used to determine the 3D position of an artefact in space. By using this 3D electronic vision system and the perpendicular reference line, the points (x_1, y_1, z_1) , (x_2, y_2, z_2) and (x_3, y_3, z_3) can be determined.

When these points are determined, they can be inserted into equations (8.1), (8.2) and (8.3) and the angles θ and α can be calculated.

By including two axial motors, the solar panel can be rotated to ensure the sun's rays are perpendicular to the solar panel.

8.6 Solar panel output angulated against the sunrays

The solar panel output was determined with the solar rays striking the solar panel at different angles. Ndlovu, 2011 indicated that solar energy as a renewable energy can be used efficiently. The solar panel was rotated 0° , 45° and 90° towards the incoming rays. The difference in output power was determined. Figure 8.4 displays how the solar panel was angulated towards the incoming sunrays.

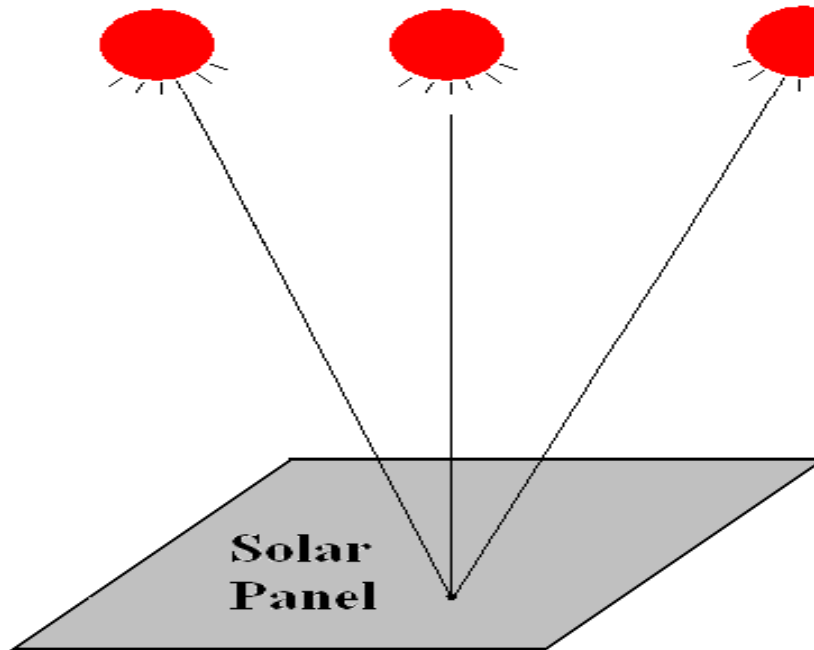


Figure 8.4: Solar panel angulated towards the incoming sunrays

Table 8.1 displays the different output power with the solar panel angulated at 0° , 45° and 90° towards the incoming rays.

Table 8.1: Difference in output power at different angles

Solar panel rotation	Open Circuit Voltage	Voltage Over resistor	Resistance	Power
90°	30.2V	12.6V	58.5 Ω	2.71W
45°	26.5V	9.1V	58.5 Ω	1.42W
0°	21.3V	5.1V	58.5 Ω	0.44W

Figure 8.5 displays the graph of the different output power with the incident rays hitting the solar panel at different angles

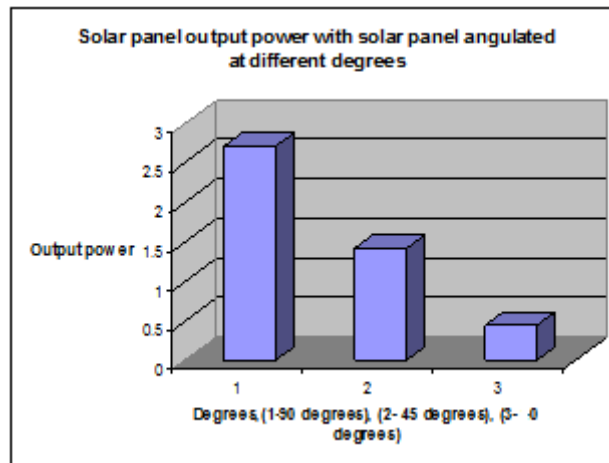


Figure 8.5: Graph of the different output power with the solar panel angled at different angles. Open circuit voltage

When the solar panel is 90° towards the incoming rays, then the highest output power is generated.

8.7 Solar panel output angulated against the sunrays

As determined from the experimental results with the solar panel angled towards the incoming rays, a reduction in output power occur when the rays don't fall 90° onto the solar panel.

In section 8.5, the method and mathematical formulae are described to obtain the angle the solar panel makes towards the incoming rays. By converting the angles obtained to rotation, these two angle values can be inserted into two axial motors and the solar panel can be rotated for the sun's rays to fall 90° onto it.

To rotate the solar panel, first the one rotation is applied and then the second one. After rotation, the solar panel will be perpendicular towards the incoming rays.

Figure 8.6 displays the methods to rotate the solar panel.

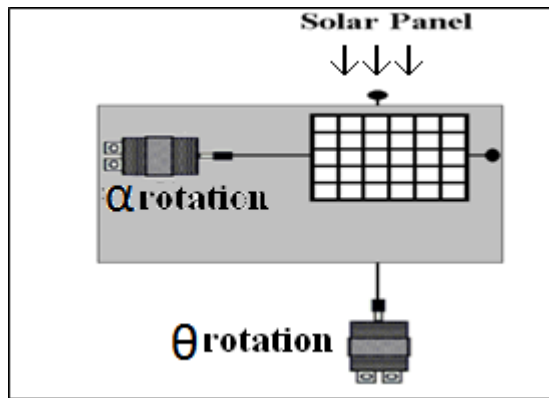


Figure 8.6: Rotation of the solar panel

8.8 Solar panel output angulated against the sunrays

To obtain the different output light intensity from the incandescent, CFL and LED lights, the solar panel was connected in the battery system as displayed in figure8.7.

The incandescent, CFL and LED lights were powered by the solar panel setup.

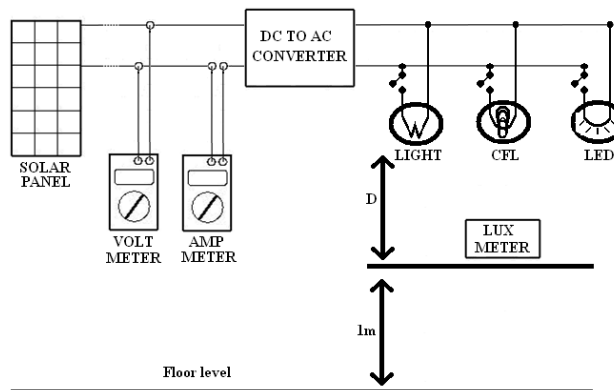


Figure 8.7: Connection and setup of the solar panel with the incandescent, CFL, and LED light

8.8.1 Light intensity output measured of the incandescent, CFL, LED and lights connected to the solar panel

The experiment was done in a room of size, 3m X 7m, with a room light connected to the grid electricity and window available for covering. To obtain no outside light enter the room through the window, the window is covered at certain stages of the measurements. Measurements were taken with the room light (room light which is connected to the grid electricity) on and window not covered, room light off with window not covered and the room light off and window covered.

To obtain the luminance of each light, the other lights as displayed in figure 7, were switched off.

Table 8.2a, Table 8.2b and Table 8.2c display the different light intensity measured with the LED, CFL and the incandescent light on. The lights were switch on individually when the intensity was measured.

Table 8.2a: Light intensity with room light on.

Room luminance measured is 45.2lux

Light source	60 W Incandescent Bulb	11W CFL	15W CFL	5W LED light
Voltage	13.4V	14.08V	13.6V	13.6V
Current	6A	1.6A	1.8A	0.8A
Light Intensity	121.6lux	117.3lux	221.6lux	82.5lux
Power	80.4W	22.53W	24.48W	10.88W

Table 8.2b: Light intensity with room light off, window not covered. Room luminance measured is 0.16lux

Light source	60 W Incandescent light	11W CFL	15W CFL	5W LED light
Voltage	13.4V	14.04V	14.1V	13.6V
Current	6A	1.8A	1.9A	0.8A
Light Intensity	79.5lux	77.4lux	145.3lux	36.1lux
Power	80.4W	25.27W	26.79W	10.88W

Table 8.2c: Light intensity with room light off, window covered. Room luminance is 0.0lux

Light source	60 W Incandescent light	11W CFL	15W CFL	5W LED light
Voltage	13.4V	14.00V	14.1V	13.6V
Current	6A	1.8A	1.9A	0.80A
Light Intensity	75.3lux	94.4lux	172.6lux	32.6lux
Power	80.4W	25.20W	26.79W	10.88W
Light intensity/power at room luminance of 0.0lux				
lux/W	0.94lux/W	3.75lux/W	6.44lux/W	3.00lux/W

A 60W incandescent light, 11W CFL and a 15W CFL were used in the experiment to determine the light intensity and the power was calculated.

8.9 Results obtained

Table 8.2c displays the luminance of the 60W incandescent bulb, 11W CFL, 15CFL and LED light with the luminance in the room measured as 0.0lux.

From the power calculation and light intensity (lux) measured, the lux/W was calculated for every light. The incandescent light produces 0.94lux/W, the 11W CFL 3.75lux/W, the 15W CFL 6.44lux/W and the LED light 3.00lux/W.

From this it indicates that the 15W CFL uses the least power for the highest amount of light intensity (lux) produced.

Figure 8.8 displays the different power as well as the lux measured for each light.

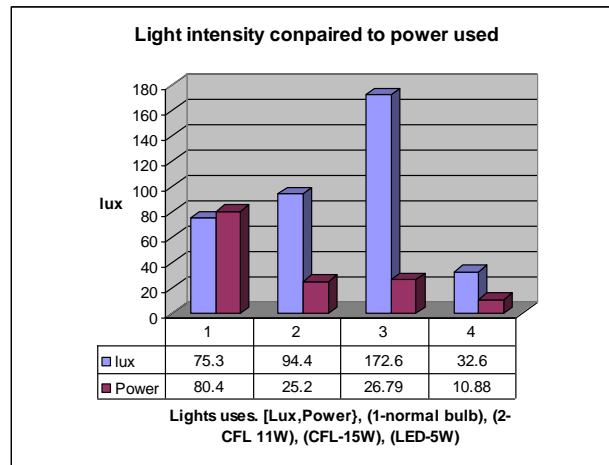


Figure 8.8: Displays both the power as well as the lux measured for every light at room luminance of 0.0lux.

According to figure 8.8, the CFL lights, produced a large amount of light intensity as compared to the amount of power used.

This graphical representation is equivalent to the calculated ratio, Table 8.2C of the lux/W as the CFL lights have a large increase in lux measured as compared to the power used.

8.10 Limitations to consider

The results obtained were done in an experimental setup with the light intensity measured at one point, 1m from the floor area. A more in depth experiment needs to be conducted with the CFL light connected in a existing room fitting or passage and the light intensity measured at different areas.

8.11 Conclusion of chapter 8

From the results, the CFL light produces the highest amount of light intensity. The light intensity measured with the CFL light was higher and this value is higher as that measured with the room lights on and window not covered.

CHAPTER 9

A model to determine the 3D-coordinates of the X-ray focus

9.1 Introduction

X-rays are part of the electromagnetic spectrum. The principles developed previously can also be used in the X-ray spectrum. The position of the X-ray focus is used in the source to image distance. Anterior-posterior (AP) and lateral (LAT) projections are normally done during an X-ray examination. By obtaining the position of the X-ray focus, it can be used to perform 3D measurements of an anatomical structure with the AP and LAT view. Kelly, 2006, indicates there is a need for measurements in radiology. There is a need for the 3D position of the X-ray focus. Palvolgyi, 2012, depicted the position of the X-ray focus in the projections of the needle's tip and the projections of the tip in a paper on Multi-parametric fit method in reconstruction of brachytherapy needles.

9.2 Aim

The aim is to describe a method to determine the 3D xyz-coordinates of the X-ray focus point.

9.3 The X-ray focus

The X-ray focus is the point where the X-rays are generated (Ball. et. al. 1989). An X-ray tube consists of a cathode and anode. It is at a point on the anode where the X-rays are generated, and is called the X-ray focus.

All X-ray foci are not point sources, and can be broad or fine focus. Also X-ray tubes can consist of rotating or stationary anodes.

Figure 9.1 displays an X-ray tube with the X-ray focus.

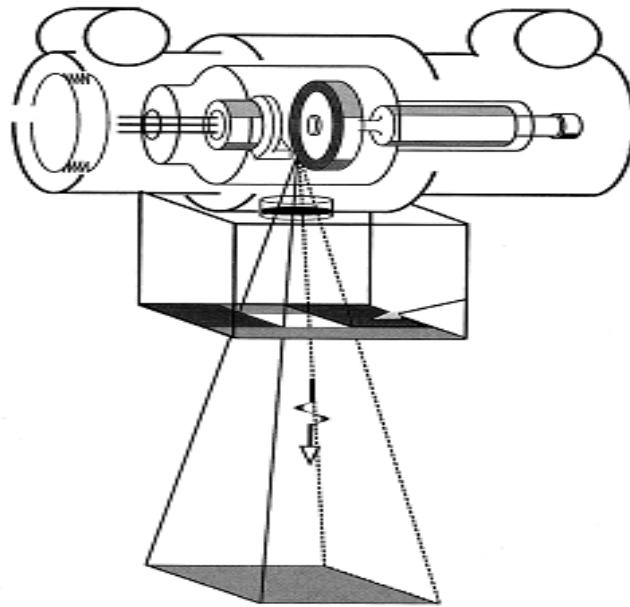


Fig 9.1: X-ray tube with X-rays being generated.
([http://miac.unibas.ch/PMI/01-BasicsOfXray.html#\(12\)](http://miac.unibas.ch/PMI/01-BasicsOfXray.html#(12))))

9.4 Method

The method used is to obtain the 3D xyz-coordinates of two artefact points in the X-ray field. With the 3D-coordinates of these two artefact points, their corresponding 3D xyz-coordinates on the X-ray image are determined.

To obtain an X-ray image with two artefact points, a metallic plate with two pinholes can be used. Figure 9.2 and figure 9.2a display the setup with a metallic plate with two pinholes and the image plane in the setup to determine the position of the X-ray focus.

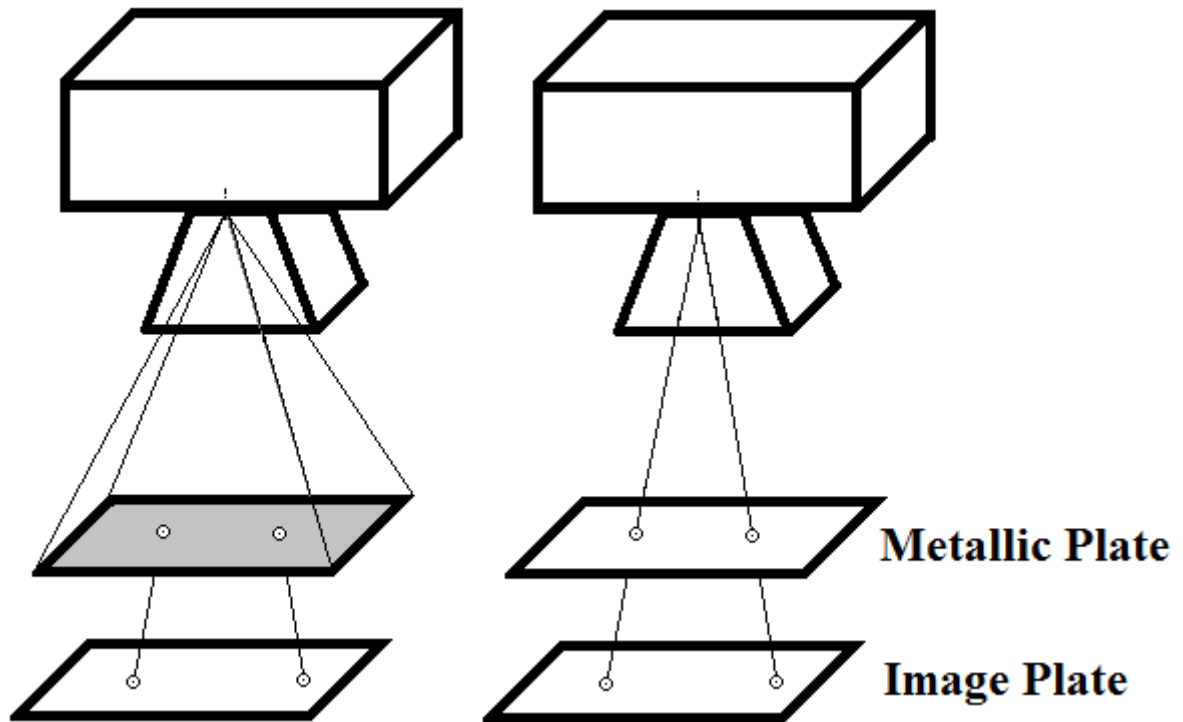


Fig 9.2: 3D Setup to determine the position of the pinhole and pinhole images. Only the pinhole image will be produced (right)

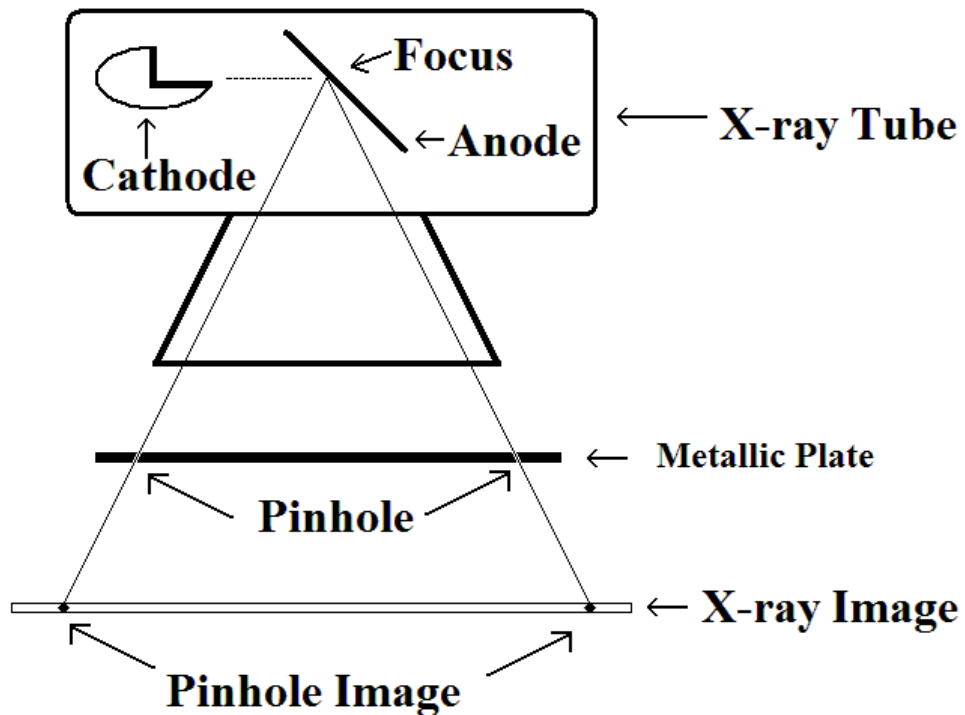


Fig 9.2a: Method to determine the xyz-position of the pinhole and pinhole images

As from figure 9.2, it indicates that two image lines are generated. The two image lines are from the different pinholes to the pinhole images on the image plate. As these two lines originate from the focus point, it indicates that these two lines intersect at the focus point.

By determining the intersection point of these two image lines, the 3D xyz-coordinates of the focus point can be determined.

9.5 Points used to generate the two image lines

From figure 9.2, the two image lines that are produced, are the one from the X-ray focus, through the left pinhole onto the image plate and the second image line is from the X-ray focus, through the right pinhole onto the image plate.

Both the pinhole points on the metallic plate as well as the pinhole points on the image plate will be described by their 3D xyz-coordinates. By using the information of the pinholes and the position of the pinhole images, the xyz-coordinates of the focus point will be calculated.

All lines in 3D space do not intersect, but as describe from above, both image lines originate from the same point, indicating an intersection point.

9.6 Mathematical method to determine the intersecting point of two lines in 3D

To determine the intersecting point of two lines in 3D

Let

$$P_1 = (x_1, y_1, z_1)$$

$$P_2 = (x_2, y_2, z_2)$$

$$P_3 = (x_3, y_3, z_3)$$

$$P_4 = (x_4, y_4, z_4)$$

As displayed in figure 9.3

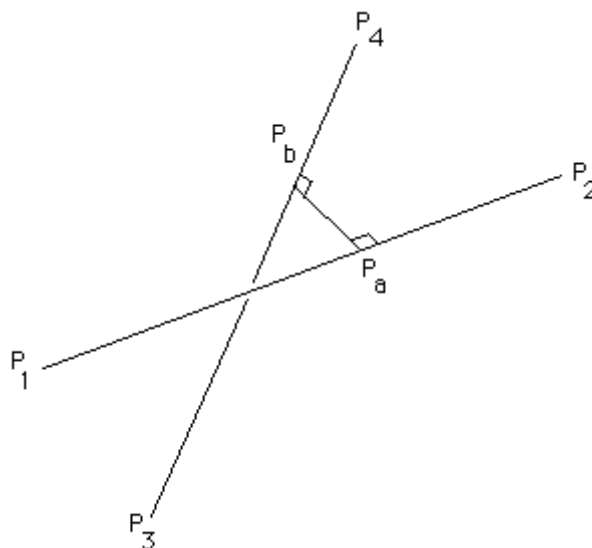


Figure 9.3: Setup to determined the shortest distance between two lines in 3D

Then as per equation (3.25), equation (3.26) and equation (3.26), the coordinates of the intersecting point are:

$$x_{ab} = \frac{x_a + x_b}{2} \quad (9.1)$$

$$y_{ab} = \frac{y_a + y_b}{2} \quad (9.2)$$

$$z_{ab} = \frac{z_a + z_b}{2} \quad (9.3)$$

with $x_a, y_a, x_b, y_b, z_a, z_b$ as:

$$x_a = \left(x_1 + \left(\frac{(((d1343)(d4321)) - ((d1321)(d4343)))}{(((d2121)(d4343)) - ((d4321)(d4321)))} \right) (x_2 - x_1) \right) \quad (9.4)$$

$$x_b = \left(x_3 + \left(\frac{\left(d1343 + d4321 \left(\frac{(((d1343)(d4321)) - ((d1321)(d4343)))}{(((d2121)(d4343)) - ((d4321)(d4321)))} \right) \right)}{d4343} \right) (x_4 - x_3) \right) \quad (9.5)$$

$$y_a = y_1 + \left(\left(\frac{(((d1343)(d4321)) - ((d1321)(d4343)))}{(((d2121)(d4343)) - ((d4321)(d4321)))} \right) (y_2 - y_1) \right) \quad (9.6)$$

$$y_b = y_2 + \left(\left(d1343 + \left(\frac{\left((d4321) \left(\frac{(((d1343)(d4321)) - ((d1321)(d4343)))}{(((d2121)(d4343)) - ((d4321)(d4321)))} \right) \right)}{d4343} \right) \right) (y_4 - y_3) \right) \quad (9.7)$$

$$z_a = z_1 + \left(\left(\frac{(((d1343)(d4321)) - ((d1321)(d4343)))}{(((d2121)(d4343)) - ((d4321)(d4321)))} \right) (z_2 - z_1) \right) \quad (9.8)$$

$$z_b = z_3 + \left(\frac{\left((d1343) + \left((d4321) \left(\frac{(((d1343)(d4321)) - ((d1321)(d4343)))}{(((d2121)(d4343)) - ((d4321)(d4321)))} \right) \right) \right)}{d4343} \right) (z_4 - z_3) \quad (9.9)$$

and

$$d1343 = ((x_1 - x_3)(x_4 - x_3)) + ((y_1 - y_3)(y_4 - y_1)) + ((z_1 - z_3) - (z_4 - z_3)) \quad (9.10)$$

$$d4321 = ((x_4 - x_3)(x_2 - x_1)) + ((y_4 - y_3)(y_2 - y_1)) + ((z_4 - z_3) - (z_2 - z_1)) \quad (9.11)$$

$$d1321 = ((x_1 - x_3)(x_2 - x_1)) + ((y_1 - y_3)(y_2 - y_1)) + ((z_1 - z_3) - (z_2 - z_1)) \quad (9.12)$$

$$d4343 = ((x_4 - x_3)(x_4 - x_3)) + ((y_4 - y_3)(y_4 - y_3)) + ((z_4 - z_3) - (z_4 - z_3)) \quad (9.13)$$

$$d2121 = ((x_2 - x_1)(x_2 - x_1)) + ((y_2 - y_1)(y_2 - y_1)) + ((z_2 - z_1) - (z_2 - z_1)) \quad (9.14)$$

9.7 Mathematical method to determine the shortest distance between two lines in 3D

To determine the distance between point (a) and point (b), the distance formulae (d_{ab} , equation 9.15) is used (Bester, et. al. 1998).

$$d_{ab} = \sqrt{(x_a - x_b)^2 + (y_a - y_b)^2 + (z_a - z_b)^2} \quad (9.15)$$

and the xyz-coordinates of the midpoint (x_{ab} , y_{ab} , z_{ab}) are:

$$x_{ab} = \frac{(x_a + x_b)}{2} \quad (9.16)$$

$$y_{ab} = \frac{(y_a + y_b)}{2} \quad (9.17)$$

$$z_{ab} = \frac{(z_a + z_b)}{2} \quad (9.18)$$

From equation 1.14 and equation 1.15 with mu_a and mu_b describe in equation 1.11 and equation 1.13 gives:

$$x_a = \left(x_1 + \left(\frac{(((d1343)(d4321)) - ((d1321)(d4343)))}{(((d2121)(d4343)) - ((d4321)(d4321)))} \right) (x_2 - x_1) \right) \quad (9.19)$$

$$x_b = \left(x_3 + \left(\frac{\left(d1343 + d4321 \left(\frac{\left(\left((d1343)(d4321) \right) - \left((d1321)(d4343) \right) \right)}{\left(\left((d2121)(d4343) \right) - \left((d4321)(d4321) \right) \right) \right)}{d4343} \right) \right) (x_4 - x_3) \right) \quad (9.20)$$

$$y_a = y_1 + \left(\frac{\left(\left((d1343)(d4321) \right) - \left((d1321)(d4343) \right) \right)}{\left(\left((d2121)(d4343) \right) - \left((d4321)(d4321) \right) \right)} (y_2 - y_1) \right) \quad (9.21)$$

$$y_b = y_2 + \left(\left(d1343 + \left(\frac{\left((d4321) \left(\frac{\left(\left((d1343) (d4321) \right) - \left((d1321) (d4343) \right) \right)}{\left(\left((d2121) (d4343) \right) - \left((d4321) (d4321) \right) \right) \right)}{d4343} \right) \right) (y_4 - y_3) \right) \quad (9.22)$$

$$z_a = z_1 + \left(\frac{\left(\left((d1343) (d4321) \right) - \left((d1321)(d4343) \right) \right)}{\left(\left((d2121) (d4343) \right) - \left((d4321) (d4321) \right) \right)} (z_2 - z_1) \right) \quad (9.23)$$

$$z_b = z_3 + \left(\frac{\left((d1343) + \left((d4321) \left(\frac{\left(\left((d1343) (d4321) \right) - \left((d1321) (d4343) \right) \right)}{\left(\left((d2121) (d4343) \right) - \left((d4321) (d4321) \right) \right) \right)}{d4343} \right) \right) (z_4 - z_3) \right) \quad (9.24)$$

With

$$d_{1343} = ((x_1 - x_3)(x_4 - x_3)) + ((y_1 - y_3)(y_4 - y_1)) + ((z_1 - z_3) - (z_4 - z_3)) \quad (9.25)$$

$$d_{4321} = ((x_4 - x_3)(x_2 - x_1)) + ((y_4 - y_3)(y_2 - y_1)) + ((z_4 - z_3) - (z_2 - z_1)) \quad (9.26)$$

$$d_{1321} = ((x_1 - x_3)(x_2 - x_1)) + ((y_1 - y_3)(y_2 - y_1)) + ((z_1 - z_3) - (z_2 - z_1)) \quad (9.27)$$

$$d_{4343} = ((x_4 - x_3)(x_4 - x_3)) + ((y_4 - y_3)(y_4 - y_3)) + ((z_4 - z_3) - (z_4 - z_3)) \quad (9.28)$$

$$d_{2121} = ((x_2 - x_1)(x_2 - x_1)) + ((y_2 - y_1)(y_2 - y_1)) + ((z_2 - z_1) - (z_2 - z_1)) \quad (9.29)$$

then inserting (P_{ab}) with $P1$, $P2$, $P3$ and $P4$ gives:

$$x_{ab} = \frac{x_a + x_b}{2} \quad (9.30)$$

$$y_{ab} = \frac{y_a + y_b}{2} \quad (9.31)$$

$$z_{ab} = \frac{z_a + z_b}{2} \quad (9.32)$$

With:

The distance between point (a) and point (b) as:

$$d_{ab} = \sqrt{(x_a - x_b)^2 + (y_a - y_b)^2 + (z_a - z_b)^2} \quad (9.33)$$

9.8 Coordinates of the focus point

Figure 9.4 displays the focus point of the X-ray tube assembly.

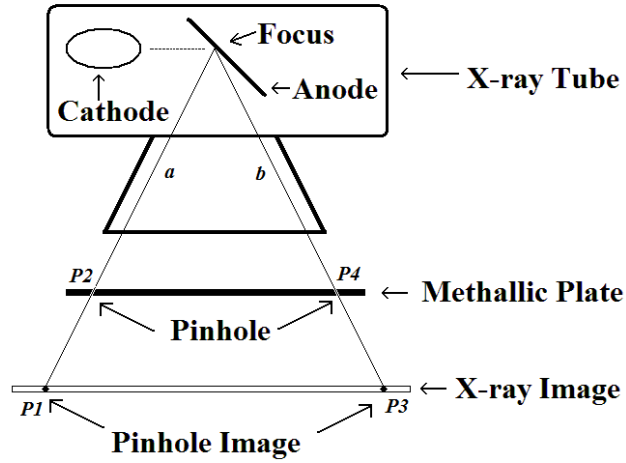


Figure 9.4: Focus point of the X-ray tube setup

Let

$$P_1 = (x_1, y_1, z_1)$$

$$P_2 = (x_2, y_2, z_2)$$

$$P_3 = (x_3, y_3, z_3)$$

$$P_4 = (x_4, y_4, z_4)$$

Then as per equation (3.25), equation (3.26) and equation (3.27), the coordinates of the X-ray focus are:

$$x_{ab} = \frac{x_a + x_b}{2} \tag{9.34}$$

$$y_{ab} = \frac{y_a + y_b}{2} \tag{9.36}$$

$$z_{ab} = \frac{z_a + z_b}{2} \tag{9.37}$$

with $x_a, y_a, x_b, y_b, z_a, z_b$ as:

$$x_a = \left(x_1 + \left(\frac{(((d1343)(d4321)) - ((d1321)(d4343)))}{(((d2121)(d4343)) - ((d4321)(d4321)))} \right) (x_2 - x_1) \right) \quad (9.38)$$

$$x_b = \left(x_3 + \left(\frac{d1343 + d4321 \left(\frac{(((d1343)(d4321)) - ((d1321)(d4343)))}{(((d2121)(d4343)) - ((d4321)(d4321)))} \right)}{d4343} \right) (x_4 - x_3) \right) \quad (9.39)$$

$$y_a = y_1 + \left(\frac{(((d1343)(d4321)) - ((d1321)(d4343)))}{(((d2121)(d4343)) - ((d4321)(d4321)))} (y_2 - y_1) \right) \quad (9.40)$$

$$y_b = y_2 + \left(\left(d1343 + \left(\frac{(d4321) \left(\frac{(((d1343) (d4321)) - ((d1321) (d4343)))}{(((d2121) (d4343)) - ((d4321) (d4321)))} \right)}{d4343} \right) \right) (y_4 - y_3) \right) \quad (9.41)$$

$$z_a = z_1 + \left(\frac{(((d1343) (d4321)) - ((d1321)(d4343)))}{(((d2121) (d4343)) - ((d4321) (d4321)))} (z_2 - z_1) \right) \quad (9.42)$$

$$z_b = z_3 + \left(\frac{\left((d1343) + \left((d4321) \left(\frac{((d1343)(d4321)) - ((d1321)(d4343))}{((d2121)(d4343)) - ((d4321)(d4321))} \right) \right) \right)}{d4343} \right) (z_4 - z_3) \quad (9.43)$$

and

$$d1343 = ((x_1 - x_3)(x_4 - x_3)) + ((y_1 - y_3)(y_4 - y_1)) + ((z_1 - z_3) - (z_4 - z_3)) \quad (9.44)$$

$$d4321 = ((x_4 - x_3)(x_2 - x_1)) + ((y_4 - y_3)(y_2 - y_1)) + ((z_4 - z_3) - (z_2 - z_1)) \quad (9.45)$$

$$d1321 = ((x_1 - x_3)(x_2 - x_1)) + ((y_1 - y_3)(y_2 - y_1)) + ((z_1 - z_3) - (z_2 - z_1)) \quad (9.46)$$

$$d4343 = ((x_4 - x_3)(x_4 - x_3)) + ((y_4 - y_3)(y_4 - y_3)) + ((z_4 - z_3) - (z_4 - z_3)) \quad (9.47)$$

$$d2121 = ((x_2 - x_1)(x_2 - x_1)) + ((y_2 - y_1)(y_2 - y_1)) + ((z_2 - z_1) - (z_2 - z_1)) \quad (9.48)$$

9.9 Discussion

By obtaining the xyz-coordinates of an X-ray focus, linear 3D measurements can be performed if two x-ray images are obtained.

To obtain any linear distance between two points in 3D, the following formula is used:

$$d = \sqrt{(x_2 - x_1)^2 + (y_2 - y_1)^2 + (z_2 - z_1)^2} \quad (9.50)$$

This indicates that if the xyz-coordinates of two 3D points can be determined, then the relative distance in 3D space with two x-ray images can be obtained.

Then by identifying any two points on the AP and LAT X-ray examination, the distance of the length on X-rays can be determined with plain X-ray imaging. Figure 9.5 displays a schematic of the setup to determine the 3D measurement with an AP and LAT view.

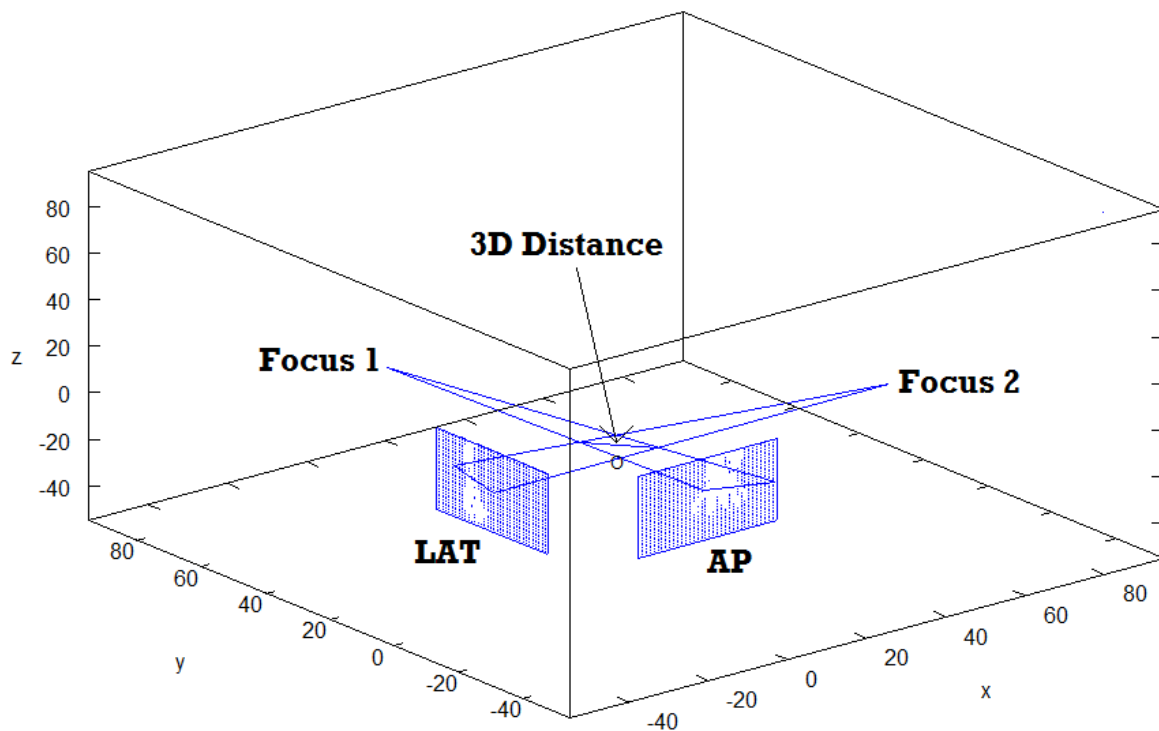


Fig 9.5: Schematic of the setup to determine the 3D distance with an AP and LAT view

Also another application is when the xyz-coordinates of a laser point is described and with the xyz-coordinates of the X-ray focus, the distance between the laser point and the X-ray focus can be determined.

Above are possible applications in application when the xyz-coordinates of the X-ray focus are obtained. Future research needs to be conducted to investigate applications of this model.

This paper describes the mathematical model to determine the 3D xyz-coordinates of the X-ray focus.

9.10 Limitations to consider

As described previously, X-rays are not generated from a point source, but the X-ray focus can be fine focus or broad focus. In this case the X-rays are being generated from a small surface area.

The above method described a method to determine the X-ray focus of a point source, but additional research needs to be performed to investigate fine and broad focus.

9.11 Conclusion of chapter 9

The model to determine the coordinates of the focus point was described.

The mathematical formulae to determine the 3D position of the X-ray focus has been derived. With this point available, measurements in 3D can be performed using the distance formula. If two X-ray exposures with the artefact in both X-ray image, then the relative distance of the object from another point can be determined. This provides the opportunity to do 3D measurements on standard AP and LAT X-ray views.

Additional research needs to be performed to apply this method in determining relative distances.

Also as X-rays follow the reverse square rule, by obtaining the distance of the X-ray focus to the patient can provide an indication in application of the reverse square rule⁹.

A model to determine the position of the X-ray focus point has been described.

CHAPTER 10

A method to determine and calculate the distance between the X-ray focus and the patient skin surface without any interaction with the patient

10.1 Introduction

The distance of the X-ray focus and the image plane are normally displayed on the X-ray Machine and can also be measured by the radiographer. The distance between the X-ray focus and the patient skin defers from patient to patient. As the topography of every patient varies, the distance from the X-ray focus and patient skin surface can be measured with interaction with the patient. This indicates that an area of interest on the patient, a measurement needs to be done. This will have multiple interactions with the patient. With this method proposed, the distance from the X-ray focus and the patient skin distance can be determined with no interaction with the patient. Not just vertical or horizontal distances can be determined, but also distances at any angle the X-ray tube have with a point on the patient skin surface.

10.2 Aim

The aim is to describe a method to determine and calculate the distance between the X-ray tube and the patient skin surface without any interaction with the patient.

10.3 The X-ray focus

The X-ray focus is the point where the X-rays are generated (Ball. et. al. 1989). An X-ray tube consists of a cathode and anode. It is at this point on the anode where the X-rays are generated, and is called the X-ray focus.

All X-ray foci are not point sources, and can be broad or fine focus. Also X-ray tubes can consist of rotating or stationary anodes.

Figure 10.1 displays an X-ray tube with the X-ray focus.

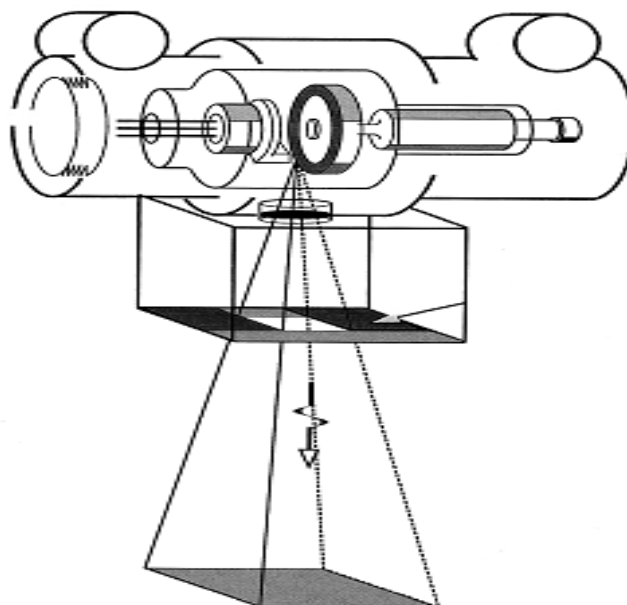


Fig 10.1: X-ray tube with X-rays being generated.
([http://miac.unibas.ch/PMI/01-BasicsOfXray.html#\(6\)](http://miac.unibas.ch/PMI/01-BasicsOfXray.html#(6)))

10.4 Point of interest on patient skin surface

The point of interest on patient skin surface is any point visible to measure the distance between the X-ray focus and the skin surface.

Figure 10.2 displays an image of a patient with the point of interest. Also a graphical setup is depicted explaining the distance that is of interest between the patient skin surface and X-ray focus.

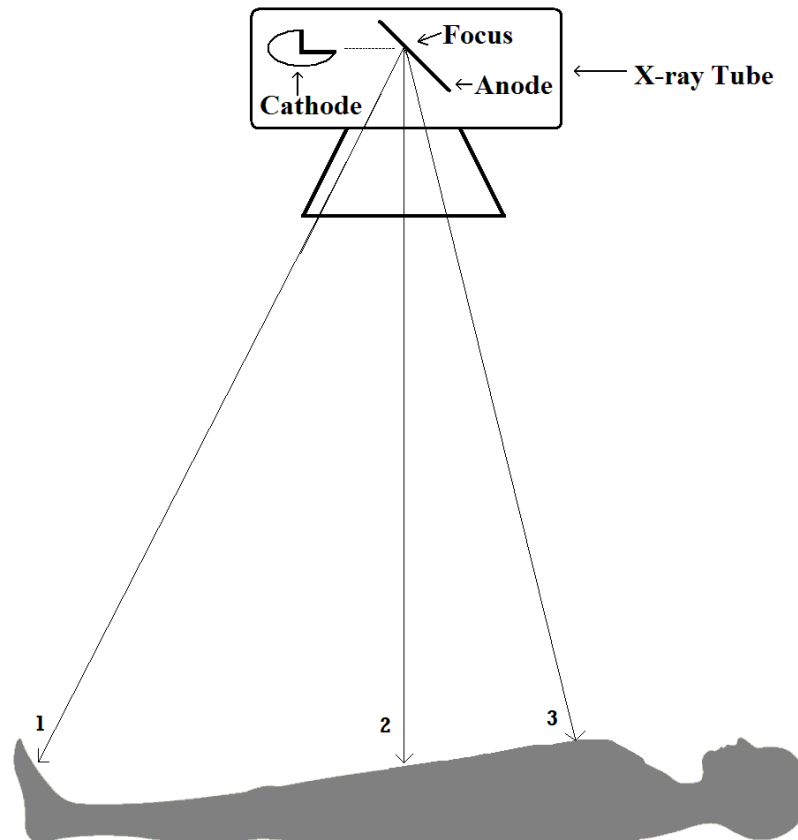


Fig 10.2: Measuring the distance between the patient skin surface and the X-ray focus

10.5 Method to determine the distance

As explained in the introduction, the method applied is to determine the xyz-coordinates of the X-ray focus as well as the xyz-coordinates of the point of interest on the patient skin surface and use the linear formulae to calculate the distance.

Formula 10.1 displays the distance formula. If the position of the X-ray focus is (x_1, y_1, z_1) and the position of the point on the patient skin surface is (x_2, y_2, z_2) , then the distance (d) between point 1 and point 2 can be calculated as:

$$d = \sqrt{(x_2 - x_1)^2 + (y_2 - y_1)^2 + (z_2 - z_1)^2} \quad (10.1)$$

Figure 10.3 depict the two points of interest to be determined to calculate the distance between the X-ray focus and the patient skin surface.

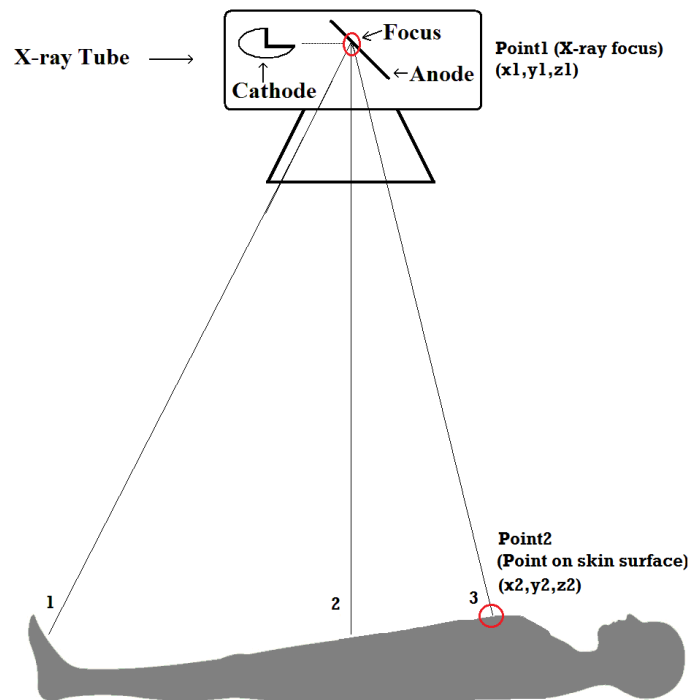


Fig 10.3: Points of interest to measure the distance between the patient skin surface and the X-ray focus

Firstly the method to determine the xyz-of the X-ray focus is explained. Then the method to determine the xyz-of the position on the patient skin surface is explained.

10.6 Coordinates of the focus point

Figure 10.4 displays the focus point and the X-ray tube assembly.

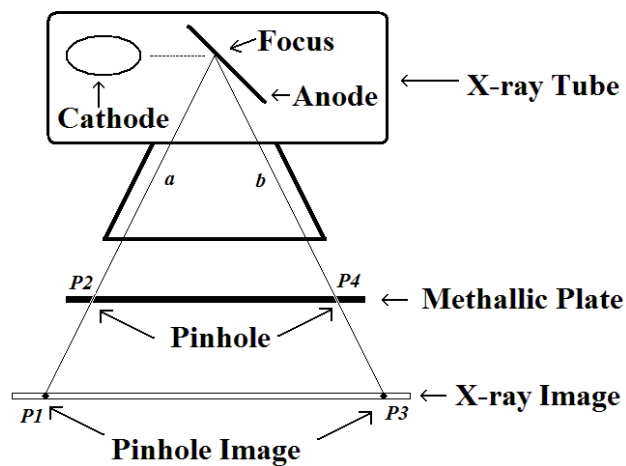


Fig 10.4: Focus point of the X-ray tube setup

Let

$$P_1 = (x_1, y_1, z_1)$$

$$P_2 = (x_2, y_2, z_2)$$

$$P_3 = (x_3, y_3, z_3)$$

$$P_4 = (x_4, y_4, z_4)$$

Then as per equation (3.25), equation (3.26) and equation (3.27) the coordinates of the X-ray focus are:

$$x_{ab} = \frac{x_a + x_b}{2} \quad (10.2)$$

$$y_{ab} = \frac{y_a + y_b}{2} \quad (10.3)$$

$$z_{ab} = \frac{z_a + z_b}{2} \quad (10.4)$$

with $x_a, y_a, x_b, y_b, z_a, z_b$ as:

$$x_a = \left(x_1 + \left(\frac{(((d1343)(d4321)) - ((d1321)(d4343)))}{(((d2121)(d4343)) - ((d4321)(d4321)))} \right) (x_2 - x_1) \right) \quad (10.5)$$

$$x_b = \left(x_3 + \left(\frac{\left(d1343 + d4321 \left(\frac{(((d1343)(d4321)) - ((d1321)(d4343)))}{(((d2121)(d4343)) - ((d4321)(d4321)))} \right) \right)}{d4343} \right) (x_4 - x_3) \right) \quad (10.6)$$

$$y_a = y_1 + \left(\frac{(((d1343)(d4321)) - ((d1321)(d4343)))}{(((d2121)(d4343)) - ((d4321)(d4321)))} \right) (y_2 - y_1) \quad (10.7)$$

$$y_b = y_2 + \left(\left(d1343 + \left(\frac{(d4321) \left(\frac{(((d1343) (d4321)) - ((d1321) (d4343)))}{(((d2121) (d4343)) - ((d4321) (d4321)))} \right) \right)}{d4343} \right) \right) (y_4 - y_3) \quad (10.8)$$

$$z_a = z_1 + \left(\left(\frac{(((d1343) (d4321)) - ((d1321)(d4343)))}{(((d2121) (d4343)) - ((d4321) (d4321)))} \right) (z_2 - z_1) \right) \quad (10.9)$$

$$z_b = z_3 + \left(\left(\frac{\left((d1343) + \left((d4321) \left(\frac{(((d1343) (d4321)) - ((d1321) (d4343)))}{(((d2121) (d4343)) - ((d4321) (d4321)))} \right) \right) \right)}{d4343} \right) (z_4 - z_3) \right) \quad (10.10)$$

and

$$d1343 = ((x_1 - x_3)(x_4 - x_3)) + ((y_1 - y_3)(y_4 - y_1)) + ((z_1 - z_3) - (z_4 - z_3)) \quad (10.11)$$

$$d4321 = ((x_4 - x_3)(x_2 - x_1)) + ((y_4 - y_3)(y_2 - y_1)) + ((z_4 - z_3) - (z_2 - z_1)) \quad (10.12)$$

$$d1321 = ((x_1 - x_3)(x_2 - x_1)) + ((y_1 - y_3)(y_2 - y_1)) + ((z_1 - z_3) - (z_2 - z_1)) \quad (10.13)$$

$$d4343 = ((x_4 - x_3)(x_4 - x_3)) + ((y_4 - y_3)(y_4 - y_3)) + ((z_4 - z_3) - (z_4 - z_3)) \quad (10.14)$$

$$d2121 = ((x_2 - x_1)(x_2 - x_1)) + ((y_2 - y_1)(y_2 - y_1)) + ((z_2 - z_1) - (z_2 - z_1)) \quad (10.15)$$

10.7 Method to determine the xyz-coordinates of the point on the patient skin surface

The method used is to obtain the 3D xyz-coordinates of the point of interest on the patient skin surface, is to use a distance laser pointer. The distance laser pointer measures the linear distance between the image plane and the laser point in vision.

To optimally use the distance of the laser pointer to the patient skin surface, the radius and the angles of rotation are used. The distance measured by the laser pointer is the radius. To obtain the angular rotation, the rotation angle around the x-axis, y-axis and z-axis is determined, the Euler angles.

To use the radius as well as the Euler angles, the spherical coordinates needs to be converted to xyz-coordinates. To determine the distance between the patient skin surface and the X-ray focus, the distance formulae can be used. The distance formula use xyz-coordinates. The coordinates of the X-ray focus is determined in the xyz-format. The position of the point of interest on the patient skin surface needs to be determined in the xyz-format to apply the distance formula. Thus the radius as well as the Euler angles, the spherical coordinates needs to be converted to xyz-coordinates.

The following displays the mathematical configuration to determine the xyz-coordinates is the radius and Euler angles are available.

10.8 Converting the radius and Euler angles to xyz-coordinates

Figure 10.5 displays the setup to with the radius as well as the rotation around the x-axis and the rotation around the y-axis.

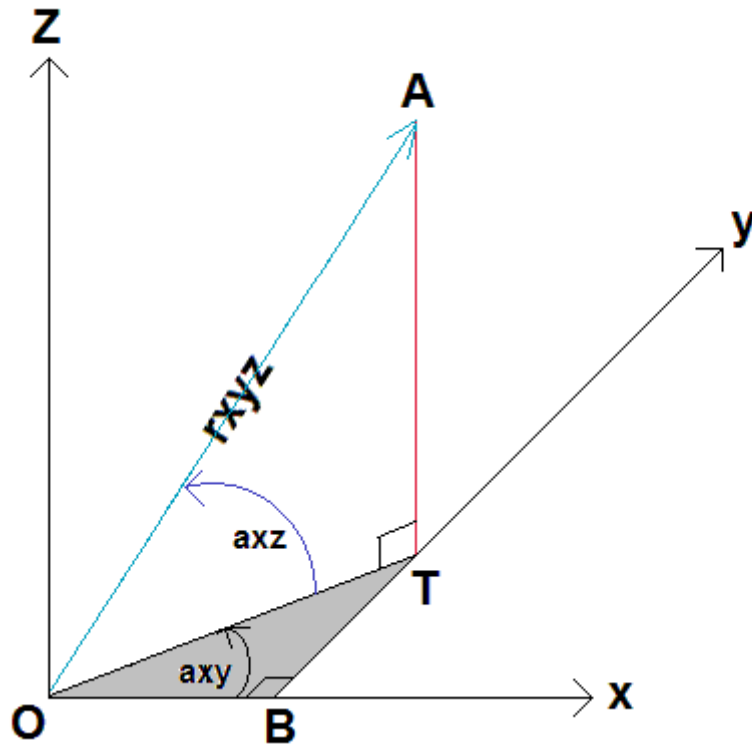


Fig. 10.5: Display of the radius and the rotations

Let:

- r_{xyz} : be the radius,
- axy : the rotation around the z-axis.
- axz : the rotation around the y-axis.
- AT : the horizontal distance from the radius to the xy-plane and
- O : the origin

Then

the vertical distance AT , z-coordinate of the radius to the xy-plane is:

$$z = r_{xyz} \sin(a_{xz}) \quad (\text{from triangle } \mathbf{OAT}) \quad (10.16)$$

But in triangle \mathbf{OAT} is:

$$OT = \sqrt{r_{xyz}^2 - z^2} \quad (10.17)$$

The x-coordinate is:

$$x = OT \cos(a_{xy}) \quad (\text{from triangle } \mathbf{OTB}) \quad (10.18)$$

Replace **OT** gives:

$$x = \sqrt{r_{xyz}^2 - z^2} \cos(a_{xy}) \quad (10.19)$$

The y-coordinate is:

$$y = OT \sin(a_{xy}) \quad (\text{from triangle } \mathbf{OTB}) \quad (10.20)$$

in triangle **OTB**.

Replace **OT** gives:

$$y = \sqrt{r_{xyz}^2 - z^2} \sin(a_{xy}) \quad (10.21)$$

Then the xyz-coordinates with the radius and Euler angles as displayed in figure 7 are:

$$x = \sqrt{r_{xyz}^2 - (r_{xyz} \sin(a_{xz}))^2} \cos(a_{xy}) \quad (10.22)$$

$$y = \sqrt{r_{xyz}^2 - (r_{xyz} \sin(a_{xz}))^2} \sin(a_{xy}) \quad (10.23)$$

$$z = r_{xyz} \sin(a_{xz}) \quad (10.24)$$

10.9 The distance between the X-ray focus and a point of interest on the patient skin surface

To determine the distance between the X-ray focus and a point of interest on the patient skin surface, the distance formula is used.

Let **(xf,yf,zf)** be the xyz-coordinates of the X-ray focus and **(xs,ys,zs)** be the xyz-coordinates of the point of interest on the patient skin surface.

Then the distance between the X-ray focus and the point of interest on the patient skin is:

$$d_{xs} = \sqrt{(x_f - x_s)^2 + (y_f - y_s)^2 + (z_f - z_s)^2} \quad (10.25)$$

with

$$x = \sqrt{r_{xyz}^2 - (r_{xyz} \sin(a_{xz}))^2} \cos(a_{xy}) \quad (10.26)$$

$$y = \sqrt{r_{xyz}^2 - (r_{xyz} \sin(a_{xz}))^2} \sin(a_{xy}) \quad (10.27)$$

$$z = r_{xyz} \sin(a_{xz}) \quad (10.28)$$

axy and axz displayed in figure 10.5.

The xyz-coordinates of the X-ray focus (**xf, yf, zf**) can be displayed as:

$$x_{ab} = \frac{x_a + x_b}{2} \quad (10.29)$$

$$y_{ab} = \frac{y_a + y_b}{2} \quad (10.30)$$

$$z_{ab} = \frac{z_a + z_b}{2} \quad (10.40)$$

with $x_a, y_a, x_b, y_b, z_a, z_b$ as described in equations 10.5 to 10.10.

10.10 Setup to measure the distance from the X-ray focus to patient skin surface

The setup to measure the distance from the X-ray focus and point of interest on patient skin surface is displayed in figure 10.6. To obtain the measured radius, a distance laser measured pointer can be used. Also the Euler angles of interest need to be obtained. When determining the xyz-coordinates of the X-ray focus it also needs to be obtained with the same origin from where the measured radius is measured. If it is not the same origin, then translation and rotation at a point other than the origin needs to be applied. The formulae to obtain the X-ray focus or the radius point if the radius point or the X-ray focus is not described with the same origin is not described in this paper. This can be done for further research.

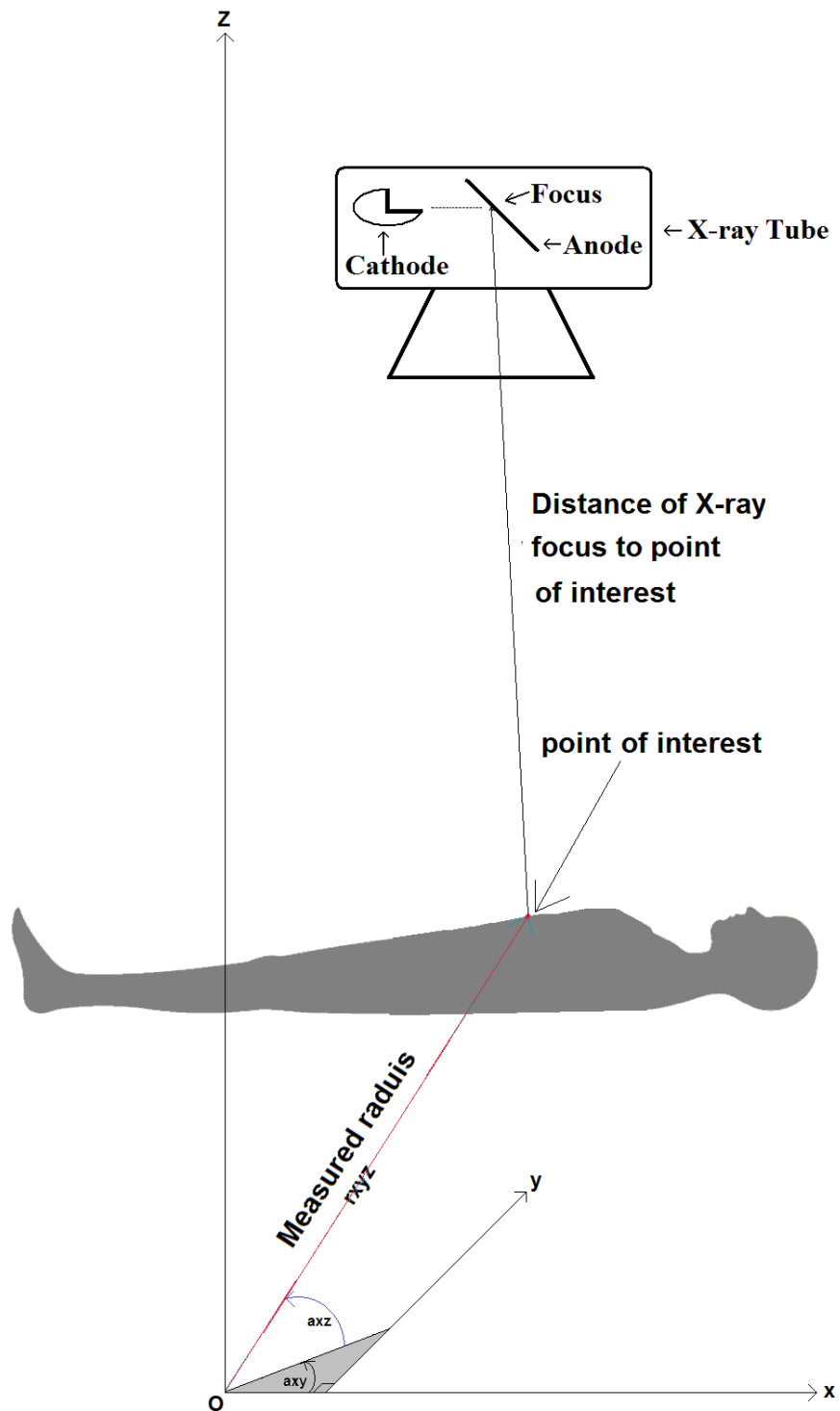


Figure 10.6: Setup to measure the distance from the X-ray focus to patient skin surface

10.11 Limitations to consider

Although there is no contact with the patient, the point of interest of the patient is identified with a laser. This indicates a minimal interaction with the patient skin surface.

As described previously, the origin of the X-ray focus and the origin from where the measured radius is measured need to be the same. This indicates that the laser

measurements instrument needs to be fixed or every time it is moved, the new values of the X-ray focus coordinates needs to be determined or the translation and rotation formulae needs to be applied.

10.12 Conclusion of chapter 10

The mathematical model to describe a method to determine the distance of the X-ray focus to the patient skin surface with no interaction with the patient is described.

If these formulae can be inserted into a program and the variables are inserted, then the distance will be calculated. As the angulations around the axis are needed and the xyz-position of the focus, it would be beneficial to insert these variables in the DICOM header.

The measured distance between the X-ray focus and a point of interest on the patient skin surface can be used in obtaining the patient to focus distance.

CHAPTER 11

A method to perform 3D measurements on routine AP and LAT X-ray examinations

11.1 Introduction

An X-ray image provide a two dimensional representation of a three dimensional structure. If measurements are done on an X-ray image, it is measurements done in 2D. To perform 3D measurements with an anterior-posterior (AP) and lateral (LAT) x-ray view can be of value in surgical planning. Kelly, 2006, indicated in an article Accuracy of Cone Beam Computed Tomography for Periodontal Defect Measurements there is a need for measurements in radiology. As X-ray images are produced from 3D structures, 3D measurements will be helpful. Three-dimensional measurements can be of value as the linear distance of a structure can be determined, even if the structure is not parallel to the image plane.

With the DICOM tag, Image Pixel Spacing (0018, 1164) the pixel size on an X-ray image can be obtained and by selecting a number of pixels, the 2D distance on the X-ray image is determined (<http://www.sno.phy.queensu.ca>). Magnification also occurs with an X-ray examination and this can influence the measurement. Also structures not parallel to the image plane will influence the measurement.

With this method proposed, 3D measurements can be obtained of structures that are magnified or not parallel with the image plane.

To perform the 3D measurement, the AP and LAT X-ray views are required, but also the position of the X-ray focus. Jenő Palvolgyi, 2012, depicted the position of the X-ray focus in the projections of the needle's tip in an article on Multi-parametric fit method in reconstruction of brachytherapy needles. This method propose will use the position of the X-ray focus and the AP and LAT X-ray image to obtain the 3D distance between two points of interest. By obtaining the position of the X-ray focus and with the position of the pixel on the X-ray image, 3D measurements with the AP and LAT X-ray views can be obtained. Also with the position of the X-ray focus, measuring the distance in 3D of a structure, even if the structure is not parallel or in close contact with the image plane can be obtained. AP and LAT projections are normally done during an X-ray examination

By providing a method to perform 3D measurement with the X-ray examinations can be useful as the 3D length of a long bone, example the forearm, femur or tibia-fibula can be obtained. This method can also be used to determine the thickness of a bone or the 3D measurement between two anatomical structures, example the size of the pedicle of a vertebra to select the correct length of a surgical screw.

11.2 Aim

The aim is to describe a model to perform 3D measurements with a routine AP and LAT view.

11.3 Method to perform 3D measurements with a routine AP and LAT X-ray examination

The user selects two points on the AP view for the proximal and distal part of the measurements. The corresponding proximal and distal points are selected on the LAT X-ray examination. The position of the X-ray focus is also determined. A line is generated from the X-ray focus, to the proximal point selected on the AP view. A second line is generated from the X-ray focus, to the proximal point on the LAT view. The intersecting point of the image lines to the proximal positions on the AP and LAT view to the X-ray focus is determined. By also determining the intersecting point on the distal points, two points in 3D are determined. By calculating the distance between these two 3D points, the distance in 3D is obtained.

The same process can be implemented if a medial and lateral point is selected. This will provide the thickness of the bone structure.

Figure 11.1 displays the AP and LAT X-ray image, the focus points as well as the 3D line to obtain the 3D measurement.

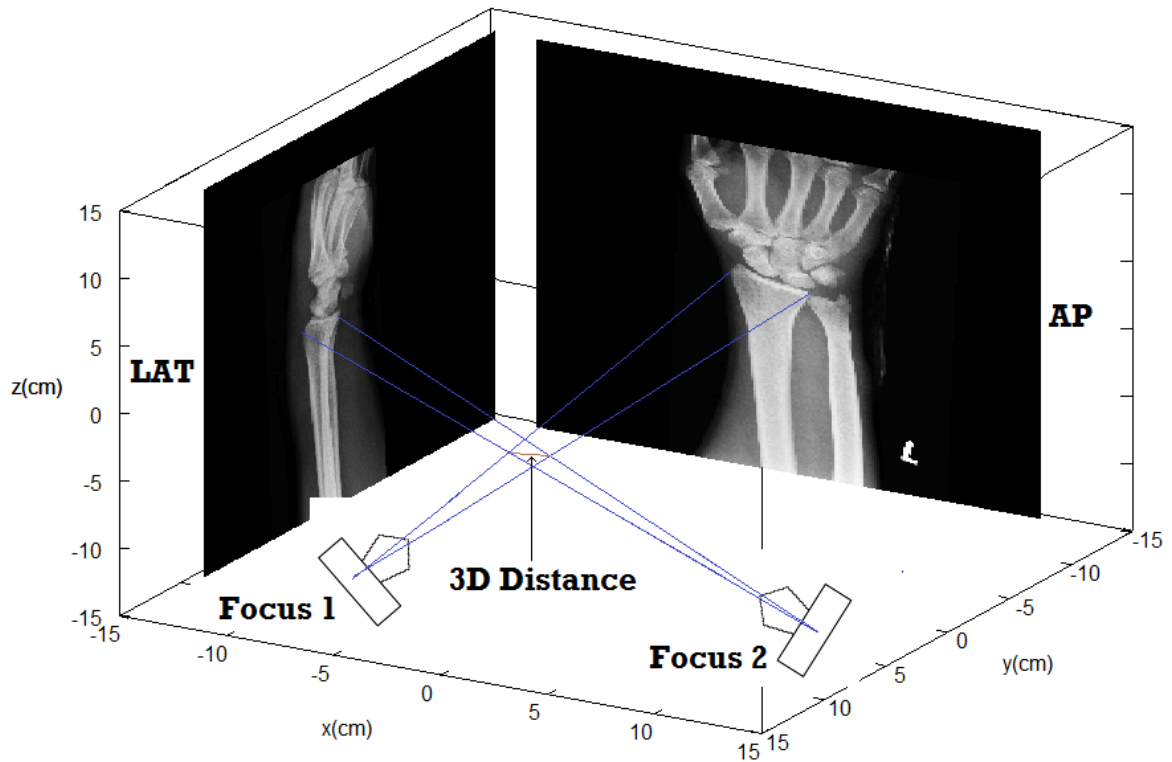
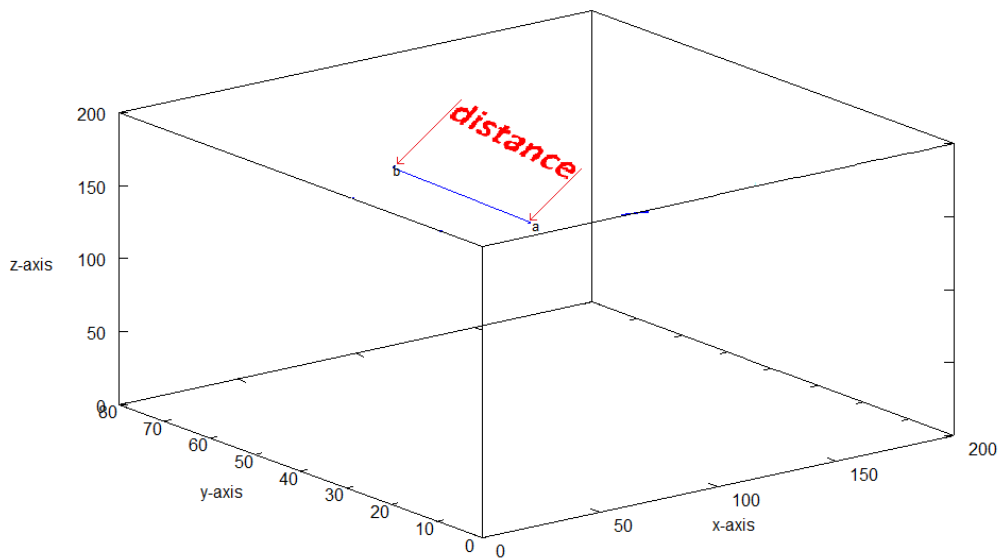


Figure 11.1: Schematic presentation of a 3D AP and LAT with the X-ray foci and the 3D measurement

To determine the position of the X-ray focus, will also be explained. As X-ray are linear, two lines will be generated, one from the X-ray focus, through the 3D point of interest and provide an image on the AP view (selected by the user). A line in 3D is generated from first focus position, through the 3D point of interest and to the point on AP image. A second line in 3D is generated from the second focus point, through the 3D point of interest and to a point on LAT image. An intersecting point of these two lines can be determined. As the user selects these two points for measuring the distance, two points in 3D will be determined. Then by obtaining the linear distance between these two points in 3D, the 3D measurements calculated as displayed in figure 11.1.1.



view: 60.0000, 322.500 scale: 1.00000, 1.00000

Figure 11.1.1: Schematic of obtaining the 3D distance from proximal and distal points of an anatomical structure

As previously described, to determine the distance in 3D, the 3D position of the X-ray focus needs to be determined. Firstly, the method to determine the 3D X-ray focus is described. Then the method to determine the position of the points of interest selected on the AP and LAT X-ray image is described. The 3D position of the points selected on the AP and LAT view is described. Lastly the distance between these two 3D points is calculated that provide the distance in 3D.

11.4 The X-ray focus

The X-ray focus is the point where the X-rays are generated. An X-ray tube consists of a cathode and anode. It is at a point on the anode where the X-rays are generated, and is called the X-ray focus. The X-ray focus can be broad or fine focus.

Figure 11.2 displays an X-ray tube with the X-ray focus.

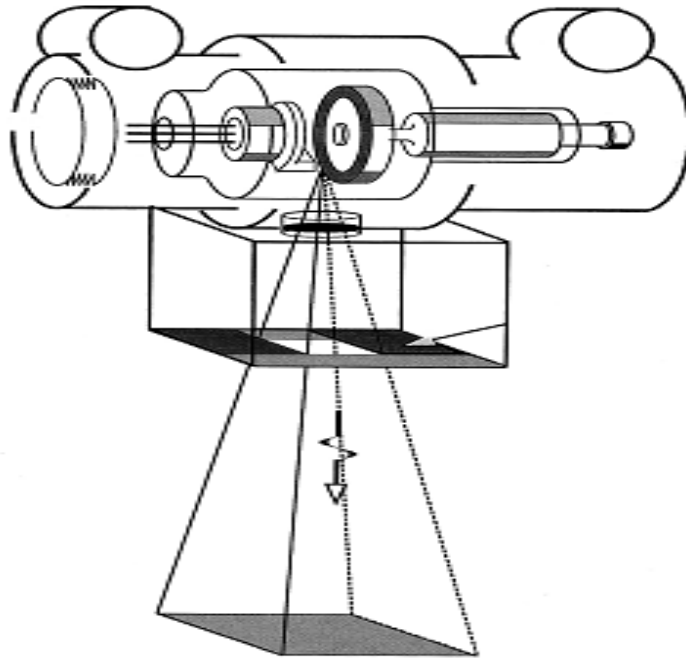


Figure 11.2: X-ray tube with X-rays being generated.
 ([http://miac.unibas.ch/PMI/01-BasicsOfXray.html#\(6\)](http://miac.unibas.ch/PMI/01-BasicsOfXray.html#(6)))

11.5 Determining the 3D-coordinates on the AP and LAT views

To determine the 3D-coordinates with the AP and LAT view, the X-ray images are viewed in the yz -plane and xz -plane as described in figure 11.3.

Normally when performing an AP and LAT view, the patients is moved through 90° . This can also be interpreted as if the tube has moved through 90° . Let the Source-to-Image-Distance (SID) be the distance from the X-ray focus to the image plate, the Image-to-Rotation-Distance (IRD) be the distance of the X-ray image to the rotation point and the Source-to-Rotation-Distance (SRD) be the distance of the X-ray focus to the to the rotation point.

Figure 11.3 displays the AP and LAT view in the yz -plane and xz -plane and the X-ray tube at 90° , with respect to the AP and LAT view. Also the SID, IRD, as well as the SRD are displayed that will be used in calculating the 3D distance.

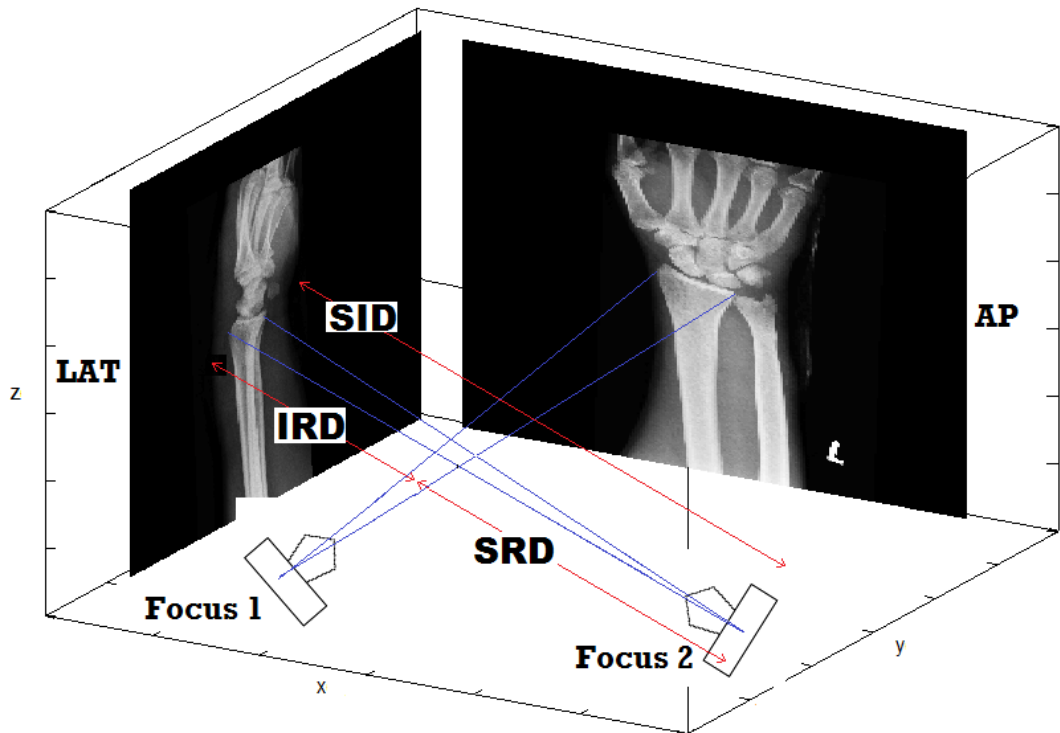


Figure 11.3: AP and LAT X-ray image

If for example a C-arm (an X-ray tube and imaging plane connected in a c-shape) is used, then the rotation point is normally in the centre of the C-arm. If an AP and LAT examination is performed in bucky (X-ray setup to obtain an X-ray image) or in contact with the X-ray cassette, then the rotation point is not midway between the SID. This provides a rotation point where the SRD and the IRD are different values.

Figure 11.4 displays an AP and LAT projection of a coin that has been X-rayed. In figure 11.4, an xyz-axial system is displayed with the AP in the xz-plane and the LAT in the yz-plane. For this setup, the rotation point is the origin. As from figure 11.4, it indicates that the x-coordinate of the AP view will be the RID. Then the x-coordinate and y-coordinate of a pixel on the AP image can be determined by multiplying the size-per-pixel with the y- position and z-position on the X-ray image.

Similarly, the same can be done on the lateral view.

This will provide the xyz-coordinates of the points selected by the user on the AP and LAT view. The xyz-coordinates of the focus point have been described. The xyz-coordinates of the points on the AP and LAT view have been determined. Then by determining the intersecting points of these two lines, the 3D points of the medial and lateral points of the structure from the AP and LAT can be determined.

11.6 Experimental results in 3D measurements with set diameter of a radiopaque structure

As the user has selected two points on AP view, two lines will be generated: one from the first focus point to the first point on the AP view and a second from the first focus point to the second point on the AP view.

Also the user select two points on LAT view and two lines will be generated: one from the first focus point to the first point on the LAT view and a second from the first focus point to the second point on the LAT view.

Again by determining the intersecting point as described in equation (3.25) to (3.27), the first 3D point and the second 3D point can be calculated.

By using the distance formula, then the distance in 3D can be determined between these two points.

Figure 11.4 displays an AP and LAT view of a coin X-rayed at SID of 100cm, IRD of 50cm and IRD of 50cm.

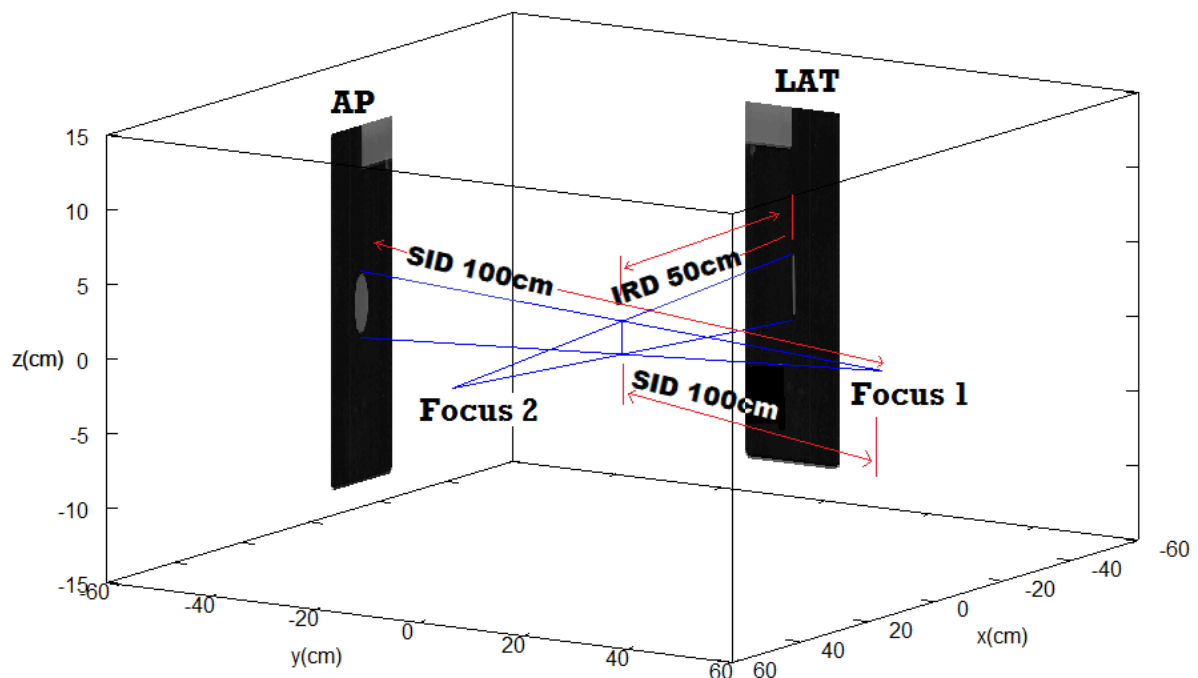


Figure 11.4 Displays an AP and LAT view of a coin

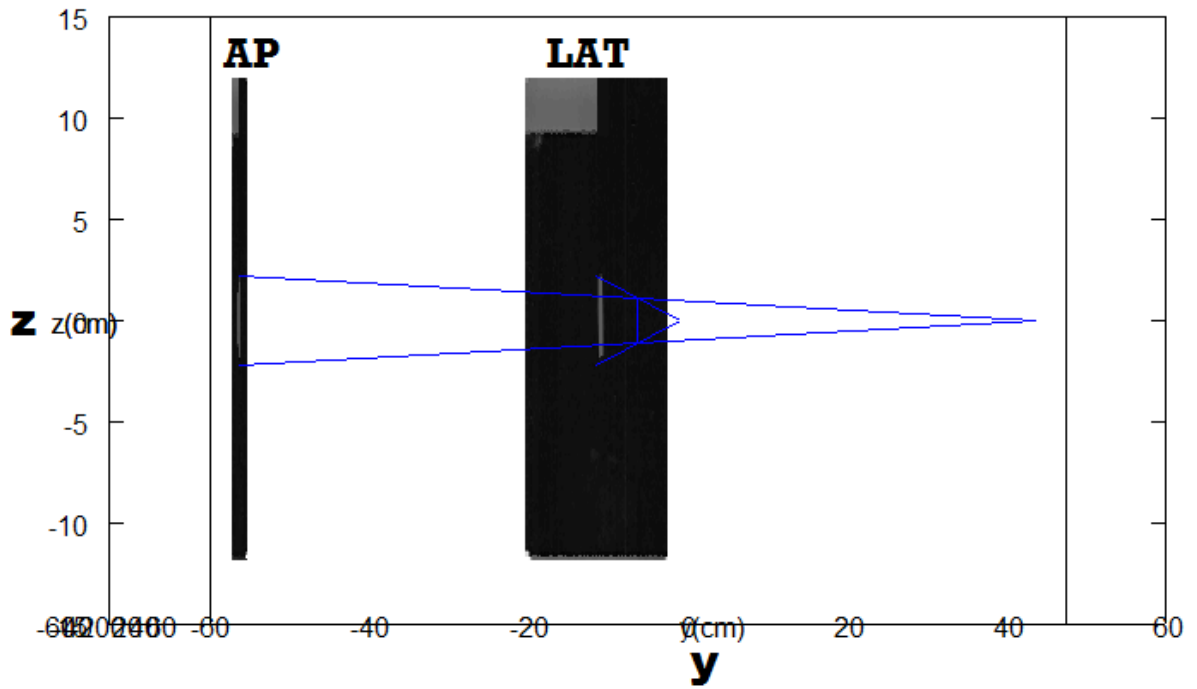


Figure 11.5: The LAT image in view and the measurement position on the LAT view.

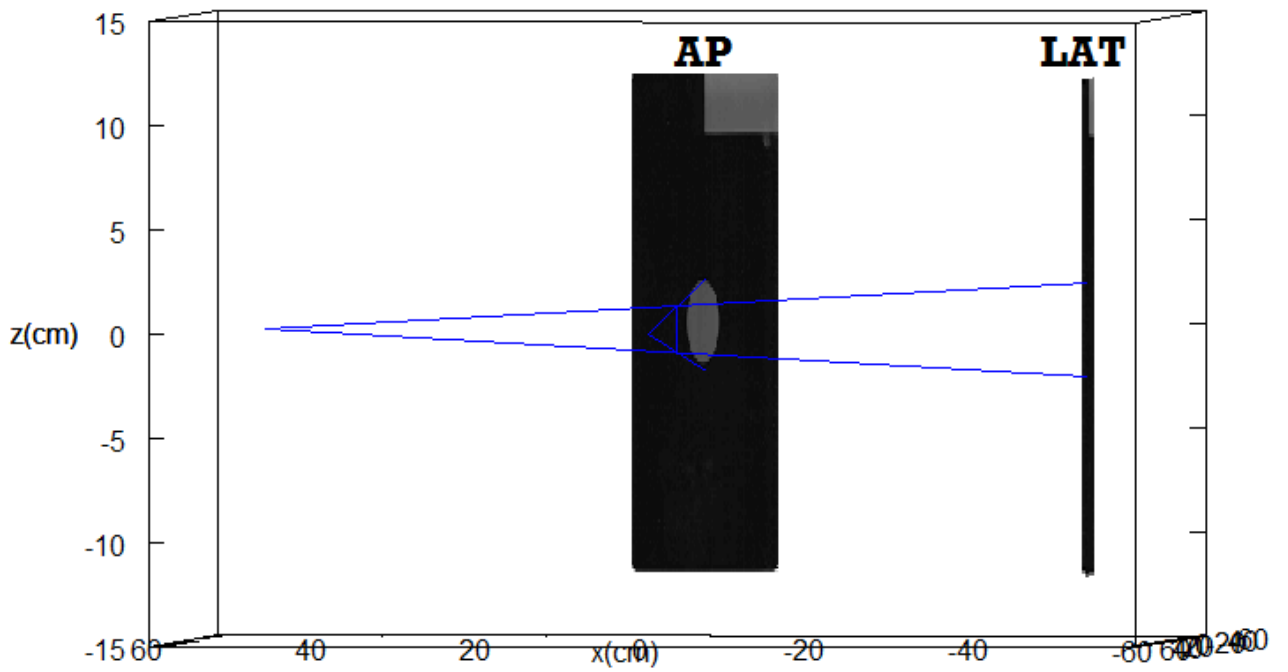


Figure 11.6: AP image in view and the measurement position on the AP view

Table 11.1: Results measurement of the coin with 1st point selected

	P1 Focus with AP view	P2 2D position of AP view	P3 Focus with LAT view	P4 2D position of LAT view	(x,y,z) 3D position of 1 st point
x	0	0	50	-50	0
y	50	-50	0	0	0
z	0	2.24	0	2.24	1.12

Table 11.2: Results measurement of the coin with 2nd point selected

	P1 Focus with AP view	P2 2D position of AP view	P3 Focus with LAT view	P4 2D position of LAT view	(x,y,z) 3D position of 2 nd point
x	0	0	50	-50	0
y	50	-50	0	0	0
z	0	-2.24	0	-2.24	-1.12

Distance of coin calculated is 2.24cm.

The diameter measured on the coin was 2.36cm. This indicates that the calculated measurement was 95% within the real distance of the coin. The user has to select the two points of interest on the AP and LAT view. This can have an influence on the accuracy of the calculated measurement. The more accurate the user selects the points and the more accurate the position of the X-ray focus is the more accurate will the calculated measurements be.

11.7 Measuring the distance of the radius

Figure 11.7 displays the method to measure the radial head distance on the AP and LAT view of the wrist. The first point of interest is a point on the lateral area of the radial head. The second point of interest is a point on the medial area of the radial head. The corresponding points on the lateral view are selected.

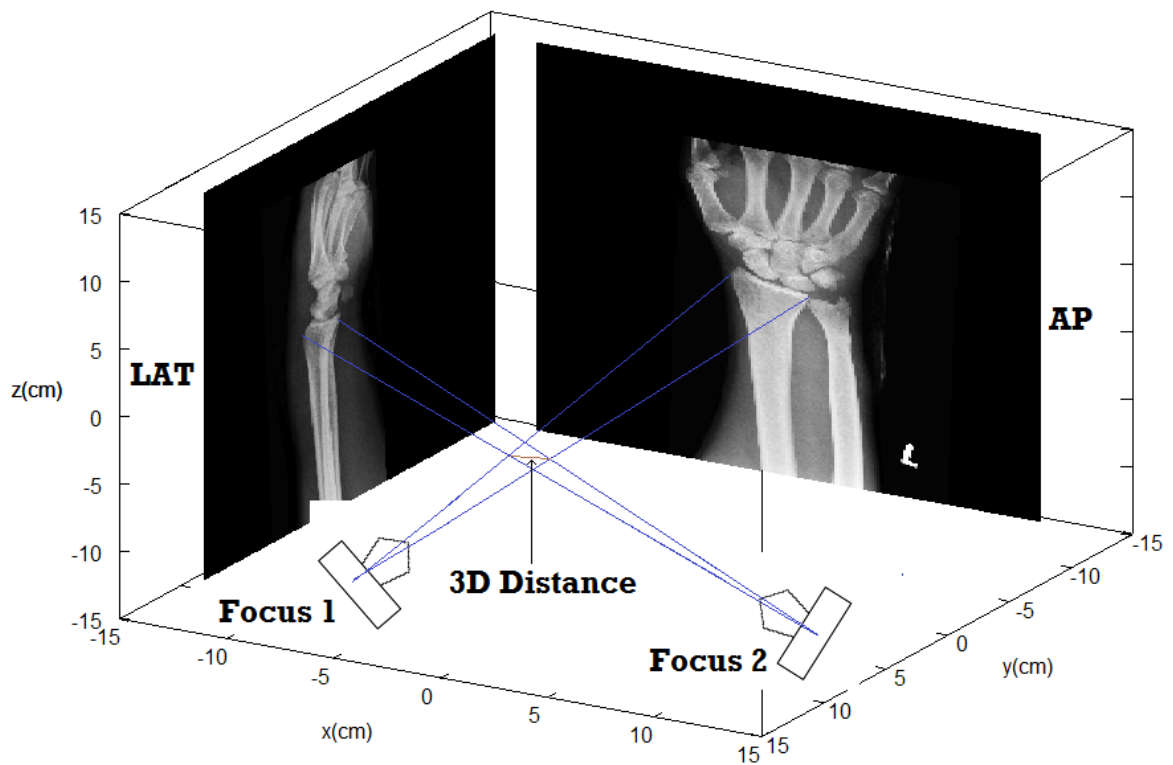


Figure 11.7: Measuring the radial transverse distance

As displayed previously, the rotation point is at (0,0,0) and the anatomical structure is in close contact with the X-ray cassette. This indicates that the rotation point is 10cm from the image plane. Figure 11.8 displays the 3D reconstruction of the AP and LAT view of the wrist to perform the 3D measurement of the radial head.

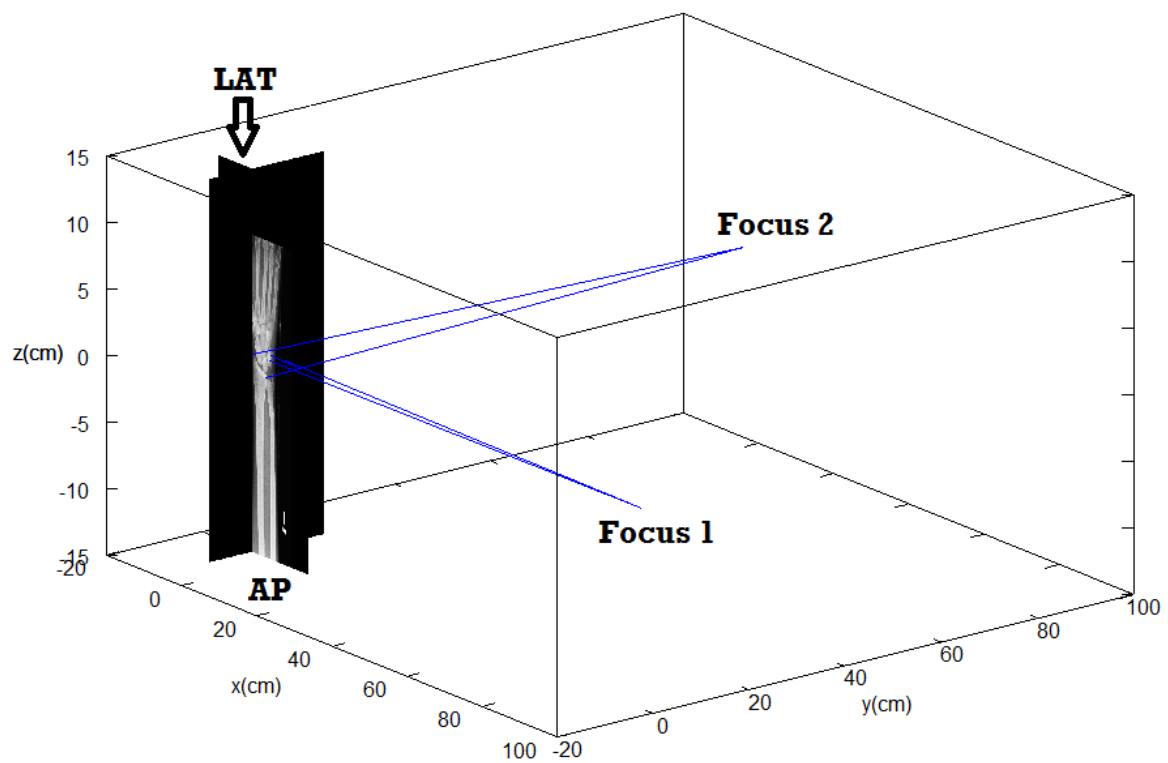


Figure 11.8: Measuring the radial transverse distance

The distance of radius at the wrist calculated is 4.35cm calculated.

Table 11.3: Results measurement of the 1st point selected on the AP and LAT view

	P1 Focus with AP view	P2 2D position of AP view	P3 Focus with LAT view	P4 2D position of LAT view	(x,y,z) 3D position of 1 st point
x	0	-2.65	97	-3	-2.55
y	97	-3	0	0.75	0.75
z	0	-0.55	0	-3.5	0.09

Table 11.4: Results measurement of the 2nd point selected on the AP and LAT view

	P1 Focus with AP view	P2 2D position of AP view	P3 Focus with LAT view	P4 2D position of LAT view	(x,y,z) 3D position of 2 nd point
x	0	0.57	97	-3	0.53
y	97	-3	0	3.86	3.73
z	0	-0.86	0	-0.56	-0.67

With the 3D position of the 1st and 2nd point, the transverse distance was calculated as 4.35cm.

11.8 Limitations to consider

The result of the 3D measurement is dependable n the points selected by the user. This indicates that the points selected on the AP view, must be indentified as on the LAT view. Points on the AP view might not be clearly visible on the LAT view, due to anatomical structures.

Also the rotation point has to be maintained from the AP to the LAT view. If using a C-arm, the rotation point can be maintained as the X-ray tube and image receptor is rotated in a circular position. The rotation point might not be maintained if the patient under examination is rotated to obtain an AP and LAT view. This can have an effect on the measured distance.

11.9 Conclusion of chapter 11

The mathematical model to perform 3D measurements on a routine AP and LAT view was obtained. This provides a method to perform linear measurements of 3D anatomical structures. Previously measurements were done in 2D, but with this method measurements are performed in 3D.

If this method can be used with a C-arm, the rotation point, SID and IRD will be known and 3D measurements can be performed. In general AP and LAT views are normally done. This method can provide an opportunity to obtain additional information with an AP and LAT view.

CHAPTER 12

Conclusion

12.1 Introduction to conclusion

The research has indicated different methods to determine the 3D position of an artefact from the visual spectrum to the X-ray spectrum.

The formula to determine the 3D position of the midpoint of the shortest line between two lines in 3D has been derived.

Using this formula, applications have been investigated in the application of a pinhole camera, 3D camera as well as the application in an X-ray system.

Technology is also moving beyond the visual spectrum and by having a method to determine measurements of the internal part of structures, can be useful in medical applications. The method to determine the length of the long bones has been introduced which can assist the medical officer in the planning of medical procedures.

12.2 Mathematical method to determine the intersecting point of two lines in 3D

The mathematical formulae to determine the intersection of two lines in 3D have been used to determine the 3D point of two lines from the object. As the lines intersect at the object point and with the position of the intersecting point, the object point was determined.

By using the method as explained by Bourke (1998) and as described in equations 3.28 to 3.37, the points describing the shortest distance between two lines in 3D was explained. As two lines in 3D do not always intersect, the shortest distance between two lines in 3D was determined. The midpoint of the shortest distance between two lines in 3D was explained in equation 3.25 to equation 3.27. Also the distance between the shortest distance of two lines in 3D was also explained in equation 3.24.

A definition can be included; example if the distance between the two points in 3D is less than a hundred of a millimetre, then it can be interpreted as a point. By using equations 3.25 to 3.27 the midpoint of the shortest distance between two lines in 3D was determined.

The method to determine the midpoint of the shortest distance between two lines in 3D was used in the pinhole setup, centre of projection method as well in the X-ray spectrum.

12.3 Formulae to determine the shortest distance between two line segments in 3D

With stereoscopic vision two different images of the same object fused together. With the use of a pinhole camera, two pinhole images were used to determine the 3D position of an object point. This was done by utilizing the pinhole position and the image point. In the use of a camera setup, the centre of projection method was used with the image point.

These methods utilize the shortest distance between two lines in 3D as well as the midpoint of the shortest distance.

The following formulae display the coordinates of the shortest distance between two lines with the coordinates of the line segment points.

Two line segments as described in figure 12.1 were used to determine the formulae of the shortest distance between the two lines with:

$$P_1 = (x_1, y_1, z_1)$$

$$P_2 = (x_2, y_2, z_2)$$

$$P_3 = (x_3, y_3, z_3)$$

$$P_4 = (x_4, y_4, z_4)$$

In

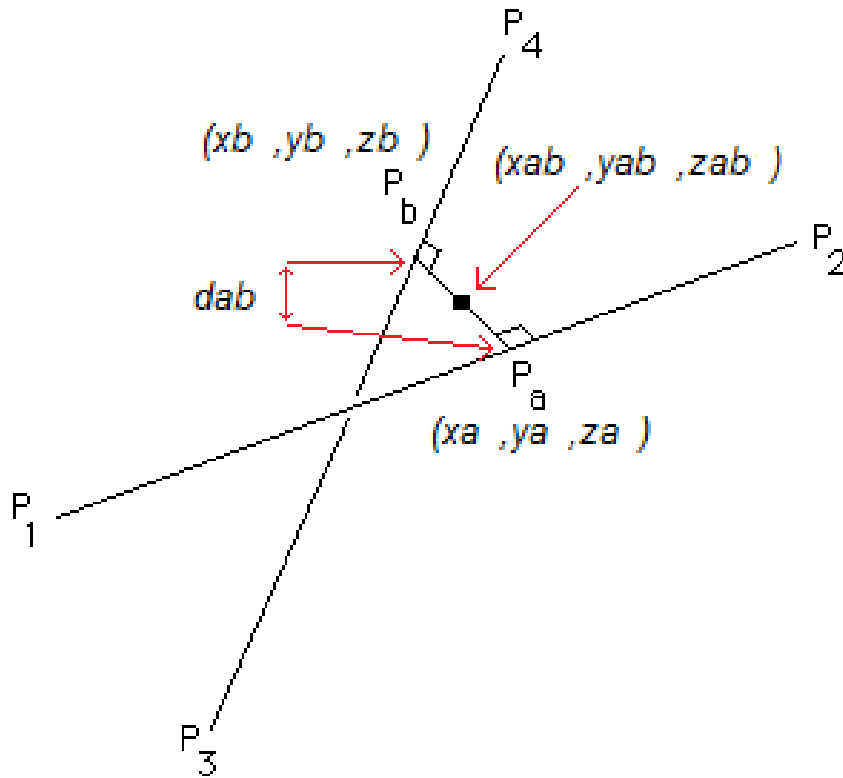


Figure 12.1: Determine the 3D co-ordinates of two lines in 3D

Having derived the main formulae to determine the intersecting point of two lines in 3D as done in this thesis, it was made possible to add it to an computer program to render the 3D position of an artefact.

This was a useful outcome and could also be applied in an embedded processor application.

As displayed in figure 12.1, the x-coordinate (x_a) of point (P_a) is described in equation 3.28.

When defining the following:

“*” as multiplication,

“/” as division,

then:

$$x_a = \frac{(x_1) + (((((x_1) - (x_3)) * ((x_4) - (x_3)) + ((y_1) - (y_3)) * ((y_4) - (y_3)) + ((z_1) - (z_3)) * ((z_4) - (z_3))) * (((x_4) - (x_3)) * ((x_2) - (x_1)) + ((y_4) - (y_3)) * ((y_2) - (y_1)) + ((z_4) - (z_3)) * ((z_2) - (z_1))) - (((x_1) - (x_3)) * ((x_2) - (x_1)) + ((y_1) - (y_3)) * ((y_2) - (y_1)) + ((z_1) - (z_3)) * ((z_2) - (z_1))) * (((x_4) - (x_3)) * ((x_4) - (x_3)) + ((y_4) - (y_3)) * ((y_4) - (y_3)) + ((z_4) - (z_3)) * ((z_4) - (z_3))))}{(((x_2) - (x_1)) * ((x_2) - (x_1)) + ((y_2) - (y_1)) * ((y_2) - (y_1)) + ((z_2) - (z_1)) * ((z_2) - (z_1))) * (((x_4) - (x_3)) * ((x_4) - (x_3)) + ((y_4) - (y_3)) * ((y_4) - (y_3)) + ((z_4) - (z_3)) * ((z_4) - (z_3))) - (((x_4) - (x_3)) * ((x_2) - (x_1)) + ((y_4) - (y_3)) * ((y_2) - (y_1)) + ((z_4) - (z_3)) * ((z_2) - (z_1))) * (((x_4) - (x_3)) * ((x_2) - (x_1)) + ((y_4) - (y_3)) * ((y_2) - (y_1)) + ((z_4) - (z_3)) * ((z_2) - (z_1))) * ((x_2) - (x_1))}$$

(12.1)

The y-coordinate (y_a) of point (Pa) is described in equation 3.30.

When defining the following:

“*” as multiplication,

“/” as division,

then:

$$y_a = \frac{y_1 + (((x_1 - x_3) * (x_4 - x_3) + (y_1 - y_3) * (y_4 - y_3) + (z_1 - z_3) * (z_4 - z_3)) * ((x_4 - x_3) * (x_2 - x_1) + (y_4 - y_3) * (y_2 - y_1) + (z_4 - z_3) * (z_2 - z_1)) - ((x_1 - x_3) * (x_2 - x_1) + (y_1 - y_3) * (y_2 - y_1) + (z_1 - z_3) * (z_2 - z_1)) * ((x_4 - x_3) * (x_4 - x_3) + (y_4 - y_3) * (y_4 - y_3) + (z_4 - z_3) * (z_4 - z_3)))}{(((x_2 - x_1) * (x_2 - x_1) + (y_2 - y_1) * (y_2 - y_1) + (z_2 - z_1) * (z_2 - z_1)) * ((x_4 - x_3) * (x_4 - x_3) + (y_4 - y_3) * (y_4 - y_3) + (z_4 - z_3) * (z_4 - z_3)) - ((x_4 - x_3) * (x_2 - x_1) + (y_4 - y_3) * (y_2 - y_1) + (z_4 - z_3) * (z_2 - z_1)) * ((x_4 - x_3) * (x_2 - x_1) + (y_4 - y_3) * (y_2 - y_1) + (z_4 - z_3) * (z_2 - z_1)))} * (y_2 - y_1)$$

(12.2)

The z-coordinate (z_a) of point (Pa) is described in equation 3.27

When defining the following:

“*” as multiplication,

“/” as division,

then:

$$z_a = \frac{z_1 + (((x_1 - x_3) * (x_4 - x_3) + (y_1 - y_3) * (y_4 - y_3) + (z_1 - z_3) * (z_4 - z_3)) * ((x_4 - x_3) * (x_2 - x_1) + (y_4 - y_3) * (y_2 - y_1) + (z_4 - z_3) * (z_2 - z_1)) - ((x_1 - x_3) * (x_2 - x_1) + (y_1 - y_3) * (y_2 - y_1) + (z_1 - z_3) * (z_2 - z_1)) * ((x_4 - x_3) * (x_4 - x_3) + (y_4 - y_3) * (y_4 - y_3) + (z_4 - z_3) * (z_4 - z_3)))}{(((x_2 - x_1) * (x_2 - x_1) + (y_2 - y_1) * (y_2 - y_1) + (z_2 - z_1) * (z_2 - z_1)) * ((x_4 - x_3) * (x_4 - x_3) + (y_4 - y_3) * (y_4 - y_3) + (z_4 - z_3) * (z_4 - z_3)) - ((x_4 - x_3) * (x_2 - x_1) + (y_4 - y_3) * (y_2 - y_1) + (z_4 - z_3) * (z_2 - z_1)) * ((x_4 - x_3) * (x_2 - x_1) + (y_4 - y_3) * (y_2 - y_1) + (z_4 - z_3) * (z_2 - z_1)))} * (z_2 - z_1)$$

(12.3)

The x-coordinate (x_b) of point (Pb) is described in equation 3.29.

When defining the following:

“*” as multiplication,

“/” as division,

then:

$$x_b = \frac{x_3 + (((x_1 - x_3) * (x_4 - x_3) + (y_1 - y_3) * (y_4 - y_3) + (z_1 - z_3) * (z_4 - z_3)) + ((x_4 - x_3) * (x_2 - x_1) + (y_4 - y_3) * (y_2 - y_1) + (z_4 - z_3) * (z_2 - z_1)) * (((x_1 - x_3) * (x_4 - x_3) + (y_1 - y_3) * (y_4 - y_3) + (z_1 - z_3) * (z_4 - z_3)) * ((x_4 - x_3) * (x_2 - x_1) + (y_4 - y_3) * (y_2 - y_1) + (z_4 - z_3) * (z_2 - z_1)) - ((x_1 - x_3) * (x_2 - x_1) + (y_1 - y_3) * (y_2 - y_1) + (z_1 - z_3) * (z_2 - z_1)) * ((x_4 - x_3) * (x_4 - x_3) + (y_4 - y_3) * (y_4 - y_3) + (z_4 - z_3) * (z_4 - z_3))))}{(((x_2 - x_1) * (x_2 - x_1) + (y_2 - y_1) * (y_2 - y_1) + (z_2 - z_1) * (z_2 - z_1)) * ((x_4 - x_3) * (x_4 - x_3) + (y_4 - y_3) * (y_4 - y_3) + (z_4 - z_3) * (z_4 - z_3)) - ((x_4 - x_3) * (x_2 - x_1) + (y_4 - y_3) * (y_2 - y_1) + (z_4 - z_3) * (z_2 - z_1)) * ((x_4 - x_3) * (x_2 - x_1) + (y_4 - y_3) * (y_2 - y_1) + (z_4 - z_3) * (z_2 - z_1)))}$$

$$z1)) * ((x4-x3) * (x4-x3) + (y4-y3) * (y4-y3) + (z4-z3) * (z4-z3)) / (((x2-x1) * (x2-x1) + (y2-y1) * (y2-y1) + (z2-z1) * (z2-z1)) * ((x4-x3) * (x4-x3) + (y4-y3) * (y4-y3) + (z4-z3) * (z4-z3)) - ((x4-x3) * (x2-x1) + (y4-y3) * (y2-y1) + (z4-z3) * (z2-z1)) * ((x4-x3) * (x2-x1) + (y4-y3) * (y2-y1) + (z4-z3) * (z2-z1)))) / (((x4-x3) * (x4-x3) + (y4-y3) * (y4-y3) + (z4-z3) * (z4-z3)) * (x4-x3)$$

(12.4)

The y-coordinate (yb) of point (Pb) is described in equation 3.31

When defining the following:

“*” as multiplication,

“/” as division,

then:

$$yb = \frac{(y3 + (((((x1-x3) * (x4-x3)) + ((y1-y3) * (y4-y3)) + ((z1-z3) * (z4-z3))) + (((x4-x3) * (x2-x1)) + ((y4-y3) * (y2-y1)) + ((z4-z3) * (z2-z1)))) * (((((x1-x3) * (x4-x3)) + ((y1-y3) * (y4-y3)) + ((z1-z3) * (z4-z3))) * (((x4-x3) * (x2-x1)) + ((y4-y3) * (y2-y1)) + ((z4-z3) * (z2-z1))) - (((x1-x3) * (x2-x1)) + ((y1-y3) * (y2-y1)) + ((z1-z3) * (z2-z1)))) * (((x4-x3) * (x2-x1)) + ((y4-y3) * (y2-y1)) + ((z4-z3) * (z2-z1)))))) / (((((x2-x1) * (x2-x1)) + ((y2-y1) * (y2-y1)) + ((z2-z1) * (z2-z1))) * (((x4-x3) * (x4-x3)) + ((y4-y3) * (y4-y3)) + ((z4-z3) * (z4-z3))) - (((x4-x3) * (x2-x1)) + ((y4-y3) * (y2-y1)) + ((z4-z3) * (z2-z1)))) * (((x4-x3) * (x2-x1)) + ((y4-y3) * (y2-y1)) + ((z4-z3) * (z2-z1)))))) / (((x4-x3) * (x4-x3)) + ((y4-y3) * (y4-y3)) + ((z4-z3) * (z4-z3))) * (y4-y3)$$

(12.5)

The z-coordinate (zb) of point (Pb) is described in equation 3.32

When defining the following:

“*” as multiplication,

“/” as division,

then:

$$zb = \frac{(z3 + (((((x1-x3) * (x4-x3)) + ((y1-y3) * (y4-y3)) + ((z1-z3) * (z4-z3))) + (((x4-x3) * (x2-x1)) + ((y4-y3) * (y2-y1)) + ((z4-z3) * (z2-z1)))) * (((((x1-x3) * (x4-x3)) + ((y1-y3) * (y4-y3)) + ((z1-z3) * (z4-z3))) * (((x4-x3) * (x2-x1)) + ((y4-y3) * (y2-y1)) + ((z4-z3) * (z2-z1))) - (((x1-x3) * (x2-x1)) + ((y1-y3) * (y2-y1)) + ((z1-z3) * (z2-z1)))) * (((x4-x3) * (x2-x1)) + ((y4-y3) * (y2-y1)) + ((z4-z3) * (z2-z1)))))) / (((((x2-x1) * (x2-x1)) + ((y2-y1) * (y2-y1)) + ((z2-z1) * (z2-z1))) * (((x4-x3) * (x4-x3)) + ((y4-y3) * (y4-y3)) + ((z4-z3) * (z4-z3))) - (((x4-x3) * (x2-x1)) + ((y4-y3) * (y2-y1)) + ((z4-z3) * (z2-z1)))) * (((x4-x3) * (x2-x1)) + ((y4-y3) * (y2-y1)) + ((z4-z3) * (z2-z1)))))) / (((x4-x3) * (x4-x3)) + ((y4-y3) * (y4-y3)) + ((z4-z3) * (z4-z3))) * (z4-z3)$$

(12.6)

The x-coordinate of the midpoint of the shortest line between two lines in 3D (x_{ab}) is:

$$x_{ab} = \frac{x_a + x_b}{2} \quad (12.7)$$

with (x_a) and (x_b) as described above.

When defining the following:

“*” as multiplication,

“/” as division,

then

$$x_{ab} = \frac{((x_1 + (((x_1 - x_3) * (x_4 - x_3) + (y_1 - y_3) * (y_4 - y_3) + (z_1 - z_3) * (z_4 - z_3))) * ((x_4 - x_3) * (x_2 - x_1) + (y_4 - y_3) * (y_2 - y_1) + (z_4 - z_3) * (z_2 - z_1))) - (((x_1 - x_3) * (x_2 - x_1) + (y_1 - y_3) * (y_2 - y_1) + (z_1 - z_3) * (z_2 - z_1))) * ((x_4 - x_3) * (x_4 - x_3) + (y_4 - y_3) * (y_4 - y_3) + (z_4 - z_3) * (z_4 - z_3))) / (((x_2 - x_1) * (x_2 - x_1) + (y_2 - y_1) * (y_2 - y_1) + (z_2 - z_1) * (z_2 - z_1))) * ((x_4 - x_3) * (x_4 - x_3) + (y_4 - y_3) * (y_4 - y_3) + (z_4 - z_3) * (z_4 - z_3))) - (((x_4 - x_3) * (x_2 - x_1) + (y_4 - y_3) * (y_2 - y_1) + (z_4 - z_3) * (z_2 - z_1))) * ((x_4 - x_3) * (x_2 - x_1) + (y_4 - y_3) * (y_2 - y_1) + (z_4 - z_3) * (z_2 - z_1))) * ((x_2 - x_1) * (x_2 - x_1) + (y_2 - y_1) * (y_2 - y_1) + (z_2 - z_1) * (z_2 - z_1))) + (x_3 + (((x_1 - x_3) * (x_4 - x_3) + (y_1 - y_3) * (y_4 - y_3) + (z_1 - z_3) * (z_4 - z_3)) + ((x_4 - x_3) * (x_2 - x_1) + (y_4 - y_3) * (y_2 - y_1) + (z_4 - z_3) * (z_2 - z_1))) * ((x_1 - x_3) * (x_4 - x_3) + (y_1 - y_3) * (y_4 - y_3) + (z_1 - z_3) * (z_4 - z_3))) * ((x_4 - x_3) * (x_2 - x_1) + (y_4 - y_3) * (y_2 - y_1) + (z_4 - z_3) * (z_2 - z_1))) - ((x_1 - x_3) * (x_2 - x_1) + (y_1 - y_3) * (y_2 - y_1) + (z_1 - z_3) * (z_2 - z_1))) * ((x_4 - x_3) * (x_4 - x_3) + (y_4 - y_3) * (y_4 - y_3) + (z_4 - z_3) * (z_4 - z_3))) / (((x_2 - x_1) * (x_2 - x_1) + (y_2 - y_1) * (y_2 - y_1) + (z_2 - z_1) * (z_2 - z_1))) * ((x_4 - x_3) * (x_4 - x_3) + (y_4 - y_3) * (y_4 - y_3) + (z_4 - z_3) * (z_4 - z_3))) - ((x_4 - x_3) * (x_2 - x_1) + (y_4 - y_3) * (y_2 - y_1) + (z_4 - z_3) * (z_2 - z_1))) * ((x_4 - x_3) * (x_2 - x_1) + (y_4 - y_3) * (y_2 - y_1) + (z_4 - z_3) * (z_2 - z_1))) / (((x_4 - x_3) * (x_4 - x_3) + (y_4 - y_3) * (y_4 - y_3) + (z_4 - z_3) * (z_4 - z_3))) * (x_4 - x_3)) / 2$$

(12.8)

The y-coordinate of the midpoint of the shortest line between two lines in 3D (y_{ab}) is:

$$y_{ab} = \frac{y_a + y_b}{2} \quad (12.9)$$

with (y_a) and (y_b) as described above.

When defining the following:

“*” as multiplication,

“/” as division,

then:

$$y_{ab} = \frac{((y_1 + (((x_1 - x_3) * (x_4 - x_3) + (y_1 - y_3) * (y_4 - y_3) + (z_1 - z_3) * (z_4 - z_3))) * ((x_4 - x_3) * (x_2 - x_1) + (y_4 - y_3) * (y_2 - y_1) + (z_4 - z_3) * (z_2 - z_1)) - ((x_1 - x_3) * (x_2 - x_1) + (y_1 - y_3) * (y_2 - y_1) + (z_1 - z_3) * (z_2 - z_1))) * ((x_4 - x_3) * (x_4 - x_3) + (y_4 - y_3) * (y_4 - y_3) + (z_4 - z_3) * (z_4 - z_3))) / (((x_2 - x_1) * (x_2 - x_1) + (y_2 - y_1) * (y_2 - y_1) + (z_2 - z_1) * (z_2 - z_1))) * ((x_4 - x_3) * (x_4 - x_3) + (y_4 - y_3) * (y_4 - y_3) + (z_4 - z_3) * (z_4 - z_3)) - ((x_4 - x_3) * (x_2 - x_1) + (y_4 - y_3) * (y_2 - y_1) + (z_4 - z_3) * (z_2 - z_1))) * ((x_4 - x_3) * (x_2 - x_1) + (y_4 - y_3) * (y_2 - y_1) + (z_4 - z_3) * (z_2 - z_1))) * (y_2 - y_1) + (y_3) + (((((x_1) - (x_3)) * ((x_4) - (x_3)) + ((y_1) - (y_3)) * ((y_4) - (y_3)) + ((z_1) - (z_3)) * ((z_4) - (z_3)))) + (((((x_4) - (x_3)) * ((x_2) - (x_1)) + ((y_4) - (y_3)) * ((y_2) - (y_1)) + ((z_4) - (z_3)) * ((z_2) - (z_1)))) * (((((x_1) - (x_3)) * ((x_4) - (x_3)) + ((y_1) - (y_3)) * ((y_4) - (y_3)) + ((z_1) - (z_3)) * ((z_4) - (z_3)))) * (((x_4) - (x_3)) * ((x_2) - (x_1)) + ((y_4) - (y_3)) * ((y_2) - (y_1)) + ((z_4) - (z_3)) * ((z_2) - (z_1)))) - (((x_1) - (x_3)) * ((x_2) - (x_1)) + ((y_1) - (y_3)) * ((y_2) - (y_1)) + ((z_1) - (z_3)) * ((z_2) - (z_1)))) * (((x_4) - (x_3)) * ((x_4) - (x_3)) + ((y_4) - (y_3)) * ((y_4) - (y_3)) + ((z_4) - (z_3)) * ((z_4) - (z_3)))) - (((x_4) - (x_3)) * ((x_2) - (x_1)) + ((y_4) - (y_3)) * ((y_2) - (y_1)) + ((z_4) - (z_3)) * ((z_2) - (z_1)))) * (((x_4) - (x_3)) * ((x_2) - (x_1)) + ((y_4) - (y_3)) * ((y_2) - (y_1)) + ((z_4) - (z_3)) * ((z_2) - (z_1)))))) / (((x_4) - (x_3)) * ((x_4) - (x_3)) + ((y_4) - (y_3)) * ((y_4) - (y_3)) + ((z_4) - (z_3)) * ((z_4) - (z_3)))) * (y_4 - y_3) / 2$$

(12.11)

The z-coordinate of the midpoint of the shortest line between two lines in 3D (z_{ab}) is:

$$z_{ab} = \frac{z_a + z_b}{2} \tag{12.12}$$

with (z_a) and (z_b) as described above.

When defining the following:

“*” as multiplication,

“/” as division,

then:

$$z_{ab} = \frac{((z_1 + (((x_1 - x_3) * (x_4 - x_3) + (y_1 - y_3) * (y_4 - y_3) + (z_1 - z_3) * (z_4 - z_3))) * ((x_4 - x_3) * (x_2 - x_1) + (y_4 - y_3) * (y_2 - y_1) + (z_4 - z_3) * (z_2 - z_1)) - ((x_1 - x_3) * (x_2 - x_1) + (y_1 - y_3) * (y_2 - y_1) + (z_1 - z_3) * (z_2 - z_1))) * ((x_4 - x_3) * (x_4 - x_3) + (y_4 - y_3) * (y_4 - y_3) + (z_4 - z_3) * (z_4 - z_3))) / (((x_2 - x_1) * (x_2 - x_1) + (y_2 - y_1) * (y_2 - y_1) + (z_2 - z_1) * (z_2 - z_1))) * ((x_4 - x_3) * (x_4 - x_3) + (y_4 - y_3) * (y_4 - y_3) + (z_4 - z_3) * (z_4 - z_3)) - ((x_4 - x_3) * (x_2 - x_1) + (y_4 - y_3) * (y_2 - y_1) + (z_4 - z_3) * (z_2 - z_1))) * ((x_4 - x_3) * (x_2 - x_1) + (y_4 - y_3) * (y_2 - y_1) + (z_4 - z_3) * (z_2 - z_1))) * (z_2 - z_1) + ((z_3) + (((x_1) - (x_3)) * ((x_4) - (x_3)) + ((y_1) - (y_3)) * ((y_4) - (y_3)) + ((z_1) - (z_3)) * ((z_4) - (z_3))) + (((x_4) - (x_3)) * ((x_2) - (x_1)) + ((y_4) - (y_3)) * ((y_2) - (y_1)) + ((z_4) - (z_3)) * ((z_2) - (z_1))) * (((x_1) - (x_3)) * ((x_4) - (x_3)) + ((y_1) - (y_3)) * ((y_4) - (y_3)) + ((z_1) - (z_3)) * ((z_4) - (z_3))) * (((x_4) - (x_3)) * ((x_2) - (x_1)) + ((y_4) - (y_3)) * ((y_2) - (y_1)) + ((z_4) - (z_3)) * ((z_2) - (z_1))) - (((x_1) - (x_3)) * ((x_2) - (x_1)) + ((y_1) - (y_3)) * ((y_2) - (y_1)) + ((z_1) - (z_3)) * ((z_2) - (z_1))) * (((x_4) - (x_3)) * ((x_4) - (x_3)) + ((y_4) - (y_3)) * ((y_4) - (y_3)) + ((z_4) - (z_3)) * ((z_4) - (z_3))) - (((x_4) - (x_3)) * ((x_2) - (x_1)) + ((y_4) - (y_3)) * ((y_2) - (y_1)) + ((z_4) - (z_3)) * ((z_2) - (z_1))) * (((x_4) - (x_3)) * ((x_2) - (x_1)) + ((y_4) - (y_3)) * ((y_2) - (y_1)) + ((z_4) - (z_3)) * ((z_2) - (z_1)))))) / (((x_4) - (x_3)) * ((x_4) - (x_3)) + ((y_4) - (y_3)) * ((y_4) - (y_3)) + ((z_4) - (z_3)) * ((z_4) - (z_3))) / 2$$

(12.13)

The distance of the shortest line between two lines in 3D (d_{ab}) is:

$$d_{ab} = \sqrt{(x_a - x_b)^2 + (y_a - y_b)^2 + (z_a - z_b)^2} \quad (12.14)$$

The above formulae can be inserted in a program to calculate the 3D position of the artefact point.

12.4 Determining the 3D xyz-position using two pinhole cameras

The principle of a pinhole camera is that light passes from an object through a pinhole to the image plane. An inverted image is created on the image plane and the image line is from the object point, through the pinhole to the image plane.

By using two pinhole cameras positioned next to each other as displayed in figure 3.1, two image lines are created from the object point, through the pinholes onto the image plane.

As the pinhole position and the position of the image point of the object point are available on the image, two lines in 3D are created from the same object point. By utilising the mathematical formulae to determine the intersection of two lines in 3D, the object point was determined using the 3D formulae.

The novelty of using a pinhole camera is with a pinhole camera, there is nearly infinite depth of view due to that the light only passes through the pinhole.

12.5 Determining the 3D xyz-position using a single lens image

The method to determine the 3D position of an artefact point with a single image was also explained. As only a single image is used, less processing is required to determine the 3D position.

To obtain stereoscopic vision two images are normally used, but a method to determine the 3D position of an artefact using only a single image have been derived. As technology is moving in the electronic field with robotics applications and even robotic exploration, a method to determine the 3D position with two images as well as a single image can be beneficial. This method does not require additional equipment to be loaded and can minimize cost if it is implemented on robotic missions.

With robotic missions, the method to determine the 3D position of an object point with only one image can be used as a backup for 3D positioning. As for stereoscopic vision two images are used and available. If one of the cameras fails, then the 3D position with a single camera can be utilised.

12.6 Determine the Centre of Projection of a camera setup

By using the centre of projection (COP) method, two image lines was used to determine the 3D position of an artefact. In this case, the two lines do not intersect at the image point, but at the COP.

Before using this method to determine the 3D position of an artefact point, the COP of a camera needs to be determined.

By utilizing the setup as displayed in figure 12.2, which displays the single camera setup with the image plane and the COP, the COP was determined. Two image lines, image line 1 and image line 2 with the set position of artefact 1, artefact 2 and the positions of the artefacts on the image plane, the COP was determined.

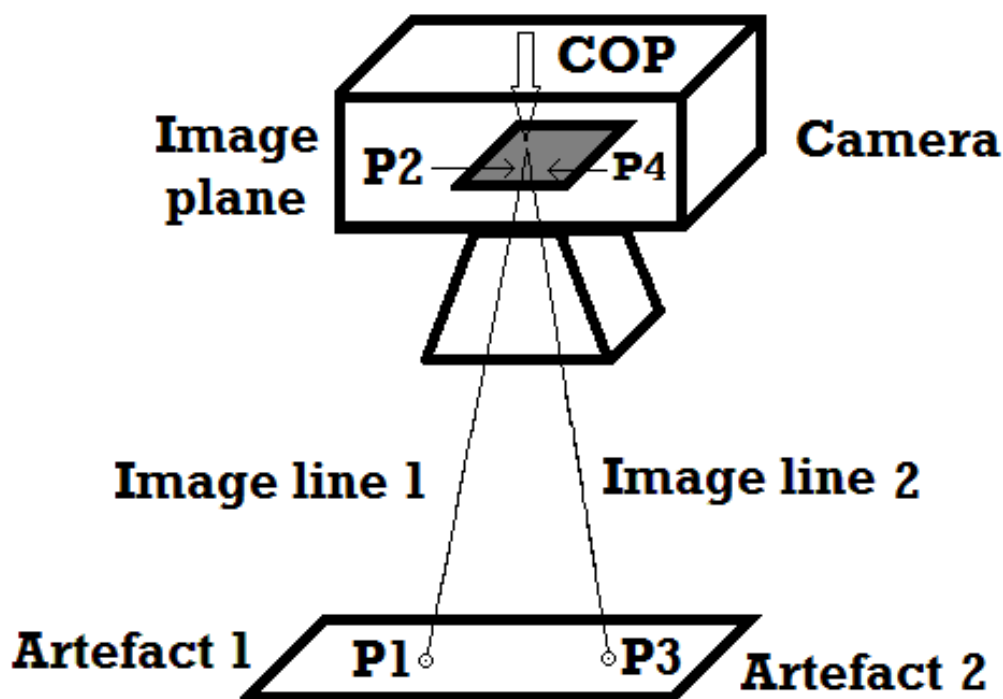


Figure 12.2: Setup to determine the COP

By utilising the formulae as described in section 12.2, the co-ordinates of the artefact points and their corresponding positions on the image plane, the 3D position of the COP was calculated.

The value of obtaining the COP position of a camera is that it can be utilised to determine the 3D position using a two camera setup.

12.7 Determining the 3D xyz-position of an X-ray focus

The X-ray focus as describe in chapter 9 is the point where the X-rays are generated. The method described to determine the intersecting point in 3D was used to determine the position of the X-ray focus.

In performing 3D measurements and planning for treatment, the position of the X-ray focus which indicates the distance from the source to the patient can be used to ensure optimum image quality for imaging. Also the inverse square rule is applicable in X-rays.

To determine the position of the X-ray focus, two image points are also utilised by using a metallic plate and the artefact position on the X-ray image as displayed in figure 12.3

Figure 12.3 displays the focus point of the X-ray tube assembly.

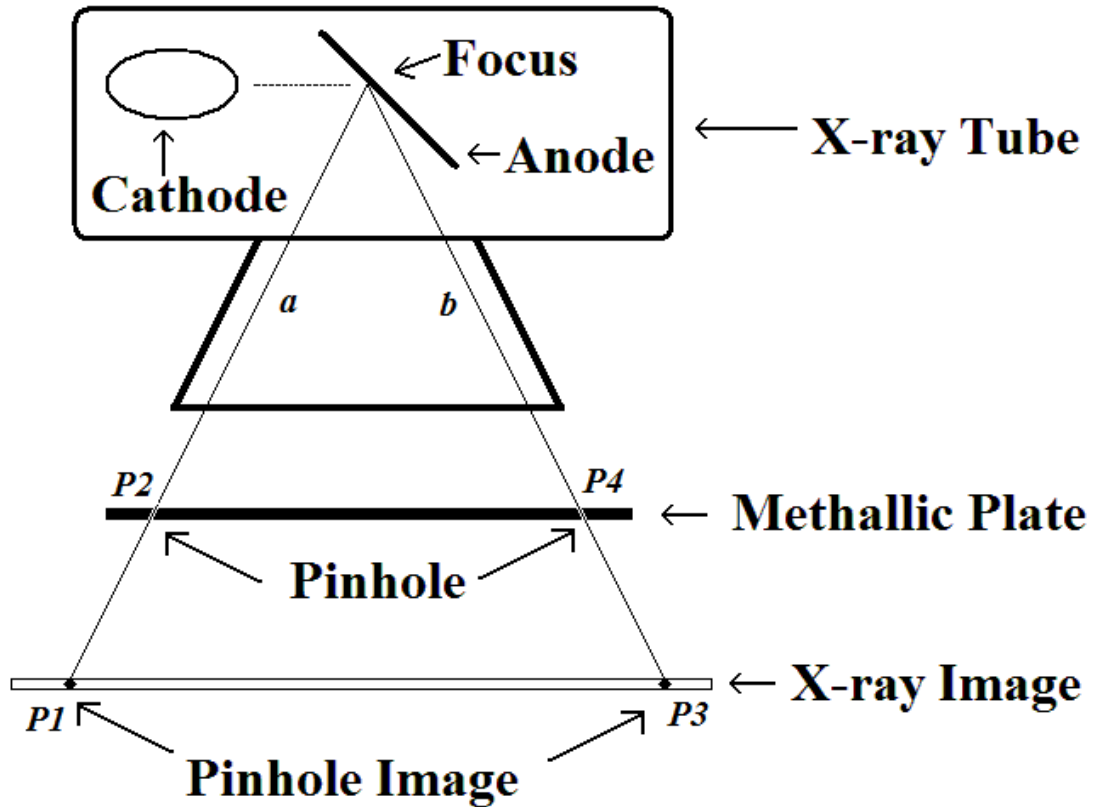


Figure 12.3: Focus point of the X-ray tube setup

By utilising the formulae as described in section 12.2, the co-ordinates of the points on the metallic plate and their corresponding positions on the X-ray image plane, the 3D position of the X-ray focus was described.

The value of obtaining the position of the X-ray focus is that it can be used to determine 3D measurements of an anatomical structure of a patient.

12.8 Determining the 3D measurements on an AP and LAT X-ray Image

Figure 12.4 displays the method to perform 3D measurements with an AP and LAT X-ray examination.

If the position of the X-ray focus 1 and X-ray focus 2 are determined then with the X-ray images available as described in figure 12.4, the 3D measurements of an anatomical structure was determined.

The anatomical structure, example the arm needs to be kept stationary with the X-ray tube rotated around a central point. With the fixed image to focus point, and the rotation angle, the positions of focus 1 and focus 2 was determined.

In this case, four image lines were generated that originating from the two X-ray foci.

By utilizing the formulae as described in section 12.2, the intersecting point of the two pairs of image lines was determined and with formulae 12.4 the 3D linear distance of the anatomical structure was obtained.

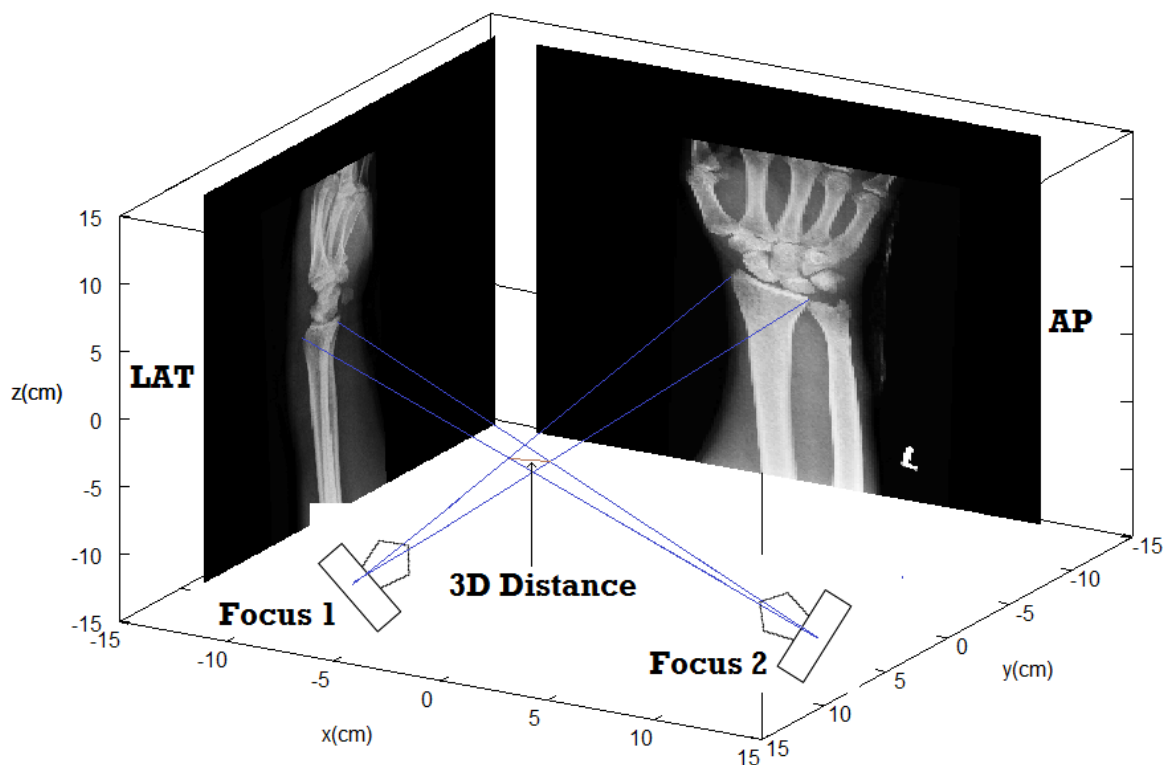


Figure 12.4: Measuring the radial transverse distance

12.9 Experimental comparison of methods derived and application

Different methods have been derived in this research to determine the 3D position of an artefact in space. These methods were applied in different experimental setup and the experimental results were within range of the calculated results.

With the method derived in the application of the pinhole camera setup, the calculated result was 20.35cm and the experimental result was 25.3cm. The method derived applied in the experiment was within of 80% of the measured results.

Also in the application of this method in the experiment measuring the distance of the coin with the X-ray visualization method, the calculated result was 2.24cm and the measured distance of the coin was 2.36cm. This gives an accuracy of 95% in applying the methods derived in an X-ray visualization method.

12.9 Conclusion

Different methods to determine the 3D position of an artefact was explained. With the formulae to obtain the 3D position of two lines in 3D, this formulae was applied in different applications.

Pinhole cameras provide nearly infinite depth of view due to that the light only passes through the pinhole. This thesis explained the method to determine the 3D position of an artefact with two pinhole cameras. Using the method for 3D positioning of an artefact with a pinhole, a number of 3D positions can be determined using the pinhole image. The novelty with a pinhole camera and the calculation of the 3D position is multiple points are available for the user to determine the 3D position.

The method to determine the 3D position of an artefact with only one image was explained in this thesis. This can be used as a backup system to obtain the 3D position of objects even when one camera is out of order. The novelty of obtaining 3D information with a single image can add in the obtaining of 3D information with minimal processing as only one image needs to be evaluated. This is a novel approach using the characteristics of a lens system.

With the utilisation of a two image system, a number of iterations are required to determine the 3D position of an artefact. With the formulae described for the 3D position of an artefact with only one image, the iterations are less. This indicates the results will be faster available when the 3D position is required. The limitations when using a single lens image, is that the image needs to be in view with the image plane.

The COP of a camera was also explained to determine the 3D position of an artefact. As explained in this thesis, the utilisation of the COP and a two camera setup was used to determine the 3D position of an artefact and also be utilized to perform 3D measurements. The value of this can be in cell phone applications. With cell phones developing rapidly and their application, utilising this method in a cell phone application with a two camera setup, 3D measurements can be obtained.

In this thesis, application of the method to determine the 3D position with an X-ray examination was explained. The diameter of a coin that was X-rayed was determined. In the X-ray spectrum, by applying this 3D formulae, the 3D length of a long bone can be determined if two X-ray images are available. With the use of computer tomography (CT), measurements can also be obtained, but the amount of radiation is less with an AP and LAT X-ray examination than that of CT. If the measurements of a long bone are required, the above method with the AP and LAT X-ray examinations can be utilised. This novel way to obtain measurements with minimum radiographic examinations was investigated in this thesis. This method can minimise radiation to the patient, but if further information are needed other examinations, example CT can be performed.

This thesis further add to the fact that with minimal radiographic examinations, additional information can be obtained using the method derived and can add benefit to surgical planning for the patient. If the lengths of surgical screws or surgical plates need to be obtained, then an application of this method can be applied and investigated.

12.10 Recommendations for further study

The pinhole camera setup provides nearly infinite depth of view, but a longer exposure time is required. With a camera setup, a shorter time is required to obtain an optimal image quality. A comparison between the application of a pinhole camera setup and a camera setup can be performed to evaluate the time effect of determining the 3D position of an artefact.

In the evaluation of the 3D position of an artefact with a single lens camera, less iterations are required to determine the 3D position as with a two camera setup. An application where both cameras are available for 3D position can be investigated with one camera failing and determine if the other camera provides the 3D position for interaction.

The strategies and applications of the formulae can be applied in both still as well as moving images. In still images, the user can select the point to determine the 3D position. Research and an investigation in the application of the above images in a moving image can be done. Also the use of panoramic images can be envisaged.

In the application in the X-ray spectrum, the 3D measurement of a linear structure has been described. Applying this in a non-linear or curved structured can be investigated. As anatomical structures have different counters. By determining the 3D length of a curve structure will be of value.

Reference

Adonis, M. & Kahn, MTE. 2006. Infrared Radiation Theory and Applications. 2006. Cape Town. CDPEs. DV8 Litho and Digital

Anderson, R. 2008. A calibration method for laser-triangulation 3D cameras. Computer Vision Laboratory: 5-7, 1. December 2008

Ball, J. & Price, T. 1989. Chesney's Radiographic Imaging. 5th Edition. Blackwell Scientific Publications. London. page 336

Bester, E. A., Ham, J., Loots, K. & Stark, A. 1998. Study & Master Mathematics. Somerset West. National Book Printers

Bourke, P. <http://paulbourke.net/geometry> (Accessed 1 March 2013)

Curtis, H. D., 2010. Orbital Mechanics for Engineering Students. 2nd Edition. Elsevier Aerospace Engineering Series.

<http://books.google.co.za/books?hl=en&lr=&id=rzw4wOHDpjQC&oi=fnd&pg=PP2&dq=%22their+dot+product+is+zero%22&ots=ULz6udNV3d&sig=gX-TWALkz4uTy3wEWVF0fgT9V5w#v=onepage&q=%22their%20dot%20product%20is%20zero%22&f=false> (Accessed: 8 March 2013)

Dektar, K., Adams, A. & Levoy, M. Gaussian lens formula.

<http://graphics.stanford.edu/courses/cs178/applets/gaussian.html> . (Accessed 18 October 2012)

Deneubourg, J. L., Goss, S. & Franks, N. 1990. The dynamics of collective sorting robot-like ants and ant-like robots. Proceedings of the first "SAB" Conference. 1990. DiBiase, D. Rectification by Stereoscopia. https://www.education.psu.edu/natureofgeoinfo/c6_p14.html. (Accessed 13 November 2012)

Engineering Talk. 2008. 3D Vision Machine System Become Mainstream. *The Engineer*, September 2006.

Fontaine, B., Termont, D., Steinicke, L., Pollefeys, M., Vergauwen, M., Moreas, R., Xu, F., Landzettel, K., Steinmetz, M., Brunner, B., Michaelis, H., Behnke, T., Dequeker, R., Degezelle, P., Bertrand, R. & Visentin, G. 2000. Autonomous operations of a micro-rover for geo-science on mars. Proceedings of 6th ESA workshop on advanced space technologies for robotics and automation - ASTRA'2000, paper no. 3.7-1 location: Noordwijk, The Netherlands. Date: December 5-7.
<http://robotics.estec.esa.int/ASTRA/Astra2000/Papers/3.7-1.pdf> (Accessed 31 July 2014)

Health and Safety Act. South Africa. 1974. *Health and Safety Act.*1974. Pretoria: Government Printers

Hollingworth, J., Butterfield, D., Swart, B. & Allsop, J. 2001. C++ Builder 5. Developer's Guide. Indiana: Sams Publishing

<http://andrewrreed.com/Writings/curricula/articles-of-potential-interest/pinhole-camera>
(Accessed on 11 October 2010)

<http://andrewrreed.com/Writings/curricula/articles-of-potential-interest/pinhole-camera>
(Accessed on 21 June 2010)

<http://education.vetmed.vt.edu/Curriculum/VM8054/EYE/BINOCS.HTM> (Accessed on 6 October 2010)

<http://inphotos.org/tag/canon/> (Accessed on 21 June 2010)

http://nasa.gov/centres/ames/news/releases/2002/02_136AR_prt.htm. (Accessed on 8 June 2011)

<http://paulbourke.net/geometry> (Accessed 1 March 2013)

<http://photo.net/pinhole/pinhole.htm> (accessed on 21 June 2010)

<http://pinhole-camera.deviantart.com/> (accessed on 11 October 2010)

http://www.gbcsa.org.za/system/data/uploads/resource/69_res.pdf (Accessed: 14 November 2011)

<http://www.greentoronto.me/effec-of-shadow-on-solar-cell-output>. (Accessed 8 June 2011)

<http://www.mathworks.com/> (Accessed: 8 March 2013)

<http://www.vision3d.com/stereo.html> (Accessed on 6 October 2010)

Ibrahim, A., "Effect of Shadow and dust on the Performance of Silicon Solar Cell"
Journal of Basic and Applied Scientific Research, 1(3), 2011, pp222-230

Joubert, S. V., Janse van Rensburg, D. P., Kruger, W. J. J. & Van der Watt, J. S.
1997. Technikon Mathematics II. 2nd Edition. Pretoria. Multigraph

Kansal, R. 2008. PIC Based Automatic Solar Radiation Tracker. Patiala .Thaper
University. (Ma-thesis)

Kelly A. M., Erica S.Y & David P.S.2006. Accuracy of Cone Beam Computed
Tomography for Periodontal Defect Measurements. 2006. *Journal of Periodontology*
(Abstract). June 2006

Klank, U., Zia, M. Z. & Beetz, M. 3D Model Selection from an Internet Database for
Robotic Vision. http://ias.in.tum.de/_media/spezial/bib/klank09icra.pdf. (Accessed 18
October 2012)

Landauer, R. S. 2013. Application of the Inverse-Square Law to Oil-Immersed Tubes.
Radiology. 2006.

Lazaros, N., Sirakoulis, G. C. and Gasteratos, A. "Review off sterio vision algorithms:
From Software to Hardware" International Journal of Optomechatronics, 2: 435–462,
2008

Liu, X., Patrangenaru, V. & Sugathadasa, S. 2007. Projective Shape Analysis for
Noncalibrated Pinhole Views. Technical Report MP03: 21-32, 17 February 2007

Microsoft Encarta Encyclopaedia, 2003

Mine, M.R. 1996. Working in a Virtual World: Interaction Techniques Used in the Chapel Hill Immersive Modeling Program. Department of Computer Science, University of North Carolina, Chapel Hill, NC 27599-3175.

[http://miac.unibas.ch/PMI/01-BasicsOfXray.html#\(12\)](http://miac.unibas.ch/PMI/01-BasicsOfXray.html#(12))
(Accessed 27 May 2014)

<http://www.cours.polymtl.ca/ind6409/Mark%20-%202012-Mine%20-%20Working%20in%20a%20Virtual%20World%20-%20Interaction%20Technique.pdf>. (Accessed 4 April 2013)

<http://www.sciencedirect.com/science/article/pii/S1120179712000300>. (Accessed 4 April 2013)

<http://www.sno.phy.queensu.ca/~phil/exiftool/TagNames/DICOM.html> (Accessed 8 October 2013)

Mokoena, S., Energy efficient lightning system implementation in 5 ESCOM buildings in the North West Region. Industrial and Commercial use of Energy. 2011. p161

Moravec, H. P. 1996. Robot Spatial Perception by Stereoscopic Vision and 3D Evidence Grids. *The Robotics Institute Carnegie Mellon University Pittsburgh, Pennsylvania 15213*. September 2006.

Mouragnon, E., Lhuillier, M., Dhôme, M., Dekeyser, F. & Sayd, P. 2006. Real Time Localization and 3D Reconstruction. September 2006

Ndlovu, M. & Lekalakala, T. Renewable energy options and base load stations for South Africa community. Industrial and Commercial use of Energy. 2011. p232

Nell, R. 2006. Theoretical method for detecting a 3D point in space with one X-ray exposure. *The South African Radiographer*, 44 (2): 21-22, November 2006.

Nell, R.D. & Kahn, M.T.E., The use of 3D electronic vision for effective utilization of solar power in a hybrid electrical supply system. International Conference. Industrial and Commercial use of Energy. 2011. p241

Palvolgyi, J. 2012. Multi-parametric fit method in reconstruction of brachytherapy needles. Abstract.

Raju, C.H. 2004. Analysis of very large scale image data using out-of-core technique and automated 3D reconstruction using calibrated images. Master's Degree Thesis. Visvesvaraya Technological University, India

Sears, F. W. 1958. Optics. Massachusetts. Addison-Wesley Publishing Company, Inc. page (90-110,372)

South African National Standard, SANS, Energy efficiency in buildings Part 2: The application of the energy efficiency requirements for buildings with natural environmental control. Edition 1. SANS 204-2:2008, p26.

Sungur, C., "Multi-axes sun-tracking system with PLC control for photovoltaic panels in Turkey" Elsevier, Renewable Energy, vol. 34, 2009, pp. 1119–1125

Swallow, R. A., Naylor, E., Roebuck, E.T. & Whitley, A. S. 2001. Clark's Positioning in Radiography. 11th Edition. Replica Press, India, Delhi. page 2 and page 386

Thakare, S.S., Rupesh, P.A. and Shahade, M. R. Artificial Intelligence with Stereo Vision Algorithms and its Methods. 2012. International Journal of Computer Applications. Proceedings on International Conference on Recent Trends in Information Technology and Computer Science (ICRTITCS-2011) icrtitcs(3):1-6, March 2012. Published by Foundation of Computer Science, New York, USA. (Abstract). 2012

The Technology Teacher. (2009).

http://www.google.co.za/url?url=http://spaceplace.nasa.gov/en/educators/pinhole_camera_web.pdf&rct=j&frm=1&q=&esrc=s&sa=U&ei=6zXaU8XiEYrN7AbKyoCwAQ&ved=0OCBMQFjAA&sig2=v1CjlcivkB-41Kct1q_Vg&usq=AFQjCNH9p-jHDN7pnX8rLUpi157fx0NrfQ. (Accessed on 31 July 2014)

Tse, K. K., Ho, M. T., Chung, H. S & Hui, S. I. 2002. A Novel Maximum Power Point Tracker for PV Panels Using Switching Frequency Modulation. IEEE TRANSACTIONS ON POWER ELECTRONICS, VOL. 17, NO. 6.

Walker, G. Evaluation MPPT converter Topologies Using a Matlab PV model. Dept of Computer Science and Electrical Engineering, University of Queensland, Australia. www.emeraldinsight.com (Accessed on 30 May 2010)

www.techdigest.tv/Pinhole-camera.png (Accessed on 21 June 2010)

APPENDICES

APPENDIX A

Calculating the intersecting point of two lines in 2D

```
function []=_2dxy()
%-----
clear all
close all
clc

x1a=rand()*100
y1a=rand()*100

x2a=rand()*100
y2a=rand()*100

x1b=rand()*100
y1b=rand()*100

x2b=rand()*100
y2b=rand()*100

ma=(y2a-y1a)/(x2a-x1a);
mb=(y2b-y1b)/(x2b-x1b);
ca=y1a-(((y2a-y1a)/(x2a-x1a))*x1a);
cb=y1b-(((y2b-y1b)/(x2b-x1b))*x1b);

%-----
xab=(cb-ca)/(ma-mb)
yab=(ma*(xab))+ca
%-----
plot([x1a,x2a],[y1a,y2a])
hold on
plot([x2a,xab],[y2a,yab])
```

```
plot([x1b,x2b],[y1b,y2b])
plot([x2b,xab],[y2b,yab])
```

```
hold off
```

```
%int2str(xab);
```

```
%int2str(yab);
```

```
%strcat('xab','(',int2str(xab),int2str(yab),')')
```

```
text(xab,yab,strcat('xab','(',int2str(xab),',',int2str(yab),')'));
```

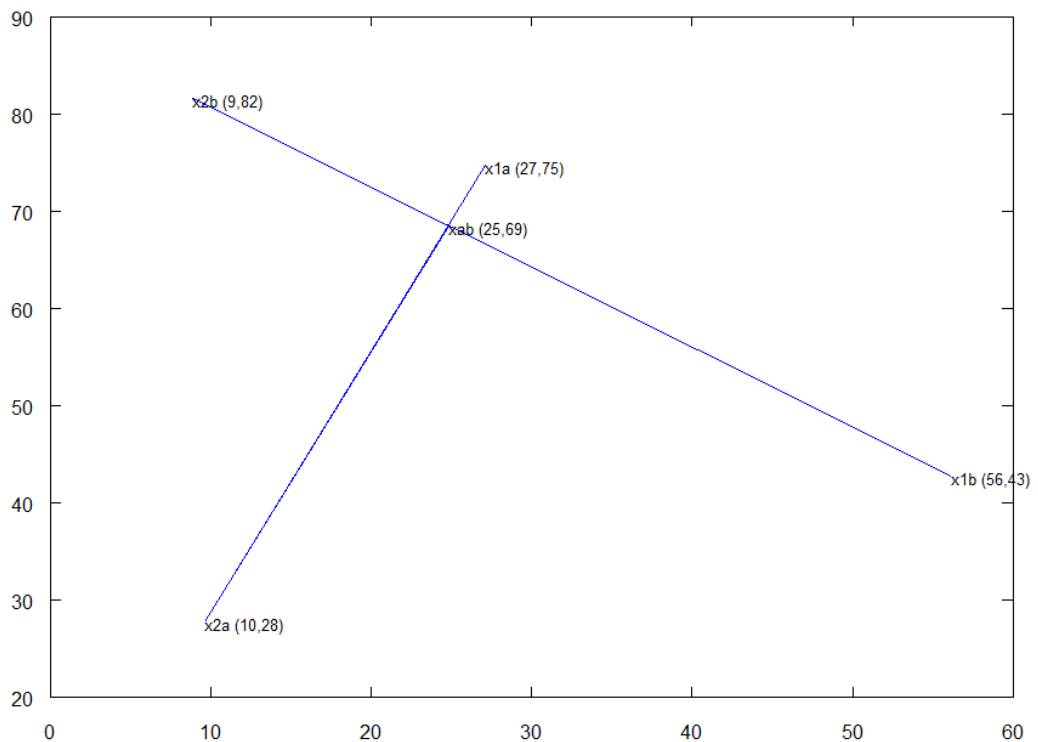
```
text(x1a,y1a,strcat('x1a','(',int2str(x1a),',',int2str(y1a),')'));
```

```
text(x1b,y1b,strcat('x1b','(',int2str(x1b),',',int2str(y1b),')'));
```

```
text(x2a,y2a,strcat('x2a','(',int2str(x2a),',',int2str(y2a),')'));
```

```
text(x2b,y2b,strcat('x2b','(',int2str(x2b),',',int2str(y2b),')'));
```

```
%-----
```



67.2810, 61.1869

APPENDIX B

Using the Centre of Projection to calculate the xyz-position

```
function []=cop4()
%-----
clear all
close all
clc
%-----
%RAND()*(b-a)+a
%rand()*((b)-(a))+(a)

xf1=rand()*(0-(-200))+(-200);
yf1=rand()*(200-(-200))+(-200);
zf1=rand()*(250-(100))+(100);

xc1=20;
yc1=0;
zc1=0;

xs1=0;
ys1=0+rand()*(-20-(-20))+(-20);
zs1=0-rand()*20;

xc2=xc1;
yc2=yc1;
zc2=zc1+70;

xs2=xs1;
ys2=ys1;
zs2=zs1-rand()*20+70;

                                xc1=20;
                                yc1=0;
                                zc1=0;

                                xs1=0;
                                ys1=-20;
                                zs1=-8.0973;

                                xc2=20;
```

```

yc2=0;
zc2=70;

xs2=0;
ys2=-20;
zs2=43.139;

p1=[xc1,yc1,zc1];
p2=[xs1,ys1,zs1];
p3=[xc2,yc2,zc2];
p4=[xs2,ys2,zs2];
[pa, pb] = LineLineIntersectIn3D(p1,p2,p3,p4);
xa=(pa(1)+pb(1))/2;
ya=(pa(2)+pb(2))/2;
za=(pa(3)+pb(3))/2;

xp=xa
yp=ya
zp=za

dfp=sqrt(...
    (xf1-xp)*(xf1-xp) + ...
    (yf1-yp)*(yf1-yp) + ...
    (zf1-zp)*(zf1-zp)...
)

%xf1=xa;
%yf1=ya;

hold on;
plot3([0,0],[-30,-30],[-30,30]);
plot3([0,0],[30,30],[-30,30]);
plot3([0,0],[-30,30],[-30,-30]);
plot3([0,0],[-30,30],[30,30]);

plot3([0,0],[-30,-30],[40,100]);
plot3([0,0],[30,30],[40,100]);
plot3([0,0],[-30,30],[40,40]);
plot3([0,0],[-30,30],[100,100]);

```

```

IRD=dfp;
SRD=dfp;
%axis([-IRD-25,SRD+25,-IRD-25,SRD+25,-IRD-25,SRD+25],"square");
axis('square');
%axis('off');

xlabel('x');
ylabel('y');
zlabel('z');

%plot3([xf1,yp],[yf1,yp],[zf1,zp]);
plot3([xc1,xs1],[yc1,ys1],[zc1,zs1]);
plot3([xc2,xs2],[yc2,ys2],[zc2,zs2]);
plot3([xc1,yp],[yc1,yp],[zc1,zp]);
plot3([xc2,yp],[yc2,yp],[zc2,zp]);

text(0,0,0,'O')
text(xp,yp,zp,'P')
text(xc1,yc1,zc1,'C1')
text(xc2,yc2,zc2,'C2')
text(xs1,ys1,zs1,'S1')
text(xs2,ys2,zs2,'S2')

legend('east');
%strcat('Origin(O)=','(',num2str(0),',',num2str(0),',',num2str(0),')'),...
legend(...
    strcat('COP1(C1)=','(',num2str(xc1),',',num2str(yc1),',',num2str(zc1),')'),...
    strcat('COP2(C2)=','(',num2str(xc2),',',num2str(yc2),',',num2str(zc2),')'),...
    strcat('Screen1(S1)=','(',num2str(xs1),',',num2str(ys1),',',num2str(zs1),')'),...
    strcat('Screen2(S2)=','(',num2str(xs2),',',num2str(ys2),',',num2str(zs2),')'),...
    strcat('P=','(',num2str(xp),',',num2str(yp),',',num2str(zp),')')...
    %strcat('Object(P)=','(',num2str(xp),',',num2str(yp),',',num2str(zp),')')...
);

hold off;

```

```

function [pa, pb] = LineLineIntersectIn3D(p1,p2,p3,p4)

%   Calculates the line segment pa_pb that is the shortest route
%   between two lines p1_p2 and p3_p4. Calculates also the values of
%   mua and mub where
%       pa = p1 + mua (p2 - p1)
%       pb = p3 + mub (p4 - p3)
%
%   Return the xyz-coordinates of pa and pb

p13(1) = p1(1) - p3(1);
p13(2) = p1(2) - p3(2);
p13(3) = p1(3) - p3(3);

p43(1) = p4(1) - p3(1);
p43(2) = p4(2) - p3(2);
p43(3) = p4(3) - p3(3);

if ((abs(p43(1)) < eps) & ...
    (abs(p43(2)) < eps) & ...
    (abs(p43(3)) < eps))
    error('Could not compute LineLineIntersect!');
end

p21(1) = p2(1) - p1(1);
p21(2) = p2(2) - p1(2);
p21(3) = p2(3) - p1(3);

if ((abs(p21(1)) < eps) & ...
    (abs(p21(2)) < eps) & ...
    (abs(p21(3)) < eps))
    error('Could not compute LineLineIntersect!');
end

d1343 = p13(1) * p43(1) + p13(2) * p43(2) + p13(3) * p43(3);
d4321 = p43(1) * p21(1) + p43(2) * p21(2) + p43(3) * p21(3);
d1321 = p13(1) * p21(1) + p13(2) * p21(2) + p13(3) * p21(3);
d4343 = p43(1) * p43(1) + p43(2) * p43(2) + p43(3) * p43(3);
d2121 = p21(1) * p21(1) + p21(2) * p21(2) + p21(3) * p21(3);

denom = d2121 * d4343 - d4321 * d4321;

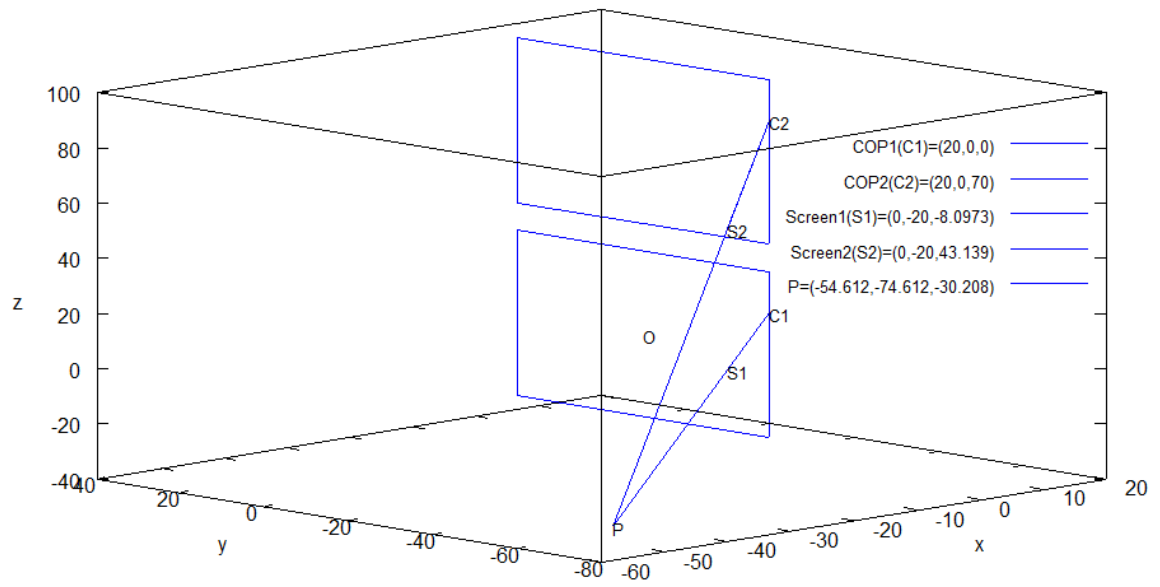
if (abs(denom) < eps)
    error('Could not compute LineLineIntersect!');
end

numer = d1343 * d4321 - d1321 * d4343;

mua = numer / denom;
mub = (d1343 + d4321 * mua) / d4343;

pa(1) = p1(1) + mua * p21(1);
pa(2) = p1(2) + mua * p21(2);
pa(3) = p1(3) + mua * p21(3);
pb(1) = p3(1) + mub * p43(1);
pb(2) = p3(2) + mub * p43(2);
pb(3) = p3(3) + mub * p43(3);

```



APPENDIX C

Get the 3D position of the midpoint of the shortest distance between two lines in 3D

```
function []=get3D()

%-----
clear all
close all
clc
%-----

%[pa, pb] = LineLineIntersectIn3D(p1,p2,p3,p4)

p1(1)=rand()*200; %x-coordinat of point(1)
p1(2)=rand()*200; %y-coordinat of point(1)
p1(3)=rand()*200 %z-coordinat of point(1)

p2(1)=rand()*200; %x-coordinat of point(2)
p2(2)=rand()*200; %y-coordinat of point(2)
p2(3)=rand()*200 %z-coordinat of point(2)

p3(1)=rand()*200; %x-coordinat of point(3)
p3(2)=rand()*200; %y-coordinat of point(3)
p3(3)=rand()*200 %z-coordinat of point(3)

p4(1)=rand()*200; %x-coordinat of point(4)
p4(2)=rand()*200; %y-coordinat of point(4)
p4(3)=rand()*200 %z-coordinat of point(4)

%-----

%{
p1(1)=212
p1(2)=225
p1(3)=100.51

p2(1)=212
p2(2)=225
p2(3)=66.90

p3(1)=212+11
```

```
p3(2)=225
p3(3)=100.51
```

```
p4(1)=212+10
p4(2)=225
p4(3)=66.90
```

```
%}
```

```
%-----
```

```
%-----
```

```
[pa, pb] = LineLineIntersectIn3D(p1,p2,p3,p4)
```

```
dab=sqrt(...
    (pa(1)-pb(1))*(pa(1)-pb(1)) + ...
    (pa(2)-pb(2))*(pa(2)-pb(2)) + ...
    (pa(3)-pb(3))*(pa(3)-pb(3))...
)
```

```
hold on
```

```
%axis('equal');
```

```
axis('square');
```

```
plot3(0,0,0, ' ');
```

```
plot3([p1(1),p2(1)],[p1(2),p2(2)],[p1(3),p2(3)])
```

```
text(p1(1),p1(2),p1(3),'1')
```

```
text(p2(1),p2(2),p2(3),'2')
```

```
plot3([p3(1),p4(1)],[p3(2),p4(2)],[p3(3),p4(3)])
```

```
text(p3(1),p3(2),p3(3),'3')
```

```
text(p4(1),p4(2),p4(3),'4')
```

```
plot3([pa(1),pb(1)],[pa(2),pb(2)],[pa(3),pb(3)])
```

```
text( (pa(1)+pb(1))/2 , (pa(2)+pb(2))/2 , (pa(3)+pb(3))/2 , 'X' )
```

```
x=(pa(1)+pb(1))/2
```

```
y=(pa(2)+pb(2))/2
```

```
z=(pa(3)+pb(3))/2
```

```
text(pa(1),pa(2),pa(3),'a')
```

```

text(pb(1),pb(2),pb(3),'b')

plot3([p1(1),pa(1)],[p1(2),pa(2)],[p1(3),pa(3)])
plot3([p2(1),pa(1)],[p2(2),pa(2)],[p2(3),pa(3)])

plot3([p3(1),pb(1)],[p3(2),pb(2)],[p3(3),pb(3)])
plot3([p4(1),pb(1)],[p4(2),pb(2)],[p4(3),pb(3)])

%legend("1",...
%    "2=8","3","4","a","b","X");

%legend("bottom");

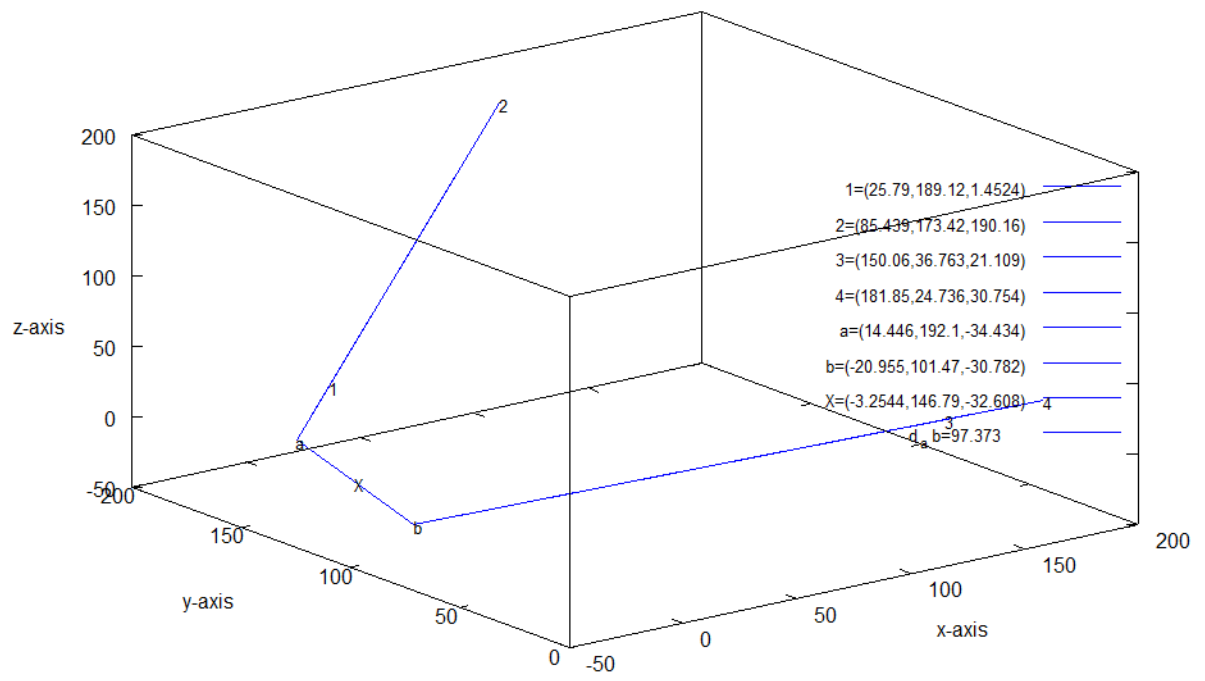
%legend(strcat("1=",(" ",num2str(p1(1))," ",num2str(p1(2))," ",num2str(p1(3)),""),...
%    "2=8","3","4","a","b","X");

legend(strcat('1=','(',num2str(p1(1))',' ',num2str(p1(2))',' ',num2str(p1(3))',')'),...
    strcat('2=','(',num2str(p2(1))',' ',num2str(p2(2))',' ',num2str(p2(3))',')'),...
    strcat('3=','(',num2str(p3(1))',' ',num2str(p3(2))',' ',num2str(p3(3))',')'),...
    strcat('4=','(',num2str(p4(1))',' ',num2str(p4(2))',' ',num2str(p4(3))',')'),...
    strcat('a=','(',num2str(pa(1))',' ',num2str(pa(2))',' ',num2str(pa(3))',')'),...
    strcat('b=','(',num2str(pb(1))',' ',num2str(pb(2))',' ',num2str(pb(3))',')'),...
    strcat('X=','(',num2str(x))',' ',num2str(y))',' ',num2str(z))',''),...
    strcat('d_ab=',num2str(dab))...
);

xlabel('x-axis');
ylabel('y-axis');
zlabel('z-axis');

hold off
%-----

```



APPENDIX D

Function to calculate the coordinates of the shortest line between two lines in 3D

```
function [pa, pb] = LineLineIntersectIn3D(p1,p2,p3,p4)

% Calculates the line segment pa_pb that is the shortest route
% between two lines p1_p2 and p3_p4. Calculates also the values of
% mua and mub where
%   pa = p1 + mua (p2 - p1)
%   pb = p3 + mub (p4 - p3)
%
% Return the xyz-coordinates of pa and pb

p13(1) = p1(1) - p3(1);
p13(2) = p1(2) - p3(2);
p13(3) = p1(3) - p3(3);

p43(1) = p4(1) - p3(1);
p43(2) = p4(2) - p3(2);
p43(3) = p4(3) - p3(3);

if ((abs(p43(1)) < eps) & ...
    (abs(p43(2)) < eps) & ...
    (abs(p43(3)) < eps))
    error('Could not compute LineLineIntersect!');
end

p21(1) = p2(1) - p1(1);
p21(2) = p2(2) - p1(2);
p21(3) = p2(3) - p1(3);

if ((abs(p21(1)) < eps) & ...
    (abs(p21(2)) < eps) & ...
    (abs(p21(3)) < eps))
    error('Could not compute LineLineIntersect!');
end

d1343 = p13(1) * p43(1) + p13(2) * p43(2) + p13(3) * p43(3);
d4321 = p43(1) * p21(1) + p43(2) * p21(2) + p43(3) * p21(3);
d1321 = p13(1) * p21(1) + p13(2) * p21(2) + p13(3) * p21(3);
d4343 = p43(1) * p43(1) + p43(2) * p43(2) + p43(3) * p43(3);
d2121 = p21(1) * p21(1) + p21(2) * p21(2) + p21(3) * p21(3);
```

```
denom = d2121 * d4343 - d4321 * d4321;
```

```
if (abs(denom) < eps)
```

```
    error('Could not compute LineLineIntersect!');
```

```
end
```

```
numer = d1343 * d4321 - d1321 * d4343;
```

```
mua = numer / denom;
```

```
mub = (d1343 + d4321 * mua) / d4343;
```

```
pa(1) = p1(1) + mua * p21(1);
```

```
pa(2) = p1(2) + mua * p21(2);
```

```
pa(3) = p1(3) + mua * p21(3);
```

```
pb(1) = p3(1) + mub * p43(1);
```

```
pb(2) = p3(2) + mub * p43(2);
```

```
pb(3) = p3(3) + mub * p43(3);
```

APPENDIX D

Obtain the maximum red pixel in an image

```
function []=maxred4()

%-----
clear all
close all
clc
%-----
%-----Determine-the-xyz=coordinants-of-a-single-most-left-red-laser-point-on-image1-----

p1=imread('SAM1b.JPG');
%p1=imread("TREE1.BMP");

%p1=imread('SAM1b.JPG');
%p1=imread('TREE1.BMP');Picture 007

rmaxRG1=0;
rmaxRB1=0;
rmax1=0;
xr1=-1;
yr1=-1;

for(x=1:size(p1,2))
    for(y=1:size(p1,1))

        if(...
            ( p1(y,x,1)-p1(y,x,2)) > 50 )&&...
            ( p1(y,x,1)-p1(y,x,3)) > 50)&&...
            ((p1(y,x,1)-p1(y,x,2))>rmaxRG1)&&...
            ((p1(y,x,1)-p1(y,x,3))>rmaxRB1)&&...
            ((p1(y,x,1)-0)>rmax1)...
        )
            rmaxRG1=p1(y,x,1)-p1(y,x,2);
            rmaxRB1=p1(y,x,1)-p1(y,x,3);
            rmax1=p1(y,x,1);
            xr1=x;
            yr1=y;
        end
    end

end
```

```

end

R1=p1(yr1,xr1,1)
G1=p1(yr1,xr1,2)
B1=p1(yr1,xr1,2)
%rmaxRG1
xr1
yr1
%-----
%-----Determine-the-xyz=coordinants-of-a-single-most-left-laser-point-on-image2-----

p2=imread('SAM2a.JPG');

rmaxRG=0;
rmaxRB=0;
rmax2=0;
xr2=-1;
yr2=-1;

for(x=1:size(p2,2))
for(y=1:size(p2,1))

if(...
(p2(y,x,1)-p2(y,x,2) > 50 )&&...
(p2(y,x,1)-p2(y,x,3) > 50)&&...
((p2(y,x,1)-p2(y,x,2))>rmaxRG)&&...
((p2(y,x,1)-p2(y,x,3))>rmaxRB)&&...
((p2(y,x,1)-0)>rmax2)...
)
rmaxRG=p2(y,x,1)-p2(y,x,2);
rmaxRB=p2(y,x,1)-p2(y,x,3);
rmax2=p2(y,x,1);
xr2=x;
yr2=y;
end

end

end

R2=p2(yr2,xr2,1)
G2=p2(yr2,xr2,2)

```



```

B2=p2(yr2,xr2,2)
%rmaxRG1
xr2
yr2
%-----
%-----Calculate the xyz-coordinants-of-the-laser-pointer-----

xc1=1; %in cm
yc1=0;
zc1=0;

xc2=1; %in cm
yc2=3;
zc2=0;

%middle (320,240)

lenght_per_pixel=0.000732; %in cm

xs1=0
ys1=(xr1-320)*lenght_per_pixel
zs1=(yr1-240)*lenght_per_pixel

xs2=0
ys2=(xr2-320)*lenght_per_pixel+yc2
zs2=(yr2-240)*lenght_per_pixel

p11=[xc1,yc1,zc1];
p22=[xs1,ys1,zs1];
p33=[xc2,yc2,zc2];
p44=[xs2,ys2,zs2];
[pa, pb] = LineLineIntersectIn3D(p11,p22,p33,p44);

dab=sqrt(...
    (pa(1)-pb(1))*(pa(1)-pb(1)) + ...
    (pa(2)-pb(2))*(pa(2)-pb(2)) + ...
    (pa(3)-pb(3))*(pa(3)-pb(3))...
)

xa=(pa(1)+pb(1))/2
ya=(pa(2)+pb(2))/2

```

```
za=(pa(3)+pb(3))/2
```

```
r=sqrt(xa*xa+ya*ya+za*za)
```

```
%-----
```

```
%-----Plot-xyz-value-on-image1-----
```

```
figure(1);
```

```
imshow(p1);
```

```
hold on;
```

```
plot(xr1,yr1,'*')
```

```
text(xr1,yr1-10,strcat(' ',int2str(xr1),',',int2str(yr1),',',int2str(zr1),' '));
```

```
hold off;
```

```
%-----
```

```
%-----Plot-xyz-value-on-image2-----
```

```
figure(2);
```

```
imshow(p2);
```

```
hold on;
```

```
if (xr1>0&&yr1>0)
```

```
plot(xr2,yr2,'*')
```

```
text(xr2,yr2-10,strcat(' ',int2str(xr2),',',int2str(yr2),',',int2str(zr2),' '));
```

```
end
```

```
hold off;
```

```
%-----
```



APPENDIX E

Measure the distance using the Centre of Projection method

```
function []=mcp1()
%=====
clear all;
close all;
clc;

% set hold on so we can show multiple plots/surfs in figure
figure(1);
hold on;
%=====
% the P1 image data you want to show a plane
%AP=imread("FilmAP2.bmp");
AP=imread("P1b.jpg");

[nr,nc, zz]=size(AP);
dpp=0.038125;

for x1=1:nr
    for y1=1:nc
        %x(x1,y1)=0;
        %y(x1,y1)=(x1*dpp)-(nr*dpp/2)-(708*0.038125);
        %z(x1,y1)=(y1*dpp)-(nc*dpp/2)+(20*0.038125);

        x(x1,y1)=0;
        y(x1,y1)=(x1*dpp)-(nr*dpp/2);
        z(x1,y1)=(y1*dpp)-(nc*dpp/2);

        planeimg1(x1,y1,1)=AP(x1,y1,1);
    endfor
endfor

colormap("gray");
%colormap("default");

% do a normal surface plot
surf(x,y,z,planeimg1, 'edgecolor','none');
```

```

%-----
% the LAT image data you want to show a plane
%LAT=imread("LAT100.bmp");
LAT=imread("P1a.jpg");

[nr,nc, zz]=size(LAT);

for x1=1:nr
  for y1=1:nc

    x(x1,y1)=0;
    y(x1,y1)=(x1*dpp)-(nr*dpp/2)-(708*0.038125);
    z(x1,y1)=(y1*dpp)-(nc*dpp/2)+(20*0.038125);

    %x(x1,y1)=0;
    %y(x1,y1)=(x1*dpp)-(nr*dpp/2);
    %z(x1,y1)=(y1*dpp)-(nc*dpp/2);
    planeimg(x1,y1,1)=LAT(x1,y1,1);
  endfor
endfor

colormap('gray');

% do a normal surface plot
surf(x,y,z,planeimg, 'edgecolor','none');

%=====
% label the axis
xlabel('x(mm)');
ylabel('y(mm)');
zlabel('z(mm)');
%axis("equal");
%axis("nolabel");
%axis("off");
%axis([-IRD-25,SRD+25,-IRD-25,SRD+25,-IRD-25,SRD+25],"square");
%axis([-120,120,-120,120,-120,120],"square");
%axis([-10,100,-10,100,-10,40],"square");

%=====
hold on
%On AP Film

```

```

FAP=[10,0,0];
AP1=[0,-1.41,1.25];
FLAT=[10,-27,0];
LAT1=[0,-27+2.36,1.33];
plot3([FAP(1),AP1(1)],[FAP(2),AP1(2)],[FAP(3),AP1(3)]);
plot3([FLAT(1),LAT1(1)],[FLAT(2),LAT1(2)],[FLAT(3),LAT1(3)]);

```

```

[pa, pb] = LineLineIntersectIn3D(FAP,AP1,FLAT,LAT1);
a=[ (pa(1)+pb(1))/2 , (pa(2)+pb(2))/2 , (pa(3)+pb(3))/2 ]

```

```

FAP=[10,0,0];
AP2=[0,2.36,1.37];
FLAT=[10,-27,0];
LAT2=[0,-27-1.18,1.26];;
%LAT2=[0,-27-2.36,1.33];
plot3([FAP(1),AP2(1)],[FAP(2),AP2(2)],[FAP(3),AP2(3)]);
plot3([FLAT(1),LAT2(1)],[FLAT(2),LAT2(2)],[FLAT(3),LAT2(3)]);

```

```

[pa, pb] = LineLineIntersectIn3D(FAP,AP2,FLAT,LAT2);
b=[ (pa(1)+pb(1))/2 , (pa(2)+pb(2))/2 , (pa(3)+pb(3))/2 ]

```

```

dab=sqrt(...
    (a(1)-b(1))*(a(1)-b(1)) + ...
    (a(2)-b(2))*(a(2)-b(2)) + ...
    (a(3)-b(3))*(a(3)-b(3))...
)

```

```

%AP2=[0,3.86-(708*0.038125),-0.56];
AP2=[0,(62*0.038125),(13*0.038125)];
%plot3([FAP(1),AP1(1)],[FAP(2),AP1(2)],[FAP(3),AP1(3)]);
%plot3([FAP(1),AP2(1)],[FAP(2),AP2(2)],[FAP(3),AP2(3)]);

```

```

FLAT=[10,0,0];
LAT1=[0,0.75,-0.35];
LAT2=[0,3.86,-0.56];
%plot3([FLAT(1),LAT1(1)],[FLAT(2),LAT1(2)],[FLAT(3),LAT1(3)]);
%plot3([FLAT(1),LAT2(1)],[FLAT(2),LAT2(2)],[FLAT(3),LAT2(3)]);

```

```
[pa, pb] = LineLineIntersectIn3D(FAP,AP1,FLAT,LAT1);
a=[ (pa(1)+pb(1))/2 , (pa(2)+pb(2))/2 , (pa(3)+pb(3))/2 ];
```

```
[pa, pb] = LineLineIntersectIn3D(FAP,AP2,FLAT,LAT2)
b=[ (pa(1)+pb(1))/2 , (pa(2)+pb(2))/2 , (pa(3)+pb(3))/2 ];
```

```
dab=sqrt(...
    (a(1)-b(1))*(a(1)-b(1)) + ...
    (a(2)-b(2))*(a(2)-b(2)) + ...
    (a(3)-b(3))*(a(3)-b(3))...
    )
```

```
%plot3([a(1),b(1)],[a(2),b(2)],[a(3),b(3)]);
```

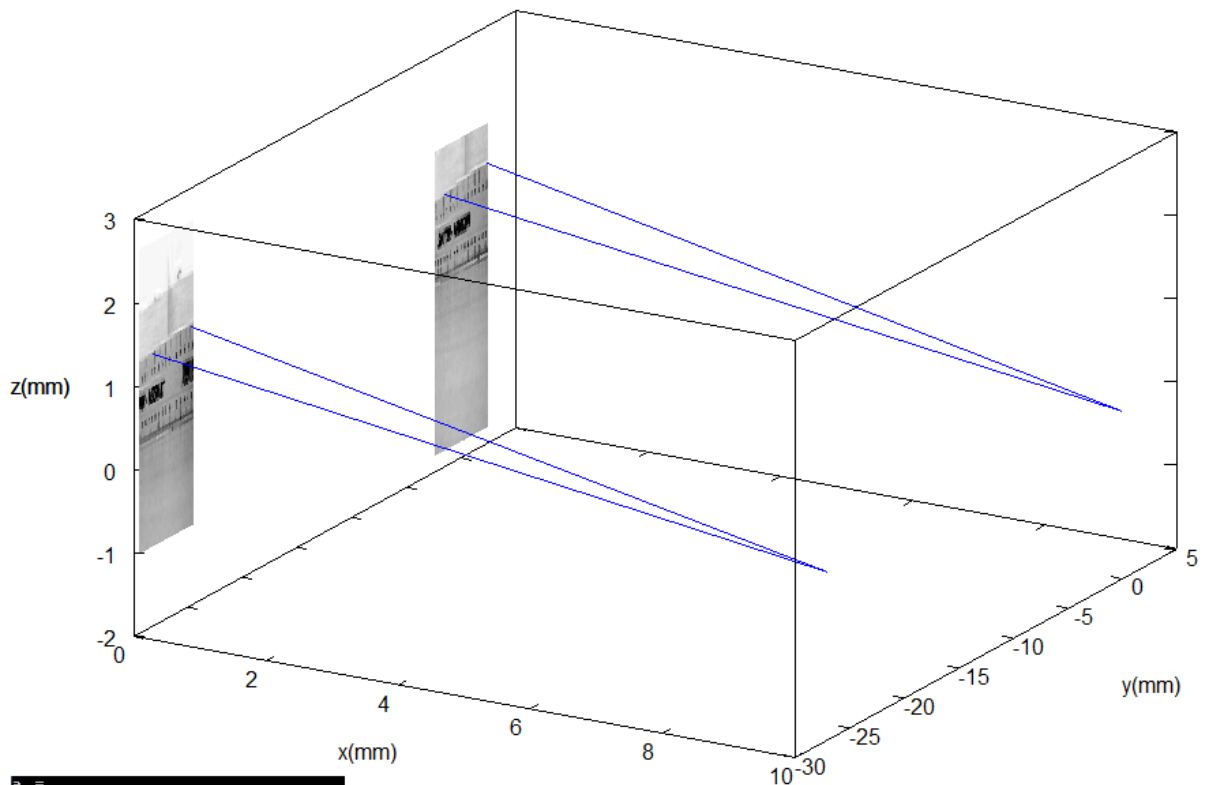
```
%-----
```

```
%=====
```

```
hold off;
```

```
%=====
```

```
endfunction
```



```
a =
-61.5954 -10.1060  9.2357
b =
 86.217  -17.987  -10.022
dab = 149.27
```

APPENDIX F

Measure the distance of a coin using an X-ray image

```
function []=mxray14()
%=====
clear all;
close all;
clc;

SID=100;
IRD=50;
SRD=SID-IRD;

% set hold on so we can show multiple plots/surfs in figure
figure(1);
hold on;
%=====
% the AP image data you want to show a plane
AP=imread("FilmAP2.bmp");

[nr,nc, zz]=size(AP);

for x1=1:nr
    for y1=1:nc
        x(x1,y1)=(x1*0.17)-(nr*0.17/2);
        y(x1,y1)=-50;
        z(x1,y1)=(y1*0.17)-(nc*0.17/2);
        planeimg1(x1,y1,1)=AP(x1,y1,1);
    endfor
endfor

colormap("gray");

% do a normal surface plot
surf(x,y,z,planeimg1, 'edgecolor','none');

%-----
% the LAT image data you want to show a plane
LAT=imread("FilmLAT2.bmp");

[nr,nc, zz]=size(LAT);
```



```

for x1=1:nr
for y1=1:nc
    x(x1,y1)=-50;
    y(x1,y1)=(x1*0.17)-(nr*0.17/2);
    z(x1,y1)=(y1*0.17)-(nc*0.17/2);
    planeimg(x1,y1,1)=LAT(x1,y1,1);
endfor
endfor

colormap('gray');

% do a normal surface plot
surf(x,y,z,planeimg, 'edgecolor','none');

%=====
% label the axis
xlabel('x(cm)');
ylabel('y(cm)');
zlabel('z(cm)');
%=====
hold on
%On AP Film

FAP=[0,50,0];
AP1=[0,-50,2.24];
AP2=[0,-50,-2.24];
plot3([FAP(1),AP1(1)],[FAP(2),AP1(2)],[FAP(3),AP1(3)]);
plot3([FAP(1),AP2(1)],[FAP(2),AP2(2)],[FAP(3),AP2(3)]);

FLAT=[50,0,0];
LAT1=[-50,0,2.24];
LAT2=[-50,0,-2.24];
plot3([FLAT(1),LAT1(1)],[FLAT(2),LAT1(2)],[FLAT(3),LAT1(3)]);
plot3([FLAT(1),LAT2(1)],[FLAT(2),LAT2(2)],[FLAT(3),LAT2(3)]);

[pa, pb] = LineLineIntersectIn3D(FAP,AP1,FLAT,LAT1);
a=[ (pa(1)+pb(1))/2 , (pa(2)+pb(2))/2 , (pa(3)+pb(3))/2 ];

[pa, pb] = LineLineIntersectIn3D(FAP,AP2,FLAT,LAT2);

```

```
b=[ (pa(1)+pb(1))/2 , (pa(2)+pb(2))/2 , (pa(3)+pb(3))/2 ];
```

```
dab=sqrt(...
```

```
    (a(1)-b(1))*(a(1)-b(1)) + ...
```

```
    (a(2)-b(2))*(a(2)-b(2)) + ...
```

```
    (a(3)-b(3))*(a(3)-b(3))...
```

```
)
```

```
plot3([a(1),b(1)],[a(2),b(2)],[a(3),b(3)]);
```

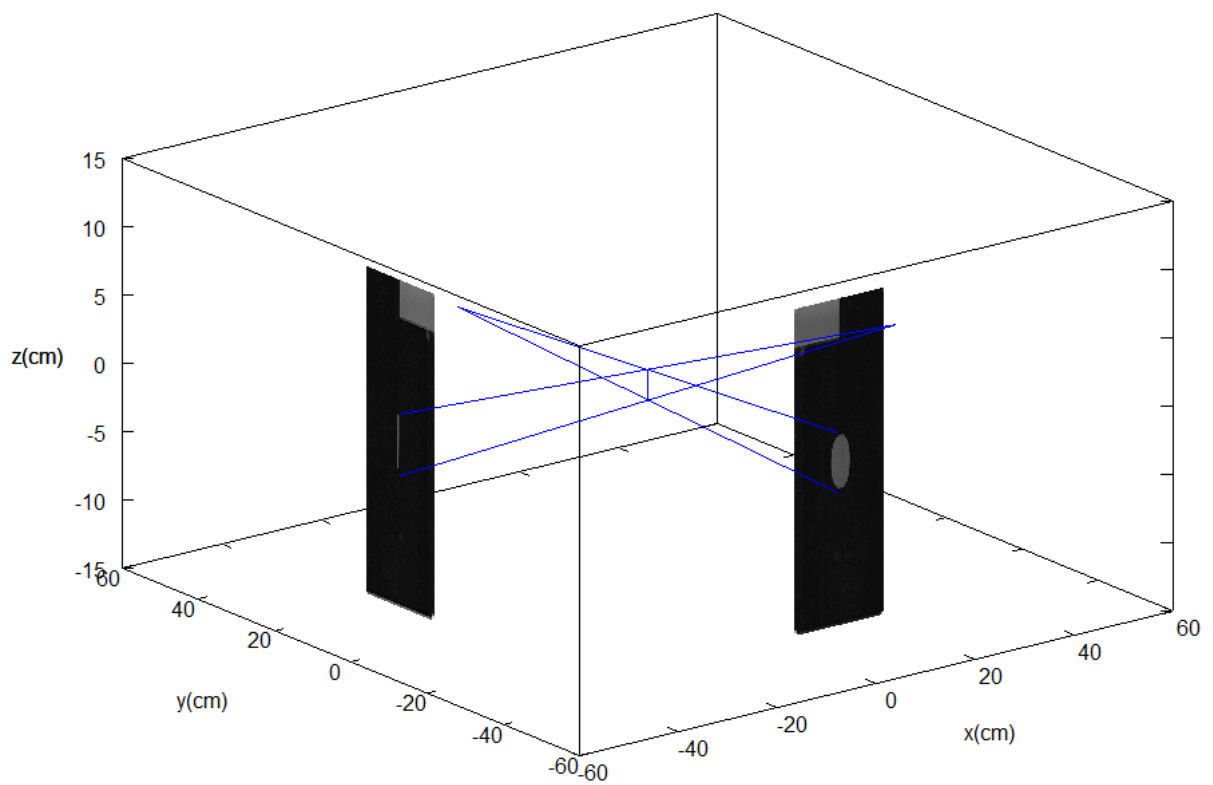
```
%-----
```

```
%=====
```

```
hold off;
```

```
%=====
```

```
endfunction
```



APPENDIX G

Measure the distance using an AP and LAT X-ray image

```
function []=mxray11()
%=====
clear all;
close all;
clc;

SID=100;
IRD=50;
SRD=SID-IRD;

% set hold on so we can show multiple plots/surfs in fugure
figure(1);
hold on;
%axis([-IRD-25,SRD+25,-IRD-25,SRD+25,-IRD-25,SRD+25],"square");
%=====
% the AP image data you want to show a plane
%AP=imread("AP.bmp");
AP=imread("AP10.bmp");

[nr,nc]=size(AP);

for x1=1:nr
for y1=1:nc
    x(x1,y1)=x1*0.115*10;
    y(x1,y1)=-60;
    z(x1,y1)=y1*0.115*10;
    planeimg1(x1,y1)=AP(x1,y1,1);
    %if(AP(x1,y1,1)<=128)
    %plot3(x,y,z, '.');
    %endif
endfor
endfor

colormap("gray");

% do a normal surface plot
surf(x,y,z,planeimg1, 'edgecolor','none');
```

```

% label the axis
xlabel('x');
ylabel('y');
zlabel('z');

%-----
% the LAT image data you want to show a plane
%LAT=imread("xray4.bmp");
LAT=imread("LAT10.bmp");

[nr,nc]=size(LAT);

for x1=1:nr
  for y1=1:nc
    x(x1,y1)=-60;
    y(x1,y1)=x1*0.115*10;
    z(x1,y1)=y1*0.115*10;
    planeimg(x1,y1)=LAT(x1,y1,1);
    %if(LAT(x1,y1,1)<=128)
    %plot3(x,y,z, '.');
    %endif
  endfor
endfor

colormap('gray');

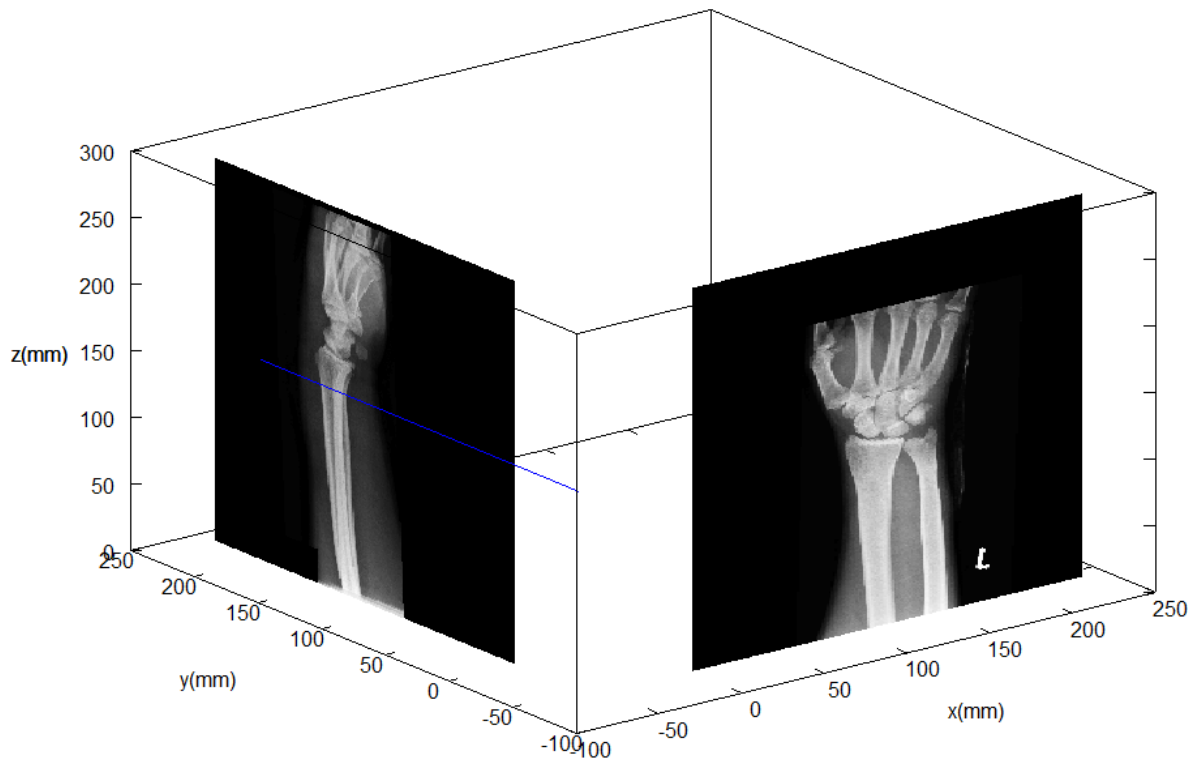
% do a normal surface plot
surf(x,y,z,planeimg, 'edgecolor','none');

% label the axis
xlabel('x(mm)');
ylabel('y(mm)');
zlabel('z(mm)');

%=====
plot3([-60,-60],[200,-50],[150,150]);

hold off;
%=====
Endfunction

```



APPENDIX H

Obtaining the xyz-coordinates of an artefact with the two cameras not aligned

```
function []=cop5()
%-----
clear all
close all
clc
%-----
%RAND()*(b-a)+a
%rand()*((b)-(a))+(a)

xf1=rand()*(0-(-200))+(-200);
yf1=rand()*(200-(-200))+(-200);
zf1=rand()*(250-(100))+(100);

%{
xc1=0;
yc1=64;
zc1=48;

xs1=0;
ys1=0+rand()*(-20-(-20))+(-20);
zs1=0-rand()*20;

xc2=xc1;
yc2=yc1;
zc2=zc1+70;

xs2=xs1;
ys2=ys1;
zs2=zs1-rand()*20+70;
%}

xc1=10;
yc1=64;
zc1=48;

xs1=0;
ys1=132-22;
zs1=52;
```

```
xc2=10;
yc2=64+150;
zc2=48;
```

```
xs2=0;
ys2=64+150;
zs2=36;
```

```
p1=[xc1,yc1,zc1];
p2=[xs1,ys1,zs1];
p3=[xc2,yc2,zc2];
p4=[xs2,ys2,zs2];
[pa, pb] = LineLineIntersectIn3D(p1,p2,p3,p4);
xa=(pa(1)+pb(1))/2;
ya=(pa(2)+pb(2))/2;
za=(pa(3)+pb(3))/2;
```

```
xp=xa
yp=ya
zp=za
```

```
dfp=sqrt(
    (xf1-xp)*(xf1-xp) + ...
    (yf1-yp)*(yf1-yp) + ...
    (zf1-zp)*(zf1-zp)
)
```

```
%xf1=xa;
%yf1=ya;
```

```
hold on;
```

```
%-----
```

```
%=====
```

```
%The image you want to show on a plane
```

```
%l=imread("TREE1b.bmp");
```

```
l=imread("Picture_035.jpg");
```

```
%The xyz-coordinates you want the image to be shown on
```

```
[nr,nc,zz]=size(l);
```

```

for y1=1:nc
for x1=1:nr
    x(x1,y1)=0;
    y(x1,y1)=x1;
    z(x1,y1)=y1;
    planeimg(x1,y1)=l (x1,y1,1);
endfor
endfor

colormap(gray);

% do a normal surface plot
surf(x,y,z,planeimg, 'edgecolor','none');
%=====
%=====
%The image you want to show on a plane
%l=imread("TREE1b.bmp");
l=imread("Picture_023.jpg");

%The xyz-coordinats you want the image to be shown on
[nr,nc,zz]=size(l);

for y1=1:nc
for x1=1:nr
    x(x1,y1)=0;
    y(x1,y1)=x1+150;
    z(x1,y1)=y1;
    planeimg(x1,y1)=l (x1,y1,1);
endfor
endfor

colormap(gray);

% do a normal surface plot
surf(x,y,z,planeimg, 'edgecolor','none');
%=====
%-----

%plot3([0,0],[-30,-30],[-30,30]);

```



```

%plot3([0,0],[30,30],[-30,30]);
%plot3([0,0],[-30,30],[-30,-30]);
%plot3([0,0],[-30,30],[30,30]);

%plot3([0,0],[-30,-30],[40,100]);
%plot3([0,0],[30,30],[40,100]);
%plot3([0,0],[-30,30],[40,40]);
%plot3([0,0],[-30,30],[100,100]);

IRD=dfp;
SRD=dfp;
%axis([-IRD-25,SRD+25,-IRD-25,SRD+25,-IRD-25,SRD+25],"square");
axis("square");
%axis("off");

xlabel("x");
ylabel("y");
zlabel("z");

%plot3([xf1,xp],[yf1,yp],[zf1,zp]);
plot3([xc1,xs1],[yc1,ys1],[zc1,zs1]);
plot3([xc2,xs2],[yc2,ys2],[zc2,zs2]);
plot3([xc1,xp],[yc1,yp],[zc1,zp]);
plot3([xc2,xp],[yc2,yp],[zc2,zp]);

text(0,0,0,'O')
text(xp,yp,zp,'P')
text(xc1,yc1,zc1,'C1')
text(xc2,yc2,zc2,'C2')
text(xs1,ys1,zs1,'S1')
text(xs2,ys2,zs2,'S2')

text(xp,yp,zp, strcat("P=", "(" , num2str(xp) , ", " , num2str(yp) , ", " , num2str(zp) , ")"));

legend("east");

legend(%strcat("Origin(O)=", "(" , num2str(0) , ", " , num2str(0) , ", " , num2str(0) , ")"),...
       strcat("COP1(C1)=", "(" , num2str(xc1) , ", " , num2str(yc1) , ", " , num2str(zc1) , ")"),...
       strcat("COP2(C2)=", "(" , num2str(xc2) , ", " , num2str(yc2) , ", " , num2str(zc2) , ")"),...)

```

```

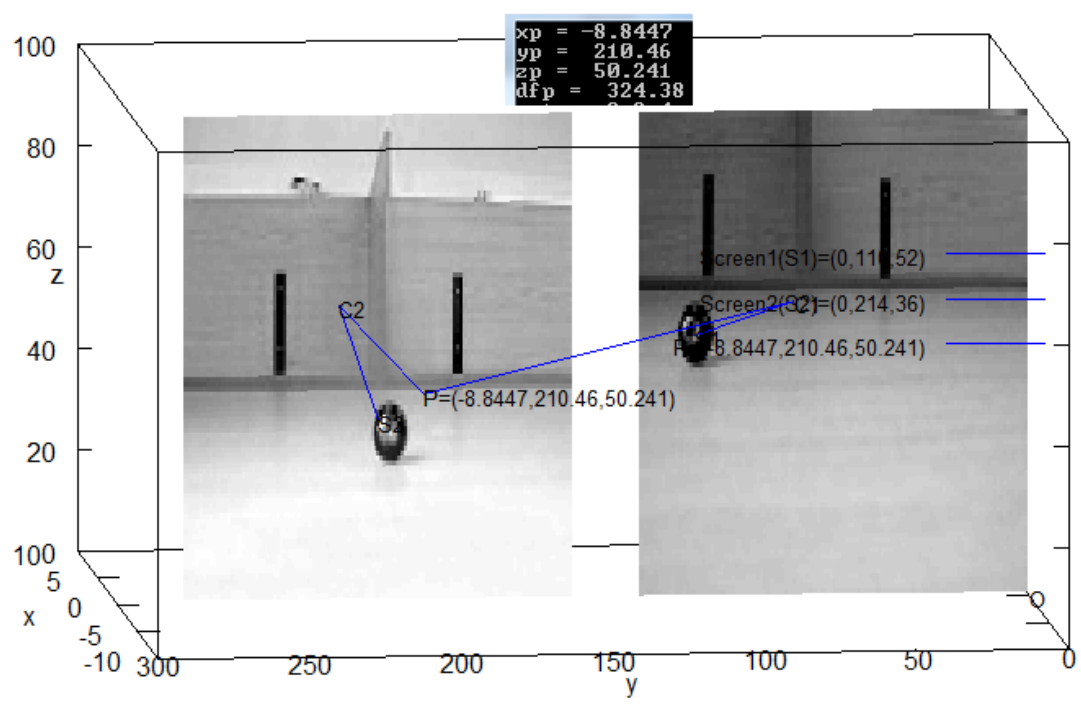
strcat("Screen1(S1)=", "(" , num2str(xs1), ", " , num2str(ys1), ", " , num2str(zs1), ")"), ...
strcat("Screen2(S2)=", "(" , num2str(xs2), ", " , num2str(ys2), ", " , num2str(zs2), ")"), ...
strcat("P=", "(" , num2str(xp), ", " , num2str(yp), ", " , num2str(zp), ")")...
%strcat("Object(P)=", "(" , num2str(xp), ", " , num2str(yp), ", " , num2str(zp), ")")...
);

```

hold off;

%-----

endfunction



APPENDIX I

Automatic detection of an object on second images as selected on first image

```
function []=vxyz03m()
%-----
clear all
close all
clc
%-----
%Read the first image
%I1=imread('Picture 002.jpg');
%I1=imread('SAM1a.jpg');
I1=imread('Picture 012a.jpg');
%Picture 010
[nr1,nc1,zz1]=size(I1);

%Do edge detection
E1=edge(rgb2gray(I1),'sobel');
%-----
%Read the first image
%I2=imread('Picture 002.jpg');
%I2=imread('SAM1a.jpg');
I2=imread('Picture 016a.jpg');

[nr2,nc2,zz2]=size(I2);

%Do edge detection
E2=edge(rgb2gray(I2),'prewitt');
%-----
figure(1)
hold on
imshow(I1);
[mx,my,mb] = ginput(1)
mx=fix(mx);
my=fix(my);
line([mx-20,mx+20],[my-20,my+20]);
%plot([mx-20,mx+20],[my,my]);
line([mx-20,mx+20],[my+20,my-20]);
text(mx,my,'*');
hold off
%-----
```

```

%-----
M=E1(my-20:my+20,mx-20:mx+20,1);
size_M=size(M);

MM=M;
[MR,MC]=size(M);

for yy=2:MC-1
for xx=2:MR-1
    if(M(yy,xx)==1)
        MM(yy-1,xx-1)=1;MM(yy-1,xx)=1;MM(yy-1,xx+1)=1;
        MM(yy,xx-1)=1;MM(yy,xx)=1;MM(yy,xx+1)=1;
        MM(yy+1,xx-1)=1;MM(yy+1,xx)=1;MM(yy+1,xx+1)=1;
    end
end
end
%-----
PMAX=-1;

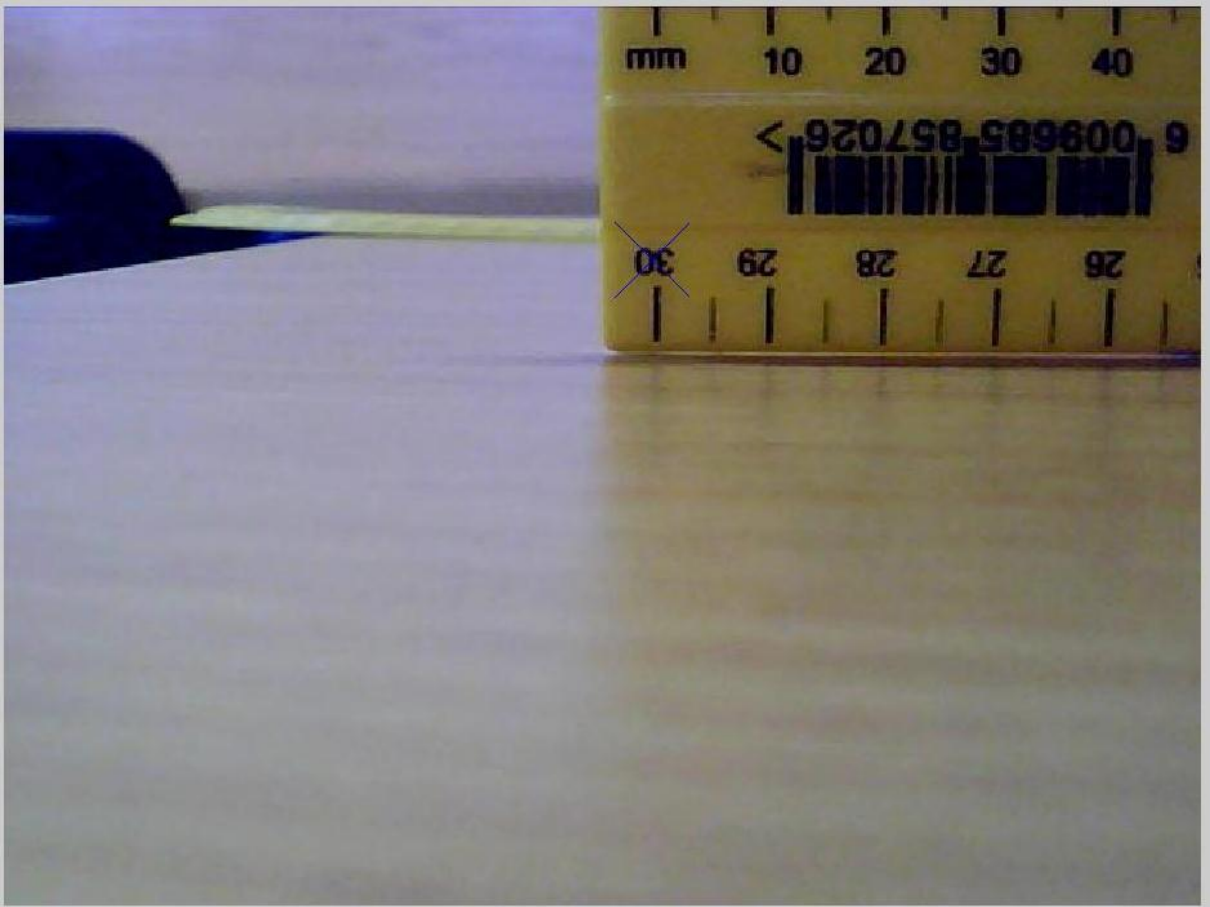
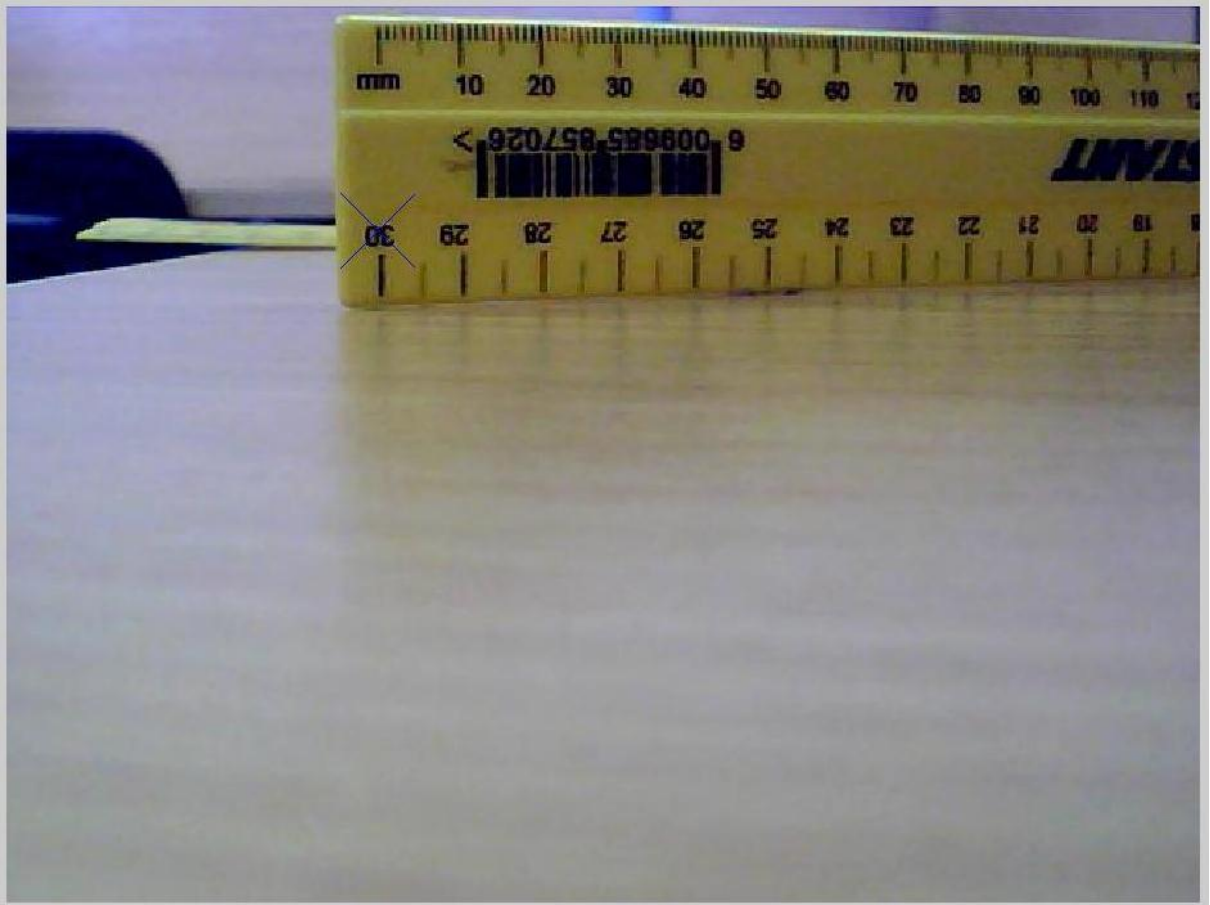
for y=21:nc2-42
for x=21:nr2-42
    K=E2(x-20:x+20,y-20:y+20,1);
    S=sum(sum(~((K&~MM)|(~K&MM))));
    P=S/1681*100;
    if(P>PMAX)
        PMAX=P;
        x1=x;
        y1=y;
    end
end
end

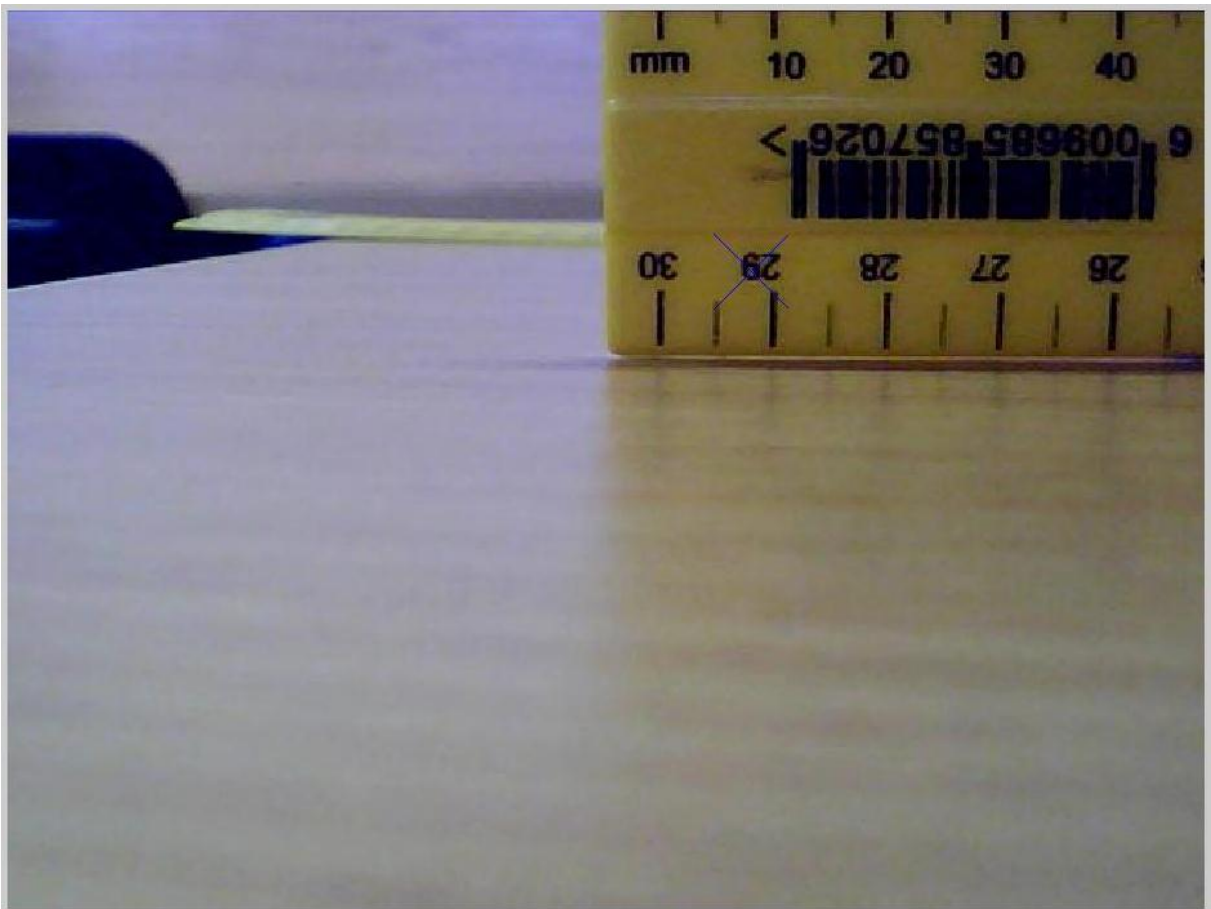
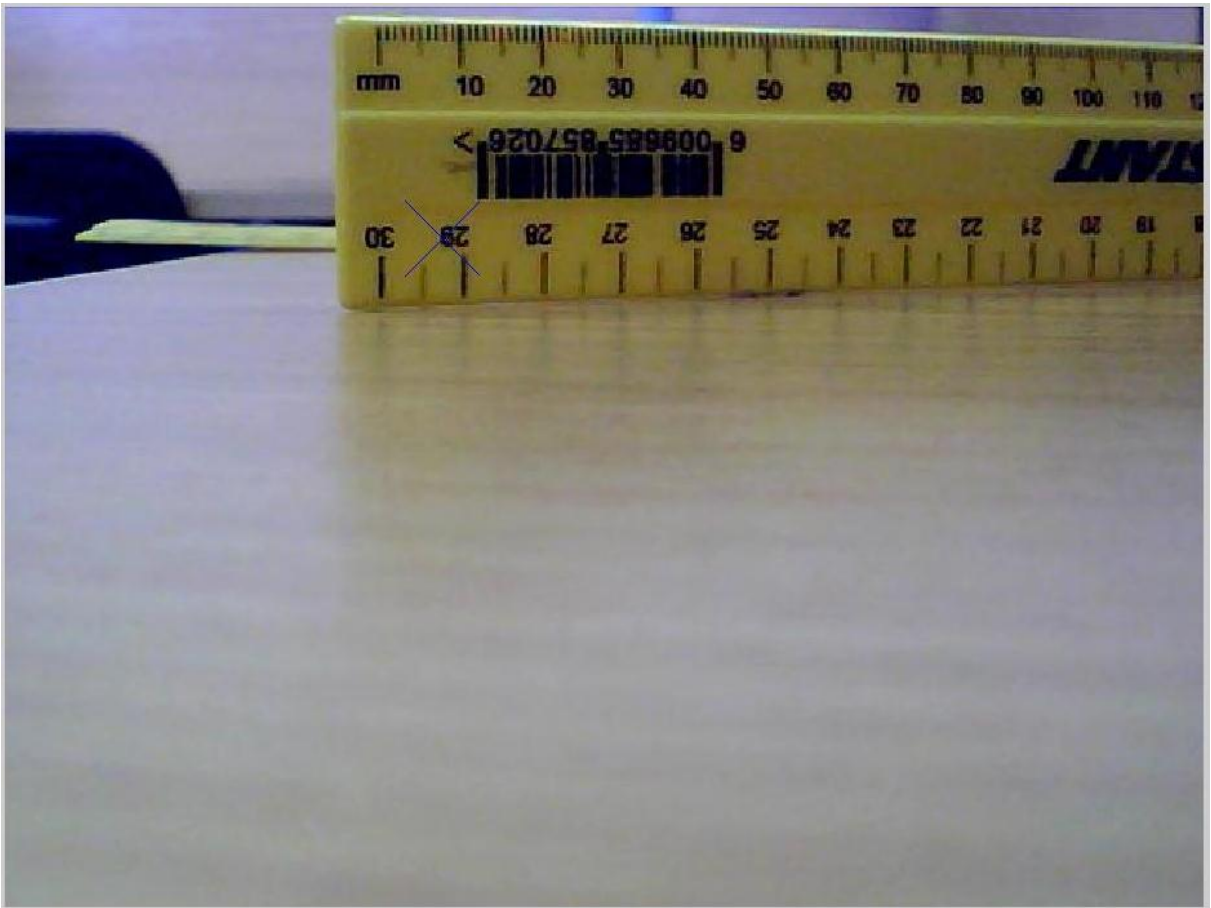
PMAX

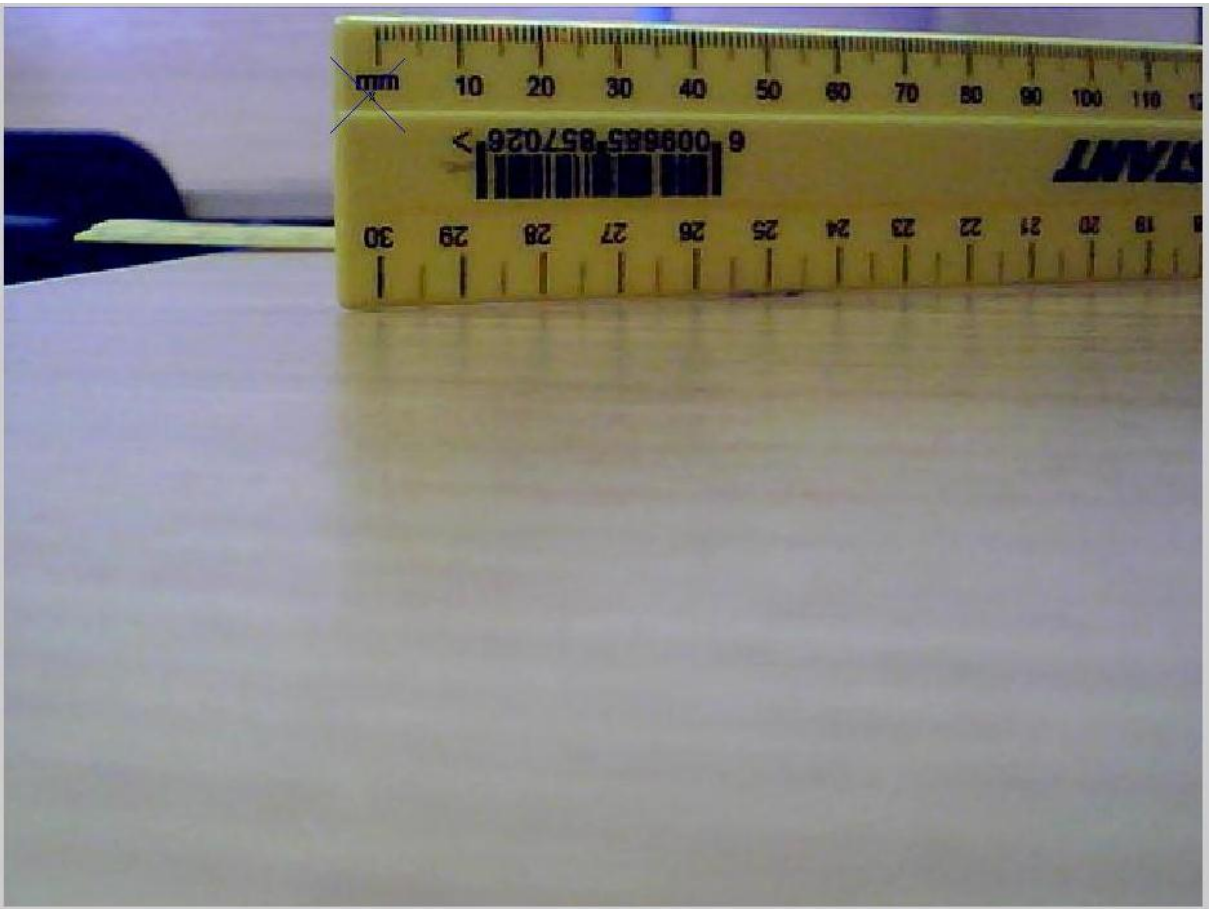
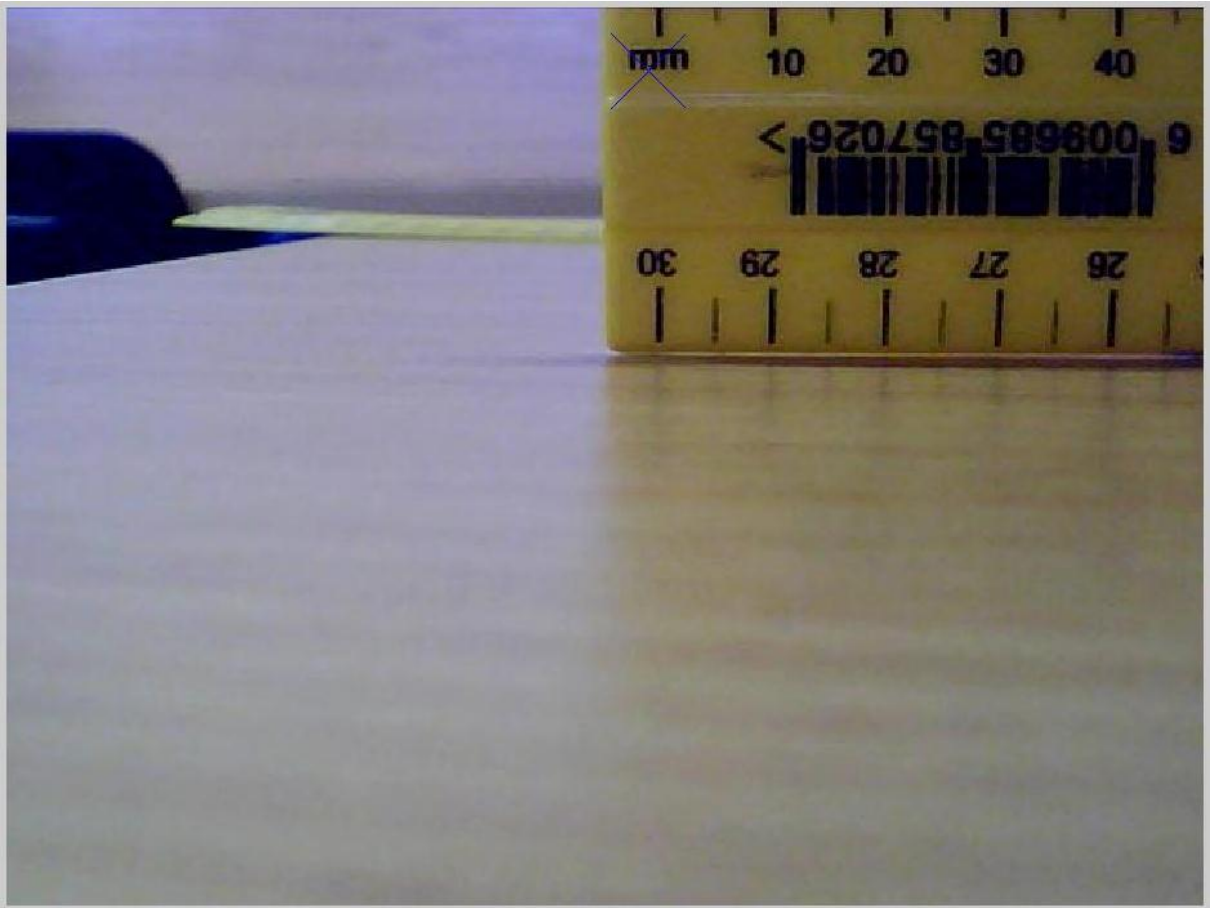
x1
y1
%-----
figure(2)
hold on
imshow(I2);
%plot([x1-20,x1+20],[y1-20,y1+20]);
line([y1-20,y1+20],[x1-20,x1+20]);

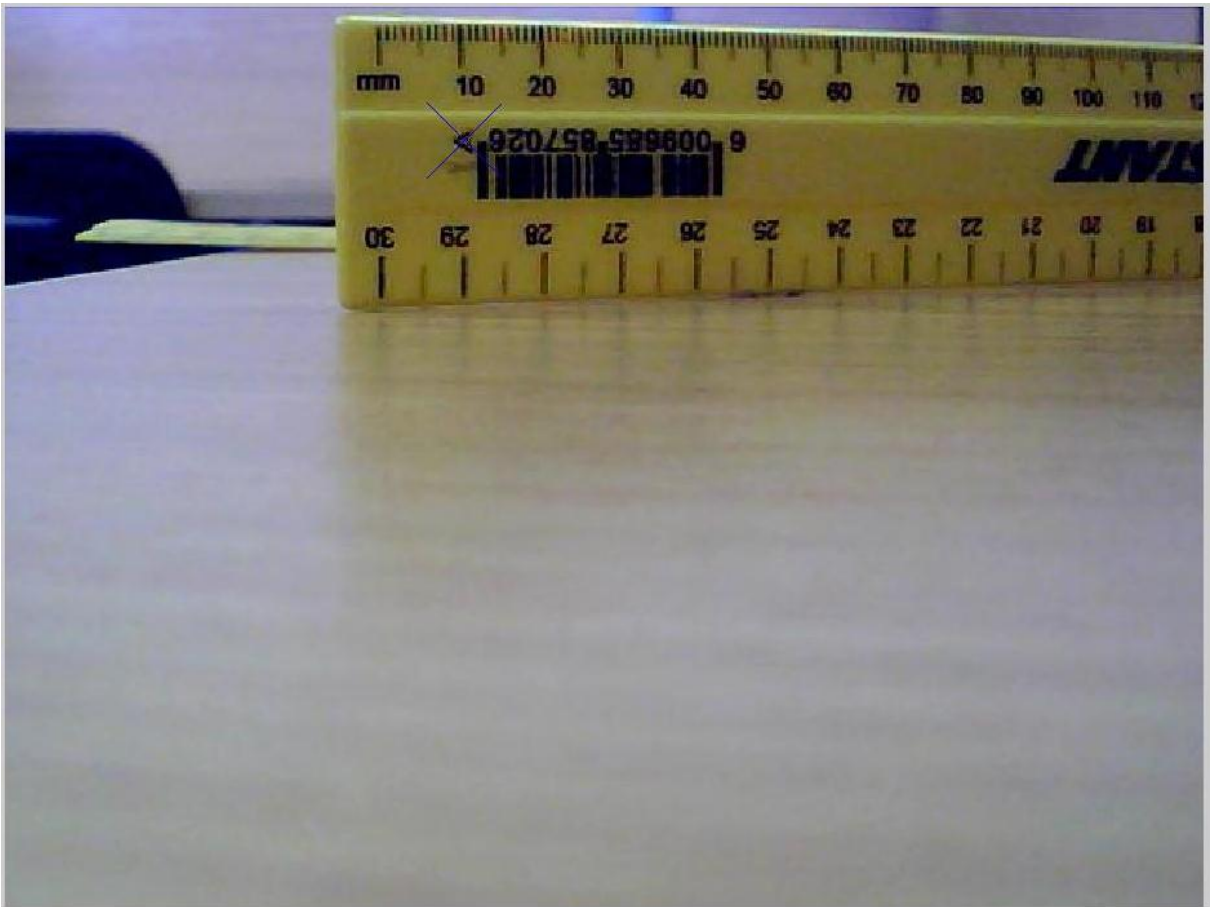
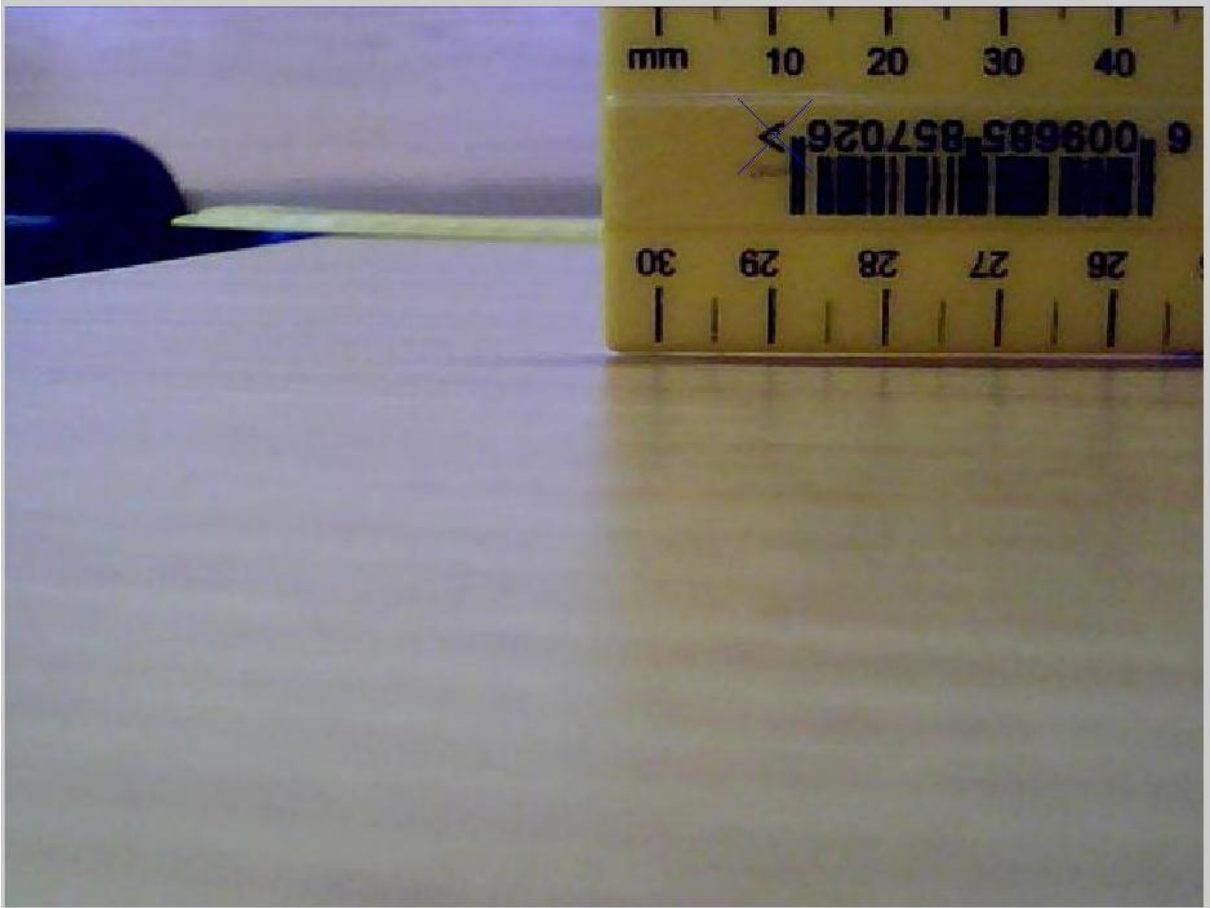
```

```
%plot([x1-20,x1+20],[y1,y1]);  
line([y1-20,y1+20],[x1+20,x1-20]);  
text(y1,x1,'x');  
hold off  
%-----
```









APPENDIX J

Let

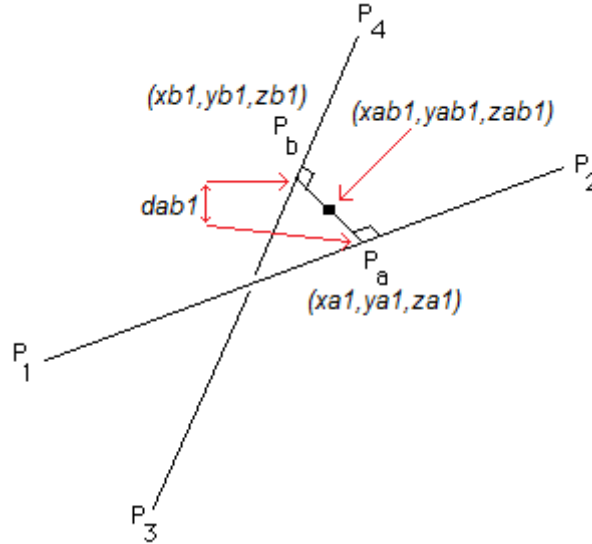
$$P_1 = (x_1, y_1, z_1)$$

$$P_2 = (x_2, y_2, z_2)$$

$$P_3 = (x_3, y_3, z_3)$$

$$P_4 = (x_4, y_4, z_4)$$

In



then

The x-coordinate (xa1) of point (Pa) is:

$$xa1 = (x1) + \frac{(((x1-x3)*(x4-x3) + (y1-y3)*(y4-y3) + (z1-z3)*(z4-z3)) * ((x4-x3)*(x2-x1) + (y4-y3)*(y2-y1) + (z4-z3)*(z2-z1)) - ((x1-x3)*(x2-x1) + (y1-y3)*(y2-y1) + (z1-z3)*(z2-z1)) * ((x4-x3)*(x4-x3) + (y4-y3)*(y4-y3) + (z4-z3)*(z4-z3)))}{(((x2-x1)*(x2-x1) + (y2-y1)*(y2-y1) + (z2-z1)*(z2-z1)) * ((x4-x3)*(x4-x3) + (y4-y3)*(y4-y3) + (z4-z3)*(z4-z3)) - ((x4-x3)*(x2-x1) + (y4-y3)*(y2-y1) + (z4-z3)*(z2-z1)) * ((x4-x3)*(x2-x1) + (y4-y3)*(y2-y1) + (z4-z3)*(z2-z1))) * (x2-x1)}$$

The y-coordinate (ya1) of point (Pa) is:

$$ya1 = y1 + \frac{(((x1-x3)*(x4-x3) + (y1-y3)*(y4-y3) + (z1-z3)*(z4-z3)) * ((x4-x3)*(x2-x1) + (y4-y3)*(y2-y1) + (z4-z3)*(z2-z1)) - ((x1-x3)*(x2-x1) + (y1-y3)*(y2-y1) + (z1-z3)*(z2-z1)) * ((x4-x3)*(x4-x3) + (y4-y3)*(y4-y3) + (z4-z3)*(z4-z3)))}{(((x2-x1)*(x2-x1) + (y2-y1)*(y2-y1) + (z2-z1)*(z2-z1)) * ((x4-x3)*(x4-x3) + (y4-y3)*(y4-y3) + (z4-z3)*(z4-z3)) - ((x4-x3)*(x2-x1) + (y4-y3)*(y2-y1) + (z4-z3)*(z2-z1)) * ((x4-x3)*(x2-x1) + (y4-y3)*(y2-y1) + (z4-z3)*(z2-z1))) * (y2-y1)}$$

The z-coordinate (za1) of point (Pa) is:

$$za1 = z1 + \frac{(((x1-x3)*(x4-x3) + (y1-y3)*(y4-y3) + (z1-z3)*(z4-z3)) * ((x4-x3)*(x2-x1) + (y4-y3)*(y2-y1) + (z4-z3)*(z2-z1)) - ((x1-x3)*(x2-x1) + (y1-y3)*(y2-y1) + (z1-z3)*(z2-z1)) * ((x4-x3)*(x4-x3) + (y4-y3)*(y4-y3) + (z4-z3)*(z4-z3)))}{(((x2-x1)*(x2-x1) + (y2-y1)*(y2-y1) + (z2-z1)*(z2-z1)) * ((x4-x3)*(x4-x3) + (y4-y3)*(y4-y3) + (z4-z3)*(z4-z3)) - ((x4-x3)*(x2-x1) + (y4-y3)*(y2-y1) + (z4-z3)*(z2-z1)) * ((x4-x3)*(x2-x1) + (y4-y3)*(y2-y1) + (z4-z3)*(z2-z1))) * (z2-z1)}$$

The x-coordinate (xb1) of point (Pb) is:

$$xb1 = x3 + \frac{(((x1-x3)*(x4-x3)+(y1-y3)*(y4-y3)+(z1-z3)*(z4-z3))+((x4-x3)*(x2-x1)+(y4-y3)*(y2-y1)+(z4-z3)*(z2-z1)))*(((x1-x3)*(x4-x3)+(y1-y3)*(y4-y3)+(z1-z3)*(z4-z3))*((x4-x3)*(x2-x1)+(y4-y3)*(y2-y1)+(z4-z3)*(z2-z1))-((x1-x3)*(x2-x1)+(y1-y3)*(y2-y1)+(z1-z3)*(z2-z1))*((x4-x3)*(x4-x3)+(y4-y3)*(y4-y3)+(z4-z3)*(z4-z3)))/(((x2-x1)*(x2-x1)+(y2-y1)*(y2-y1)+(z2-z1)*(z2-z1))*((x4-x3)*(x4-x3)+(y4-y3)*(y4-y3)+(z4-z3)*(z4-z3))-((x4-x3)*(x2-x1)+(y4-y3)*(y2-y1)+(z4-z3)*(z2-z1))*((x4-x3)*(x2-x1)+(y4-y3)*(y2-y1)+(z4-z3)*(z2-z1))))}{((x4-x3)*(x4-x3)+(y4-y3)*(y4-y3)+(z4-z3)*(z4-z3))*((x4-x3))}$$

The y-coordinate (yb1) of point (Pb) is:

$$yb1 = (y3) + \frac{(((x1)-(x3))*((x4)-(x3))+((y1)-(y3))*((y4)-(y3))+((z1)-(z3))*((z4)-(z3)))+((x4)-(x3))*((x2)-(x1))+((y4)-(y3))*((y2)-(y1))+((z4)-(z3))*((z2)-(z1)))*(((x1)-(x3))*((x4)-(x3))+((y1)-(y3))*((y4)-(y3))+((z1)-(z3))*((z4)-(z3)))*((x4)-(x3))*((x2)-(x1))+((y4)-(y3))*((y2)-(y1))+((z4)-(z3))*((z2)-(z1)))-((x1)-(x3))*((x2)-(x1))+((y1)-(y3))*((y2)-(y1))+((z1)-(z3))*((z2)-(z1)))*((x4)-(x3))*((x4)-(x3))+((y4)-(y3))*((y4)-(y3))+((z4)-(z3))*((z4)-(z3)))/(((x2)-(x1))*((x2)-(x1))+((y2)-(y1))*((y2)-(y1))+((z2)-(z1))*((z2)-(z1)))*((x4)-(x3))*((x4)-(x3))+((y4)-(y3))*((y4)-(y3))+((z4)-(z3))*((z4)-(z3))-((x4)-(x3))*((x2)-(x1))+((y4)-(y3))*((y2)-(y1))+((z4)-(z3))*((z2)-(z1)))*((x4)-(x3))*((x2)-(x1))+((y4)-(y3))*((y2)-(y1))+((z4)-(z3))*((z2)-(z1))))}{((x4)-(x3))*((x4)-(x3))+((y4)-(y3))*((y4)-(y3))+((z4)-(z3))*((z4)-(z3))*((y4)-(y3))}$$

The z-coordinate (zb1) of point (Pb) is:

$$zb1 = (z3) + \frac{(((x1)-(x3))*((x4)-(x3))+((y1)-(y3))*((y4)-(y3))+((z1)-(z3))*((z4)-(z3)))+((x4)-(x3))*((x2)-(x1))+((y4)-(y3))*((y2)-(y1))+((z4)-(z3))*((z2)-(z1)))*(((x1)-(x3))*((x4)-(x3))+((y1)-(y3))*((y4)-(y3))+((z1)-(z3))*((z4)-(z3)))*((x4)-(x3))*((x2)-(x1))+((y4)-(y3))*((y2)-(y1))+((z4)-(z3))*((z2)-(z1)))-((x1)-(x3))*((x2)-(x1))+((y1)-(y3))*((y2)-(y1))+((z1)-(z3))*((z2)-(z1)))*((x4)-(x3))*((x4)-(x3))+((y4)-(y3))*((y4)-(y3))+((z4)-(z3))*((z4)-(z3)))/(((x2)-(x1))*((x2)-(x1))+((y2)-(y1))*((y2)-(y1))+((z2)-(z1))*((z2)-(z1)))*((x4)-(x3))*((x4)-(x3))+((y4)-(y3))*((y4)-(y3))+((z4)-(z3))*((z4)-(z3))-((x4)-(x3))*((x2)-(x1))+((y4)-(y3))*((y2)-(y1))+((z4)-(z3))*((z2)-(z1)))*((x4)-(x3))*((x2)-(x1))+((y4)-(y3))*((y2)-(y1))+((z4)-(z3))*((z2)-(z1))))}{((x4)-(x3))*((x4)-(x3))+((y4)-(y3))*((y4)-(y3))+((z4)-(z3))*((z4)-(z3))*((z4)-(z3))}$$

The x-coordinate of the midpoint of the shortest line between two lines in 3D (xab1) is:

$$xab1 = \frac{((x1) + (((x1-x3)*(x4-x3)+(y1-y3)*(y4-y3)+(z1-z3)*(z4-z3))*((x4-x3)*(x2-x1)+(y4-y3)*(y2-y1)+(z4-z3)*(z2-z1)) - ((x1-x3)*(x2-x1)+(y1-y3)*(y2-y1)+(z1-z3)*(z2-z1))*((x4-x3)*(x4-x3)+(y4-y3)*(y4-y3)+(z4-z3)*(z4-z3)))/(((x2-x1)*(x2-x1)+(y2-y1)*(y2-y1)+(z2-z1)*(z2-z1))*((x4-x3)*(x4-x3)+(y4-y3)*(y4-y3)+(z4-z3)*(z4-z3)) - ((x4-x3)*(x2-x1)+(y4-y3)*(y2-y1)+(z4-z3)*(z2-z1))*((x4-x3)*(x2-x1)+(y4-y3)*(y2-y1)+(z4-z3)*(z2-z1))))}{2} + x3 + \frac{(((x1-x3)*(x4-x3)+(y1-y3)*(y4-y3)+(z1-z3)*(z4-z3))+((x4-x3)*(x2-x1)+(y4-y3)*(y2-y1)+(z4-z3)*(z2-z1)))*(((x1-x3)*(x4-x3)+(y1-y3)*(y4-y3)+(z1-z3)*(z4-z3))*((x4-x3)*(x2-x1)+(y4-y3)*(y2-y1)+(z4-z3)*(z2-z1))-((x1-x3)*(x2-x1)+(y1-y3)*(y2-y1)+(z1-z3)*(z2-z1))*((x4-x3)*(x4-x3)+(y4-y3)*(y4-y3)+(z4-z3)*(z4-z3)))/(((x2-x1)*(x2-x1)+(y2-y1)*(y2-y1)+(z2-z1)*(z2-z1))*((x4-x3)*(x4-x3)+(y4-y3)*(y4-y3)+(z4-z3)*(z4-z3))-((x4-x3)*(x2-x1)+(y4-y3)*(y2-y1)+(z4-z3)*(z2-z1))*((x4-x3)*(x2-x1)+(y4-y3)*(y2-y1)+(z4-z3)*(z2-z1))))}{((x4-x3)*(x4-x3)+(y4-y3)*(y4-y3)+(z4-z3)*(z4-z3))*((x4-x3))}$$

The y-coordinate of the midpoint of the shortest line between two lines in 3D (yab1) is:

$$yab1 = (y1) + \frac{(((x1-x3)*(x4-x3)+(y1-y3)*(y4-y3)+(z1-z3)*(z4-z3))*((x4-x3)*(x2-x1)+(y4-y3)*(y2-y1)+(z4-z3)*(z2-z1)) - ((x1-x3)*(x2-x1)+(y1-y3)*(y2-y1)+(z1-z3)*(z2-z1))*((x4-x3)*(x4-x3)+(y4-y3)*(y4-y3)+(z4-z3)*(z4-z3)))/(((x2-x1)*(x2-x1)+(y2-y1)*(y2-y1)+(z2-z1)*(z2-z1))*((x4-x3)*(x4-x3)+(y4-y3)*(y4-y3)+(z4-z3)*(z4-z3))-((x4-x3)*(x2-x1)+(y4-y3)*(y2-y1)+(z4-z3)*(z2-z1))*((x4-x3)*(x2-x1)+(y4-y3)*(y2-y1)+(z4-z3)*(z2-z1))))}{((x4-x3)*(x4-x3)+(y4-y3)*(y4-y3)+(z4-z3)*(z4-z3))*((y4-y3))}$$

$$\frac{((y3) * ((y4) - (y3)) + ((z1) - (z3)) * ((z4) - (z3))) + (((x4) - (x3)) * ((x2) - (x1)) + ((y4) - (y3)) * ((y2) - (y1)) + ((z4) - (z3)) * ((z2) - (z1))) * (((x1) - (x3)) * ((x4) - (x3)) + ((y1) - (y3)) * ((y4) - (y3)) + ((z1) - (z3)) * ((z4) - (z3))) * (((x4) - (x3)) * ((x2) - (x1)) + ((y4) - (y3)) * ((y2) - (y1)) + ((z4) - (z3)) * ((z2) - (z1))) - (((x1) - (x3)) * ((x2) - (x1)) + ((y1) - (y3)) * ((y2) - (y1)) + ((z1) - (z3)) * ((z2) - (z1))) * (((x4) - (x3)) * ((x4) - (x3)) + ((y4) - (y3)) * ((y4) - (y3)) + ((z4) - (z3)) * ((z4) - (z3))) / (((x2) - (x1)) * ((x2) - (x1)) + ((y2) - (y1)) * ((y2) - (y1)) + ((z2) - (z1)) * ((z2) - (z1))) * (((x4) - (x3)) * ((x4) - (x3)) + ((y4) - (y3)) * ((y4) - (y3)) + ((z4) - (z3)) * ((z4) - (z3))) - (((x4) - (x3)) * ((x2) - (x1)) + ((y4) - (y3)) * ((y2) - (y1)) + ((z4) - (z3)) * ((z2) - (z1))) * (((x4) - (x3)) * ((x2) - (x1)) + ((y4) - (y3)) * ((y2) - (y1)) + ((z4) - (z3)) * ((z2) - (z1)))) / (((x4) - (x3)) * ((x4) - (x3)) + ((y4) - (y3)) * ((y4) - (y3)) + ((z4) - (z3)) * ((z4) - (z3))) * ((y4) - (y3)) / 2$$

The z-coordinate of the midpoint of the shortest line between two lines in 3D (zab1) is:

$$zab1 = \frac{((z1 + (((x1 - x3) * (x4 - x3) + (y1 - y3) * (y4 - y3) + (z1 - z3) * (z4 - z3)) * ((x4 - x3) * (x2 - x1) + (y4 - y3) * (y2 - y1) + (z4 - z3) * (z2 - z1)) - ((x1 - x3) * (x2 - x1) + (y1 - y3) * (y2 - y1) + (z1 - z3) * (z2 - z1))) * ((x4 - x3) * (x4 - x3) + (y4 - y3) * (y4 - y3) + (z4 - z3) * (z4 - z3))) / (((x2 - x1) * (x2 - x1) + (y2 - y1) * (y2 - y1) + (z2 - z1) * (z2 - z1))) * ((x4 - x3) * (x4 - x3) + (y4 - y3) * (y4 - y3) + (z4 - z3) * (z4 - z3)) - ((x4 - x3) * (x2 - x1) + (y4 - y3) * (y2 - y1) + (z4 - z3) * (z2 - z1))) * ((x4 - x3) * (x2 - x1) + (y4 - y3) * (y2 - y1) + (z4 - z3) * (z2 - z1))) * (z3) + (((x1) - (x3)) * ((x4) - (x3)) + ((y1) - (y3)) * ((y4) - (y3)) + ((z1) - (z3)) * ((z4) - (z3))) * (((x4) - (x3)) * ((x2) - (x1)) + ((y4) - (y3)) * ((y2) - (y1)) + ((z4) - (z3)) * ((z2) - (z1))) * (((x1) - (x3)) * ((x4) - (x3)) + ((y1) - (y3)) * ((y4) - (y3)) + ((z1) - (z3)) * ((z4) - (z3))) * (((x4) - (x3)) * ((x2) - (x1)) + ((y4) - (y3)) * ((y2) - (y1)) + ((z4) - (z3)) * ((z2) - (z1))) - (((x1) - (x3)) * ((x2) - (x1)) + ((y1) - (y3)) * ((y2) - (y1)) + ((z1) - (z3)) * ((z2) - (z1))) * (((x4) - (x3)) * ((x4) - (x3)) + ((y4) - (y3)) * ((y4) - (y3)) + ((z4) - (z3)) * ((z4) - (z3))) / (((x2) - (x1)) * ((x2) - (x1)) + ((y2) - (y1)) * ((y2) - (y1)) + ((z2) - (z1)) * ((z2) - (z1))) * (((x4) - (x3)) * ((x4) - (x3)) + ((y4) - (y3)) * ((y4) - (y3)) + ((z4) - (z3)) * ((z4) - (z3))) - (((x4) - (x3)) * ((x2) - (x1)) + ((y4) - (y3)) * ((y2) - (y1)) + ((z4) - (z3)) * ((z2) - (z1))) * (((x4) - (x3)) * ((x2) - (x1)) + ((y4) - (y3)) * ((y2) - (y1)) + ((z4) - (z3)) * ((z2) - (z1)))) / (((x4) - (x3)) * ((x4) - (x3)) + ((y4) - (y3)) * ((y4) - (y3)) + ((z4) - (z3)) * ((z4) - (z3))) * ((z4) - (z3)) / 2$$

The distance of the shortest line between two lines in 3D (dab1) is:

$$dab1 = \sqrt{((xa1 - xb1) * (xa1 - xb1)) + ((ya1 - yb1) * (ya1 - yb1)) + ((za1 - zb1) * (za1 - zb1))}$$

APPENDIX K

Obtaining the xyz-coordinates of using the formulae describing the line segment points in xyz-coordinate system

```
function []=short3D6()
%-----
%Calculating the shortest distance between two lines in 3D
%-----
clear all
close all
clc

%RAND()*(b-a)+a
%xa1=rand()*((-17.5)-17.5)+17.5;
%-----
focus_AP=[0,97,0]
focus_LAT=[97,0,0]

point1_AP=[-2.65,-3,-0.55]
point2_AP=[0.57,-3,-0.86]

point1_LAT=[-3,0.75,-0.5]
point2_LAT=[-3,3.86,-0.56]
%-----
x1=focus_AP(1,1)
y1=focus_AP(1,2)
z1=focus_AP(1,3)

x2=point1_AP(1,1)
y2=point1_AP(1,2)
z2=point1_AP(1,3)

x3=focus_LAT(1,1)
y3=focus_LAT(1,2)
z3=focus_LAT(1,3)

x4=point1_LAT(1,1)
y4=point1_LAT(1,2)
z4=point1_LAT(1,3)
```


$$\begin{aligned}
& ((y_4)-(y_3))^*((y_2)-(y_1))+((z_4)-(z_3))^*((z_2)-(z_1)))-(((x_1)-(x_3))^*((x_2)-(x_1))+((y_1)-(y_3))^*((y_2)-(y_1))+((z_1)-(z_3))^*... \\
& ((z_2)-(z_1)))^*((x_4)-(x_3))^*((x_4)-(x_3))+((y_4)-(y_3))^*((y_4)-(y_3))+((z_4)-(z_3))^*((z_4)-(z_3)))/(((x_2)-(x_1))^*((x_2)-(x_1))+... \\
& ((y_2)-(y_1))^*((y_2)-(y_1))+((z_2)-(z_1))^*((z_2)-(z_1)))^*((x_4)-(x_3))^*((x_4)-(x_3))+((y_4)-(y_3))^*((y_4)-(y_3))+((z_4)-(z_3))^*((z_4)-... \\
& (z_3)))-(((x_4)-(x_3))^*((x_2)-(x_1))+((y_4)-(y_3))^*((y_2)-(y_1))+((z_4)-(z_3))^*((z_2)-(z_1)))^*((x_4)-(x_3))^*((x_2)-(x_1))+((y_4)-(y_3))^*... \\
& ((y_2)-(y_1))+((z_4)-(z_3))^*((z_2)-(z_1))))^*((x_2)-(x_1))+x_3+(((x_1-x_3)^*(x_4-x_3)+(y_1-y_3)^*(y_4-y_3)+(z_1-z_3)^*(z_4-z_3))+((x_4-x_3))^*... \\
& (x_2-x_1)+(y_4-y_3)^*(y_2-y_1)+(z_4-z_3)^*(z_2-z_1))^*((x_1-x_3)^*(x_4-x_3)+(y_1-y_3)^*(y_4-y_3)+(z_1-z_3)^*(z_4-z_3))^*((x_4-x_3)^*(x_2-x_1)+(y_4-y_3))^*... \\
& (y_2-y_1)+(z_4-z_3)^*(z_2-z_1))-((x_1-x_3)^*(x_2-x_1)+(y_1-y_3)^*(y_2-y_1)+(z_1-z_3)^*(z_2-z_1))^*((x_4-x_3)^*(x_4-x_3)+(y_4-y_3)^*(y_4-y_3)+(z_4-z_3))^*... \\
& (z_4-z_3))/(((x_2-x_1)^*(x_2-x_1)+(y_2-y_1)^*(y_2-y_1)+(z_2-z_1)^*(z_2-z_1))^*((x_4-x_3)^*(x_4-x_3)+(y_4-y_3)^*(y_4-y_3)+(z_4-z_3)^*(z_4-z_3))-((x_4-x_3))^*... \\
& (x_2-x_1)+(y_4-y_3)^*(y_2-y_1)+(z_4-z_3)^*(z_2-z_1))^*((x_4-x_3)^*(x_2-x_1)+(y_4-y_3)^*(y_2-y_1)+(z_4-z_3)^*(z_2-z_1)))/((x_4-x_3)^*(x_4-x_3)+(y_4-y_3))^*... \\
& (y_4-y_3)+(z_4-z_3)^*(z_4-z_3))^*(x_4-x_3))/2
\end{aligned}$$

$$\begin{aligned}
yab1 = & ((y_1+(((x_1-x_3)^*(x_4-x_3)+(y_1-y_3)^*(y_4-y_3)+(z_1-z_3)^*(z_4-z_3))^*((x_4-x_3)^*(x_2-x_1)+(y_4-y_3)^*(y_2-y_1)+(z_4-z_3)^*(z_2-z_1))-((x_1-x_3)^*(x_2-x_1)+(y_1-y_3)^*(y_2-y_1)+(z_1-z_3)^*(z_2-z_1))^*((x_4-x_3)^*(x_4-x_3)+(y_4-y_3)^*(y_4-y_3)+(z_4-z_3)^*(z_4-z_3)))/(((x_2-x_1)^*(x_2-x_1)+(y_2-y_1)^*(y_2-y_1)+(z_2-z_1)^*(z_2-z_1))^*((x_4-x_3)^*(x_4-x_3)+(y_4-y_3)^*(y_4-y_3)+(z_4-z_3)^*(z_4-z_3))-((x_4-x_3)^*(x_2-x_1)+(y_4-y_3)^*(y_2-y_1)+(z_4-z_3)^*(z_2-z_1)))^*(y_2-y_1))+((y_3+(((x_1-x_3)^*(x_4-x_3)+(y_1-y_3)^*((y_4)-(y_3))+((z_1)-(z_3))^*((z_4)-(z_3)))+((x_4)-(x_3))^*((x_2)-(x_1))+((y_4)-(y_3))^*((y_2)-(y_1))+((z_4)-(z_3))^*((z_2)-(z_1)))^*((x_1)-(x_3))^*((x_4)-(x_3))+((y_1)-(y_3))^*((y_4)-(y_3))+((z_1)-(z_3))^*((z_4)-(z_3))^*((x_4)-(x_3))^*((x_2)-(x_1))+((y_4)-(y_3))^*((y_2)-(y_1))+((z_4)-(z_3))^*((z_2)-(z_1)))-((x_1)-(x_3))^*((x_2)-(x_1))+((y_1)-(y_3))^*((y_2)-(y_1))+((z_1)-(z_3))^*((z_2)-(z_1)))^*((x_4)-(x_3))^*((x_4)-(x_3))+((y_4)-(y_3))^*((y_4)-(y_3))+((z_4)-(z_3))^*((z_4)-(z_3)))/(((x_2)-(x_1))^*((x_2)-(x_1))+((y_2)-(y_1))^*((y_2)-(y_1))+((z_2)-(z_1))^*((z_2)-(z_1)))^*((x_4)-(x_3))^*((x_4)-(x_3))+((y_4)-(y_3))^*((y_4)-(y_3))+((z_4)-(z_3))^*((z_4)-... \\
& (z_3)))-((x_4)-(x_3))^*((x_2)-(x_1))+((y_4)-(y_3))^*((y_2)-(y_1))+((z_4)-(z_3))^*((z_2)-(z_1)))^*((x_4)-(x_3))^*((x_2)-(x_1))+((y_4)-(y_3))^*((y_2)-(y_1))+((z_4)-(z_3))^*((z_2)-(z_1)))/(((x_4)-(x_3))^*((x_4)-(x_3))+((y_4)-(y_3))^*((y_4)-(y_3))+((z_4)-(z_3))^*((z_4)-(z_3)))/2
\end{aligned}$$

$$\begin{aligned}
zab1 = & ((z_1+(((x_1-x_3)^*(x_4-x_3)+(y_1-y_3)^*(y_4-y_3)+(z_1-z_3)^*(z_4-z_3))^*((x_4-x_3)^*(x_2-x_1)+(y_4-y_3)^*(y_2-y_1)+(z_4-z_3)^*(z_2-z_1))-((x_1-x_3)^*(x_2-x_1)+(y_1-y_3)^*(y_2-y_1)+(z_1-z_3)^*(z_2-z_1))^*((x_4-x_3)^*(x_4-x_3)+(y_4-y_3)^*(y_4-y_3)+(z_4-z_3)^*(z_4-z_3)))/(((x_2-x_1)^*(x_2-x_1)+(y_2-y_1)^*(y_2-y_1)+(z_2-z_1)^*(z_2-z_1))^*((x_4-x_3)^*(x_4-x_3)+(y_4-y_3)^*(y_4-y_3)+(z_4-z_3)^*(z_4-z_3))-((x_4-x_3)^*(x_2-x_1)+(y_4-y_3)^*(y_2-y_1)+(z_4-z_3)^*(z_2-z_1)))^*(z_2-z_1))+((z_3+(((x_1-x_3)^*(x_4-x_3)+(y_1-y_3)^*((y_4)-(y_3))+((z_1)-(z_3))^*((z_4)-(z_3)))+((x_4)-(x_3))^*((x_2)-(x_1))+((y_4)-(y_3))^*((y_2)-(y_1))+((z_4)-(z_3))^*((z_2)-(z_1)))^*((x_1)-(x_3))^*((x_4)-(x_3))+((y_1)-(y_3))^*((y_4)-(y_3))+((z_1)-(z_3))^*((z_4)-(z_3))^*((x_4)-(x_3))^*((x_2)-(x_1))+((y_4)-(y_3))^*((y_2)-(y_1))+((z_4)-(z_3))^*((z_2)-(z_1)))-((x_1)-(x_3))^*((x_2)-(x_1))+((y_1)-(y_3))^*((y_2)-(y_1))+((z_1)-(z_3))^*((z_2)-(z_1)))^*((x_4)-(x_3))^*((x_4)-(x_3))+((y_4)-(y_3))^*((y_4)-(y_3))+((z_4)-(z_3))^*((z_4)-... \\
& (z_3)))-((x_4)-(x_3))^*((x_2)-(x_1))+((y_4)-(y_3))^*((y_2)-(y_1))+((z_4)-(z_3))^*((z_2)-(z_1)))^*((x_4)-(x_3))^*((x_2)-(x_1))+((y_4)-(y_3))^*((y_2)-(y_1))+((z_4)-(z_3))^*((z_2)-(z_1)))/(((x_4)-(x_3))^*((x_4)-(x_3))+((y_4)-(y_3))^*((y_4)-(y_3))+((z_4)-(z_3))^*((z_4)-(z_3)))/2
\end{aligned}$$

$$\frac{((x3)+(y4)-(y3))*((y4)-(y3))+((z4)-(z3))*((z4)-(z3)))/(((x2)-(x1))*((x2)-(x1))+((y2)-(y1))*((y2)-(y1))+((z2)-(z1))*((z2)-(z1)))*(((x4)-(x3))*((x4)-(x3))+((y4)-(y3))*((y4)-(y3))+((z4)-(z3))*((z4)-(z3)))-(((x4)-(x3))*((x2)-(x1))+((y4)-(y3))*((y2)-(y1))+((z4)-(z3))*((z2)-(z1)))*(((x4)-(x3))*((x2)-(x1))+((y4)-(y3))*((y2)-(y1))+((z4)-(z3))*((z2)-(z1)))))/(((x4)-(x3))*((x4)-(x3))+((y4)-(y3))*((y4)-(y3))+((z4)-(z3))*((z4)-(z3)))*((z4)-(z3)))/2$$

$$dab1=\sqrt{((xa1-xb1)*(xa1-xb1))+((ya1-yb1)*(ya1-yb1))+((za1-zb1)*(za1-zb1)))}$$

%-----

$$x5=\text{focus_AP}(1,1)$$

$$y5=\text{focus_AP}(1,2)$$

$$z5=\text{focus_AP}(1,3)$$

$$x6=\text{point2_AP}(1,1)$$

$$y6=\text{point2_AP}(1,2)$$

$$z6=\text{point2_AP}(1,3)$$

$$x7=\text{focus_LAT}(1,1)$$

$$y7=\text{focus_LAT}(1,2)$$

$$z7=\text{focus_LAT}(1,3)$$

$$x8=\text{point2_LAT}(1,1)$$

$$y8=\text{point2_LAT}(1,2)$$

$$z8=\text{point2_LAT}(1,3)$$

$$xa2=(x5)+((((x5)-(x7))*((x8)-(x7))+((y5)-(y7))*((y8)-(y7))+((z5)-(z7))*((z8)-(z7)))*((x8)-(x7))*((x6)-(x5))+((y8)-(y7))*((y6)-(y5))+((z8)-(z7))*((z6)-(z5)))-(((x5)-(x7))*((x6)-(x5))+((y5)-(y7))*((y6)-(y5))+((z5)-(z7))*((z6)-(z5)))*(((x8)-(x7))*((x8)-(x7))+((y8)-(y7))*((y8)-(y7))+((z8)-(z7))*((z8)-(z7)))/(((x6)-(x5))*((x6)-(x5))+((y6)-(y5))*((y6)-(y5))+((z6)-(z5))*((z6)-(z5)))*(((x8)-(x7))*((x8)-(x7))+((y8)-(y7))*((y8)-(y7))+((z8)-(z7))*((z8)-(z7)))-(((x8)-(x7))*((x6)-(x5))+((y8)-(y7))*((y6)-(y5))+((z8)-(z7))*((z6)-(z5)))*(((x8)-(x7))*((x6)-(x5))+((y8)-(y7))*((y6)-(y5))+((z8)-(z7))*((z6)-(z5)))))*((x6)-(x5))$$

$$ya2=y5+((((x5-x7)*(x8-x7)+(y5-y7)*(y8-y7)+(z5-z7)*(z8-z7))*((x8-x7)*(x6-x5)+(y8-y7)*(y6-y5)+(z8-z7)*(z6-z5))-((x5-x7)*(x6-x5)+(y5-y7)*(y6-y5)+(z5-z7)*(z6-z5))*((x8-x7)*(x8-x7)+(y8-y7)*(y8-y7)+(z8-z7)*(z8-z7)))/(((x6-x5)*(x6-x5)+(y6-y5)*(y6-y5)+(z6-z5)*(z6-z5))*((x8-x7)*(x8-x7)+(y8-y7)*(y8-y7)+(z8-z7)*(z8-z7))-((x8-x7)*(x6-x5)+(y8-y7)*(y6-y5)+(z8-z7)*(z6-z5))*((x8-x7)*(x6-x5)+(y8-y7)*(y6-y5)+(z8-z7)*(z6-z5))))*(y6-y5)$$

$$za2=z5+((((x5-x7)*(x8-x7)+(y5-y7)*(y8-y7)+(z5-z7)*(z8-z7))*((x8-x7)*(x6-x5)+(y8-y7)*(y6-y5)+(z8-z7)*(z6-z5))-((x5-x7)*(x6-x5)+(y5-y7)*(y6-y5)+(z5-z7)*(z6-z5))*((x8-x7)*(x8-x7)+(y8-y7)*(y8-y7)+(z8-z7)*(z8-z7)))/(((x6-x5)*(x6-x5)+(y6-y5)*(y6-y5)+(z6-z5)*(z6-z5))*((x8-x7)*(x8-x7)+(y8-y7)*(y8-y7)+(z8-z7)*(z8-z7))-((x8-x7)*(x6-x5)+(y8-y7)*(y6-y5)+(z8-z7)*(z6-z5))*((x8-x7)*(x6-x5)+(y8-y7)*(y6-y5)+(z8-z7)*(z6-z5))))*(z6-z5)$$

$$\begin{aligned}
&xb2=x7+((((x5-x7)*(x8-x7)+(y5-y7)*(y8-y7)+(z5-z7)*(z8-z7))+((x8-x7)*(x6-x5)+(y8-y7)*(y6-y5)+(z8- \\
&z7)*(z6-z5))*(((x5-x7)*(x8-x7)+(y5-y7)*(y8-y7)+(z5-z7)*(z8-z7))*((x8-x7)*(x6-x5)+(y8-y7)*(y6-y5)+(z8- \\
&z7)*(z6-z5))-((x5-x7)*(x6-x5)+(y5-y7)*(y6-y5)+(z5-z7)*(z6-z5))*((x8-x7)*(x8-x7)+(y8-y7)*(y8-y7)+(z8- \\
&z7)*(z8-z7)))/(((x6-x5)*(x6-x5)+(y6-y5)*(y6-y5)+(z6-z5)*(z6-z5))*((x8-x7)*(x8-x7)+(y8-y7)*(y8-y7)+(z8- \\
&z7)*(z8-z7))-((x8-x7)*(x6-x5)+(y8-y7)*(y6-y5)+(z8-z7)*(z6-z5))*((x8-x7)*(x6-x5)+(y8-y7)*(y6-y5)+(z8- \\
&z7)*(z6-z5))))/((x8-x7)*(x8-x7)+(y8-y7)*(y8-y7)+(z8-z7)*(z8-z7)))*(x8-x7) \\
&yb2=(y7)+((((x5)-(x7))*((x8)-(x7))+((y5)-(y7))*((y8)-(y7))+((z5)-(z7))*((z8)-(z7)))+((x8)-(x7))*((x6)- \\
&(x5))+((y8)-(y7))*((y6)-(y5))+((z8)-(z7))*((z6)-(z5)))*(((x5)-(x7))*((x8)-(x7))+((y5)-(y7))*((y8)- \\
&(y7))+((z5)-(z7))*((z8)-(z7)))*((x8)-(x7))*((x6)-(x5))+((y8)-(y7))*((y6)-(y5))+((z8)-(z7))*((z6)-(z5)))-((x5)- \\
&(x7))*((x6)-(x5))+((y5)-(y7))*((y6)-(y5))+((z5)-(z7))*((z6)-(z5)))*((x8)-(x7))*((x8)-(x7))+((y8)-(y7))*((y8)- \\
&(y7))+((z8)-(z7))*((z8)-(z7)))/(((x6)-(x5))*((x6)-(x5))+((y6)-(y5))*((y6)-(y5))+((z6)-(z5))*((z6)- \\
&(z5)))*((x8)-(x7))*((x8)-(x7))+((y8)-(y7))*((y8)-(y7))+((z8)-(z7))*((z8)-(z7)))-((x8)-(x7))*((x6)-(x5))+((y8)- \\
&(y7))*((y6)-(y5))+((z8)-(z7))*((z6)-(z5)))*((x8)-(x7))*((x6)-(x5))+((y8)-(y7))*((y6)-(y5))+((z8)-(z7))*((z6)- \\
&(z5))))/((x8)-(x7))*((x8)-(x7))+((y8)-(y7))*((y8)-(y7))+((z8)-(z7))*((z8)-(z7)))*(y8)-(y7) \\
&zb2=(z7)+((((x5)-(x7))*((x8)-(x7))+((y5)-(y7))*((y8)-(y7))+((z5)-(z7))*((z8)-(z7)))+((x8)-(x7))*((x6)- \\
&(x5))+((y8)-(y7))*((y6)-(y5))+((z8)-(z7))*((z6)-(z5)))*(((x5)-(x7))*((x8)-(x7))+((y5)-(y7))*((y8)- \\
&(y7))+((z5)-(z7))*((z8)-(z7)))*((x8)-(x7))*((x6)-(x5))+((y8)-(y7))*((y6)-(y5))+((z8)-(z7))*((z6)-(z5)))-((x5)- \\
&(x7))*((x6)-(x5))+((y5)-(y7))*((y6)-(y5))+((z5)-(z7))*((z6)-(z5)))*((x8)-(x7))*((x8)-(x7))+((y8)-(y7))*((y8)- \\
&(y7))+((z8)-(z7))*((z8)-(z7)))/(((x6)-(x5))*((x6)-(x5))+((y6)-(y5))*((y6)-(y5))+((z6)-(z5))*((z6)- \\
&(z5)))*((x8)-(x7))*((x8)-(x7))+((y8)-(y7))*((y8)-(y7))+((z8)-(z7))*((z8)-(z7)))-((x8)-(x7))*((x6)-(x5))+((y8)- \\
&(y7))*((y6)-(y5))+((z8)-(z7))*((z6)-(z5)))*((x8)-(x7))*((x6)-(x5))+((y8)-(y7))*((y6)-(y5))+((z8)-(z7))*((z6)- \\
&(z5))))/((x8)-(x7))*((x8)-(x7))+((y8)-(y7))*((y8)-(y7))+((z8)-(z7))*((z8)-(z7)))*(z8)-(z7) \\
&xab2=((x5)+((((x5)-(x7))*((x8)-(x7))+((y5)-(y7))*((y8)-(y7))+((z5)-(z7))*((z8)-(z7)))*((x8)-(x7))*((x6)- \\
&(x5)))+... \\
&((y8)-(y7))*((y6)-(y5))+((z8)-(z7))*((z6)-(z5)))-((x5)-(x7))*((x6)-(x5))+((y5)-(y7))*((y6)-(y5))+((z5)- \\
&(z7))*... \\
&((z6)-(z5))*((x8)-(x7))*((x8)-(x7))+((y8)-(y7))*((y8)-(y7))+((z8)-(z7))*((z8)-(z7)))/(((x6)-(x5))*((x6)- \\
&(x5)))+... \\
&((y6)-(y5))*((y6)-(y5))+((z6)-(z5))*((z6)-(z5)))*((x8)-(x7))*((x8)-(x7))+((y8)-(y7))*((y8)-(y7))+((z8)- \\
&(z7))*((z8)-... \\
&(z7))-((x8)-(x7))*((x6)-(x5))+((y8)-(y7))*((y6)-(y5))+((z8)-(z7))*((z6)-(z5)))*((x8)-(x7))*((x6)-(x5))+((y8)- \\
&(y7))*... \\
&((y6)-(y5))+((z8)-(z7))*((z6)-(z5))))*((x6)-(x5))+x7+(((x5-x7)*(x8-x7)+(y5-y7)*(y8-y7)+(z5-z7)*(z8- \\
&z7))+((x8-x7)*... \\
&(x6-x5)+(y8-y7)*(y6-y5)+(z8-z7)*(z6-z5))*(((x5-x7)*(x8-x7)+(y5-y7)*(y8-y7)+(z5-z7)*(z8-z7))*((x8- \\
&x7)*(x6-x5)+(y8-y7)*... \\
&(y6-y5)+(z8-z7)*(z6-z5))-((x5-x7)*(x6-x5)+(y5-y7)*(y6-y5)+(z5-z7)*(z6-z5))*((x8-x7)*(x8-x7)+(y8- \\
&y7)*(y8-y7)+(z8-z7)*... \\
&(z8-z7)))/(((x6-x5)*(x6-x5)+(y6-y5)*(y6-y5)+(z6-z5)*(z6-z5))*((x8-x7)*(x8-x7)+(y8-y7)*(y8-y7)+(z8- \\
&z7)*(z8-z7))-((x8-x7)*...
\end{aligned}$$


```

AP=imread("AP10.bmp");

[nr,nc, zz]=size(AP);
% 28.75 X 23.552 (2500 X 2048 ) [250 X 205] 0.0115
dpp=0.115;

for xx1=1:nr
for yy1=1:nc
    xx(xx1,yy1)=(xx1*dpp)-(nr*dpp/2);
    yy(xx1,yy1)=-3;
    zz(xx1,yy1)=(yy1*dpp)-(nc*dpp/2);
    planeimg1(xx1,yy1,1)=AP(xx1,yy1,1);
endfor
endfor

colormap("gray");

% do a normal surface plot
surf(xx,yy,zz,planeimg1, 'edgecolor','none');

%=====
%axis("square");
plot3([x1,x2],[y1,y2],[z1,z2],"r");
    %text(x1,y1,z1,"(x1,y1,z1)");
    %%text(x1,y1,z1,"1");
    %text(x2,y2,z2,"(x2,y2,z2)");
    %%text(x2,y2,z2,"2");
plot3([x1,xa1],[y1,ya1],[z1,za1],"r");
    %text(xa1,ya1,za1,"(xa1,ya1,za1)");
    %%text(xa1,ya1,za1,"a1");
plot3([x2,xa1],[y2,ya1],[z2,za1],"r");

plot3([x3,x4],[y3,y4],[z3,z4],"r");
    %text(x3,y3,z3,"(x3,y3,z3)");
    %%text(x3,y3,z3,"3");
    %text(x4,y4,z4,"(x4,y4,z4)");
    %%text(x4,y4,z4,"4");
plot3([x3,xb1],[y3,yb1],[z3,zb1],"r");
    %text(xb1,yb1,zb1,"(xb1,yb1,zb1)");
    %%text(xb1,yb1,zb1,"b1");
plot3([x4,xb1],[y4,yb1],[z4,zb1],"r");

```

```

plot3([xa1,xb1],[ya1,yb1],[za1,zb1],"r");
        %text(xab1,yab1,zab1,"(xab1,yab1,zab1)");
        %%text(xab1,yab1,zab1,"ab1");
        %%text(0,0,0,"O");

```

```

plot3([xab1,xab2],[yab1,yab2],[zab1,zab2],"g");
        %text(xab2,yab2,zab2,"(xab2,yab2,zab2)");
        %%text(xab2,yab2,zab2,"ab2");

```

%-----

```

plot3([x5,x6],[y5,y6],[z5,z6],"b");
        %text(x5,y5,z5,"(x5,y5,z5)");
        %%text(x5,y5,z5,"5");
        %text(x6,y6,z6,"(x6,y6,z6)");
        %%text(x6,y6,z6,"6");

```

```

plot3([x5,xa2],[y5,ya2],[z5,za2],"b");
        %text(xa2,ya2,za2,"(xa2,ya2,za2)");
        %%text(xa2,ya2,za2,"a2");

```

```

plot3([x6,xa2],[y6,ya2],[z6,za2],"b");

```

```

plot3([x7,x8],[y7,y8],[z7,z8],"b");
        %text(x7,y7,z7,"(x7,y7,z7)");
        %%text(x7,y7,z7,"7");
        %text(x8,y8,z8,"(x8,y8,z8)");
        %%text(x8,y8,z8,"8");

```

```

plot3([x7,xb2],[y7,yb2],[z7,zb2],"b");
        %text(xb2,yb2,zb2,"(xb2,yb2,zb2)");
        %%text(xb2,yb2,zb2,"b2");

```

```

plot3([x8,xb2],[y8,yb2],[z8,zb2],"b");

```

```

plot3([xa2,xb2],[ya2,yb2],[za2,zb2],"b");
        %text(xab2,yab2,zab2,"(xab2,yab2,zab2)");
        %%text(xab2,yab2,zab2,"ab2");
        %text(0,0,0,"O");

```

%-----

```

xlabel("x");

```

```

ylabel("y");
xlabel("z");

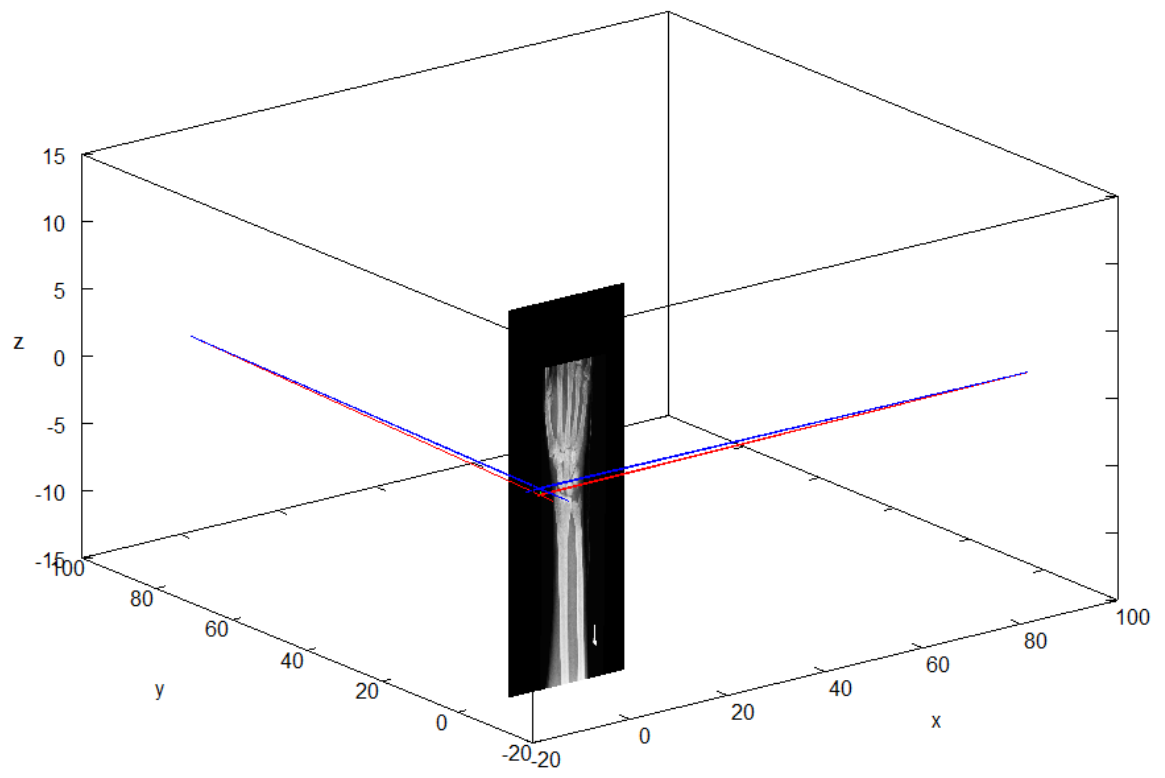
%legend("east");
%{
legend(%strcat("Origin(O)=","(",num2str(0),"",num2str(0),"",num2str(0),"),"),...

strcat("(xab,yab,zab,dab)=","(",num2str(xab),"",num2str(yab),"",num2str(zab),"",num2str(dab),"),"),...
%strcat("(xab,yab,zab,dab)=","(",num2str(xab),"",num2str(yab),"",num2str(zab),"),"),...
strcat("(x1,y1,z1)=","(",num2str(x1),"",num2str(y1),"",num2str(z1),"),"),...
strcat("(x2,y2,z2)=","(",num2str(x2),"",num2str(y2),"",num2str(z2),"),"),...
strcat("(x3,y3,z3)=","(",num2str(x3),"",num2str(y3),"",num2str(z3),"),"),...
strcat("(x4,y4,z4)=","(",num2str(x4),"",num2str(y4),"",num2str(z4),"),"),...
strcat("(xa,ya,za)=","(",num2str(xa),"",num2str(ya),"",num2str(za),"),"),...
strcat("(xb,yb,zb)=","(",num2str(xb),"",num2str(yb),"",num2str(zb),"),")...
%strcat("(xb,yb,zb)=","(",num2str(xb),"",num2str(yb),"",num2str(zb),"),")...
%strcat("(xab,yab,zab)=","(",num2str(xab),"",num2str(yab),"",num2str(zab),"),")...
);

%}
hold off
%-----
endfunction

```

x1 = 0	dab1 = 0.031639
y1 = 97	x5 = 0
z1 = 0	y5 = 97
x2 = -2.6500	z5 = 0
y2 = -3	x6 = 0.57000
z2 = -0.55000	y6 = -3
x3 = 97	z6 = -0.86000
y3 = 0	x7 = 97
z3 = 0	y7 = 0
x4 = -3	z7 = 0
y4 = 0.75000	x8 = -3
z4 = -0.50000	y8 = 3.8600
xa1 = -2.5507	z8 = -0.56000
ya1 = 0.74680	xa2 = 0.53166
za1 = -0.52939	ya2 = 3.7260
xb1 = -2.5509	za2 = -0.80216
yb1 = 0.74663	xb2 = 0.53011
zb1 = -0.49775	yb2 = 3.7237
xab1 = -2.5508	zb2 = -0.54023
yab1 = 0.74672	xab2 = 0.53088
zab1 = -0.51357	yab2 = 3.7249
dab1 = 0.031639	zab2 = -0.67119
x5 = 0	dab2 = 0.26194
y5 = 97	dab = 4.2885



APPENDIX L

Publications and conference proceedings

Peer reviewed conference and journal Publications

Nell, R. D. & Kahn, M.T.E. The use of 3D electronic vision for effective utilization of solar power in a hybrid electrical supply setup. DUE 2011. IEEE, Xplore

Nell, R. D. & Kahn, M.T.E. Measuring the light intensity of a hybrid powered CFL/LED lighting using 3D electronic vision. ICUE 2012. IEEE, Xplore

Rachel Griggs, Savvas Andronikou, **Raymond Nell**, Natasha O'Connell, Amanda Dehaye & Maria Ines Boechat. World Federation of Pediatric Imaging (WFPI) volunteer outreach through tele-reading: the pilot project in South Africa. Journal of Paediatric Radiology. **Springer-Verlag**, Berlin Heidelberg 2014

International Conference presentations

Nell, R. D. & Kahn, M.T.E. A method to determine and calculate the distance between the X-ray tube and the patient skin surface without any interaction with the patient ISRRT Congress, Canada 2011

Nell, R. D. & Kahn, M.T.E. A method for external surface reconstruction to provide both the external and internal 3D image of the patient in a hybrid radiography examination. Canada, 2011

Nell, R. D. & Kahn, M.T.E. A method to perform 3D measurements with an AP and LAT X-ray examination. SORSA-RSSA Imaging Congress. Durban 2013

Nell, R. D. The independent equipment record (IER) assisting the radiographer in quality assurance. SORSA-RSSA Imaging Congress. Durban 2013

International Conference poster presentations

Nell, R. D. Theoretical Method for Detecting a 3D Point in Space with One X-ray Exposure. Australia, ISRRT Congress. 2010

Nell, R. D. TB protection methods for the protection of the Radiographer against TB infection in the X-ray department. Australia, ISRRT Congress. 2010

Nell, R. D. A basic telemedicine system that uses email and a hospital computer to link primary health care centres to major hospitals. Southern African Telemedicine Conference .Stellenbosch University and Medical Research Council. Cape Town 2010

IEEE.org | IEEE Xplore Digital Library | IEEE Standards | IEEE Spectrum | More Sites Cart (0) | Create Account | Sign In

IEEE Xplore
DIGITAL LIBRARY

Access provided by:
Cape Peninsula University of
Technology
Sign Out

BROWSE MY SETTINGS MY PROJECTS WHAT CAN I ACCESS? RESOURCES

SEARCH

Author Search | Advanced Search | Preferences | Search Tips | More Search Options

Browse Conference Publications > Industrial and Commercial Use ...

The use of 3D electronic vision for effective utilization of solar power in a hybrid electrical supply setup

Full Text as PDF

2 Author(s) Nell, R.D. ; Electr. Eng., Cape Peninsula Univ. of Technol., Cape Town, South Africa ; Kahn, M.T.E.

Abstract Authors References Cited By Keywords Metrics Similar

Download Citations Email

Three-dimensional (3D) electronic vision can provide recognition of objects and also orientation of an object to its surrounding. With recognition of objects, possible interaction can be obtained and readjustment of their position. When a solar panel is used in a hybrid electrical supply setup, recognition of objects and their casing shadow can be used to reposition a solar panel to obtain

12:04 12/Jan/14

IEEE.org | IEEE Xplore Digital Library | IEEE Standards | IEEE Spectrum | More Sites Cart (0) | Create Account | Sign In

IEEE Xplore
DIGITAL LIBRARY

Access provided by:
Cape Peninsula University of
Technology
Sign Out

BROWSE MY SETTINGS MY PROJECTS WHAT CAN I ACCESS? RESOURCES

SEARCH

Author Search | Advanced Search | Preferences | Search Tips | More Search Options

Browse Conference Publications > Domestic Use of Energy Confer ...

Measuring the light intensity of a hybrid powered CFL and LED lighting using 3D electronic vision in rotation of the solar panel

Full Text as PDF
Full Text in HTML

2 Author(s) Nell, R.D. ; Dept. of Electr. Eng., Cape Peninsula Univ. of Technol., Cape Town, South Africa ; Kahn, M.T.E.

Abstract Authors References Cited By Keywords Metrics Similar

Download Citations Email

This paper describes how 3D electronic vision can be used in rotation of the solar panel for optimal use of sunlight to power an incandescent, CFL and LED light. The light intensity from the CFL and LED lighting powered by the solar panel is measured and how the solar panel, battery setup and grid supply is used in a hybrid electrical setup for both daytime and night time lighting. The method used is

12:03 12/Jan/14

Springer Link

Search

Home • Contact Us

Download PDF (251 KB) View Article

Pediatric Radiology
June 2014, Volume 44, Issue 6, pp 648-654

World Federation of Pediatric Imaging (WFPI) volunteer outreach through tele-reading: the pilot project in South Africa

Rachel Griggs, Savvas Andronikou, Raymond Nell, Natasha O'Connell, Amanda Dehaye, Maria Ines Boechat

Download PDF (251 KB)

View Article

Abstract

Background
Shortages in radiology services are estimated to affect 3.5–4.7 billion people worldwide. Teleradiology is a potential means of alleviating this shortage.

Do you want AutoComplete to remember web form entries? Learn about AutoComplete

ESPR, SPR, AOSPR and SLARP

Within this Article

- Introduction
- Materials and methods
- Results

12:01 12/7Jun/14

Presentations - Windows Internet Explorer

http://www.ie.ssa.ac.za/index.php/conferences/satelemed@BoechatConf/satelemed2015/paper.aspx?view&path%5D%3D%3D129

ABSTRACTS SUBMISSION

HOME ABOUT LOG IN ACCOUNT SEARCH ARCHIVE *** GO BACK TO SA TELEMEDICINE CONFERENCE ***

Home > Presentations

Presentations

A BASIC RADIOGRAPHY TELEMEDICINE SYSTEM THAT USES EMAIL AND HOSPITAL COMPUTER NETWORK TO LINK PRIMARY HEALTH CARE CENTRES TO MAJOR HOSPITALS

Raymond Donovan Nell

Internet | Protected Mode On

03:06 PM 2014/07/31

